frontiers | Research Topics

Highly consanguineous populations and rare genetic diseases in pediatrics

Edited by
Naglaa M. Kamal and Laila Sherief

Published in
Frontiers in Genetics
Frontiers in Pediatrics

ISSN 1664-8714
ISBN 978-2-83251-016-2
DOI 10.3389/978-2-83251-016-2

About Frontiers

Frontiers is more than just an open access publisher of scholarly articles: it is a pioneering approach to the world of academia, radically improving the way scholarly research is managed. The grand vision of Frontiers is a world where all people have an equal opportunity to seek, share and generate knowledge. Frontiers provides immediate and permanent online open access to all its publications, but this alone is not enough to realize our grand goals.

Frontiers journal series

The Frontiers journal series is a multi-tier and interdisciplinary set of open-access, online journals, promising a paradigm shift from the current review, selection and dissemination processes in academic publishing. All Frontiers journals are driven by researchers for researchers; therefore, they constitute a service to the scholarly community. At the same time, the *Frontiers journal series* operates on a revolutionary invention, the tiered publishing system, initially addressing specific communities of scholars, and gradually climbing up to broader public understanding, thus serving the interests of the lay society, too.

Dedication to quality

Each Frontiers article is a landmark of the highest quality, thanks to genuinely collaborative interactions between authors and review editors, who include some of the world's best academicians. Research must be certified by peers before entering a stream of knowledge that may eventually reach the public - and shape society; therefore, Frontiers only applies the most rigorous and unbiased reviews. Frontiers revolutionizes research publishing by freely delivering the most outstanding research, evaluated with no bias from both the academic and social point of view. By applying the most advanced information technologies, Frontiers is catapulting scholarly publishing into a new generation.

What are Frontiers Research Topics?

Frontiers Research Topics are very popular trademarks of the *Frontiers journals series*: they are collections of at least ten articles, all centered on a particular subject. With their unique mix of varied contributions from Original Research to Review Articles, Frontiers Research Topics unify the most influential researchers, the latest key findings and historical advances in a hot research area.

Find out more on how to host your own Frontiers Research Topic or contribute to one as an author by contacting the Frontiers editorial office: frontiersin.org/about/contact

Highly consanguineous populations and rare genetic diseases in pediatrics

Topic editors

Naglaa M. Kamal — Cairo University, Egypt

Laila Sherief — Zagazig University, Egypt

Citation

Kamal, N. M., Sherief, L., eds. (2022). *Highly consanguineous populations and rare genetic diseases in pediatrics*. Lausanne: Frontiers Media SA.

doi: 10.3389/978-2-83251-016-2

Table of contents

frontiers in Genetics

BRIEF RESEARCH REPORT
published: 11 February 2022
doi: 10.3389/fgene.2022.761178

A Novel Variant of the *CHD2* Gene Associated With Developmental Delay and Myoclonic Epilepsy

Lina Zhu[1†], *Fujun Peng*[2†], *Zengwen Deng*[3], *Zhichun Feng*[1] *and Xiuwei Ma*[1*]

[1]Faculty of Pediatrics, Chinese PLA General Hospital, BaYi Children's Hospital, The Seventh Medical Center of PLA General Hospital, Beijing, China, [2]School of Basic Medical Sciences, Weifang Medical University, Weifang, China, [3]Hospital of Jvlu County, Xingtai, China

OPEN ACCESS

Edited by:
Naglaa M. Kamal,
Cairo University, Egypt

Reviewed by:
Jing Chen,
Cincinnati Children's Hospital Medical Center, United States
Vanesa Nieto-Estévez,
University of Texas at San Antonio, United States
Marina Trivisano,
Bambino Gesù Children's Hospital (IRCCS), Italy
Amy McTague,
University College London, United Kingdom

***Correspondence:**
Xiuwei Ma
pony007@vip.sina.com

[†]These authors have contributed equally to this work and share first authorship

Specialty section:
This article was submitted to Genetics of Common and Rare Diseases, a section of the journal Frontiers in Genetics

Received: 19 August 2021
Accepted: 12 January 2022
Published: 11 February 2022

Citation:
Zhu L, Peng F, Deng Z, Feng Z and Ma X (2022) A Novel Variant of the CHD2 Gene Associated With Developmental Delay and Myoclonic Epilepsy. Front. Genet. 13:761178. doi: 10.3389/fgene.2022.761178

Pathogenic variants in *CHD2* have been reported to have a wide range of phenotypic variability in neurodevelopmental disorders, such as early-onset epileptic encephalopathy, developmental delay, and behavior problems. So far, there is no clear correlation between genotypes and phenotypes. This study reports a Chinese patient with a novel heterozygous *CHD2* mutation (c.4318C>T, pArg1440*). Her main clinical manifestations include developmental delay, myoclonic epilepsy, and hypothyroidism. Then, we reviewed a total of 144 individuals carrying *CHD2* variants with epileptic encephalopathy. In terms of clinical manifestations, these patients are usually described with variable epilepsy phenotypes, including idiopathic photosensitive occipital epilepsy, Dravet syndrome, Jeavons syndrome, Lennox–Gastaut syndrome, juvenile myoclonic epilepsy, and non-specific epileptic encephalopathy. Among them, myoclonic seizures and generalized tonic-clonic seizures are the main seizure types in all patients hosting *CHD2* single-nucleotide or indel variants (non-CNVs). At the molecular level, there are 102 types of *CHD2* non-CNVs in 126 patients, almost one mutational type corresponding to one person, and there is no difference in the incidence ratio of each position. Furthermore, we summarized that a small proportion of patients inherited *CHD2* variants, and not all patients with *CHD2* variants had seizures. Importantly, the phenotypes, especially seizures control and fever sensitivity, and genotypes had a relative association. These results enriched the database of CHD2-relative neurodevelopmental disorders and provided a theoretical foundation for researching the relationship between genotypes and phenotypes.

Keywords: whole-exome sequencing, *CHD2* variants, developmental delay, myoclonic epilepsy, epileptic encephalopathy

INTRODUCTION

Chromodomain helicase DNA-binding protein 2 (CHD2, MIM: 615369) is a member of the CHD family, which is only known to cause the brain-restricted phenotypes when disrupted in humans. It is mapped to chromosome 15q26.1 and is considered an ATP-dependent chromatin remodeling that regulates the transcription expression of many genes (Lamar and Carvill, 2018; Carvill and Mefford, 2015). Some studies have demonstrated that pathogenic variants of the *CHD2* gene are associated with childhood-onset developmental and epileptic encephalopathy (DEE), which is a severe form of neurodevelopmental disorder with a wide range of phenotypic variability, including autism spectrum

disorder (ASD), intellectual disability (ID), developmental delay, microcephalus, behavioral anomalies, facial dysmorphisms, and several types of epilepsy (Carvill and Mefford, 2015; Thomas et al., 2015; Verhoeven et al., 2016; Chen et al., 2020). Recently, Chen et al. presented the largest single case series of patients with CHD2-related epilepsy and then comprehensively reviewed 53 published cases in the literature through seizure onset age, seizure types, developmental outcome, electroencephalogram (EEG), brain magnetic resonance imaging (MRI), and diagnoses, among others, which improved the understanding on the relationship between genotype and phenotype (Chen et al., 2020). In 2021, De Maria et al. reported 18 new patients and reviewed 84 previously reported patients, getting the results that the median age of seizures onset in 92% of patients was 2.5 years, and there was no clear association between genotypes and phenotypes (De Maria et al., 2021).

This study reported a novel variant in the *CHD2* gene in a Chinese girl with developmental delay and myoclonic epilepsy through whole-exome sequencing (WES). We also systematically reviewed the published literature, provided a thorough overview of clinical, neuroimaging, physical, and genetic findings in CHD2-related epilepsy patients, and built the possible relationship between genotypes and phenotypes.

MATERIALS AND METHODS

Case Collection

A total of 59 papers, including 144 cases, were considered candidates (**Table 1** and **Supplementary Table S1**). These cases were collected from studies and databases and reported to associate with the *CHD2* mutations. The main process is as follows: 1) the keywords "CHD2" and "neurodevelopmental disorders" or "epileptic encephalopathy" were used to search the PubMed database for relevant papers; 2) the full text of each eligible publication was downloaded and read carefully. The papers and review articles on these cases were saved; 3) using the "CHD2" gene as the keyword, relevant papers in the HGMD database were acquired, downloaded, screened, and reserved, and these papers were associated with CHD2-related epileptic encephalopathy; 4) the collected review articles were used to confirm the conclusions from the obtained papers and complement the lacking literature; 5) patient information, including clinical information, neuroimaging, physical, and genetic findings, was extracted from these papers, such as gender, inheritance, and diagnostic findings; and 6) all results were checked by more than two researchers, and the opposite consequences were verified after discussion.

Whole-Exome Sequencing

Genomic DNA was extracted from the peripheral blood of all the family members using DNA Isolation Kit (Blood DNA Kit V2, CW2553) according to standard procedure. Whole-exome capture and sequencing were performed using SureSelect Human All Exon V6 (60 Mb) kit (Agilent, Santa Clara, USA, and sequenced on the Illumina Nova series platform (Illumina, San Diego, USA), generating 150 bp paired-end pairs. The raw reads of sequencing underwent the process of trimming, depolluting, and filtering to get only the high-quality reads. Only those that passed these filtrations could be used for the downstream analyses. High-quality paired-end reads were aligned to the human reference genome sequence from the UCSC database (build 37.1 version hg19, http://genome.ucsc.edu/) using the Burrows–Wheeler Alignment tool. We estimated quality scores and made the consensus SNP and insertions and deletions (indels) calling using GATK [1]. All the called variants were annotated with ANNOVAR software to give the variant position, variant type, allele frequency, conservation prediction, and so forth, which would help locate mutations relative to diseases. All variants were filtered using the 1000 Genomes, ExAC, ChES, and gnomAD databases, as well as a minor allele frequency (MAF) ≤ 1%. Then, a series of analyses were used with OMIM database, HGMD database, and phenotypes-genotypes association analysis. Finally, the candidate variants were judged according to the ACMG standard and validated by Sanger sequencing. All samples were obtained with written informed consent from patients.

Statistical Analyses

All the statistical analyses were performed using SPSS 22.0. Pearson $\chi 2$ test was used to assess the significance of differences between groups. In the study of the number of patients with various seizure types (**Table 2** and **Supplementary Table S2**), the average value was introduced, which was equal to the number of all the patients except for unclassified generalized seizures (GS), unclassified seizures, and not applicable (NA) divided by the number of seizure types containing at least one patient. Similarly, the average concept was introduced in the study of the number of patients with various epilepsy types/syndrome (**Figure 3** and **Supplementary Table S3**). In the study of the incidence rate of variants in different domains of *CHD2* (**Figure 4A** and **Supplementary Table S4**), the incidence rate was calculated by dividing the mutational numbers in one domain divided by mRNA sequence lengths of this domain, and the average value was equal to the number of all the variants divided by the length of mRNA sequence in *CHD2* gene. In the studies of seizures control, photosensitivity, and fever sensitivity (**Figures 4B,C** and **Supplementary Table S5**), the difference values were presented among different domains of CHD2. A two-sided p-value < 0.05 was considered statistically significant and was adjusted by the Bonferroni correction.

Clinical Report

The proband was a 3-year and 2-month old girl, who was a full-term baby born by a healthy and unrelated Chinese couple through cesarean section, weighing 3,900 g, without intrauterine distress, suffocation, and neonatal jaundice (**Figure 1A**). Three days after birth, a thyroid function test suggested hypothyroidism, and the child took thyroxine tablets regularly to maintain normal thyroid function. She started to roll over at 6 months and sit at 8 months. At 17 months, she could not walk alone, and her Development Screen Test (DST) presented DQ < 70 and MI < 70. The DQ scores of Gesell Developmental Assessment (GDA) are listed below: gross movement is 71, fine

TABLE 1 | The seizure types of patients with *CHD2* mutations.

	Single-nucleotide or indel variants (*n* = 126)	Copy number variants (*n* = 18)
Gender	F (43), M (61), NA (22)	F (11), M (7)
Age	0~6 years (26), 6~12 years (27), >12 years (37), NA (36)	0~6 years (3), 6~12 years (4), >12 years (8), NA (3)
Inheritance	*De novo* (111), mother (2), father (3), NA (10)	*de novo* (18), mother (0), father (0), NA (0)
Age of seizure onset	≤1 year (16), 1~6 years (70), 6~12 years (5), >12 years (2), NA (33)	≤1 year (2), 1~6 years (11), 6~12 years (3), >12 years (1), NA (1)
Development before seizure onset	Delay (47), normal (22), NA (57)	Delay (12), normal (0), NA (6)
Seizure control	Yes (18), no (36), NA (72)	Yes (6), no (9), NA (3)
Introduce factors		
Photosensitivity	Yes (45), no (37), NA (44)	Yes (5), no (1), NA (12)
Fever sensitivity	Yes (14), no (37), NA (75)	Yes (0), no (4), NA (14)
Cognition/development outcome		
ASD	Yes (34), no (48), NA (44)	Yes (7), no (5), NA (6)
ADHD	Yes (12), no (48), NA (66)	Yes (1), no (8), NA (9)
ID	Yes (76), no (8), NA (42)	Yes (15), no (3), NA (0)
Behavior problem	Yes (47), no (2), NA (77)	Yes (10), no (0), NA (8)
Other abnormal findings[#]	Yes (78), no (8), NA (40)	Yes (16), no (0), NA (2)
Physical development		
Height	Normal (17), short stature (6), tall stature (1), NA (102)	Normal (4), short stature (6), tall stature (0), NA (8)
Weight	Normal (11), underweight (5), obesity (2), NA (108)	Normal (6), underweight (1), obesity (2), NA (9)
Head circumference	Normal (15), microcephaly (9), NA (102)	Normal (2), microcephaly (3), NA (13)
EEG	Normal (2), abnormal (80), NA (44)	Normal (0), abnormal (9), NA (9)
MRI	Normal (64), abnormal (8), NA (54)	Normal (9), abnormal (5), NA (4)
Facial dysmorphisms	yes (11), no (7), NA (108)	Yes (12), no (0), NA (6)

Abbreviations: d, day; m, month; y, year; ADHD, attention deficit hyperactivity disorder; ASD, autism spectrum disorder; EEG, electroencephalography; F, female; ID, intellectual disability; M, male; MRI, magnetic resonance imaging; NA, not applicable; #, other abnormal findings mainly contained delay in motor and language development, learning disability, illusions or hearing odd sounds, defective social communications, poor balance, short-term memory problems, etc.

movement is 76, adaptive skills score is 71, language is 53, and social score is 71. Brain magnetic resonance imaging (MRI) revealed no severe abnormalities. Then, the patient was required to do a series of rehabilitation training, which resulted in her ability to walk alone at 1.5 years, and run and navigate stairs at 2.5 years. However, she still could not jump or execute instructions and presented poor balance. The development delay was shown in her intelligence and language; for example, she spoke a single word at 2 years and said two or three words at 3 years. She liked to run around and open her mouth and did not like to play with other children. At the age of 2 years and 8 months, she started to experience seizures, and there was no obvious cause such as photosensitivity and fever sensitivity. The seizures were manifested by a rapid shaking of the entire body, which relieved in 1-2 s and occurred several times per day. After remission, the mental reaction was as usual. There was no special family history. The video electroencephalogram (VEEG) showed high-amplitude spike waves, and slow spike waves were burst throughout the brain, especially in the frontal, central, and middle posterior temporal regions (**Figures 2A,B**). When she had seizures, VEEG showed a generalized polyspike wave (**Figure 2C**). Other auxiliary examinations results were normal and mainly contained electrocardiogram, blood routine, urine routine, stool routine, biochemistry, myocardial enzymes, thyroid function, blood ammonia, lactic acid, blood tandem mass spectrometry analysis of amino acids and acylcarnitine, and urine organic acid analysis. Oral anti-epileptic treatment with sodium valproate was gradually increased to 30 mg/kg·d, and seizure was controlled.

The girl came to our hospital because of mental retardation with seizures when she was 3 years and 2 months old. She presented normal facial features, active behavior, poor execution, and lacking eye contact with people. The physical examination results revealed a total length of 96 cm, weight of 15 kg, and head circumference of 49 cm. The cardiopulmonary and abdominal examinations showed no abnormality. Dystonia of limbs did not exist, sputum culture reflexes were drawn symmetrically, and pathological signs were negative. The second DQ scores were a gross movement of 60, fine movement of 69, adaptive skills of 66, language of 50, and social score of 67. Brainstem auditory evoked response (BAER) showed a delay in the peripheral conduction of the binaural auditory pathway. Visual evoked potential (VEP) showed that the incubation period of bilateral P100 was prolonged. Integrating the above information, the girl was diagnosed with developmental delay and myoclonic epilepsy.

Genetic Analysis

Whole-exome sequencing was performed on the proband and her parents. Overall, more than 8 Gb of the sequence generated per patient covered all the exome and splice site regions of genes. The proband revealed a *de novo* heterozygous variant in *CHD2* (c. 4318C>T, p. Arg1440*). This nonsense variant was localized in the 30th exon out of 39 total exons in the *CHD2* gene (NM_001271.4) and was predicted to cause premature termination of translation. In addition, the mutation does not exist in the 1000 Genomes, ExAC, ChES, and gnomAD databases (Macdonald et al., 2014; Lek et al., 2016), and to our knowledge, it has not been reported in affected individuals in the published literature.

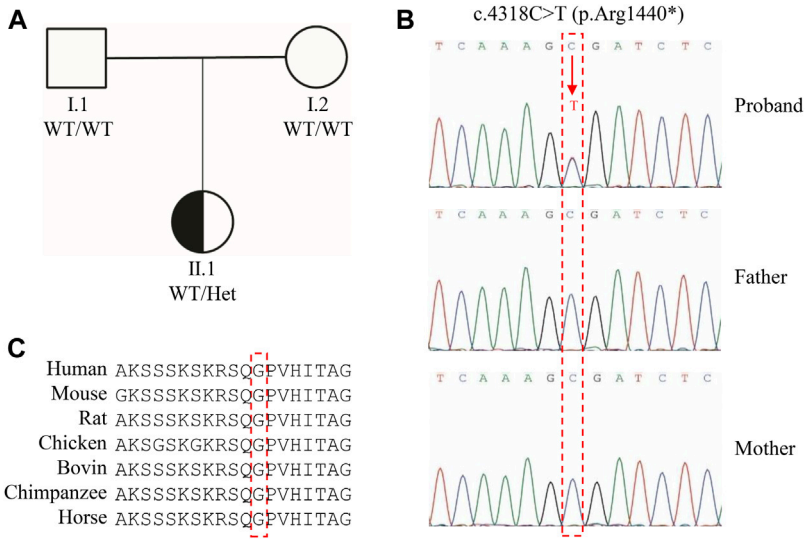

FIGURE 1 | Genetic characterization of the proband. **(A)** Family pedigree. **(B)** Analysis of CHD2 c.4318C>T (NM_001271.4, p. Arg1440*) in a non-related Chinese family. **(C)** Homology alignment of the protein encoded by CHD2.

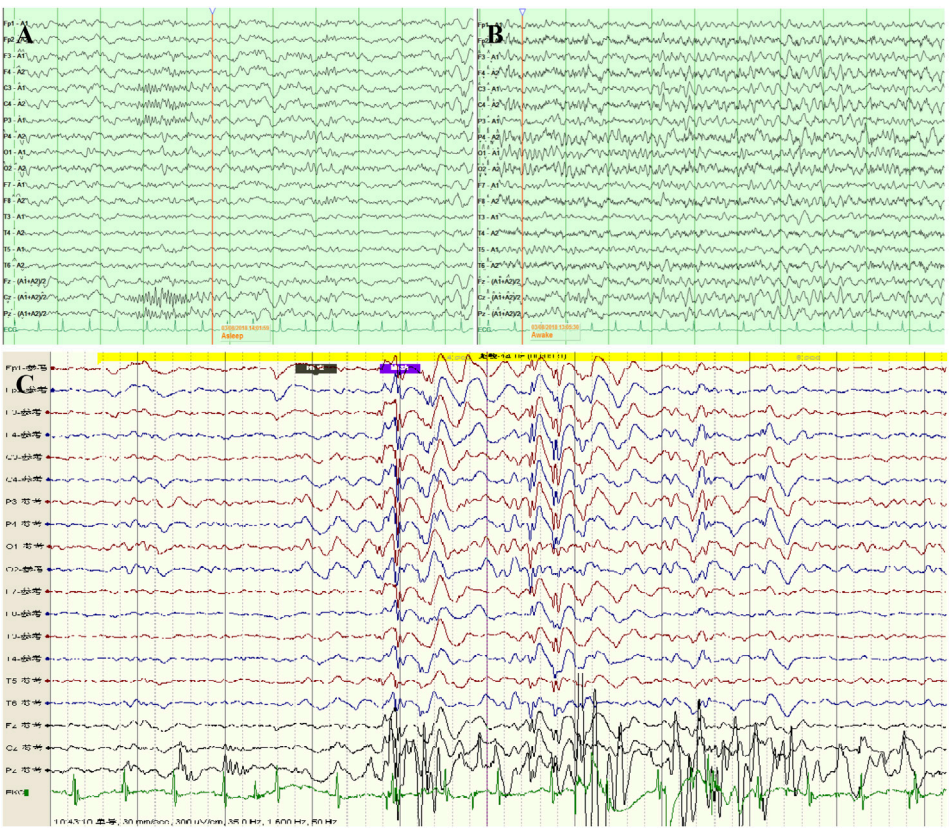

FIGURE 2 | Video electroencephalogram (VEEG) of the proband with development disorders. **(A)** During the sleeping period, a small amount of medium amplitude sharp waves and sharp slow waves were emitted asynchronously in bilateral frontal, central, parietal, and right occipital regions, and sporadic in the right anterior temporal region. **(B)** During the awake period, there had 7-8 Hz low amplitude, a, and Θ mixed waves in the bilateral occipital area. **(C)** When she had myoclonic seizures, the results showed a generalized polyspike wave.

TABLE 2 | Clinical characteristics of persons with a *CHD2* mutation in published cases.

	Single-nucleotide or indel variants			Copy number variants		
Seizure types	**First**	**Further**	**All**	**First**	**Further**	**All**
aAS	3	**11**[b]	**14**[b]	0	0	0
AbS	5	**13**[b]	**18**[b]	5	0	5
aMAS	**0**[a]	0	**0**[a]	1	0	1
AtS	4	**15**[b]	**19**[b]	0	0	0
CSE	2	3	5	0	0	0
DA	**0**[a]	1	1	0	0	0
EMA	8	4	**12**[b]	1	1	2
EMs	**0**[a]	1	1	0	1	1
ES	2	0	2	0	0	0
FCS	**0**[a]	0	**0**[a]	0	1	1
FoS	3	**15**[b]	**18**[b]	1	0	1
FoSID	1	0	1	1	0	1
FS	14	5	**19**[b]	3	0	3
GCS	**0**[a]	0	**0**[a]	0	1	1
GTCS	**17**	**30**[b]	**47**[b]	2	**5***	**6***
HD	**0**[a]	2	2	0	1	1
MA	1	6	7	0	0	0
MAS	3	8	10	0	0	0
MCS	**0**[a]	1	1	0	0	0
MS	**24**[b]	**30**[b]	**52**[b]	0	4	4
NCSE	**0**[a]	10	10	0	1	1
NS	**0**[a]	1	1	0	0	0
SE	**0**[a]	8	8	0	0	0
TCS	5	7	12	0	0	0
TS	1	**11**[b]	12	0	2	2
Unclassified GS	4	0	4	3	1	3
Unclassified seizures	33	0	28	1	0	1
NA	1	67	0	0	10	0

*Abbreviations: aAS, atypical absence seizures; AbS, absence seizures; aMAS, atypical myoclonic-absence seizures; AtS, atonic seizures; CNVs, copy number variants; CSE, convulsive status epilepticus; DA, drop attack; EMA, eyelid myoclonia with absence; EMs, eyelid myoclonias; ES, epileptic spasm; FCS, febrile clonic seizures; FoS, focal seizures; FoSID, focal seizure with impairment of awareness; FS, febrile seizures; GCS, generalized clonic seizure; GS, generalized seizures; GTCS, generalized tonic-clonic seizures; HD, head drops; MA, myoclonic absence seizures; MAS, myoclonic-atonic seizures; MCS, myotonic-clonic seizures; MS, myoclonic seizures; NA, not applicable; NCSE, non-convulsive status epilepticus; NS, non-epileptic seizures; SE, status epilepticus; TCS, tonic-clonic seizures; TS, tonic seizures; *, the difference did not exist using the Bonferroni correction.*

[a]*tendence and p-value <0.05;*

[b]*resistance and p-value <0.05.*

This variant was also validated by Sanger sequencing. Meanwhile, the *CHD2* genes of her parents were normal (**Figures 1A,B**). No other significant variants were found in the other genes. Multiple sequence alignment analysis revealed that the p. Arg1440* substitution occurred on an amino acid residue which was evolutionarily highly conserved among different species (**Figure 1C**).

DISCUSSION

The CHD protein family (containing CHD1–CHD9) is mainly involved in the ATP-dependent chromatin remodelers that contribute to the reorganization of chromatin structure and deposition of histone variants necessary for regulating gene transcription expression. Among the nine CHD family members, the *CHD2* pathogenic variants only lead to a brain-restricted phenotype when disrupted in humans, which indicates a unique role for this gene in neurodevelopment (Lamar and Carvill, 2018).

CHD2 mutation-related epilepsy was first published in 2009 (Veredice et al., 2009). This paper described a 30-month-old girl with refractory myoclonic epilepsy associated with mental retardation, growth delay, peculiar facial appearance, minor physical anomalies, and photosensitivity. In the patient, a 15q26.1–15q26.2 deletion including *CHD2* was detected by CGH-array. To date, there are 144 reported individuals encompassing 126 single-nucleotide or indel variants (non-CNVs) and 18 copy number variants (CNVs) with CHD2-related epileptic encephalopathy (**Table 1** and **Supplementary Table S1**). From **Table 1** and **Supplementary Table S1**, almost all patients were diagnosed at over 1 year or even over 6 years of age. Up to now, most *CHD2* variants have been reported *de novo* in patients with epilepsy rather than in an inherited mode. Nevertheless, in 2015, the first patients diagnosed with eyelid myoclonia with absence (EMA) inherited it from an unaffected mother, who carried the *CHD2* variant c.653C>T (p. Pro218Leu) (Galizia et al., 2015). In 2018, the patient who inherited a pathogenic *CHD2* variant c.628G>T (p. Glu218*) from the affected mother was published (Petersen et al., 2018). The distressing thing is that compared with her daughter's refractory epilepsy, her seizures have always been well controlled (Petersen et al., 2018). In 2020, Chen et al. reported

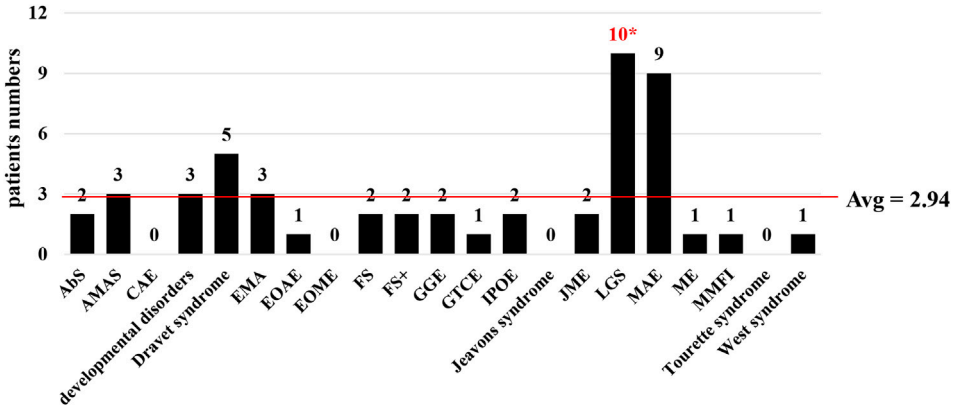

FIGURE 3 | Statistical analysis of all reported CHD2-non-CNVs patients with epilepsy. Distributions of patients according to epilepsy syndrome in the overall cohort, including 126 non-CNVs patients. The epilepsy syndrome did not contain DEE, non-specific GE, non-specific EE, and unclassified epilepsy. The average value = patients' numbers of epilepsy syndrome/numbers of epilepsy types. Abbreviations: AbS, absence seizures; CAE, childhood absence epilepsy; DEE, developmental and epileptic encephalopathy; EE, epileptic encephalopathy; EMA, eyelid myoclonia with absence; EOAE, early-onset absence epilepsy; EOME, early-onset myoclonic epilepsy; FS, febrile seizures; FS+, febrile seizure plus; GE, generalized epilepsy; GGE, genetic generalized epilepsy; GTCE, generalized tonic-clonic epilepsy; IPOE, idiopathic photosensitive occipital epilepsy; JME, juvenile myoclonic epilepsy; LGS, Lennox-Gastaut syndrome; MAE, myoclonic atonic epilepsy; ME, myoclonic epilepsy; MMFI, malignant migrating focal seizures in infancy; non-CNVs, single-nucleotide or indel variants; *, the difference did not exist using the Bonferroni correction.

a sporadic case inherited from an unaffected father with c.5153+2T>C variant of *CHD2* gene and dizygotic twins inherited from the affected father with c.5232G>A (p. Met1744Ile) (Chen et al., 2020). To our surprise, the five mutations in patients did not occur again in other cases. In *CHD2* CNVs patients, the inherited patients were not reported. These findings indicate that *CHD2* variants, with the exception of *CHD2* CNVs, can be inherited (**Table 1**).

Previously, *CHD2* variants were generally considered to be childhood-onset epileptic encephalopathy. However, more and more individuals with *CHD2* mutants were published, and the ages of seizure onset were different from infancy to childhood (**Table 1** and **Supplementary Table S1**). We had also found that different patients had different development in pre-seizure onset. For example, Carvill et al. reported that two out of six patients with epileptic encephalopathies caused by *CHD2* mutations had normal development and another four were abnormal (Carvill et al., 2013). Interestingly, all the patients with *CHD2* CNVs could lead to developmental delays in pre-seizure onsets, such as motor and speech developmental delays (**Table 1** and **Supplementary Table S1**). In addition, the inducing factors, including photosensitivity and fever sensitivity, EEG results, and facial dysmorphisms, were also various among *CHD2* variants' patients. Galizia et al. performed photosensitivity tests on zebrafish larvae with *CHD2* gene knockout and found that the *CHD2* gene knockout significantly enhanced the photosensitivity of congenital zebrafish larvae. Their results had confirmed that this gene was related to photosensitive epilepsy (Galizia et al., 2015). Except for the twin patients mentioned above, most patients had abnormal EEG results (Chen et al., 2020). We also found that the reported patients had behavior problems such as aggressive behavior. In other aspects of patients, the findings showed diversity, such as ASD, height, and MRI (**Table 1** and **Supplementary Table S1**).

The patients have variable seizure types, including absence seizures (AbS), atonic seizures, tonic-clonic seizures, and myoclonic absence seizures. Importantly, an individual can have multiple seizure types; even the first seizure and the later seizure could be of different types (**Supplementary Table S1**). Based on these phenomena, we summarized and analyzed the seizure types of patients with *CHD2* non-CNVs and CNVs (**Table 2** and **Supplementary Table S2**). In the *CHD2* non-CNVs patients, both the myoclonic seizures (MS, 27.3%, 24/88) and generalized tonic-clonic seizures (GTCS, 19.3%, 17/88) were the top two types of the first seizures, which presented the difference than average value (5.87 people/seizure types). Some seizure types, including atypical myoclonic-absence seizures (aMAS, 0%) and febrile clonic seizures (FCS, 0%), did not exist. In contrast, MS (50.8%, 30/59), GTCS (50.8%, 30/59), atonic seizures (AtS, 25.4%, 15/59), focal seizures (FoS, 25.4%, 15/59) and andother three seizure types were the main types of second and later seizures compared to average value (2.95 people/seizure types). In general, MS, GTCS, AtS, febrile seizures (FS), absence seizures (AbS), FoS, atypical absence seizures (aAS), and eyelid myoclonia with absence (EMA) were the main seizure types in *CHD2* non-CNVs (**Table 2** and **Supplementary Table S2**). Interestingly, the main type for *CHD2* CNVs patients could be GTCS, which did not exist using the Bonferroni correction. This phenomenon could be related to the small samples. Furthermore, the patients' numbers in different epileptic encephalopathy were analyzed using the above methods (**Figure 3** and **Supplementary Table S3**). The results showed that Lennox–Gastaut syndrome (LGS) was usually diagnosed in

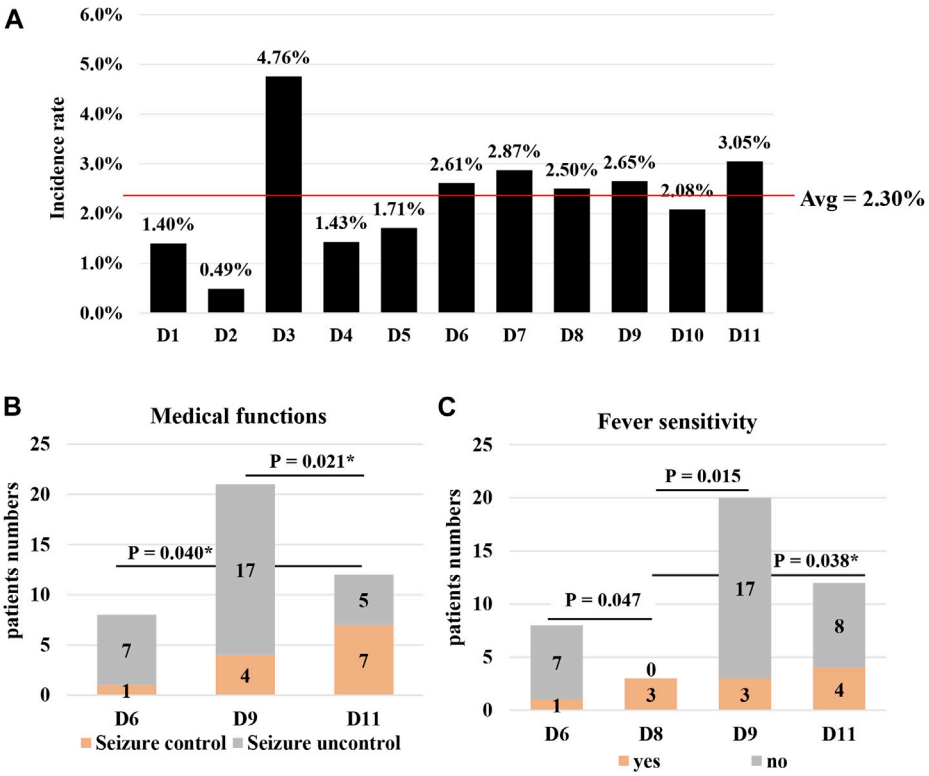

FIGURE 4 | Association analysis between genotypes and phenotypes in *CHD2* non-CNVs patients. **(A)** Distributions of the incidence rate of 126 non-CNVs in different *CHD2* domains. The incidence rate was the mutational numbers in one domain divided by mRNA sequence lengths of this domain and the average value equal to all the variants numbers divided by mRNA sequence lengths of the *CHD2* gene. **(B,C)** The association analysis between *CHD2* genotypes in different domains and phenotypes including seizure control and fever sensitivity in *CHD2* non-CNVs patients. Abbreviations: non-CNVs, single-nucleotide or indel variants; reference protein sequences, NP_001262.3; *, the difference did not exist using Bonferroni correction; D1, 1-262aa; D2, 263-330aa, chromodomain; D3, 331-337aa; D4, 378-447aa, chromodomain; D5, 448-486aa; D6, 487-767aa, SNF2 family; D7, 768-825aa; D8, 826-905aa, helicase conserved C-terminal domain; D9, 906-1458aa; D10, 1459-1554aa, domain of unknown function; D11, 1555-1828aa.

CHD2 non-CNVs patients, which presented the difference compared to the average value (2.94 people/epileptic encephalopathy) using the Pearson $\chi 2$ test, and the adjusted difference with the Bonferroni correction was disappearance (**Supplementary Table S3**). The *CHD2* CNVs individuals did not exist in these results (**Supplementary Table S3**).

Though a series of studies indicated that there was no clear correlation between genotypes and phenotype in CHD2-related epileptic encephalopathy (Epi et al., 2013; Chen et al., 2020; De Maria et al., 2021), we thought that it was necessary to further research the association between genotypes and phenotypes. We referred to the mRNA sequences NM_001271.4 and protein sequences NP_001262.3 to analyze all the *CHD2* non-CNVs related epilepsy patients (Thomas et al., 2015; Carvill and Mefford, 2015) (**Figure 4** and **Supplementary Tables S4, S5**). The whole protein sequences were divided into 11 fragments (D1–D11), including four conserved domains (Thomas et al., 2015). There were 102 types of *CHD2* non-CNVs in 126 patients, and almost one mutational type corresponded to one patient. Among them, the c.4173dupA (p. Gln1392Thrfs*17) and c.5035C>T (p. Arg1679*) could be the hotspot variants but only occurred five times, respectively (**Supplementary Table S4**). The *CHD2* variants were distributed in the whole protein sequences and focused on the D9 fragments (906-1458aa, 33.92%, 37/126) (**Supplementary Table S4**), which led to a serious shortcoming because the longer the domain, the more the number. In order to address this shortcoming, the incidence rate was applied. Though the D11 fragments (1554-1828aa, 3.05%, 25/825) tended to host the *CHD2* variants, the difference value was not shown than the average value (2.30%) (**Figure 4A** and **Supplementary Table S4**). Meanwhile, The D3 fragment was too short and was not further analyzed. Interestingly, the incidence rate presented the difference between D1 and D11 (**Supplementary Table S4**). We also analyzed the relationship between *CHD2* genotypes and seizure control, inducing factors including photosensitivity and fever sensitivity in all the *CHD2* non-CNVs patients, and found a significant correlation between genotypes and phenotypes (**Figures 4B,C** and **Supplementary Table S5**). The patients with *CHD2* variants in D11 tended to have better seizure control, and patients with *CHD2* variants in D6 and D9 tended to have worse seizure

control. Similarly, there also was a difference in fever sensitivity among D6, D8, D9, and D11. The patients in D8 tended to have more serious fever sensitivity compared to D6, D9, and D11. Though the difference for photosensitivity did not present with *CHD2* variants in D6, D9, and D11, patients with *CHD2* variants in D9 suffered photosensitivity more easily than *CHD2* variants in D6 and D11. These results suggested that there could be associations between genotypes and phenotypes, which were further demonstrated by the dizygotic or monozygotic twins (Pinto et al., 2016; Wang et al., 2017; Chen et al., 2020). Pinto et al. reported that the monozygosity cases had the same seizure onset at 2 years and 6 months old, carried the c.4173dupA (p. Gln1392Thrfs*17) mutations, and presented a set of similar clinical features phenotypes, including autism spectrum disorder, hypotonia, postnatal microcephaly, stereotypic movements, circadian rhythm alterations, and AbS (Pinto et al., 2016). Wang et al. also reported that the monozygotic twins had the same mutation c.5035C>T (p. Arg1679*) and showed similar clinical features (Wang et al., 2017). In another paper, the dizygotic twins were diagnosed with febrile seizure plus (FS+), carried the c.5232G>A (p. Met1744Ile) mutation inherited from the affected father, showed similar clinical descriptions such as fever introduce, MRI normal, EEG normal, first seizure type GTCS, and seizure control except for seizure onset and further seizure type (Chen et al., 2020).

A large number of studies demonstrated the phenotypic heterogeneity of CHD2-associated epilepsy. So far, 144 patients have been reported to have epileptic seizures and associated *CHD2* variants (**Table 1** and **Supplementary Table S1**). However, not all patients with *CHD2* variants have seizures. Up to now, a total of 9 patients with *CHD2* variants were reported to have no epilepsy (Bhakta et al., 2005; Kulkarni et al., 2008; Chenier et al., 2014; Hamdan et al., 2014; Pinto et al., 2014; Chen et al., 2017; Cabrera-Salcedo et al., 2019), For example, Hamdan et al. found that a severe ID girl with motor and speech development delays and *CHD2* variant c.335C>G (p. Ser112*) did not have the history of epilepsy (Hamdan et al., 2014). Interestingly, patients without epilepsy tended to be *CHD2* CNVs patients (Bhakta et al., 2005; Kulkarni et al., 2008; Chenier et al., 2014; Hamdan et al., 2014; Pinto et al., 2014). So far, five patients carrying *CHD2* CNVs but without epilepsy have been reported. For example, Pinto et al. reported a patient with a *de novo* deletion in the *CHD2* gene, with ASD, mild ID, and dysmorphic features including micrognathia and protruding ears, but no seizures (Pinto et al., 2014). However, his ASD-affected brother carried the same deletion of the *CHD2* gene, had similar dysmorphic features and mild ID, and experienced an epilepsy onset at 9 years of age. Kulkarni et al. described a *de novo* translocation t(X; 15) (p22.2; q26.1) dn disrupting *CHD2* in a child with developmental delay, scoliosis, and hirsutism (Kulkarni et al., 2008).

According to the data, seizures in about 1/4 of patients are controlled through single or multiple anti-epileptic drugs (**Table 1** and **Supplementary Table S1**). Interestingly, the ages of seizure onset of patients who were seizures control and carried *CHD2* non-CNVs were from 1 to 12 years, and generalized tonic-clonic seizures (GTCS, 61.1%, 11/18) and myoclonic seizures (MS, 38.9%, 7/18) were the top two seizure types (**Supplementary Table S1**). However, most patients with CHD2-related neurodevelopmental disorders remain refractory to treatment. Although in some epilepsy syndromes, a ketogenic diet could have vital benefits (Daci et al., 2018; Zhou et al., 2018), a total of four patients with *CHD2* variants were treated with the ketogenic diet, which did not produce significant effects (Thomas et al., 2015; Costain et al., 2019). Therefore, a large sample size and follow-up studies would be helpful to define the treatment and prognosis of CHD2-related epilepsy.

CONCLUSION

In this study, a girl with developmental delay and myoclonic epilepsy caused by a new mutation c.4318C>T (pArg1440*) in the *CHD2* gene was studied using WES. The mutation produced a nonsense variant and disrupted the CHD2 protein structure.

Subsequently, all patients with reported neurodevelopmental disorder and variants in the *CHD2* gene were systematically reviewed and analyzed. A total of 144 patients, including 126 non-CNVs and 18 CNVs with *CHD2* pathogenic variants, were analyzed. We found that, except for *CHD2* CNV, a small portion of patients obtained *CHD2* variants by inheritance rather than *de novo*. The ages of seizure onset with *CHD2* mutants varied from infancy to childhood, even adults. The patients with *CHD2* non-CNVs had a certain tendency toward the seizure types, such as MS and GTCS. Meanwhile, not all patients with *CHD2* variants had seizures. Although almost one mutational type corresponded to one person, there may be an association between genotypes and phenotypes, especially for seizure control and fever sensitivity. The above results can provide a theoretical basis for better research on CHD2-related neurodevelopmental disorders.

DATA AVAILABILITY STATEMENT

The datasets for this article are not publicly available due to concerns regarding participant/patient anonymity. Requests to access the datasets should be directed to the corresponding author.

ETHICS STATEMENT

The studies involving human participants were reviewed and approved by the Ethical Committee of the Seventh Medical Center of PLA General Hospital. Written informed consent to participate in this study was provided by the participant's legal guardian/next of kin. Written informed consent was obtained from the individual(s), and minor(s)' legal guardian/next of kin for the publication of any potentially identifiable images or data included in this article.

AUTHOR CONTRIBUTIONS

LZ, FP, and XM conducted and designed the experiment. LZ and FP wrote the manuscript, performed the experiment, and analyzed the data. LZ and ZD collected the samples. ZF and XM were responsible for the supervision and coordination of the study process. All authors approved the final manuscript as submitted and agreed to be accountable for all aspects of the work.

FUNDING

All phases of this study were supported by the Seventh Medical Center of PLA General Hospital. This project has received funding from the National Key Research and Development Projects (2016YFC1000707), Weifang Medical College Doctoral Start Fund (2020BSQD40), and Natural Science Foundation of Shandong Province (ZR2021QH367).

ACKNOWLEDGMENTS

The authors would thank the patients for their participation in this study and the teachers for providing critical advice in data analysis.

SUPPLEMENTARY MATERIAL

The Supplementary Material for this article can be found online at: https://www.frontiersin.org/articles/10.3389/fgene.2022.761178/full#supplementary-material

REFERENCES

Bhakta, K. Y., Marlin, S. J., Shen, J. J., and Fernandes, C. J. (2005). Terminal Deletion of Chromosome 15q26.1: Case Report and Brief Literature Review. *J. Perinatol* 25, 429–432. doi:10.1038/sj.jp.7211301

Cabrera-Salcedo, C., Hawkes, C. P., Tyzinski, L., Andrew, M., Labilloy, G., Campos, D., et al. (2019). The GenomicsTargeted Searches of the Electronic Health Record and Genomics Identify an Etiology in Three Patients with Short Stature and High IGF-I Levels. *Horm. Res. Paediatr.* 92, 186–195. doi:10.1159/000504884

Carvill, G. L., Heavin, S. B., Yendle, S. C., Mcmahon, J. M., O'roak, B. J., Cook, J., et al. (2013). Targeted Resequencing in Epileptic Encephalopathies Identifies De Novo Mutations in CHD2 and SYNGAP1. *Nat. Genet.* 45, 825–830. doi:10.1038/ng.2646

Carvill, G. L., Mefford, H. C., Adam, M. P., Ardinger, H. H., Pagon, R. A., Wallace, S. E., et al. (2015). "CHD2-Related Neurodevelopmental Disorders," in *GeneReviews((R))* (Seattle (WA). [updated 2021 Jan 21]).

Chen, C.-P., Chen, C.-Y., Chern, S.-R., Wu, P.-S., Chen, S.-W., Lai, S.-T., et al. (2017). Molecular Cytogenetic Characterization of a Duplication of 15q24.2-q26.2 Associated with Anencephaly and Neural Tube Defect. *Taiwanese J. Obstet. Gynecol.* 56, 550–553. doi:10.1016/j.tjog.2017.06.003

Chen, J., Zhang, J., Liu, A., Zhang, L., Li, H., Zeng, Q., et al. (2020). CHD2 -related Epilepsy: Novel Mutations and New Phenotypes. *Dev. Med. Child. Neurol.* 62, 647–653. doi:10.1111/dmcn.14367

Chénier, S., Yoon, G., Argiropoulos, B., Lauzon, J., Laframboise, R., Ahn, J. W., et al. (2014). CHD2 Haploinsufficiency Is Associated with Developmental Delay, Intellectual Disability, Epilepsy and Neurobehavioural Problems. *J. Neurodevelop Disord.* 6, 9. doi:10.1186/1866-1955-6-9

Costain, G., Cordeiro, D., Matviychuk, D., and Mercimek-Andrews, S. (2019). Clinical Application of Targeted Next-Generation Sequencing Panels and Whole Exome Sequencing in Childhood Epilepsy. *Neuroscience* 418, 291–310. doi:10.1016/j.neuroscience.2019.08.016

Daci, A., Bozalija, A., Jashari, F., and Krasniqi, S. (2018). Individualizing Treatment Approaches for Epileptic Patients with Glucose Transporter Type1 (GLUT-1) Deficiency. *Int. J. Mol. Sci.* 19. doi:10.3390/ijms19010122

De Maria, B., Balestrini, S., Mei, D., Melani, F., Pellacani, S., Pisano, T., et al. (2021). Expanding the Genetic and Phenotypic Spectrum of CHD2-Related Disease: From Early Neurodevelopmental Disorders to Adult-Onset Epilepsy. *Am. J. Med. Genet. A.* 188 (2), 522–533. doi:10.1002/ajmg.a.62548

Epi, K. C., Allen, A. S., Berkovic, S. F., Cossette, P., Delanty, N., Dlugos, D., et al. (2013). De Novo mutations in Epileptic Encephalopathies. *Nature* 501, 217–221. doi:10.1038/nature12439

Galizia, E. C., Myers, C. T., Leu, C., De Kovel, C. G. F., Afrikanova, T., Cordero-Maldonado, M. L., et al. (2015). CHD2variants Are a Risk Factor for Photosensitivity in Epilepsy. *Brain* 138, 1198–1208. doi:10.1093/brain/awv052

Hamdan, F. F., Srour, M., Capo-Chichi, J.-M., Daoud, H., Nassif, C., Patry, L., et al. (2014). De Novo mutations in Moderate or Severe Intellectual Disability. *Plos Genet.* 10, e1004772. doi:10.1371/journal.pgen.1004772

Kulkarni, S., Nagarajan, P., Wall, J., Donovan, D. J., Donell, R. L., Ligon, A. H., et al. (2008). Disruption of Chromodomain Helicase DNA Binding Protein 2 (CHD2) Causes Scoliosis. *Am. J. Med. Genet.* 146A, 1117–1127. doi:10.1002/ajmg.a.32178

Lamar, K.-M. J., and Carvill, G. L. (2018). Chromatin Remodeling Proteins in Epilepsy: Lessons from CHD2-Associated Epilepsy. *Front. Mol. Neurosci.* 11, 208. doi:10.3389/fnmol.2018.00208

Lek, M., Karczewski, K. J., Karczewski, K. J., Minikel, E. V., Samocha, K. E., Banks, E., et al. (2016). Analysis of Protein-Coding Genetic Variation in 60,706 Humans. *Nature* 536, 285–291. doi:10.1038/nature19057

Macdonald, J. R., Ziman, R., Yuen, R. K. C., Feuk, L., and Scherer, S. W. (2014). The Database of Genomic Variants: a Curated Collection of Structural Variation in the Human Genome. *Nucl. Acids Res.* 42, D986–D992. doi:10.1093/nar/gkt958

Petersen, A. K., Streff, H., Tokita, M., and Bostwick, B. L. (2018). The First Reported Case of an Inherited Pathogenic CHD2 Variant in a Clinically Affected Mother and Daughter. *Am. J. Med. Genet.* 176, 1667–1669. doi:10.1002/ajmg.a.38835

Pinto, A. M., Bianciardi, L., Mencarelli, M. A., Imperatore, V., Di Marco, C., Furini, S., et al. (2016). Exome Sequencing Analysis in a Pair of Monozygotic Twins Re-evaluates the Genetics behind Their Intellectual Disability and Reveals a CHD2 Mutation. *Brain Dev.* 38, 590–596. doi:10.1016/j.braindev.2015.12.006

Pinto, D., Delaby, E., Merico, D., Barbosa, M., Merikangas, A., Klei, L., et al. (2014). Convergence of Genes and Cellular Pathways Dysregulated in Autism Spectrum Disorders. *Am. J. Hum. Genet.* 94, 677–694. doi:10.1016/j.ajhg.2014.03.018

Thomas, R. H., Zhang, L. M., Carvill, G. L., Archer, J. S., Heavin, S. B., Mandelstam, S. A., et al. (2015). CHD2 Myoclonic Encephalopathy Is Frequently Associated with Self-Induced Seizures. *Neurology* 84, 951–958. doi:10.1212/wnl.0000000000001305

Veredice, C., Bianco, F., Contaldo, I., Orteschi, D., Stefanini, M. C., Battaglia, D., et al. (2009). Early Onset Myoclonic Epilepsy and 15q26 Microdeletion: Observation of the First Case. *Epilepsia* 50, 1810–1815. doi:10.1111/j.1528-1167.2009.02078.x

Verhoeven, W., Egger, J., Knegt, A., Zuydam, J., and Kleefstra, T. (2016). Absence Epilepsy and the CHD2 Gene: an Adolescent Male with Moderate Intellectual Disability, Short-Lasting Psychoses, and an Interstitial Deletion in 15q26.1–q26.2. *Ndt* 12, 1135–1139. doi:10.2147/ndt.s102272

Wang, Y., Du, X., Bin, R., Yu, S., Xia, Z., Zheng, G., et al. (2017). Genetic Variants Identified from Epilepsy of Unknown Etiology in Chinese Children by Targeted Exome Sequencing. *Sci. Rep.* 7, 40319. doi:10.1038/srep40319

Zhou, P., He, N., Zhang, J.-W., Lin, Z.-J., Wang, J., Yan, L.-M., et al. (2018). Novel Mutations and Phenotypes of Epilepsy-Associated Genes in Epileptic Encephalopathies. *Genes, Brain Behav.* 17, e12456. doi:10.1111/gbb.12456

Conflict of Interest: The authors declare that the research was conducted in the absence of any commercial or financial relationships that could be construed as a potential conflict of interest.

Publisher's Note: All claims expressed in this article are solely those of the authors and do not necessarily represent those of their affiliated organizations, or those of the publisher, the editors, and the reviewers. Any product that may be evaluated in this article, or claim that may be made by its manufacturer, is not guaranteed or endorsed by the publisher.

frontiers | Frontiers in Genetics

CASE REPORT
published: 26 April 2022
doi: 10.3389/fgene.2022.845967

Case Report: DARS Mutations Responsible for Hypomyelination With Brain Stem and Spinal Cord Involvement and Leg Spasticity

Meijun Liu†, Wen Xiao†, Fang Yang, Xueqing Wang, Chao Chen, Shuoguo Jin, Ningjing Ran†, Weiyin Chen* and Dongdong Yang**

Neurology Department, Hospital of Chengdu University of Traditional Chinese Medicine, Chengdu, China

OPEN ACCESS

Edited by:
Laila Sherief,
Zagazig University, Egypt

Reviewed by:
Hasan Orhan Akman,
Columbia University Irving Medical Center, United States
Wanjin Chen,
First Affiliated Hospital of Fujian Medical University, China

***Correspondence:**
Ningjing Ran
doctoranran@outlook.com
Weiyin Chen
chenwydoctor@sina.com
Dongdong Yang
1241668186@qq.com

†These authors have contributed equally to this work

Specialty section:
This article was submitted to Genetics of Common and Rare Diseases, a section of the journal Frontiers in Genetics

Received: *30 December 2021*
Accepted: *07 April 2022*
Published: *26 April 2022*

Citation:
Liu M, Xiao W, Yang F, Wang X, Chen C, Jin S, Ran N, Chen W and Yang D (2022) Case Report: DARS Mutations Responsible for Hypomyelination With Brain Stem and Spinal Cord Involvement and Leg Spasticity. Front. Genet. 13:845967. doi: 10.3389/fgene.2022.845967

Objective: Hypomyelination with brain stem and spinal cord involvement and leg spasticity (HBSL) is a rare form of leukodystrophy presenting with varying clinical and imaging features. We report a case of HBSL to investigate the clinical and radiological characteristics of HBSL resulting from cytoplasmic aspartyl-tRNA synthetase gene (DARS) mutations.

Subjects: We report a patient of HBSL with compound heterozygous mutations in DARS1. To study the potential genetic variations of the patient, targeted next-generation sequencing, whole-exome sequencing, and Sanger sequencing were used. We reviewed the clinical and radiological features of the patient. The literature was thoroughly evaluated.

Results: The patient suffered from developmental regression associated with lower limbs spasticity, developmental delay, and paralysis of the lower limbs since childhood. Decreased T1 and increased T2 signals were observed on the bilateral basal, centrum ovale, frontal lobe, parietal lobe, and ganglia in cervical cord magnetic resonance imaging (MRI). The patient had two compound heterozygous mutations (NM_001349:c.1363T > C and NM_001349:c.821C > G) in the DARS1 gene.

Conclusion: Two mutations in DARS1 were found to be associated with HBSL, one of them being reported for the first time. These findings can be valuable for diagnosing and providing genetic counseling to HBSL patients in the future.

Keywords: posterior leukoencephalopathy sgndrome, HBSL, DARS1, mutation, case reprot

1 INTRODUCTION

HBSL was first reported in 2013 (Ryan et al., 2013) in an autosomal recessive inheritance (Mendelian Inheritance in Man (OMIM): 6,15,281). Currently, HBSL is a rarely reported condition, and the occurrence of HBSL associated with the mutation in DARS is presented in a few studies (Ryan et al., 2013; Nicole et al., 2015). One of the involved enzymes is cytosolic aspartyl-tRNA synthetase DARS (DARS-AspRS), which pairs aspartate with its corresponding tRNA, and its expression is most pronounced in brain tissue (Ryan et al., 2013). Therefore, missense mutations in the gene encoding DARS result in the occurrence of HBSL with a distinct pattern of hypomyelination, motor

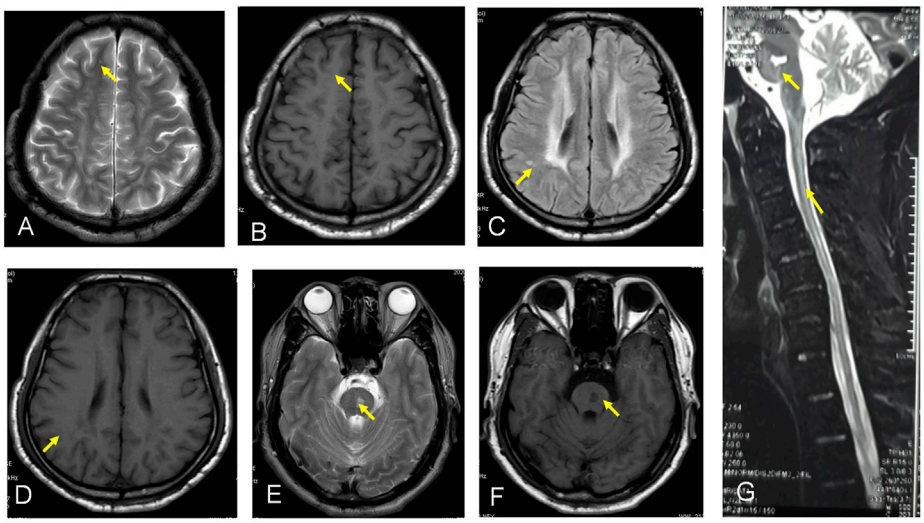

FIGURE 1 | (A–G) show the MRI by a decreased signal on the T1 sequence and increased signal intensity on the T2/FLAIR sequance showed a of the bilateral basal, certain ovale, frontal lobe, and parietal lobe, and F shows increased signal on the T2 sequence showed a of ganglia cervical cord.

abnormalities, and cognitive impairment (Zhang et al., 2018). In addition, MRI is characterized by broad symmetry high signal in T2Wimages and iso-intensity in T1W images of supratentorial white matter, brain stem, and cerebellar region. High signals in T2W images are observed in the dorsal spinal cord.

2 PATIENT AND RESULT

We report a case of HBSL in a 45-year old Han Chinese man of Sichuan Province. He had a history of normal birth and development of bilateral lower limb paralysis and delay in motor functions since 2 years of age. He complained of difficulty in walking, abnormal posture, and difficulty in standing after squatting down. By the age of 4 years, the patient could walk only with support, and by 5 years of age, he required support to stand as well. However, both the upper limbs had normal motor and cognitive functions. The patient did not receive any treatment due to poor economic background leading to a delay in diagnosis and treatment. He came for medical advice 1-year back due to progressive weakening in both upper limbs. At the time of consultation, the patient was unable to stand up, faced difficulty in raising upper limbs, and his cognitive function was deranged. On physical examination, findings were muscle strength grade 3 in both the upper limbs, hypermyotonia, hyperreflexia in bilateral upper and lower limbs (+++), positive bilateral Hoffman sign, higher muscle tension in both lower limbs, and a positive bilateral Babinski sign. Laboratory examination revealed plasma thrombin time 15.8 s, rheumatoid factor 21 IU/ml, and blood transferrin level 1.79 g/L. Routine blood test, urine test, and stool test were within normal limits. Liver and kidney function tests, electrolytes, tumor marker, and autoimmune antibody profile revealed no abnormality. An electrocardiogram showed a sinus heart rate of 69 beats per minute. The heart ultrasound showed no significant abnormalities in cardiac structure and blood flow. The electromyogram demonstrated normal right anterior tibial nerve insertion potential, incomplete light and strong contraction, the right dorsal inter bone muscle and bilateral medial femoral myoneurogenic injury, and myogenic damage. Multifocal lesions were detected on MRI by a decreased signal on the T1 sequence, increased signal intensity on the T2/FLAIR, and diffusion-weighted imaging (DWI) sequence showed a of the bilateral basal, centrum ovale, frontal lobe, and parietal lobe, and increased signal on the T2 sequence showed a of ganglia cervical cord (**Figure 1**).

Whole-exome sequencing analysis was performed using whole-exome capture with NimbleGen2.0, detecting the distribution and concentration of qPCR amplified libraries by AgilentBioanalyzer2100 and Hiseq2500 sequencing. Variant annotation was performed using the PolyPhen-2.2.2 software, ANNOVAR software, HGMD, dbSNP, and 1,000 genome database. Mutations in DARS1 detected were, c.1363T > C (p.Y455H) (of maternal origin) and c.821C > G (p.A274G). Moreover, his elder brothers and sister's mutations in DARS1 detected were c.1363T > C (p.Y455H) and c.821C > G (p.A274G). And his mother's mutations in DARS1 were detected, namely, c.1363T > C (p.Y455H). The two elder brothers and sister of the proband developed weakness of lower limbs and walking unstable, when they were teenagers. The mother of proband has no obvious clinical symptoms at present, but it couldn not rule out the possibility she has no clinical symptoms in the future. (**Figure 2**). The mutations in DARS1 of the proband and his sibings were c.1363T > C (p.Y455H) (of maternal origin) and c.821C > G (p.A274G) (of paternal origin), and his father died when he was 12 and his gene could not be detected. We speculated that the cause of his father's death was gene mutation (**Figure 2**; **Table 1**). The mutations are termed as

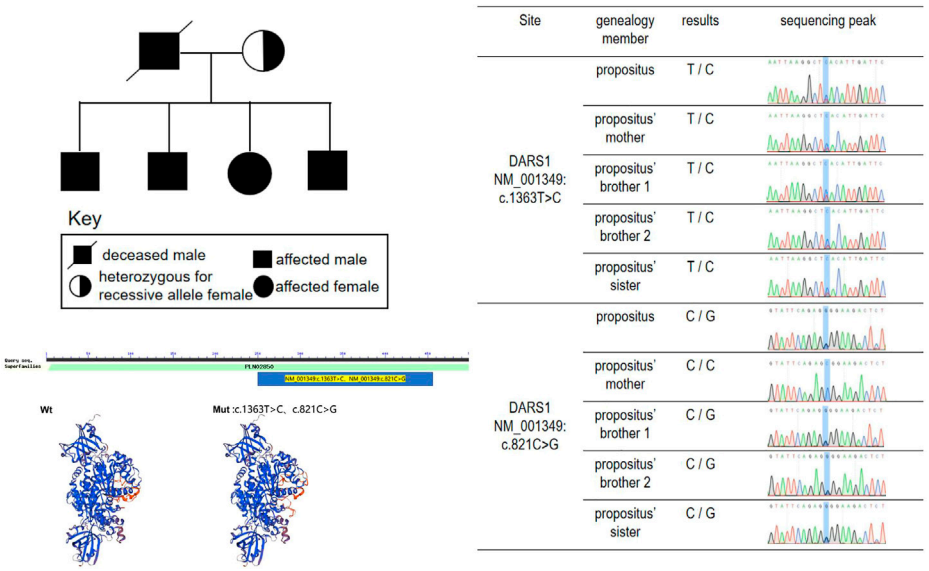

FIGURE 2 | The genetic mutation and genetic lineage map.

TABLE 1 | DARS Mutations associated of the Patient.

Genomic Position (hg19)	Nucleotide Alterations	Exon	Protein Alteration	Inheritance
chr2:136 6,68,760	NM_001349 c.1363T > C	15	p.Y455H	Maternal
chr2:136 6,78,161	NM_001349 c.821C > G	10	p.A274G	paternal

"pathogenic" and "likely pathogenic" according to the American College of Medical Genetics and Genomics (ACMG) guidelines, and a diagnosis of HBSL was made. The c.1363T > C (p.Y455H) gene was obtained from his mother.

Since HBSL is characterized by hypomyelination, the treatment is essential to promote myelin repair. The patient was prescribed vitamin B1 (Yangzhou Eddie Pharmaceutical Co., Ltd.) 10 mg orally three times a day, methylcobalamin tablets (Wei Material, China Pharmaceutical Co., Ltd.) 0.5 mg three times a day, and cytophosphate choline sodium tablets (Sichuan Zitonggong Pharmaceutical Co., Ltd.) 0.2 g three times a day for a year. On a follow-up visit after 1 year, the patient could lift heavy weight and ambulate with the support of crutches.

3 DISCUSSION

The characteristic manifestation of HBSL is that severe spasms occur in the first year of life and motor paraparesis occur, resulting in difficulty in walking independently. HBSL symptoms also include hypoevolutism in motor development, nystagmus, and cognitive developmental delays. HBSL is a rare hereditary disease, and only a few cases of infants or children with HBSL have been reported. Since this patient failed to receive medical aid in early childhood, he was diagnosed with HBSL in adulthood. At present, he is the oldest patient reported on a global scale, has a 43-years course of the disease, involving mobility of lower limbs, and upper limbs with normal cognitive function. This further reinforces the fact that the main clinical symptom of HBSL is limb paralysis and has little effect on cognitive function. The main clinical symptoms of classic early-onset HBSL are delayed motor development, progressive lower limb spasm, inability to walk, and normal cognitive function. Patients with the late-onset disease are mainly teenagers, with symptoms of dyskinesia and lower limb spasm. Before the onset of the disease, their movements, and cognitive functions are normal. MRI shows symmetric high signal intensity in T2W images in bilateral periventricular white matter. Subcortical white matter, corpus callosum, or internal capsule is not involved (Zhang et al., 2018). The disease in our patient started in early childhood, which is also evident by the radiological features matching the description of the classic early-onset HBSL.

Hypomyelination with brain stem and spinal cord involvement and leg spasticity (HBSL) is a leukodystrophy caused by missense mutations of the aspartyl-tRNA synthetase-encoding gene DARS1. Homozygous as well as compound heterozygous point mutations of the DARS gene that confer non-synonymous amino-acid substitutions to

FIGURE 3 | Sequence alignment of the DARS in different species. Comparison of the amino acid sequence show its high conversation among species. Amino acids that differ from the sequence of the insert in humans are indicated in different colors. Mutation site (N304 and N485) are marked in yellow and purple.

highly conserved residues in the catalytic domain cause the white matter disorder Hypomyelination with Brain stem and Spinal cord involvement and Leg spasticity (HBSL) (Ryan et al., 2013; Nicole et al., 2015). The mutant gene associated with HBSL is DARS, located on the 2q21.3 chromosome. The DARS gene encodes the cytoplasmic aspartyl-tRNA synthetase (Kim et al., 2013), which functions as a dimer and consists of an N-terminal anticodon recognition domain and a C-terminal catalytic domain. The mutations in tRNA synthetases can cause a broad range of neurologic disorders. It's the first time that HBLS-related mutant genes were reported by Ryan et al. They performed an investigation of DARS expression in humans and mice by using a curated set of publicly available data found that DARS is a core component of the translational machinery, and it is diffusely localized in cytoplasm and broadly expressed in the central nervous system. These data are consistent with HBSL's clinical presentation. (Ryan et al., 2013). The encoded protein is highly expressed in brain tissue, especially the cerebellum, brain stem, thalamencephalon, hippocampus, basal ganglia, and spinal cord (Dominik et al., 2017). A study on a biopsied sample of the cerebellum of a patient with HBSL has demonstrated a very high expression of the DARS gene (Dominik et al., 2018). The study of the expression of DARS in the central nervous system is crucial for the treatment of HBSL using targeted therapies. One study analyzed endogenous DARS expression on the mRNA and protein level brain and in human stem cell-derived neurons, oligodendrocytes, and astrocytes (Dominik et al., 2018). Oligodendrocyte plays an important role in myelination; hence DARS gene mutation results in the demyelination of white matter by decreasing the expression of endogenous DARS in oligodendrocytes. Gene mutations were also detected in DARS1 in this patient. The full length of DASR1 coding sequence is 1506 bp, and the protein sequence length is 501 amino acids. We found the patient's mutation position occurs at the 821st base position of the coding sequence (C-G), resulting in the amino acid changing from alanine (Ala) to glycine (Gly), in addition, at the 1363st base position of the coding sequence (T-C), resulting in the amino acid tyrosine (Tyr) becoming histidine (His). The two point mutations result in amino acid changes (**Table 1**). Sequence alignment of the DARS in different species. Comparisons of the amino acid sequence show its high conservation among species(**Figure 3**).

Data available on the treatment of HBSL at present is lacking. Mecobalamin participates in the synthesis of the myelin, which is one of the important components of the myelin sheath. Mecobalamin can improve the activity of methionine synthetase and promote the synthesis of lipid lecithin, which is one of the main structures of the myelin sheath, thereby improving the formation of the myelin sheath, promoting Schwann's cell metabolism, and repairing the damaged myelin sheath (Ma et al., 2010). Citicoline is a nucleic acid derivative that is enzymatically catalyzed to produce phosphatidylcholine, a part of the bilayer lipid membrane. Moreover, citicoline plays an important role in the synthesis of lecithin and improves nerve function by promoting the synthesis of lecithin. When the nerve cell membrane is damaged, exogenous citicoline is continuously supplemented to synthesize phosphatidylcholine, which participates in the repair of the nerve cell membrane (Jain-bo et al., 2010). Phospholipids, including phospholithin, cerebral phospholipid, and sphingolipids are one of the important components of the lipid layer and myelin sheath is composed of protein and lipid (Richard, 2002). Moreover, phosphatidylcholine and sphingolipid in the nerve cell membrane are degraded if choline is deficient, leading to cell apoptosis. Continuous supplementation of choline in exogenous cytohocholine catabolism can prevent nerve cell membrane damage and cholinergic neurodeath (Yen et al., 1999). In this case, after treatment with vitamin B1, methocobalamin, and cytophosphocholine sodium, an improvement in limb movement was observed. We conclude that mecobalamin and vitamin B1 could promote myelination and may be effective in HBSL. However, comprehensive clinical research is still needed to confirm it in the future.

DATA AVAILABILITY STATEMENT

The original contributions presented in the study are included in the article/Supplementary Material, further inquiries can be directed to the corresponding authors.

ETHICS STATEMENT

Written informed consent was obtained from the individual(s) for the publication of any potentially identifiable images or data included in this article.

AUTHOR CONTRIBUTIONS

NR, WC, and DY: conceived and designed the manuscript. XW and CC: clinical data acquisition. SJ and FY: analyzed the clinical and genetic data. ML, NR, and WX: wrote the paper. All authors contributed to the article and approved the submitted version.

ACKNOWLEDGMENTS

We would like to thank the patient, his family, the many clinicians and the clinical laboratory scientists who contributed to this research.

REFERENCES

Fröhlich, D., Suchowerska, A. K., Spencer, Z. H. T., von Jonquieres, G., Klugmann, C. B., Bongers, A., et al. (2017). *In Vivo* characterization of the Aspartyl-tRNA Synthetase DARS: Homing in on the Leukodystrophy HBSL. *Neurobiol. Dis.* 97 (Pt A), 24–35. doi:10.1016/j.nbd.2016.10.008

Fröhlich, D., Suchowerska, A. K., Voss, C., He, R., Wolvetang, E., von Jonquieres, G., et al. (2018). Expression Pattern of the Aspartyl-tRNA Synthetase DARS in the Human Brain. *Front. Mol. Neurosci.* 11, 81. doi:10.3389/fnmol.2018.00081

Jian-bo, L., Cheng-ya, W., Jia-wei, C., Xiao-lu, L., and Zhen-qing, F. (2010). The Preventive Efficacy of Methylcobalamin on Rat Peripheral Neuropathy Influenced by Diabetes via Neural IGF-1 Levels. *Nutr. Neurosci.* 13 (2), 79–86. doi:10.1179/147683010X12611460763607

Kim, K. R., Park, S. H., Kim, H. S., Rhee, K. H., Kim, B. G., Kim, D. G., et al. (2013). Crystal Structure of Human Cytosolic Aspartyl-tRNA Synthetase, a Component of Multi-tRNA Synthetase Complex. *Proteins* 81 (10), 1840–1846. doi:10.1002/prot.24306

Ma, J., Li, W., Tian, R., and Lei, W. (2010). Ginsenoside Rg1 Promotes Peripheral Nerve Regeneration in Rat Model of Nerve Crush Injury. *Neurosci. Lett.* 478 (2), 66–71. doi:10.1016/j.neulet.2010.04.064

Richard, M. Z. (2002). Membrane Stabilizer: Citicoline. *Curr. Med. Res. Opin.* 2, s14–7. doi:10.1185/030079902125000679

Taft, R. J., Vanderver, A., Leventer, R. J., Damiani, S. A., Simons, C., Grimmond, S. M., et al. (2013). Mutations in DARS Cause Hypomyelination with Brain Stem and Spinal Cord Involvement and Leg Spasticity. *Am. J. Hum. Genet.* 92 (5), 774–780. doi:10.1016/j.ajhg.2013.04.006

Wolf, N. I., Toro, C., Kister, I., Latif, K. A., Leventer, R., Pizzino, A., et al. (2015). DARS-associated Leukoencephalopathy Can Mimic a Steroid-Responsive Neuroinflammatory Disorder. *Neurology* 84 (3), 226–230. doi:10.1212/WNL.0000000000001157

Yen, C. L., Mar, M. H., and Zeisel, S. H. (1999). Choline Deficiency-Induced Apoptosis in PC12 Cells Is Associated with Diminished Membrane Phosphatidylcholine and Sphingomyelin, Accumulation of Ceramide and Diacylglycerol, and Activation of a Caspase. *FASEB J.* 13 (1), 135–142. doi:10.1096/fasebj.13.1.135

Zhang, J., Liu, M., Zhou, L., Zhang, Z. B., Wang, J. M., Jiang, Y. W., et al. (2018). DARS Mutations Responsible for Hypomyelination with Brain Stem and Spinal Cord Involvement and Leg Spasticity: Report of Two Cases and Review of Literature. *Zhonghua Er Ke Za Zhi* 56 (3), 211–215. doi:10.3760/cma.j.issn.0578-1310.2018.03.011

Conflict of Interest: The authors declare that the research was conducted in the absence of any commercial or financial relationships that could be construed as a potential conflict of interest.

Publisher's Note: All claims expressed in this article are solely those of the authors and do not necessarily represent those of their affiliated organizations, or those of the publisher, the editors and the reviewers. Any product that may be evaluated in this article, or claim that may be made by its manufacturer, is not guaranteed or endorsed by the publisher.

frontiers | Frontiers in Genetics

ORIGINAL RESEARCH
published: 26 April 2022
doi: 10.3389/fgene.2022.868942

Description of the Molecular and Phenotypic Spectrum of Lesch-Nyhan Disease in Eight Chinese Patients

Lu Li[1†], Xiaohui Qiao[2†], Fei Liu[1], Jingjing Wang[1], Huijun Shen[1], Haidong Fu[1] and Jian-Hua Mao[1]*

[1]*Department of Nephrology, Children's Hospital, National Clinical Research Center for Child Health, National Children's Regional Medical Center, Zhejiang University School of Medicine, Hangzhou, China,* [2]*Department of Nephrology, Ningbo Women and Children's Hospital, Ningbo, China*

Background: Lesch-Nyhan disease (LND) is a rare disorder involving pathogenic variants in the *HPRT1* gene encoding the enzyme hypoxanthine-guanine phosphoribosyltransferase (HGPRT) that result in hyperuricemia, intellectual disability, dystonic movement disorder, and compulsive self-mutilation. The purpose of the present study was to characterize the genetic basis of LND and describe its phenotypic heterogeneity by identifying the variation in the *HPRT1* gene in a cohort of Chinese LND patients.

Results: The median age at diagnosis was 31 mo (interquartile range (IQR): 7–76 mo), and the initial manifestations were mainly head control weakness and motor development delay. The median age of self-mutilation behavior onset was 19 mo (IQR: 17–24 mo), and all patients were required to travel in a wheelchair and fall into the predicament of compulsive self-harm behavior. There were two patients whose blood uric acid levels were normal for their high urinary acid excretion fraction without taking uric acid-lowering drugs. Seven different pathogenic variants of the *HPRT1* gene were identified among eight independent pedigrees, including four novel mutations [c.299 (exon 3) T > A; loss (exon: 6) 84 bp; c.277_281delATTGC; c.468_470delGAT]. The pathogenic variant sites were mainly concentrated in exon 3, and truncating mutations (including frameshift mutations and nonsense mutations) were the most common genetic variant types (5/7, 71.4%).

Conclusion: The present study described the phenotypic and molecular spectrum of LND in eight Chinese families, including four novel mutations, which expands our understanding of LND.

Keywords: Lesch-Nyhan disease, HPRT1 gene, self-mutilation, hyperuricemia, dystonia

OPEN ACCESS

Edited by:
Naglaa M. Kamal,
Cairo University, Egypt

Reviewed by:
H. A. (Buz) Jinnah, Emory University, United States
Lynette Fairbanks, Guy's and St Thomas' NHS Foundation Trust, United Kingdom

***Correspondence:**
Jian-Hua Mao
maojh88@zju.edu.cn

[†]These authors have contributed equally to this work

Specialty section:
This article was submitted to Genetics of Common and Rare Diseases, a section of the journal Frontiers in Genetics

Received: *03 February 2022*
Accepted: *25 March 2022*
Published: *26 April 2022*

Citation:
Li L, Qiao X, Liu F, Wang J, Shen H, Fu H and Mao J-H (2022) Description of the Molecular and Phenotypic Spectrum of Lesch-Nyhan Disease in Eight Chinese Patients. Front. Genet. 13:868942. doi: 10.3389/fgene.2022.868942

Abbreviations: BWA, Burrows–Wheeler Aligner; ESP, Exome Sequencing Project; ExAC, Exome Aggregation Consortium; GAKT, Genome Analysis Toolkit; HGMD, Human Gene Mutation Database; HGPRT, hypoxanthine-guanine phosphoribosyltransferase; IQR, interquartile range; LND, Lesch-Nyhan disease; MDT, multidisciplinary team; MRI, magnetic resonance imaging; NCBI, National Center for Biotechnology Information; OMIM, Online Mendelian Inheritance in Man; PolyPhen-2, Polymorphism Phenotyping v2; SAMe, S-adenosylmethionine; SIB, self-injurious behavior; SIFT, Scale-invariant feature transform; SNPs, single nucleotide polymorphisms; SNPs, single nucleotide polymorphisms; US, ultrasound.

INTRODUCTION

Lesch-Nyhan disease (LND: OMIM 3000322) is a rare neurogenetic disorder involving pathogenic variants in the *HPRT1* gene encoding the enzyme hypoxanthine-guanine phosphoribosyltransferase (HGPRT). The *HPRT1* gene spans ~44 kb of DNA at Xq26.2-q26.3, including 8 introns and 9 exons, encoding a total of 218 amino acids with a protein size of 24.5 kDa (Torres and Puig, 2007; Fu et al., 2014). To date, more than 600 pathogenic variants associated with LND have been identified (Nguyen et al., 2017). Deficiency of the enzyme HGPRT is usually associated with clinical evidence for overproduction of uric acid and a series of neurobehavioral problems. Patients with enzyme HGPRT activity less than 2% often have characteristic self-injurious behaviors (buccal mucosa biting, lip biting, tongue and finger biting), dystonic movement disorder, intellectual disability and hyperuricemia, namely, LND (Jinnah). The prevalence of LND is approximately 1/380,000 live births in Canada (Crawhall et al., 1972) and 1/235,000 live births in Spain (Roche et al., 2009). The life expectancy of LND patients can reach 20–40 years old under effective clinical management (Jinnah). Aspiration pneumonia and renal failure are the main causes of death (Fasullo and Endres, 2015). Patients with LND are troubled and hurt by self-injurious behaviour (SIB) (Schretlen et al., 2005). Until now, there has been no effective drug that can control SIBs, as the pathophysiology between SIBs and HGPRT deficiency is not clear (Seifert, 2016). Although reports about LND are not uncommon around the world (Puig et al., 2001; Schretlen et al., 2013; Cho et al., 2019), there are only a few single-case reports about LND in Chinese patients (Huang et al., 2018; Jian* et al., 2013; Lee et al., 1995). The present study aims to describe Chinese patients with LND with the purpose of improving knowledge of the natural history of the disease and outlining the background for future management recommendations.

MATERIALS AND METHODS

Patients and Ethical Approval

This study was approved by the Ethics Committee of Children's Hospital of Zhejiang University and followed the Declaration of Helsinki. Informed consent was obtained from the parents of the patients. A total of eight pediatric patients from eight unrelated families diagnosed with LND in the Children's Hospital of Zhejiang University School of Medicine from May 2018 to August 2021 were included in this study. LND was diagnosed according to recognized criteria: evidence of excess uric acid production, characteristic neurobehavioral phenotype, a pathogenic variant in *HPRT1* identified by molecular genetic testing and/or HGPRT enzyme activity <2% (Jinnah; Jinnah et al., 2006). Clinical features such as hyperuricemia, motor dysfunction, and SIB were retrospectively reviewed from the medical records. The assessment of the patient's renal function followed the updated Schwartz (CKiDCr) eGFR = 0.413 × L (cm)/PCr (mg/dl) (Schwartz et al., 2009).

Targeted Next-Generation Sequencing and Data Analysis

Genomic DNA was extracted from peripheral blood, and its integrity was assessed by 0.8% agarose gel electrophoresis. The whole-exome library was constructed by a Roche Nimble Gen SEQ EZ exome enrichment kit v2.0 and seq EZ exome enrichment kit v2.0 according to industrial instructions. The samples were sequenced using the Illumina NovaSeq 6,000 series sequencer (PE150) according to the standard manual. After deleting adapters, low-quality read filters, and other quality control protocols, the raw data were cleaned up. The clean data were aligned with the NCBI human reference genome (hg18) using Burrows Wheeler Aligner (BWA), and variants were called using Genome Analysis Toolkit (GATK). Samtools and Pindel were used to call single nucleotide polymorphisms (SNPs) and InDels (insertion-deletions), respectively. The clean data were then filtered according to the quality of the sequencing for further analysis. Nonsynonymous substitutions and SNPs with minor allele frequencies (MAFs) lower than 5% were filtered using Scale-invariant feature transform (SIFT). Then, the function and pathogenicity of the mutant gene were analysed referencing the dbSNP (http://www3.ncbi.nlm.nih.gov/SNP/), 1000 Genomes Project (ftp://ftp-trace.ncbi.nih.gov/1000genomes/), ExAC (https://exac.broadinstitute.org/), ESP (https://evs.gs.washington.edu/EVS/), OMIM (ncbi.nlm.nih.gov/omim/), Swiss-Var (http://swissvar.expasy.org), HGMD (http://www.hgmd.org), ClinVar (https://www.ncbi.nlm.nih.gov/clinvar/), and other disease databases. Protein structure prediction software, such as PROVEAN (http://provean.jcvi.org/index.php), SIFT (http://sift.jcvi.org/), PolyPhen-2 (http://genetics.bwh.harvard.edu/pph2/), and Mutationtaster (http://mutationtaster.org), was used to screen variants with unknown single base pathogenicity. MaxEntScan (http://genes.mit.edu/burgelab/maxent/Xmaxentscan_scoreseq.html) was used to screen potential splice sites. The classification and pathogenicity of variants were conducted according to the variant-interpretation guidelines from the American College of Medical Genetics and Genomics (AGMG) (Richards et al., 2015).

RESULTS

Clinical Characteristics

Overview

Table 1 summarizes the clinical characteristics of eight patients with LND when they were diagnosed in the present study. The median age of self-mutilation behavior onset was 19 mo (interquartile range (IQR): 17–24 mo), and the median age of diagnosis was 31 mo (IQR: 7–76 mo). Two patients were diagnosed by gene testing before the appearance of SIB. All eight patients presented baseline hypotonia, severe action dystonia and compulsive SIB. SIB mainly manifests as biting lips, buccal mucosa, tongue, and fingers. No patient showed any aggressive behavior towards other people or objects. One patient observed a seizure. There was no obvious abnormality in brain magnetic resonance imaging (MRI), except for some cases with a widening of the extracerebral space or dysmyelination. All eight

TABLE 1 | Clinical features of eight Chinese patients from eight unrelated families with LND when they are diagnosed.

Patients	P1	P2	P3	P4	P5	P6	P7	P8
Sex	M	M	M	M	M	M	M	M
Family history	–	–	–	+	–	–	–	–
Age at presentation	5 m	4 m	4 m	3 m	4 m	3 m	4 m	5 m
Age of diagnosis	151 m	42 m	6 m	76 m	7 m	96 m	20 m	12 m
Age of self-mutilation onset	36 m	17 m	14 m	36 m	21 m	24 m	17 m	17 m
Baseline hypotonia	+	+	+	+	+	+	+	+
Twisting	+	+	–	+	+	–	+	–
Spasms	+	+	+	+	+	+	+	+
Developmental delay	+	+	+	+	+	+	+	+
Self-injurious behavior	+	+	+	+	+	+	+	+
Brain MRI	Nor	ESW	Nor	Nor	ESW	ESW	Nor	DML
Epilepsy	+	–	–	–	–	–	–	–
[a]Serm uric acid (umol/L)	439	671	677	592	924	327	378	569
Renal ultrasonography	KS	UBBCM	NPC	NA	KS	Nor	Nor	KC
Blood creatinine (umol/L)	65	66	18	38	19	39	25	24
eGFR(ml/min/1.73 m2)	68.5	53	117	103	115	112	102	106
Proteinuria	–	+	–	–	–	–	–	–
Hematuria	–	–	–	–	–	–	–	–
Gouty arthritis	–	–	–	–	–	–	–	–
Megaloblastic anemia	–	+	–	–	–	–	–	–
Eating disorder	+	+	+	+	+	+	+	+
Sleep disorder	+	+	+	+	+	+	+	+
Body restraints	+	+	+	+	+	+	+	–
Dental pads	–	–	–	–	–	–	–	–

[a]Serm uric acid (μmol/L): The normal range for the plasma uric acid in male children refers to the previous literature reported[19]: <5 years 214 ± 53.6; 5–10 years 244 ± 59.5; 10–12 years 262 ± 65.5; 12–15 years 333 ± 65.5.

DML, dysmyelination; ESW, extracerebral space widened; KC, Kidney Crystal; KS, Kidney stones; M, male; Nor, normal; NPC, nephrocalcinosis; UBBCM, unclear boundary between the cortex and the medulla; eGFR, estimated glomerular filtration rate, following the updated Schwartz (CKiDCr) eGFR = 0.413 × L (cm)/PCr (mg/dl)[17].

patients had varying degrees of eating disorders (chewing and swallowing dysfunction). Megaloblastic anemia was observed in one patient. Hyperuricaemia manifested in seven patients, and two patients maintained normal blood uric acid without taking urate-lowering drugs. Three patients were found to have kidney stones or crystals at the time of diagnosis, one patient had nephrocalcinosis, and one patient showed an unclear boundary between the renal cortex and medulla at the time of diagnosis. Two patients showed varying degrees of decline in renal function, one of which was complicated with microalbuminuria. Sleep disorders (difficulty falling asleep and/or frequent waking up) plagued every patient. Seven patients needed body restraints (such as elbow restraints, gloves, and bandages) to prevent self-injury. None of the eight patients had their teeth extracted. Some patients (patients 1, 2, 4, and 6) were misdiagnosed with "cerebral palsy" before the diagnosis of LND, and patient 7 was misdiagnosed with "global developmental delay" before the symptoms of SIB.

Developmental Delay Characteristics

All eight patients denied a history of perinatal trauma and showed abnormal motor development with poor head control at the age of 3–5 months. All patients were never able to sit alone, crawl or walk and relied on a wheelchair to get around. Two patients (patient 2 and patient 8) showed regression of motor development because they were able to control their heads at the age of 3 months. All patients underwent rehabilitation for at least 6 months to 2 years, but the effect was poor.

Self-Mutilation Behavior Characteristics

Most patients have shocking and cruel SIB, mainly manifesting as biting of the lips, buccal mucosa, tongue, and fingers. The median age of SIB onset was 19 mo (IQR: 17–24 mo). S-adenosylmethionine (SAMe) (23 mg/kg.d) was administered to patient 8 for more than 3 months, while symptoms of self-injury did not improve. SIB can be aggravated when patients are nervous, unfamiliar, and sick. Often, muscle tone increases when they feel nervous and restless. As shown in **Figure 1**: Patient 1's lower lip became thinner and the tongue became shorter due to long-term SIB; patient 2's right lower lip became thinner due to his bite, and the lower central and lateral incisors were also worn away by himself; patient 6's lip became mutilated due to SIB, and the tip of his tongue was often battered by his bite; Patient 8's self-mutilation behavior was the least among all patients, and he likes to bite the oral mucosa. The parents of patients 1 and 6 reported that children with LND felt anxious and scared when the protective restraint device was removed or not properly applied.

Characteristics of Hyperuricaemia

Six patients presented with hyperuricemia at the time of diagnosis, with an average uric acid level of 580.5 μmol/L (IQR: 378–671 μmol/L). However, the blood uric acid levels of patient 6 and patient 7 were near-normal (327 μmol/L and 378 μmol/L, respectively, as shown in **Table 1**; the normal range for the plasma uric acid in male children refers to the previous literature reported (Wilcox, 1996))when they were diagnosed with LND without taking uric acid-lowering drugs.

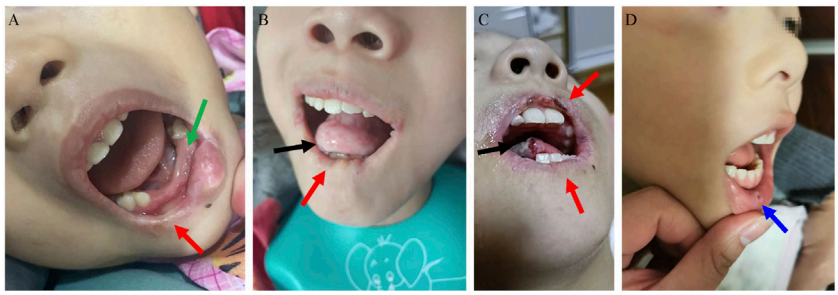

FIGURE 1 | Self-mutilation symptoms in LND. **(A)**: Patient 2's right lower lip became thinner (red arrow) due to his bite, and the lower central and lateral incisors were also worn away by himself (green arrow). **(B)**: Patient 1's lower lip became thinner (red arrow), and the tongue became shorter due to long-term self-injurious behaviour (SIB). **(C)**: Patient 6's lip became mutilated due to SIB (red arrow), and the tip of his tongue was often battered by his bite (black arrow). **(D)**: Bitting of the mucosa in patient 8 (blue arrow).

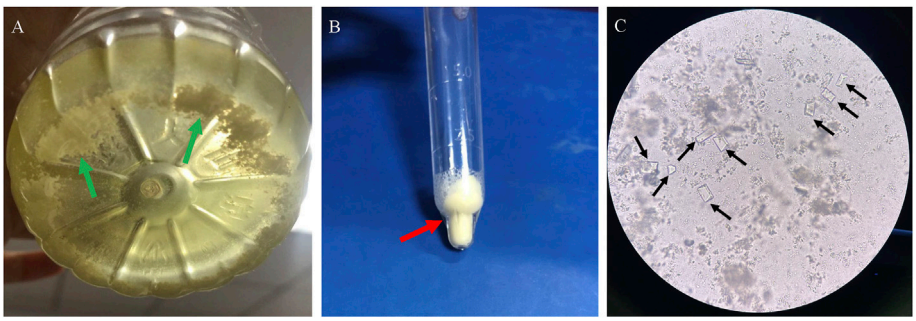

FIGURE 2 | Crystalline urine in patient 8 of LND. **(A)**: Small white crystals deposited in urine **(B)**: small crystals after centrifugal precipitation, **(C)**: microscope (×200): square columnar magnesium ammonium phosphate crystal with strong refraction (black arrow).

The ratios of urine uric acid/creatinine were 3.0 and 2.7, respectively, which suggested increased uric acid excretion. None of the eight patients had any manifestations of gouty arthritis.

Characteristics of Kidney Stones

Three patients had kidney stones or crystals (patients 1, 5, and 8) at the time of LND diagnosis. Before the diagnosis of LND in patient 1, he had a history of multiple urinary tract stones and repeated urinary tract infections, and analysis of his stone revealed that it was hydrogen urate. Although patient 5 had been taking uric acid-lowering drugs since he was 7 months old, there were still small crystals in his kidneys at the last follow-up when he was 2 years old. For patient 8, although uric acid-lowering drugs were taken in time after diagnosis, there were still small kidney stones during the 1-year follow-up. He had excreted crystalline urine twice, and microscopic examination revealed crystals of magnesium ammonium phosphate (**Figure 2**).

Characteristics of Kidney Function

Patients 1 and 2 had decreased renal function at the time of diagnosis of LND. Before the diagnosis of LND, patient 1 had a history of multiple urinary tract stones and repeated urinary tract infections. He was once subjected to percutaneous nephrolithotomy due to severe renal obstruction and infection caused by stones, and analysis of the stone composition revealed that it was hydrogen urate. His urinalysis showed that the specific gravity of urine was normal, and there was no albuminuria or microalbuminuria except for a small number of white blood cells. The ultrasound (US) examination of patient 2 showed that the kidney size was normal, the renal parenchyma echo was enhanced, the cortex and pulp boundary were unclear, and no urinary calculi were found. Urinalysis showed that α1 microglobulin and β2 microglobulin were elevated, and the specific gravity of urine was normal. The parents of both patients refused further kidney pathological examination.

Dysarthria and Dysphagia

All patients had a delay of language development and dysarthria, could only pronounce monosyllabic words and individual simple reduplicated words, and could not speak complete sentences. Usually, only their caregivers can understand their pronunciation. All eight patients had difficulty chewing and swallowing to varying degrees and could only eat a liquid diet.

Characteristics of Drugs Taken

After diagnosis, among the six patients with a high uric acid phenotype, five patients took allopurinol (2.5–8 mg/kg.d) to control uric acid. Patient 8 took febuxostat (0.25 mg/kg.d) to

TABLE 2 | Molecular analysis of the *HPRT1* gene in 8 Chinese patients from 8 unrelated families with LND.

Patient No	Mutation type	Exon	Variants	Amino acid alteration	Source	AGMG classification
1	Missense	exon3	c.212_c.213insG	p.Tyr72fsTer2	mother	LP
2	Nonsense	exon3	c.151C > T	p.R51X,168	mother	LP
3	Nonsense	exon3	c.151C > T	p.R51X,168	mother	LP
4	Missense	**exon3**	**c.299T > A**	**p.I100N**	mother	LP
5	Deletion	**exon3**	**c.277_281delATTGC**	**p.Ile93fsTyr12**	De nove	LP
6	Deletion	**exon6**	**loss**	**84 bp**	mother	LP
7	Deletion	**exon6**	**c.468_470delGAT**	**p.Lys156_Met157delinsLys**	mother	LP
8	Nonsense	exon7	c.508C > T	p.R170X,49	mother	P

Bold, novel mutations; others represent mutations that have been reported in the Human Gene Mutation Database (URL http://www.hgmd.cf.ac.uk/ac/index.php).

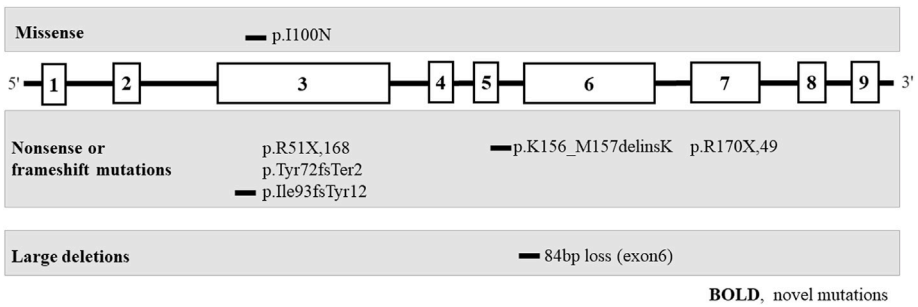

FIGURE 3 | Pathogenic variants of the *HPRT1* gene (bold, novel mutation) in eight unrelated Chinese families with Lesch-Nyhan disease. Most are private genetic variants, p. R51X,168, which were confirmed in two families.

control uric acid, and as of the last follow-up (3 years after taking febuxostat), no adverse reactions related to febuxostat were observed. Six patients took clonazepam (0.04–0.08 mg/kg.d) to stabilize mood and reduce muscle tension. S-Adenosylmethionine (SAMe, 23 mg/kg.d) was administered to patient 8 for more than 3 3 months, but symptoms of self-injury did not improve. Clonazepam was not observed to be helpful in reducing self-harm behavior. Patient 1 took estazolam (0.05 mg/kg.d) to control epilepsy. Most of them received sodium bicarbonate or sodium-potassium hydrogen citrate granules to alkalize the urine. During intermittent follow-up of 3 months to 3 years, there was no evidence that any of these drugs could improve dyskinesia or self-mutilation.

Genetics

The genetic phenotypes of the eight patients are provided in **Table 2**; **Figure 3**.

Eight different pathogenic variants in HPRT1 were identified from 8 independent pedigrees, including four novel mutations [c.299 (exon 3) T > A; loss (exon: 6) 84 bp; c.277_281delATTGC; c.468_470delGAT]. There were no evident mutational hotspots. Truncating pathogenic variants, including frameshift and nonsense mutations, were the most common (5/7, 71.4%), followed by missense mutations (1/7, 14.3%) and large deletions (1/7, 14.3%). Family screening was performed in all eight patients. Pathogenic variants in seven probands (87.5%) were inherited from their mothers, and *de novo* mutations occurred in one of eight probands (12.5%). All heterozygous females were clinically normal. Variants of unknown significance identified in Patient 1–8 were listed in **Supplementary Tables 1** to **8**.

DISCUSSION

Although it was characterized 56 years ago (Lesch and Nyhan, 1964), it is still unclear how HGPRT enzyme deficiency causes such profound neurobehavioral symptoms. As mentioned above, the disease characteristics we observed are mostly consistent with the results obtained by other countries and centers (Bertelli et al., 2004; Madeo et al., 2019). However, we are shocked by the burden of disease on patients and their families, which is what we want to emphasize. The hyperuricaemia of individual patients was ignored without standardized management and treatment. Since the emergence of SIB is age-related, the diagnosis of LND is often delayed until self-mutilation becomes evident (Nyhan, 2008). As in our study, only two patients were diagnosed before self-injurious symptoms appeared. What bothers family members most is that their children are constantly hurt by self-mutilation, and there is no effective method or medicine to help them out of the predicament. Although individuals experience pain from these behaviors, they cannot stop the behavior on their own.

Harm behavior that violates personal wishes and is beyond the control of the individual is the behavioral phenotype of LND (Torres et al., 2012). Harm behavior in LND is usually grouped

into four categories: (Torres and Puig, 2007): self-inflicted harm; (Fu et al., 2014); harm/damage to other people/objects; (Nguyen et al., 2017); harm to communication in progress; and (Jinnah) harm to activity in progress (Sebesta et al., 2008). The harmful behaviors of LND patients in our study were mainly self-inflicted harm (biting buccal mucosa, fingers, lips, and tongue). Due to the severity of SIB and its impact on quality of life, the management of SIB is necessary and challenging. Drug treatment often becomes an important part of the treatment plan. It has been reported that SAMe can improve SIBs and reduce dystonia. However, a drug clinical trial of SMAe showed that most people's behavior deteriorates (Dolcetta et al., 2013). Our study also showed that SMAe has a poor effect on improving SIB and mood. It has also been reported that risperidone has an antagonistic effect on SIBs in patients with LND (Allen and Rice, 1996), 5-hydroxytryptophan produces a significant reduction in athetoid movement and has a sedative effect in LND (Frith et al., 1976), and ecopipam may reduce the severity of SIBs in LND (Khasnavis et al., 2016). However, there is no high-quality evidence to support any drug treatment for SIBs. In nondrug therapy, pediatricians and patients' caregivers also supported tooth extraction as one of the important means to control SIB (James et al., 1989; Cotton et al., 2018), while dental experts preferred to rely on tooth protectors or lip protectors to reduce injuries (Limeres et al., 2013). Jinnah et al. suggested that rapid tooth extraction should be considered as part of the nursing standard when necessary (Goodman et al., 2014). However, in our study, 3 patients had permanent facial disfigurement, and none of the parents chose tooth extraction to control self-harm behavior. Parents were afraid of bleeding, infection, and anesthesia risks during tooth extraction. Perhaps the underlying reason was a cultural identity. In other words, tooth extraction is a big deal in Chinese, they think although it is only a small tooth, it is still a part of the body.

From birth, LND will produce too much uric acid, and hyperuricemia is a common phenomenon in LND (Torres et al., 2012), which is often overlooked because hyperuricemia may be mild. Rarely, the serum uric acid concentration can be normal (Sebesta et al., 2008). In our study, two patients (patient 6 and patient 7) had near-normal blood uric acid levels without taking uric acid-lowering drugs, and the ratio of urine uric acid/creatinine was 2.7 and 3.0, respectively. In infants and young children, increased renal clearance can effectively remove uric acid from the blood; therefore, there may be borderline hyperuricemia in *HPRT1* disorders (Torres et al., 2012). Some scholars suggest that the ratio of urine uric acid/creatinine can be used as a screening test for hereditary purine metabolism disorders based on the age of patients (Kaufman et al., 1968). The difference in the degree of hyperuricaemia in LND may be related to GLUT9 single nucleotide polymorphisms (SNPs) (Torres and Puig, 2018). The management of hyperuricemia in LND remains a clinical challenge. Allopurinol, as the first-line drug for the treatment of children with hyperuricemia, is most commonly used in patients with LND. However, there are no current consensus guidelines for the optimal dosage of allopurinol to avoid the risk of iatrogenic xanthine urolithiasis, and the recommended dosage of allopurinol starts at 5–10 mg/kg per day (Pais et al., 2006). Taking allopurinol (average dose 6.44 mg/kg/d) can reduce the serum uric acid concentration in LND by 50% (Torres et al., 2006). As a new specific xanthine oxidase inhibitor, febuxostat has a good effect of lowering uric acid and is especially suitable for patients with chronic renal insufficiency. Due to its high price and potential cardiovascular risk, the guidelines only recommend febuxostat as the first-line uric acid-lowering treatment drug for gout patients (Khanna et al., 20122012). However, there is insufficient evidence that febuxostat increases the risk of sudden cardiac death in Asian populations (White et al., 2018). Patient 8 had been taking febuxostat since the diagnosis of LND, his blood uric acid was well controlled, and no adverse reactions related to febuxostat were observed during the follow-up of 3 years. We found that both patients in our study who had decreased renal function at the time of diagnosis had a history of delayed diagnosis and treatment of hyperuricaemia. In previously published cases, the main cause of renal insufficiency seems to be attributed to urate nephropathy and acute obstructive nephropathy (Pela et al., 2008; Thumfart et al., 2016; Ambarsari et al., 2020). It has also been reported that pathogenic variants in the *HPRT1* gene lead to renal calcinosis and renal insufficiency (Vargiami et al., 2016). Whether there is a mechanism other than hyperuricemia in patients with renal insufficiency needs to be further observed and studied.

This is the first study to summarize the natural history of LND patients in mainland China. We describe four new mutations: c.299 (exon 3) T > A; loss (exon: 6) 84 bp; c.277_281delATTGC; and c.468_470delGAT. There were still some limitations in our study. First, functional analyses of novel mutations were not performed to confirm the results; second, HGPRT enzymatic testing was not performed to further improve the diagnosis; however, as recommended in GeneReviews: a male proband with suggestive clinical and laboratory findings, a hemizygous pathogenic variant in *HPRT1* identified by molecular genetic testing and/or low HGPRT enzyme activity can be diagnosed as *HPRT1* disorder (Jinnah). Four of the eight variants we reported have previously been confirmed to be LND-related pathogenic variants (Jinnah et al., 2000; Yamada et al., 2011). Among the four new mutations, there is one missense mutation and three deletion mutations, which change the type and sequence of polypeptide chain amino acids and affect the expression of the HGPRT protein. Moreover, the clinical characteristics of all patients are highly consistent with LND. Therefore, the detection of HGPRT enzyme activity is not necessary. However, commercialized HGPRT enzyme activity detection reagents are indeed conducive to clinicians' screening of suspected HPRT1 diseases and early diagnosis. Finally, our study lacks data on the intelligence and cognitive function of LND patients because most of the patients show fear and insecurity when exposed to strange environments or people, which induces aggravation of self-injurious behavior and/or unstoppable crying.

Similar to other rare diseases, the management of LND involves a multidisciplinary team (neurology, rehabilitation, oral cavity, kidney, metabolism, etc.). Although there are various multidisciplinary team (MDT) teams in most third-

class hospitals in China, the MDT team for LND has not been established in any hospital. Patients with LND often cannot be fully managed after diagnosis. Children with LND often become scared and anxious when in the hospital, and their behavior and neuromotor disorders will worsen, which makes it more difficult for doctors to evaluate and treat them. Therefore, we suggest that LND screening should be carried out in patients with intellectual disability, dystonic movement disorder and hyperuricemia, and the commercial HGPRT enzyme activity detection reagent can greatly improve the detection efficiency and reduce the screening cost. We believe that increasing public attention to LND with the help of social forces can improve the situation of LND patients, and increasing the publicity and popularization of LND among medical professionals can reduce missed diagnoses and misdiagnoses. The promotion of basic research, drug development (such as enzyme replacement therapy) and gene therapy research on LND will fundamentally change the long-term prognosis of children with LND.

CONCLUSION

With this study, we have described the phenotypic and molecular spectrum of LND in eight Chinese families, including four novel mutations, which improve the knowledge of the natural history of the disease and expand our understanding of LND, outlining the background for future management recommendations.

DATA AVAILABILITY STATEMENT

The datasets presented in this article are not readily available because data cannot be shared publicly because of patient confidentiality. Data are available from Children's Hospital of Zhejiang University Institutional Data Access/Ethics Committee (contact via zuchiec@163.com) for researchers who meet the criteria for access to confidential data. Requests to access the datasets should be directed to zuchiec@163.com.

ETHICS STATEMENT

The studies involving human participants were reviewed and approved by the Ethics Committee of the Children's Hospital of Zhejiang University School of Medicine. Written informed consent to participate in this study was provided by the participants' legal guardian/next of kin. Written informed consent was obtained from the individual(s), and minor(s)' legal guardian/next of kin, for the publication of any potentially identifiable images or data included in this article.

AUTHOR CONTRIBUTIONS

LL and XQ drafted the manuscript. LL, XQ, J-HM, JW, HS, and HF participated in data collection. J-HM and FL provided academic suggestions and revised the manuscript. LL, XQ, and J-HM were in charge of the project administration. J-HM acquired the funding. All authors reviewed the final manuscript and agreed to the published version of the manuscript.

FUNDING

This article is funded by the National Natural Science Foundation of China (Grant No. U20A20351). The funder helped in the preparation of the manuscript.

ACKNOWLEDGMENTS

The authors would like to thank "China LNS Care Home" for assisting in communicating with the families of LND patients. The authors would like to thank the patients and their parents for their kind cooperation and their contribution to this report.

SUPPLEMENTARY MATERIAL

The Supplementary Material for this article can be found online at: https://www.frontiersin.org/articles/10.3389/fgene.2022.868942/full#supplementary-material

Supplementary Table S1 | Variants of unknown significance identified in Patient 1.

Supplementary Table S2 | Variants of unknown significance identified in Patient 2.

Supplementary Table S3 | Variants of unknown significance identified in Patient 3.

Supplementary Table S4 | Variants of unknown significance identified in Patient 4.

Supplementary Table S5 | Variants of unknown significance identified in Patient 5.

Supplementary Table S6 | Variants of unknown significance identified in Patient 6.

Supplementary Table S7 | Variants of unknown significance identified in Patient 7.

Supplementary Table S8 | Variants of unknown significance identified in Patient 8.

REFERENCES

Allen, S. M., and Rice, S. N. (1996). Risperidone Antagonism of Self-Mutilation in a Lesch-Nyhan Patient. *Prog. Neuro-Psychopharmacology Biol. Psychiatry* 20 (5), 793–800. doi:10.1016/0278-5846(96)00059-0

Ambarsari, C. G., Cahyadi, D., Sari, L., Satria, O., Sahli, F., Darmadi, T. L., et al. (2020). Late Diagnosis of Lesch-Nyhan Disease Complicated with End-Stage Renal Disease and Tophi Burst: a Case Report. *Ren. Fail.* 42 (1), 113–121. doi:10.1080/0886022X.2020.1713805

Bertelli, M., Randi, D., Micheli, V., Gallo, S., Andrighetto, G., Parmigiani, P., et al. (2004). Molecular Basis of Hypoxanthine-Guanine Phosphoribosyltransferase Deficiency in Italian Lesch-Nyhan Patients: Identification of Nine Novel Mutations. *J. Inherit. Metab. Dis.* 27 (6), 767–773. doi:10.1023/B:BOLI.0000045799.78633.23

Cho, J. H., Choi, J.-H., Heo, S. H., Kim, G.-H., Yum, M.-S., Lee, B. H., et al. (2019). Phenotypic and Molecular Spectrum of Korean Patients with Lesch-Nyhan

Syndrome and Attenuated Clinical Variants. *Metab. Brain Dis.* 34 (5), 1335–1340. doi:10.1007/s11011-019-00441-0

Cotton, A. C., Bell, R. B., and Jinnah, H. A. (2018). Expert Opinion vs Patient Perspective in Treatment of Rare Disorders: Tooth Removal in Lesch-Nyhan Disease as an Example. *JIMD Rep.* 41, 25–27. doi:10.1007/8904_2017_80

Crawhall, J. C., Henderson, J. F., and Kelley, W. N. (1972). Diagnosis and Treatment of the Lesch-Nyhan Syndrome. *Pediatr. Res.* 6 (5), 504–513. doi:10.1203/00006450-197205000-00004

Dolcetta, D., Parmigiani, P., Salmaso, L., Bernardelle, R., Cesari, U., Andrighetto, G., et al. (2013). Quantitative Evaluation of the Clinical Effects ofS-Adenosylmethionine on Mood and Behavior in Lesch-Nyhan Patients. *Nucleosides, Nucleotides and Nucleic Acids* 32 (4), 174–188. doi:10.1080/15257770.2013.774012

Fasullo, M., and Endres, L. (2015). Nucleotide Salvage Deficiencies, DNA Damage and Neurodegeneration. *Ijms* 16 (5), 9431–9449. doi:10.3390/ijms16059431

Frith, C. D., Johnston, E. C., Joseph, M. H., Powell, R. J., and Watts, R. W. (1976). Double-blind Clinical Trial of 5-hydroxytryptophan in a Case of Lesch-Nyhan Syndrome. *J. Neurol. Neurosurg. Psychiatry* 39 (7), 656–662. doi:10.1136/jnnp.39.7.656

Fu, R., Ceballos-Picot, I., Torres, R. J., Larovere, L. E., Yamada, Y., Nguyen, K. V., et al. (2014). Genotype-phenotype Correlations in Neurogenetics: Lesch-Nyhan Disease as a Model Disorder. *Brain* 137 (Pt 5), 1282–1303. doi:10.1093/brain/awt202

Goodman, E. M., Torres, R. J., Puig, J. G., and Jinnah, H. A. (2014). Consequences of Delayed Dental Extraction in Lesch-Nyhan Disease. *Mov Disord. Clin. Pract.* 1 (3), 225–229. doi:10.1002/mdc3.12040

Huang, J., Zhang, C., Guo, Q., Zhang, X., Ma, L., Zhan, Y., et al. (2018). Lesch-Nyhan Syndrome in a Chinese Family with Mutation in the Hypoxanthine-Guanine Phosphoribosyltransferase Gene. *Clin. Lab.* 64 (1), 197–200. doi:10.7754/Clin.Lab.2017.170813

James, P., Vorherr, T., Krebs, J., Morelli, A., Castello, G., McCormick, D. J., et al. (1989). Modulation of Erythrocyte Ca2+-ATPase by Selective Calpain Cleavage of the Calmodulin-Binding Domain. *J. Biol. Chem.* 264 (14), 8289–8296. doi:10.1016/s0021-9258(18)83181-7

Jian*, W.-X., Peng*, W.-H., Li, H.-L., Feng, Q.-W., Wang, W.-X., and Su, Q. (2013). Molecular Characterization and Structure Analysis of HPRT in a Chinese Patient with Lesch-Nyhan Disease. *Nucleosides, Nucleotides and Nucleic Acids* 32 (4), 189–195. doi:10.1080/15257770.2013.774013

Jinnah, H. A. *HPRT1 Disorders Synonyms: HGprt Deficiency, HPRT Deficiency, Hypoxanthine-Guanine Phosphoribosyltransferase Deficiency*.

Jinnah, H. A., De Gregorio, L., Harris, J. C., Nyhan, W. L., and O'Neill, J. P. (2000). The Spectrum of Inherited Mutations Causing HPRT Deficiency: 75 New Cases and a Review of 196 Previously Reported Cases. *Mutat. Research/Reviews Mutat. Res.* 463 (3), 309–326. doi:10.1016/s1383-5742(00)00052-1

Jinnah, H. A., Visser, J. E., Harris, J. C., Verdu, A., Larovere, L., Ceballos-Picot, I., et al. (2006). Delineation of the Motor Disorder of Lesch-Nyhan Disease. *Brain* 129 (Pt 5), 1201–1217. doi:10.1093/brain/awl056

Kaufman, J. M., Greene, M. L., and Seegmiller, J. E. (1968). Urine Uric Acid to Creatinine Ratio-A Screening Test for Inherited Disorders of Purine Metabolism. *J. Pediatr.* 73 (4), 583–592. doi:10.1016/s0022-3476(68)80274-4

Khanna, D., Fitzgerald, J. D., Khanna, P. P., Bae, S., Singh, M. K., Neogi, T., et al. (20122012). 2012 American College of Rheumatology Guidelines for Management of Gout. Part 1: Systematic Nonpharmacologic and Pharmacologic Therapeutic Approaches to Hyperuricemia. *Arthritis Care Res.* 64 (10), 1431–1446. doi:10.1002/acr.21772

Khasnavis, T., Reiner, G., Sommerfeld, B., Nyhan, W. L., Chipkin, R., and Jinnah, H. A. (2016). A Clinical Trial of Safety and Tolerability for the Selective Dopamine D1 Receptor Antagonist Ecopipam in Patients with Lesch-Nyhan Disease. *Mol. Genet. Metab.* 117 (4), 401–406. doi:10.1016/j.ymgme.2016.02.005

Lee, W. J., Lee, H. M., Chi, C. S., Yang, M. T., Lin, H. Y., and Lin, W. H. (1995). Genetic Analysis of the HPRT Mutation of Lesch-Nyhan Syndrome in a Chinese Family. *Zhonghua Yi Xue Za Zhi (Taipei)* 56 (6), 359–366.

Lesch, M., and Nyhan, W. L. (1964). A Familial Disorder of Uric Acid Metabolism and Central Nervous System Function. *Am. J. Med.* 36, 561–570. doi:10.1016/0002-9343(64)90104-4

Limeres, J., Feijoo, J. F., Baluja, F., Seoane, J. M., Diniz, M., and Diz, P. (2013). Oral Self-Injury. An Update. *Dent Traumatol.* 29 (1), 8–14. doi:10.1111/j.1600-9657.2012.01121.x

Madeo, A., Di Rocco, M., Brassier, A., Bahi-Buisson, N., De Lonlay, P., and Ceballos-Picot, I. (2019). Clinical, Biochemical and Genetic Characteristics of a Cohort of 101 French and Italian Patients with HPRT Deficiency. *Mol. Genet. Metab.* 127 (2), 147–157. doi:10.1016/j.ymgme.2019.06.001

Nguyen, K. V., Naviaux, R. K., and Nyhan, W. L. (2017). Novel Mutation in the Human HPRT1 Gene and the Lesch-Nyhan Disease. *Nucleosides, Nucleotides and Nucleic Acids* 36 (11), 704–711. doi:10.1080/15257770.2017.1395037

Nyhan, W. L. (2008). Lesch-Nyhan Disease. *Nucleosides, Nucleotides and Nucleic Acids* 27 (6), 559–563. doi:10.1080/15257770802135745

Pais, V. M., Jr., Lowe, G., Lallas, C. D., Preminger, G. M., and Assimos, D. G. (2006). Xanthine Urolithiasis. *Urology* 67 (5), e9–1084. doi:10.1016/j.urology.2005.10.057

Pela, I., Donati, M. A., Procopio, E., and Fiorini, P. (2008). Lesch-Nyhan Syndrome Presenting with Acute Renal Failure in a 3-Day-Old Newborn. *Pediatr. Nephrol.* 23 (1), 155–158. doi:10.1007/s00467-007-0588-x

Puig, J. G., Torres, R. J., Mateos, F. A., Ramos, T. H., Arcas, J. M., Buño, A. S., et al. (2001). The Spectrum of Hypoxanthine-Guanine Phosphoribosyltransferase (HPRT) Deficiency. *Medicine* 80 (2), 102–112. doi:10.1097/00005792-200103000-00003

Richards, S., Aziz, N., Bale, S., Bick, D., Das, S., Gastier-Foster, J., et al. (2015). Standards and Guidelines for the Interpretation of Sequence Variants: a Joint Consensus Recommendation of the American College of Medical Genetics and Genomics and the Association for Molecular Pathology. *Genet. Med.* 17 (5), 405–424. doi:10.1038/gim.2015.30

Roche, A., Pérez-Dueñas, B., Camacho, J. A., Torres, R. J., Puig, J. G., García-Cazorla, A., et al. (2009). Efficacy of Rasburicase in Hyperuricemia Secondary to Lesch-Nyhan Syndrome. *Am. J. Kidney Dis.* 53 (4), 677–680. doi:10.1053/j.ajkd.2008.09.011

Schretlen, D. J., Varvaris, M., Ho, T. E., Vannorsdall, T. D., Gordon, B., Harris, J. C., et al. (2013). Regional Brain Volume Abnormalities in Lesch-Nyhan Disease and its Variants: a Cross-Sectional Study. *Lancet Neurol.* 12 (12), 1151–1158. doi:10.1016/s1474-4422(13)70238-2

Schretlen, D. J., Ward, J., Meyer, S. M., Yun, J., Puig, J. G., Nyhan, W. L., et al. (2005). Behavioral Aspects of Lesch-Nyhan Disease and its Variants. *Dev. Med. Child. Neurol.* 47 (10), 673–677. doi:10.1017/S0012162205001374

Schwartz, G. J., Muñoz, A., Schneider, M. F., Mak, R. H., Kaskel, F., Warady, B. A., et al. (2009). New Equations to Estimate GFR in Children with CKD. *Jasn* 20 (3), 629–637. doi:10.1681/ASN.2008030287

Sebesta, I., StibÅrková, B., Dvorakova, L., Hrebicek, M., Minks, J., Stolnaja, L., et al. (2008). Unusual Presentation of Kelley-Seegmiller Syndrome. *Nucleosides, Nucleotides and Nucleic Acids* 27 (6), 648–655. doi:10.1080/15257770802143863

Seifert, R. (2016). Towards Rational Drug Treatment of Lesch-Nyhan Disease. *Mol. Genet. Metab.* 118 (3), 145–146. doi:10.1016/j.ymgme.2016.05.004

Thumfart, J., Weschke, B., Ringe, H., Weinhold, N., and Müller, D. (2016). Acute Renal Failure Unmasking Lesch-Nyhan Disease in a Patient with Tuberous Sclerosis Complex. *Eur. J. Paediatric Neurol.* 20 (4), 649–651. doi:10.1016/j.ejpn.2016.04.014

Torres, R. J., Prior, C., and Puig, J. G. (2006). Efficacy and Safety of Allopurinol in Patients with the Lesch-Nyhan Syndrome and Partial Hypoxanthine-Phosphoribosyltransferase Deficiency: a Follow-Up Study of 18 Spanish Patients. *Nucleosides, Nucleotides and Nucleic Acids* 25 (9-11), 1077–1082. doi:10.1080/15257770600893974

Torres, R. J., and Puig, J. G. (2018). GLUT9 Influences Uric Acid Concentration in Patients with Lesch-Nyhan Disease. *Int. J. Rheum. Dis.* 21 (6), 1270–1276. doi:10.1111/1756-185X.13323

Torres, R. J., and Puig, J. G. (2007). Hypoxanthine-guanine Phosophoribosyltransferase (HPRT) Deficiency: Lesch-Nyhan Syndrome. *Orphanet J. Rare Dis.* 2, 48. doi:10.1186/1750-1172-2-48

Torres, R. J., Puig, J. G., and Jinnah, H. A. (2012). Update on the Phenotypic Spectrum of Lesch-Nyhan Disease and its Attenuated Variants. *Curr. Rheumatol. Rep.* 14 (2), 189–194. doi:10.1007/s11926-011-0231-5

Vargiami, E., Printza, N., Papadimiditriou, E., Batzios, S., Kyriazi, M., Papachristou, F., et al. (2016). Nephrocalcinosis and Renal Failure in Lesch-Nyhan Syndrome: Report of Two Familial Cases and Review of the Literature. *Urology* 97, 194–196. doi:10.1016/j.urology.2016.04.004

White, W. B., Saag, K. G., Becker, M. A., Borer, J. S., Gorelick, P. B., Whelton, A., et al. (2018). Cardiovascular Safety of Febuxostat or Allopurinol in Patients with Gout. *N. Engl. J. Med.* 378 (13), 1200–1210. doi:10.1056/NEJMoa1710895

Wilcox, W. D. (1996). Abnormal Serum Uric Acid Levels in Children. *J. Pediatr.* 128 (6), 731–741. doi:10.1016/s0022-3476(96)70322-0

Yamada, Y., Wakamatsu, N., Taniguchi, A., Kaneko, K., and Fujimori, S. (2011). Hypoxanthine Guanine Phosphoribosyltransferase (HPRT) Mutations in the Asian Population. *Nucleosides, Nucleotides and Nucleic Acids* 30 (12), 1248–1255. doi:10.1080/15257770.2011.603714

Conflict of Interest: The authors declare that the research was conducted in the absence of any commercial or financial relationships that could be construed as a potential conflict of interest.

Publisher's Note: All claims expressed in this article are solely those of the authors and do not necessarily represent those of their affiliated organizations, or those of the publisher, the editors and the reviewers. Any product that may be evaluated in this article, or claim that may be made by its manufacturer, is not guaranteed or endorsed by the publisher.

frontiers | Frontiers in Genetics

CASE REPORT
published: 18 May 2022
doi: 10.3389/fgene.2022.847397

Case Report: Adolescent-Onset Isolated Nephronophthisis Caused by a Novel Homozygous Inversin Mutation

Zhengxia Zhong[1], Xiaoyong Yan[1], Zhengying Fang[2], Yijun Dong[1], Jiaxing Tan[3], Jingyuan Xie[2], Linhong Hu[1], Shibin Zhang[4]* and Wei Qin[3]*

[1]Division of Nephrology, Department of Medicine, Affiliated Hospital of Zunyi Medical University, Zunyi, China, [2]Department of Nephrology, Shanghai Ruijin Hospital, Shanghai Jiao Tong University School of Medicine, Shanghai, China, [3]Division of Nephrology, Department of Medicine, West China Hospital, Sichuan University, Chengdu, China, [4]Laboratory Animal Centers, Zunyi Medical University, Zunyi, China

OPEN ACCESS

Edited by:
Naglaa M. Kamal,
Cairo University, Egypt

Reviewed by:
Priyanka Upadhyai,
Manipal Academy of Higher Education, India
Yuki Hitomi,
National Center For Global Health and Medicine, Japan

***Correspondence:**
Zhengxia Zhong
snkzzx1002@163.com
Shibin Zhang
574610922@qq.com

Specialty section:
This article was submitted to Genetics of Common and Rare Diseases, a section of the journal Frontiers in Genetics

Received: 02 January 2022
Accepted: 07 April 2022
Published: 18 May 2022

Citation:
Zhong Z, Yan X, Fang Z, Dong Y, Tan J, Xie J, Hu L, Zhang S and Qin W (2022) Case Report: Adolescent-Onset Isolated Nephronophthisis Caused by a Novel Homozygous Inversin Mutation. Front. Genet. 13:847397. doi: 10.3389/fgene.2022.847397

Objective: Nephronophthisis (NPHP) is a rare autosomal recessive inherited kidney disease that can cause cystic enlargement of the kidneys, and lead to end-stage renal disease (ESRD) before the age of 30 years. Herein we describe a case of adolescent-onset NPHP with a novel homozygous mutation in the inversin gene (*INVS*).

Methods: The patient was a 15-year-old Chinese boy who presented with ESRD. Genetic testing was performed via whole exome sequencing and validated *via* Sanger sequencing. A novel homozygous *INVS* mutation was identified (c. 1909C > T; p. Gln637Ter).

Results: The results of laboratory examinations included urinary protein 1.05 g/24 h, urine erythrocyte count 5/high-power field, serum creatinine 1,026.2 μmol/L, and estimated glomerular filtration rate 5.8 ml/min/1.73 mm^2. Extrarenal features included hypertension and moderate anemia, and his parents were consanguineous (first cousins). A homozygous 1-bp substitution resulting in a nonsense mutation (c. 1909C > T; p. Gln637Ter) in exon 15 of *INVS* was detected via whole exome sequencing, and validated via Sanger sequencing. According to the classification system of the American College of Medical Genetics and Genomics, the mutated gene in *INVS* is strongly pathogenic (PVS1+PM2+*P*P3+*P*P5). His parents and a younger brother were heterozygous carriers. Based on the above results he was diagnosed with juvenile type 2 NPHP. He underwent hemodialysis, and received a kidney transplant after 2 months. He is currently recovering well, with a serum creatinine level of 117 μmol/L and an estimated glomerular filtration rate of 79.6 ml/min/1.73 mm^2.

Conclusion: Here we have described an extremely rare case of adolescent-onset type 2 NPHP caused by a homozygous *INVS* mutation. The patient had progressed to ESRD by the age of 15 years. The current report will deepen our understanding of the clinical and genetic basis of this disease.

Keywords: adolescent-onset, homozygous mutation, INVs, NPHP2, ESRD

INTRODUCTION

Nephronophthisis (NPHP) is an extremely rare autosomal recessive kidney disease characterized by renal tubulointerstitial lesions, tubular basement membrane disruption, and renal cyst formation that progresses to end-stage renal disease (ESRD) in children (Otto et al., 2003). In addition to renal symptoms NPHP is often complicated with diverse extrarenal features, and approximately 20% of patients suffer from ciliopathy syndrome, including retinal degeneration, bone abnormalities, and liver fibrosis (Srivastava et al., 2017). Genetic studies have identified more than 20 genes that are causally associated with NPHP in humans. Juvenile type I NPHP (NPHP1) is most commonly caused by homozygous pathogenic variants in *NPHP1*, which encodes an SH3 domain protein (Hildebrandt et al., 1997a; Otto et al., 2008). Type 2 NPHP (NPHP2) has also been identified in patients with infantile NPHP, and is distinguished from other types of NPHP by an early age of onset and cystic enlargement of the kidneys. O'Toole et al. (2006) first reported *NPHP2* mutation in a 2-year-old Arab boy with retinitis degeneration and kidney failure. Here in we report the novel *INVS* mutation p. Gln637Ter in an adolescent patient with NPHP2.

CASE

A 15-year-old Chinese boy who had been experiencing headache and vomiting for 1 week was admitted to the hospital (IV-2 in **Figure 1**). Ophthalmic examination did not reveal any obvious abnormalities, there were no neurological symptoms, and he did not exhibit short stature. His clinical symptoms were sudden and severe, and mainly manifested as hypertension and severe kidney failure. His blood pressure was 170/123 mmHg, his serum creatinine level was 1,026.2 μmol/L, and no prior symptoms were reported. His parents were consanguineous (first cousins), and his older brother had succumbed to an undiagnosed kidney disease at 8 years of age, without a kidney biopsy. The current patient was initially admitted to our medical center on 21 May 2021.

Ultrasonography depicted small kidneys and diffuse lesions (85–90 mm in diameter) in both kidneys, but no cystic enlargement of the kidneys. Laboratory tests revealed a hemoglobin level of 67 g/L and a urinary protein level of 1.05 g/24 h. Chest computed tomography was normal. Laboratory investigations on admission included screening for hepatitis B virus surface antigen, antinuclear antibodies, anti-double-stranded DNA antibodies, anti-glomerular basement membrane antibodies, and anti-neutrophil cytoplasmic antibodies, all of which were negative. The patient was started on hemodialysis. Fortunately he received a kidney transplant after 2 months of dialysis. He is currently recovering well, with a serum creatinine level of 117 μmol/L and an estimated glomerular filtration rate of 79.6 ml/min/1.73 mm^2. Whole exome sequencing was performed to further investigate the cause of his illness, and segregation was validated via Sanger sequencing in him and his family. Written informed consent was obtained from all family members.

METHODS

Blood samples were collected and DNA was extracted via a DNeasy Blood Kit (Qiagen, catalogue number 69504). DNA of the human exon region was highly enriched via an Agilent SureSelectHuman All ExonV6 Kit, and whole exome sequencing was performed using the Illumina platform. Sanger sequencing was then used to validate the exome sequencing results, and the loci of variation were analyzed in accordance with the standards and guidelines for the interpretation of genetic variants developed by the American College of Medical Genetics and Genomics in 2015 (Richards et al., 2015).

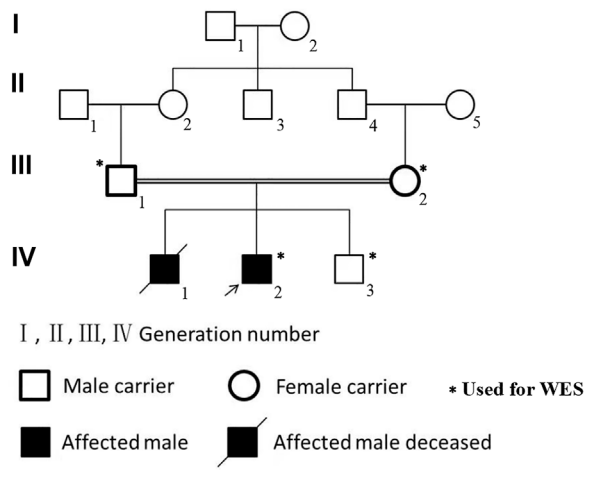

FIGURE 1 | The pedigree of the family with NPHP2/INVS mutation (c.1909C > T) in the exon 15. Affected brothers of INVS mutation are represented by black symbols. Males are represented by squares, and females are represented by round symbols. Crossed symbols represent deceased individuals.

TABLE 1 | Clinical characteristics of the patient and his family.

Parameter	Proband	Father	Mother	Brother
Age (years)	15	50	48	12
Height (cm)	173	165	155	140
Hemoglobin (g/L)	69	151	143	139
Serum albumin (g/L)	42.1	38.9	43.9	47
Scr (μmol/L)	1,026.2	79	69	57
eGFR (mL/min/1.73 $m^{2)}$	5.8	99.5	89.8	148.6
Uric acid (mmol/L)	382	335	207	298
Urine protein (g/24 h)	1.05	0.10	0.09	0.05
U-RBC (/HPF)	5	0	0	0

Scr, serum creatinine; eGFR, estimated glomerular filtration rate; U-RBC/HPF, red blood cell per high power field in urine.

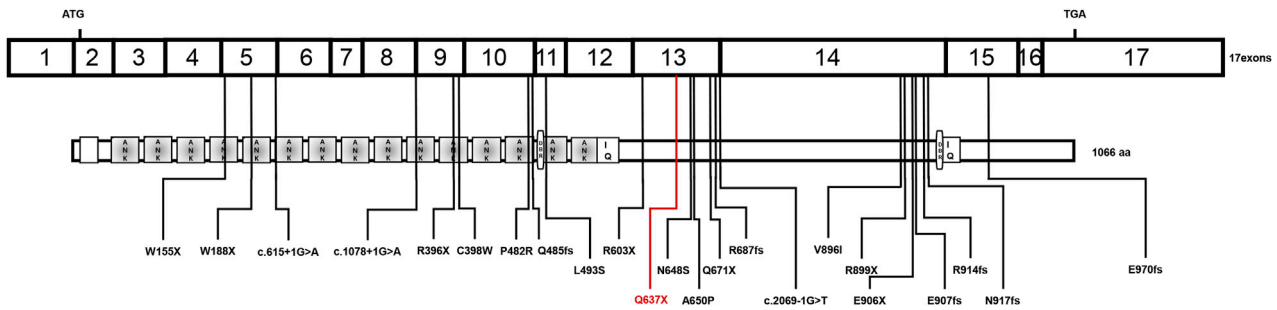

FIGURE 2 | Schematic diagram of the reported INVS mutations. ANK: ankyrin repeats, IQ: IQ calmodulin-binding domains, DBR: destruction box regions.

RESULTS

Laboratory results included urinary protein 1.05 g/24 h, urine erythrocyte count 5/high-power field, serum creatinine 1,026.2 μmol/L, and an estimated glomerular filtration rate of 5.8 ml/min/1.73 mm^2. Extrarenal features mainly manifested as hypertension and moderate anemia. His parents (III-1 and III-2 in **Figure 1**) and younger brother (IV-3 in **Figure 1**) were in good health, and the results of their medical examinations were normal (**Table 1**). Mutational analysis of the inversin gene (*INVS*) identified a homozygous mutation in exon 15:c.1909C > T, with a predicted coding sequence change of p. Gln637Ter. A cytosine to thymidine substitution at nucleotide 1909 is predicted to result in glutamine at amino acid 637 being replaced by a stop codon, prematurely terminating the protein (**Figure 2**). According to the classification system of the American College of Medical Genetics and Genomics the *INVS* mutation identified is strongly pathogenic (PVS1+PM2+*p*P3+*p*P5). The presence of this mutation was then assessed in his immediate family members by sequencing the corresponding site via the Sanger method. The patient's father, mother, and a younger brother were heterozygous carriers of the same mutation, indicating that it resulted in ESRD in the patient, and originated from his parents who were first cousins (**Figure 3**). This novel variant has not been reported in the Human Gene Mutation Database or ClinVar before.

DISCUSSION

NPHP is an uncommon autosomal recessive renal tubular interstitial disease known to cause renal ciliopathy. It is divided into infantile, juvenile, and adolescent forms based on respective median ages of onset and progression to ESRD of 1, 13, and 19 years. It is reportedly a common genetic condition that leads to ESRD in children and adolescents at the early stage of disease, characterized by polyuria, polydipsia, and anemia (Hildebrandt et al., 2009). Molecular genetic studies have identified more than 20 different *NPHP* genes that cause NPHP (Luo and Tao, 2018; Srivastava et al., 2018). To date the prevalence of NPHP with renal failure has not been thoroughly evaluated. Data from countries other than China indicate an incidence of approximately 1 per 20 million members of the population (König et al., 2017). *NPHP1* causes the most common form, accounting for approximately 20% of cases (Hildebrandt et al., 1997b), but the incidence rate of NPHP in China has not been reported. The clinical features of NPHP can be complex and nonspecific, and they can include growth retardation and anemia followed by progressive deterioration of kidney function. Histological kidney pathology typically includes basement membrane splitting and thickening of renal tubules, and interstitial fibrosis or interstitial cell infiltration.

The current patient was a 15-year-old child who presented with classical symptoms including headache, hypertension, anemia, and renal failure accompanied by ESRD. A novel homozygous pathogenic variant c.1909C > T in exon 15 of *INVS* was detected that is predicted to cause premature truncation of the inversin protein. Ultrasonography of the kidneys revealed hyperechogenic diffuse lesions, and the kidneys were shrunken. Clinically, the opportunity for renal pathological biopsy had been lost, so it was difficult to identify the etiology of his condition. Considering the consanguineous marriage of his parents, and that his older brother had died of ESRD, exome sequencing was performed in his entire immediate family. A novel and strongly pathogenic mutation was identified in the *INVS* gene, which may be associated with the ESRD in this patient. Inversin, the protein defective in NPHP2 patients, localizes to the primary cilia of renal epithelial cells and has been identified in patients with the infantile form of NPHP (Eley et al., 2004). Currently little is known about its specificity and potential interactions. Tory et al. (Tory et al., 2009) described five *NPHP2* mutations that were recurrent in unrelated families, and the frequency of *INVS* mutations is reportedly up to 78% in patients who develop ESRD before 2 years of age. There are previous reports of patients with homozygous *INVS* mutations who developed renal failure before 5 years of age (Otto et al., 2008; O'Toole et al., 2006). Bellavia et al. (Bellavia et al., 2010) also described a patient with an *INVS* mutation who developed ESRD at the age of 11. Previous studies have demonstrated that *NPHP2* mutations can cause ESRD, mainly the infantile-onset NPHP2 form. The age at which previously described patients progressed to ESRD differed from that of the current patient. The novel homozygous gene mutation identified in the current Chinese

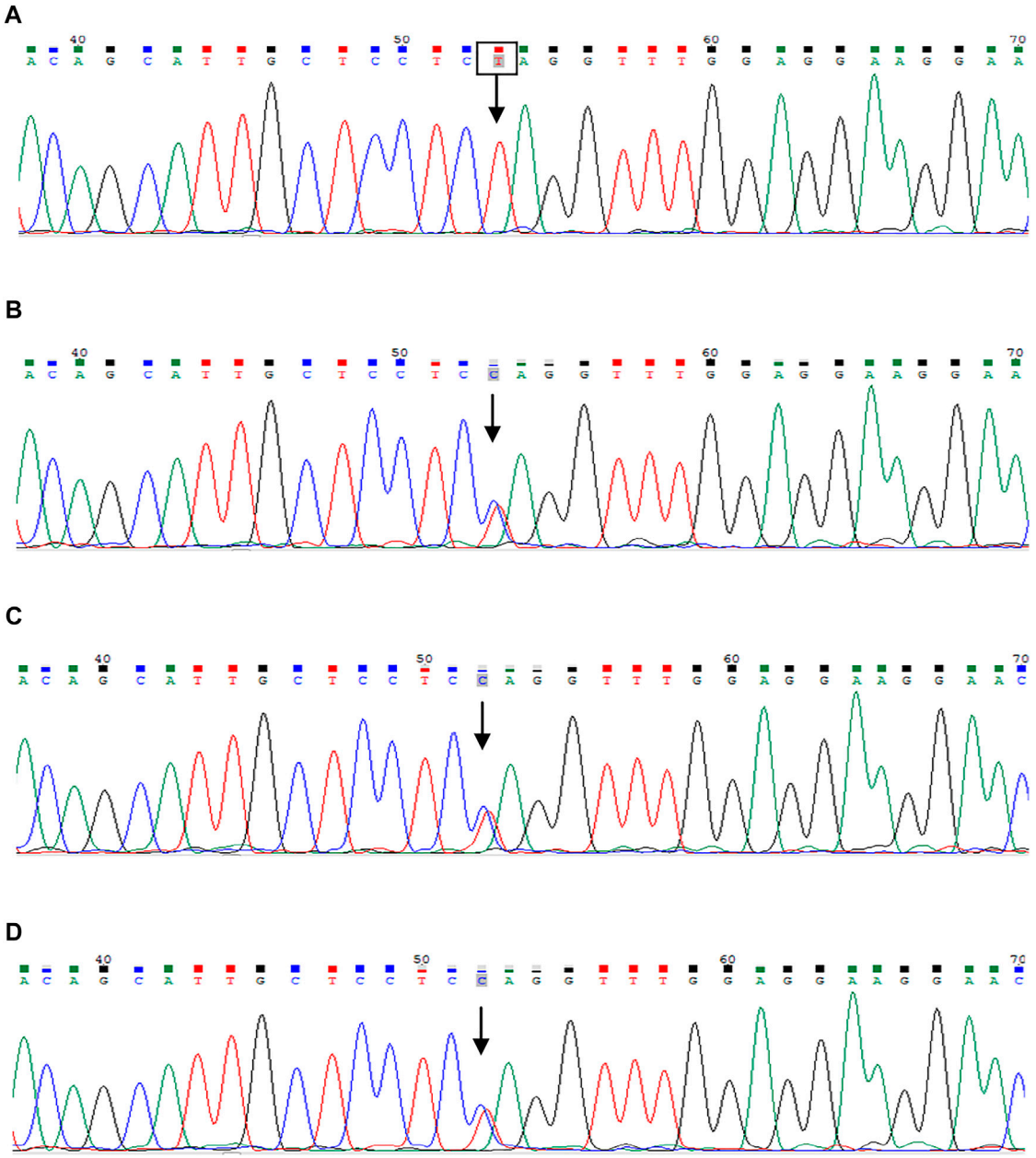

FIGURE 3 | Sanger sequencing of the INVS gene. The patient was identified with 1-bp substitution; **(C)** C1909T, NM_001318382, Chr9:103059299 **(A)**. His parents and younger brother are heterozygous carriers **(B–D)**, and the arrows show the position of the mutation.

patient with the adolescent form of NPHP2 has not been previously reported, thus this report adds to the *NPHP2* variation spectrum.

There is currently a lack of effective therapy for NPHP2, so close long-term follow-up and supportive care strategies focused on attenuating the progression of renal impairment are generally utilized, sometimes in conjunction with alternative therapies. Kidney transplantation is preferred over replacement therapy when NPHP2 develops to ESRD. NPHP2 is a rare genetically heterogeneous disease accompanied by insidious clinical features and nonspecific manifestations, and it is easily misdiagnosed. Most patients have progressed to stage 5 chronic kidney disease by the time NPHP is diagnosed, and a kidney biopsy is not feasible due to the small size of the kidneys. It is thus very important to acquire family history, growth history, and other information for the diagnosis of NPHP. The possibility of undescribed pathogenic genes should also be fully considered in younger patients presenting with kidney disease.

The present case demonstrates that the clinical diagnosis of atypical NPHP2 is difficult. We have reported the first severe phenotype in a Chinese NPHP2 patient with

adolescent-onset ESRD, and a novel *INVS* mutation was detected via whole exome sequencing. The case serves as a reminder to clinicians that precise medical genetic diagnostics are needed in cases of strongly suspected genetic diseases, especially in patients with a family history of consanguineous marriage.

DATA AVAILABILITY STATEMENT

The original contributions presented in the study are included in the article/Supplementary Material, further inquiries can be directed to the corresponding authors.

ETHICS STATEMENT

Written informed consent was obtained from the individual(s) for the publication of any potentially identifiable images or data included in this article.

AUTHOR CONTRIBUTIONS

JX, XY and QW designed the study and critically revised the work. ZZ and SZ performed the experiments, collected the data, and wrote the manuscript. ZZ, JT, ZF and SZ performed the statistical analyses. YD and LH collected blood samples. All authors have read and approved the final manuscript.

REFERENCES

Bellavia, S., Dahan, K., Terryn, S., Cosyns, J.-P., Devuyst, O., and Pirson, Y. (2010). A Homozygous Mutation in INVS Causing Juvenile Nephronophthisis with Abnormal Reactivity of the Wnt/beta-Catenin Pathway. *Nephrol. Dial. Transpl.* 25, 4097–4102. doi:10.1093/ndt/gfq519

Eley, L., Turnpenny, L., Yates, L. M., Craighead, A. S., Morgan, D., Whistler, C., et al. (2004). A Perspective on Inversin. *Cell Biol Int* 28, 119–124. doi:10.1016/j.cellbi.2003.11.009

Hildebrandt, F., Attanasio, M., and Otto, E. (2009). Nephronophthisis: Disease Mechanisms of a Ciliopathy. *Jasn* 20, 23–35. doi:10.1681/asn.2008050456

Hildebrandt, F., Otto, E., Rensing, C., Nothwang, H. G., Vollmer, M., Adolphs, J., et al. (1997). A Novel Gene Encoding an SH3 Domain Protein Is Mutated in Nephronophthisis Type 1. *Nat. Genet.* 17, 149–153. doi:10.1038/ng1097-149

Hildebrandt, F., Strahm, B., Nothwang, H.-G., Gretz, N., Schnieders, B., Singh-Sawhney, I., et al.Members of the APN Study Group (1997). Molecular Genetic Identification of Families with Juvenile Nephronophthisis Type 1: Rate of Progression to Renal Failure. *Kidney Int.* 51, 261–269. doi:10.1038/ki.1997.31

König, J., Kranz, B., König, S., Schlingmann, K. P., Titieni, A., Tönshoff, B., et al. (2017). Gesellschaft für Pädiatrische Nephrologie (GPN). Phenotypic spectrum of children with nephronophthisis and related ciliopathies. *Clin. J. Am. Soc. Nephrol.* 12, 1974–1983.

Luo, F., and Tao, Y. H. (2018). Nephronophthisis: A Review of Genotype-Phenotype Correlation. *Nephrology* 23, 904–911. doi:10.1111/nep.13393

O'Toole, J. F., Otto, E. A., Frishberg, Y., and Hildebrandt, F. (2006). Retinitis Pigmentosa and Renal Failure in a Patient with Mutations in INVS. *Nephrol. Dial. Transpl.* 21, 1989–1991. doi:10.1093/ndt/gfl088

Otto, E. A., Helou, J., Allen, S. J., O'Toole, J. F., Wise, E. L., Ashraf, S., et al. (2008). Mutation Analysis in Nephronophthisis Using a Combined Approach of Homozygosity Mapping, CEL I Endonuclease Cleavage, and Direct Sequencing. *Hum. Mutat.* 29, 418–426. doi:10.1002/humu.20669

Otto, E. A., Schermer, B., Obara, T., O'Toole, J. F., Hiller, K. S., Mueller, A. M., et al. (2003). Mutations in INVS Encoding Inversin Cause Nephronophthisis Type 2, Linking Renal Cystic Disease to the Function of Primary Cilia and Left-Right axis Determination. *Nat. Genet.* 34, 413–420. doi:10.1038/ng1217

Richards, S., Aziz, N., Bale, S., Bick, D., Das, S., Gastier-Foster, J., et al. (2015). Standards and Guidelines for the Interpretation of Sequence Variants: a Joint Consensus Recommendation of the American College of Medical Genetics and Genomics and the Association for Molecular Pathology. *Genet. Med.* 17, 405–424. doi:10.1038/gim.2015.30

Srivastava, S., Molinari, E., Raman, S., and Sayer, J. A. (2017). Many Genes-One Disease? Genetics of Nephronophthisis (NPHP) and NPHP-Associated Disorders. *Front. Pediatr.* 5, 287. doi:10.3389/fped.2017.00287

Srivastava, S., Molinari, E., Raman, S., and Sayer, J. A. (2018). Many Genes-One Disease? Genetics of Nephronophthisis (NPHP) and NPHP-Associated Disorders. *Front. Pediatr.* 5, 287. doi:10.3389/fped.2017.00287

Tory, K., Rousset-Rouvière, C., Gubler, M.-C., Morinière, V., Pawtowski, A., Becker, C., et al. (2009). Mutations of NPHP2 and NPHP3 in Infantile Nephronophthisis. *Kidney Int.* 75, 839–847. doi:10.1038/ki.2008.662

Conflict of Interest: The authors declare that the research was conducted in the absence of any commercial or financial relationships that could be construed as a potential conflict of interest.

Publisher's Note: All claims expressed in this article are solely those of the authors and do not necessarily represent those of their affiliated organizations, or those of the publisher, the editors and the reviewers. Any product that may be evaluated in this article, or claim that may be made by its manufacturer, is not guaranteed or endorsed by the publisher.

frontiers | Frontiers in Genetics

CASE REPORT
published: 23 May 2022
doi: 10.3389/fgene.2022.802402

Case Report: Clinical and Genetic Characteristics of Pearson Syndrome in a Chinese Boy and 139 Patients

Yanqin Ying, Yan Liang, Xiaoping Luo and Ming Wei*

Department of Pediatrics, Tongji Hospital, Tongji Medical College, Huazhong University of Science and Technology, Wuhan, China

Background: Pearson's syndrome (PS) is a rare multi-system disorder caused by mitochondrial DNA deletion. Most PS cases in the literature are individual reports, and there is a lack of systematic analysis of clinical features and gene mutations in large samples.

Objective: To report a case of PS and summarize the clinical features and genetic characteristics of PS by reviewing the literature.

Methods: We reported a case of PS in a boy with severe anemia and multi-system disorder. Genetic etiology was identified by mitochondrial DNA sequencing and whole-exon sequencing. Clinical features and gene mutations were summarized by literature review.

Results: The patient had major clinical manifestations with recurrent anemia and multiple organ failure after infection. Mitochondrial DNA sequencing revealed a *de novo* heteroplasmic deletion of 3.063 kb (nt 6,224–9,287) with 75% heteroplasmy in peripheral blood. A total of 139 PS cases were retrieved after a literature search. The most common initial symptom was refractory anemia requiring repeated blood transfusion (86.2%), digestive system symptoms (26.9%), and failure to thrive (15.4%). During the course of disease, the observed symptoms were bone marrow failure (100%), metabolic disorders (61.87%) and gastrointestinal symptoms (61.87%), failure to thrive (48.9%), renal disorders (42.45%), and pancreatic exocrine insufficiency (39.6%). The mean heteroplasmy of mitochondrial DNA mutation in peripheral blood in deaths (76.29 ± 11.86%, $n = 29$) was higher than that in survivals (59.92 ± 23.87%, $n = 26$, $p < 0.01$). Among the patients with the 4.977 kb deletion, the heteroplasmy in peripheral blood in deaths (79.64 ± 9.71%, $n = 11$) was higher than that in survivals (56.67 ± 27.65%, n = 9, $p < 0.05$).

Conclusion: PS can affect multiple systems, and mitochondrial DNA sequencing should be performed early. The heteroplasmy in peripheral blood is related to prognosis.

Keywords: Pearson's syndrome, anemia, mitochondrial DNA deletion, clinical features, gene mutations

OPEN ACCESS

Edited by:
Francesca Luisa Sciacca, IRCCS Carlo Besta Neurological Institute Foundation, Italy

Reviewed by:
Baoheng Gui, the Second Affiliated Hospital of Guangxi Medical University, China
Nicole J. Lake, Yale University, United States

****Correspondence:***
Yan Liang
liangyan2010@sina.com

Specialty section:
This article was submitted to Genetics of Common and Rare Diseases, a section of the journal Frontiers in Genetics

Received: *26 October 2021*
Accepted: *09 May 2022*
Published: *23 May 2022*

Citation:
Ying Y, Liang Y, Luo X and Wei M (2022) Case Report: Clinical and Genetic Characteristics of Pearson Syndrome in a Chinese Boy and 139 Patients. Front. Genet. 13:802402. doi: 10.3389/fgene.2022.802402

INTRODUCTION

Pearson syndrome (PS, OMIM: 557,000), also known as Pearson marrow pancreas syndrome, was first reported by Pearson et al., in 1979 (Pearson et al., 1979). PS is a congenital multi-system disorder caused by mitochondrial DNA (mtDNA) mutation and characterized by severe anemia with neutropenia and (or) thrombocytopenia, ring sideroblasts in the bone marrow, pancreatic exocrine insufficiency, and hyperlactic acidemia (Rötig et al., 1990). Most patients tend to have symptoms in early infancy or even the neonatal period and die before the age of three. Some survivors develop Kearns–Sayre syndrome (KSS), which is characterized by ophthalmoplegia, ataxia, retinitis pigmentosa, conduction defects, and myopathy, while the hematological signs disappear (Giese et al., 2007; Tumino et al., 2011). PS is very rare mitochondriopathies, and mtDNA mutations are rather homogeneous since the same 4.977 kb deletion constitutes the most common lesion (Rötig et al., 1995)) and is generally sporadic. The true incidence of PS is still unknown. The current literature regarding PS mainly were individual reports and some reports summarized the clinical features (Manea et al., 2009; Pronman et al., 2019). There is a lack of large sample systematic analyses of the clinical features and the relationship between mtDNA mutations and clinical features. Here, we report one Chinese child with PS. In addition, we have also reviewed the literature to summarize the clinical features and gene mutation of PS.

CASE REPORT AND METHODS

Case Data

The patient was a male child with full-term natural birth and 2.5 kg of birth weight. His family history was unremarkable. At the age of 7 months, anemia was observed, and serum hemoglobin (Hb) levels was 80 g/L. No special treatment was given. At 10 months of age, he was admitted to the pediatric intensive care unit (PICU) because of fever and vomiting for 5 days. The blood examination revealed anemia (Hb 86 g/L), neutropenia (0.57×10^9/L), and thrombocytopenia (71×10^9/L). Serum ferritin levels was 121.7 ug/L (30–400 ug/l). Bone marrow aspirate showed markedly active myeloproliferation with impaired megakaryocyte maturation (**Figure 1A**). The patient had high levels of ALT (146 U/L) and AST (227 U/L). Pancreatic amylase level was 4 U/L (13–53 U/L), and lipase level was 226 U/L (13–60 U/L). Serum lactic acid level was 9.3 mmol/L (0.5–2.2 mmol/L), while blood glucose, serum ammonia were normal. No specific metabolites were detected by blood amino acids and tandem mass spectrometry of urine. The patient was discharged after 12 days of hospitalization upon symptoms relief. After the discharge, the growth and development of the child were normal, and he had frequent bowel movements.

At the age of 17 months, the patient was readmitted to the PICU for vomiting and a poor appetite. He had epileptic seizures and went into a coma. The blood examination revealed anemia and thrombocytopenia, while neutrophils were within the normal range. The patient had decreased amylase levels, hypoglycemia, metabolic acidosis, hyperlactic acidemia, increased ALT level, and increased ammonia level (673 umol/L). High-sensitivity cardiac troponin I and brain natriuretic peptide (BNP) increased to 160.3 pg/ml (<40 pg/ml) and 3,006 pg/ml, respectively. The second bone marrow aspiration also revealed sideroblast anemia. A brain diffusion-weighted imaging (DWI) scan (**Figure 1B**) showed linear hyperintensity in the left occipital lobe. Video electroencephalogram (VEEG) showed background diffuse δ slow waves, high-amplitude slow waves and sharp slow-wave rhythmic bursts in bilateral frontal and mid-frontal areas,

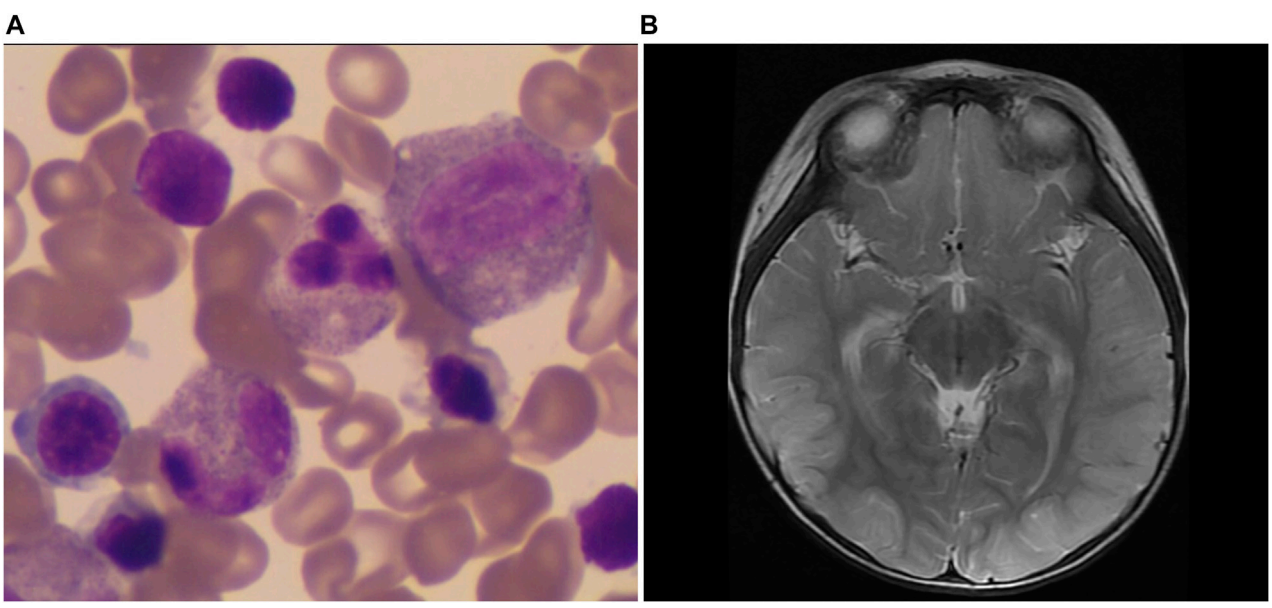

FIGURE 1 | The patient's main clinical characters. **(A)** Bone marrow aspirate showed markedly active myeloproliferation with impaired megakaryocyte maturation. **(B)** The brain DWI image. It showed linear hyperintensity in the left occipital lobe on diffusion-weighted imaging (DWI).

while no sleep spindles were recorded. Whole-exon sequencing was performed, but no pathogenic gene mutations were detected. The patient was discharged after 18 days. At the time of discharge, his limbs muscle strength was decreased to grade III, and he was unable to walk. His stool frequency was increased.

One month later, the child was hospitalized for vomiting and anemia. Pupillary light reflexes were weak in both eyes. The hearing was normal. Pancreatic function exocrine function was reduced. Folic acid, vitamin B12, renal function, and tubular function proteins were all normal. The mitochondrial disease was suspected, and mitochondrial gene sequencing was performed.

The patient was administered multivitamins, L-carnitine, CoQ10, and other supportive therapies. After discharge, he was given repeated blood transfusions. His platelets and neutrophils were within the normal range, and he still had metabolic acidosis, hyperlactic academia, and elevated liver enzymes. At 25 months of age, his muscle strength was increased, and his pupillary light reflex became normal. There was no significant lag in growth and mental development. At 31 months of age, the patient died from a severe infection.

Whole-Exon Sequencing and Whole Mitochondrial Genome Sequencing Analysis

Four milliliter of venous blood was drawn from the child and the parents. Both nuclear genome and mitochondrial genome sequencing in peripheral blood proceeded as previous publication (Liang et al., 2020). In brief, The fragmented DNA library was captured using GenCap of 23,000 genes and Mitochondrial DNA Capture Kits. Sequencing was carried out using the Illumina HiSeq X ten platform for paired-reading of 150 bp. After sequencing, the raw data were saved in a FASTQ format. Both Illumina sequencing adapters and low-quality reads were filtered using the cutadaptor software (http://code.google.com/p/cutadapt/). The clean reads of nuclear genome were aligned to human reference genome (hg19, UCSC) using the sentieon software (https://www.sentieon.com/). The clean reads of mitochondrial genome were aligned to each human reference (hg38, UCSC) using the sentieon software (https://www.sentieon.com/). Duplicated reads were removed, and only unique mapping reads were used for the next variation detection. Both SNVs and Indels of the nuclear genome and mitochondrial genome were detected using the HaplotypeCaller module of the GATK software (https://software.broadinstitute.org/gatk/). In addition, the relative copy numbers were calculated using the tools of fix, segment, and call of the CNVkit software (https://cnvkit.readthedocs.io/en/stable/).

Ethical Approval

The study was approved by the Ethics Committee of Tongji Hospital, Tongji Medical College of Huazhong University of Science and Technology.

Literature Search

Based on PubMed, Human Gene Mutation Database (HGMD), Online Mendelian Inheritance in Man (OMIM), China National Knowledge Infrastructure (CNKI), and Wanfang Data searches using keywords "Pearson marrow pancreas syndrome", "mtDNA deletion syndrome" and "Pearson syndrome", we identified and compiled 105 papers containing PS case reports published before March 2021. After removing duplicates, 139 PS cases with a complete medical history and gene mutation data were obtained (**Figure 2**). The onset age was defined as the time the first symptom was recorded in study. The age of diagnosis referred to the age that the genetic mutation was confirmed or the PS was diagnosed in the study.

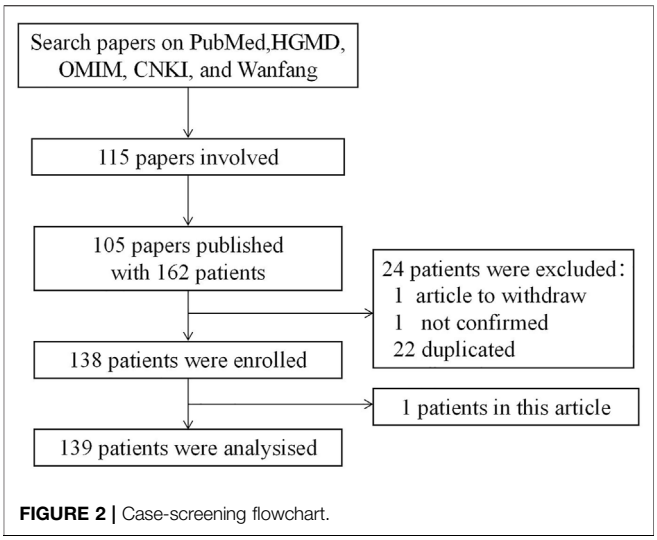

FIGURE 2 | Case-screening flowchart.

All the patients were divided into survivals and deaths groups according to the status at the end of the follow-up period.

Statistical Analysis

Descriptive statistical analysis was used for clinical features. The mtDNA heteroplasmy was expressed as a percentage. The heteroplasmy from peripheral blood in the deaths and survivals groups were expressed as mean ± SD. The comparison of gene heteroplasmy between the two groups was performed using two-sided *t*-tests, and $p < 0.05$ was considered statistically significant.

RESEARCH RESULTS

Genetic Test Results

No pathogenic gene mutations were detected by whole-exon sequencing. The mtDNA sequencing indicated that the patient had a 3.063 kb deletion in the area of chrM: 6,224–9,287 (**Figure 3**), including part of MT-CO1, all MT-TS1, MT-TD, MT-CO2, MT-TK, MT-ATP8, MT-ATP6, MT-CO3, and the heteroplasmy was 75% in peripheral blood. The mother didn't carry the same mutation. It was a ***de novo*** mutation since this mutation had not been reported and published at mitobreak (http://mitobreak.portugene.com/cgi-bin/Mitobreak_home.cgi/).

General Characteristics of Pearson Syndrome

Among the 139 PS cases, a total of 131 cases had clear gender records, which included 60 females and 71 males (**Supplementary data S1**).

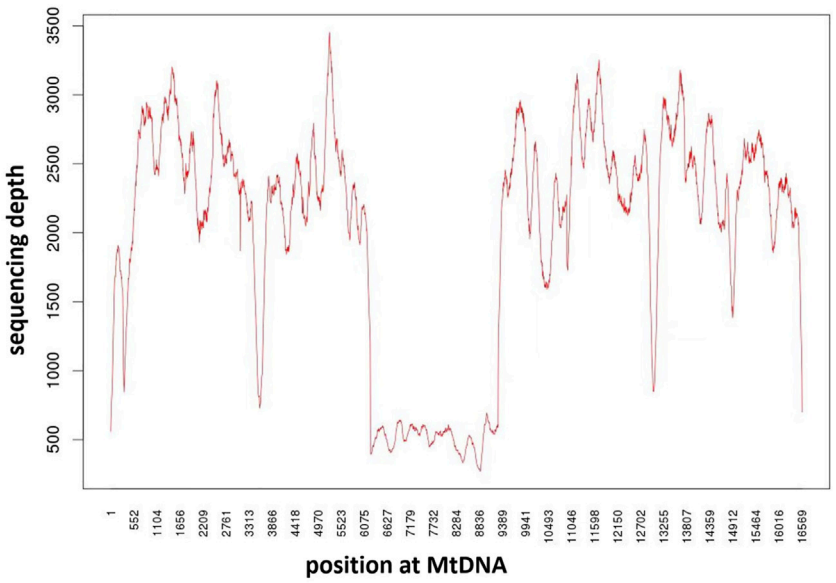

FIGURE 3 | Mitochondrial DNA mutation in the patients. Analysis of mitochondrial DNA mutations in the child's blood showed a heteroplasmic deletion of mitochondrial DNA 3.063 kb (nt 6,224–9,287).

The onset age was mostly within 1 month after birth (54/128, 42.2%), followed by 1 month–6 months (41/128, 32.0%), **Figure 4A**. While only 8/105 (7.6%) patients were diagnosed within 1 month of age. Most patients were diagnosed after 1 year of age (60/105, 57.2%).

From onset to diagnosis, the most common duration was 1–3 years (27/103, 26.2%), followed by less than 1 month (23/103, 22.3%). Out of 139 patients, 130 had documented outcomes. Among them, total of 69 cases (52.3%) died, and 17 cases (24.6%) died within 1 year of age, 32 cases (46.4%) died within 1–3 years, and 20 cases died after 3 years of age (29.0%). Among the surviving cases, 2 cases developed to KSS.

Pregnancy and birth history were recorded in 67 cases, which included 4 cases (6.0%) with preterm delivery, 7 cases (10.4%) with intrauterine growth restriction, 5 cases (7.5%) with intrauterine distress, 2 cases (3.0%) with meconium-stained amniotic fluid, and 2 cases (3.0%) with oligohydramnios during pregnancy. Only 57 cases with the record of family history were reported. Among them, four cases had related family history including 1 case with a maternal diagnosis of progressive external ophthalmoplegia (PEO), 1 case with the death of the first three fetuses in the family, 1 case with tremors in the mother and grandmother, 1 case with the family history of PS in a sibling. One case had an unrelated family history with sudden infant death syndrome in paternal uncle.

Initial Symptoms

There were 130 cases with clearly recorded initial symptoms (**Figure 4B**). The most common initial symptom was refractory anemia requiring repeated blood transfusions (112 cases, 86.2%). Among the patients with anemia, there were 27 cases (20.8%) of anemia with neutropenia or thrombocytopenia. None of the patients had initial symptoms as separated neutropenia or thrombocytopenia. Anemia was the only initial symptom in 58 cases (44.6%). In addition, there were 35 cases (26.9%) with gastrointestinal symptoms, including vomiting, diarrhea, and feeding difficulties, 20 cases (15.4%) with failure to thrive, 19 cases (14.6%) with metabolic disorders, including metabolic acidosis, hyperlactic acidemia, hypoglycemia, and electrolyte disorders, and 8 cases (6.2%) with pancreatic exocrine insufficiency.

Symptoms Observed During the Course of the Disease

Multiple symptoms were observed in 139 cases during the course of the disease (**Figure 4C**). Bone marrow failure was reported in all 139 cases (100%), presenting as refractory anemia with or without neutropenia and (or) thrombocytopenia. Both metabolic disorders and gastrointestinal symptoms occurred in 86 cases (61.9%), failure to thrive in 68 cases (48.9%), renal disorders in 59 cases (42.5%), pancreatic exocrine insufficiency in 55 cases (39.6%), recurrent infections in 47 cases (33.8%), impaired vision with ocular and limb muscles disability in 33 patients (23.7%), central nervous system affected in 42 patients (30.2%), cardiac disease in 28 cases (20.1%), and diabetes mellitus in 25 cases (18.0%).

Mitochondrial DNA Mutation

Among the 139 PS cases, mitochondrial DNA mutation was documented in 135 cases, all of which were heteroplasmy mutations, including 8 cases with duplication in addition to heteroplasmic deletion. There were 30 cases (22.2%) of 4.977 kb deletion and 105 cases (77.8%) of other

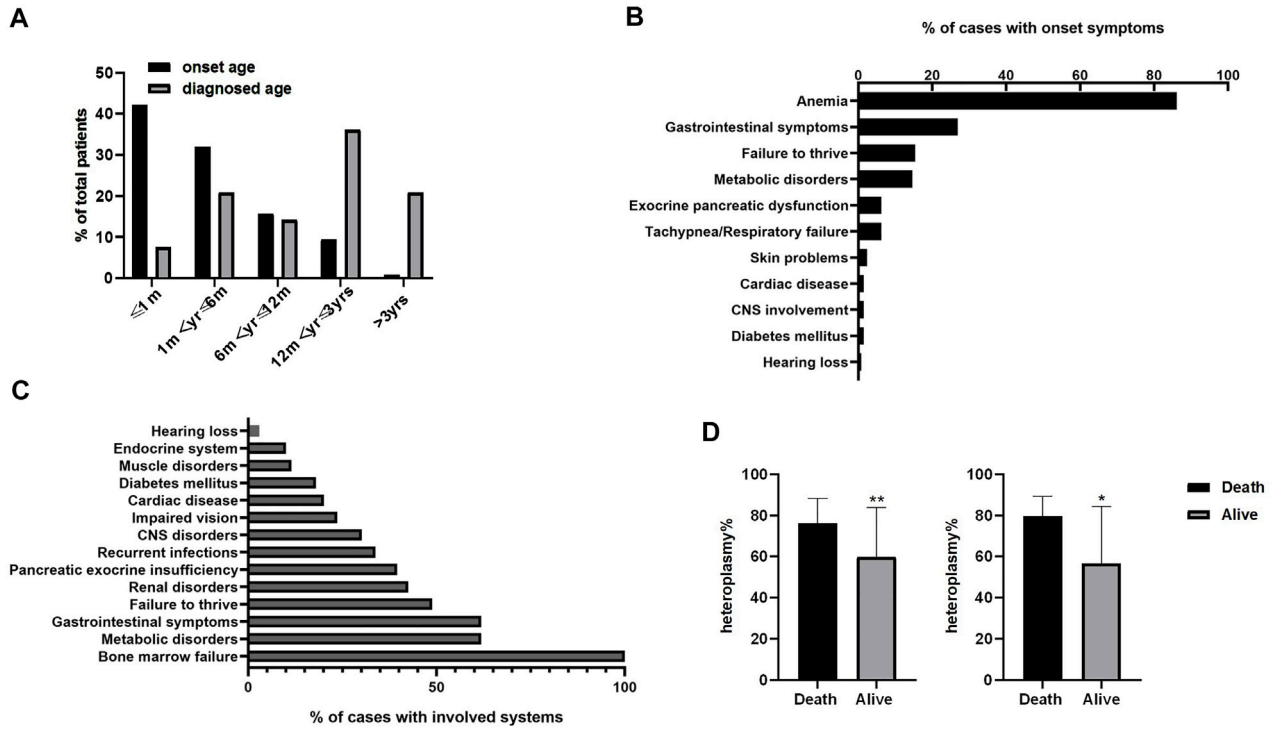

FIGURE 4 | Disease characteristics of 139 patients. **(A)** Age of onset and diagnosis time from the onset in Pearson syndrome patients. **(B)** The percentage of initial symptoms observed in patients. **(C)** The percentage of symptoms observed in patients during the course of the disease. [a] refers to diarrhea and vomiting;[b] refers to hypothyroidism, growth hormone deficiency, and adrenal insufficiency. **(D)** Comparison of mitochondrial mutation heteroplasmy in peripheral blood between the death group and the survival group. The mean heteroplasmy of mitochondrial DNA mutation in peripheral blood was statistically higher in the deaths (76.29 ± 11.86%, n = 29) than that in survivals (59.92 ± 23.87%, n = 26; t = 3.272, p < 0.01. left). For patients with 4.977 kb deletion (right), the mean heteroplasmy of mitochondrial DNA mutation genes in peripheral blood was statistically higher in the deaths (79.64 ± 9.71%,n = 11) than that in survivals (56.67 ± 27.65%, n = 9) (t = 2.58, p < 0.05). Error bar represents the SD of heteroplasmy from peripheral blood in the deaths and survivals groups. **Supplementary data S1** The data of patients summarized from the literature review. **Supplementary data S2** Correlation between heteroplasmy of mitochondrial DNA deletion in peripheral blood and the age of onset. **Supplementary data S3** Correlation between heteroplasmy of 4.977 kb deletion in peripheral blood and the age of onset.

mitochondrial DNA mutations. Mitochondrial gene deletion sites were between nt.6074 and nt.16082, and the genes involved included MT-CO1, MT-TS1, MT-TD, MT-CO2, MT-TK, MT-ATP8, MT-ATP6, MT-CO3, MT-TG, MT-ND3, MT-TR, MT-ND4L, MT-ND4, MT-TH, MT-TS2, MT-TL2, MT-ND5, MT-ND6, MT-TE, MT-CYB, MT-TT, and MT-TP.

Mitochondrial DNA Deletion Heteroplasmy

Heteroplasmy in peripheral blood and/or bone marrow was detected in 85 cases, ranging from 20 to 100%. There was no significant correlation between heteroplasmy of mtDNA deletion in peripheral blood and age of onset, and heteroplasmy of 4.977 kb deletion in peripheral blood and age of onset (**Supplementary data S2** and **Supplementary data S3**). The mean heteroplasmy of mtDNA mutation in peripheral blood was statistically higher in the deaths (76.29 ± 11.86%, n = 29) than that in survivals (59.92 ± 23.87%, n = 26; t = 3.272, p < 0.01), **Figure 4D** left. For patients with 4.977 kb deletion, the mean heteroplasmy of mtDNA mutation genes in peripheral blood was statistically higher in the deaths (79.64 ± 9.71%, n = 11) than that in survivals (56.67 ± 27.65%, n = 9) (t = 2.58, p < 0.05), **Figure 4D** right.

DISCUSSION

Pearson's syndrome is a maternally inherited disease caused by the heteroplasmic deletion of mitochondrial DNA. The mutation leads to mitochondrial respiratory chain dysfunction and insufficient cellular energy supply (Smith et al., 1995; Williams et al., 2012). Most cases are sporadic, and those with a clear family history are rare. In this case, the patient had no obvious family history, and the mother had no symptoms of mitochondrial pathology. Among the 139 cases reported in the literature, only 57 cases had family history provided. Five cases had a clear family history. Due to genetic heteroplasmy, clinical manifestations were variable among siblings (Köklü et al., 2010).

PS has an early onset and can even occur in the uterus with anemic fetal hydrops and cardiomegaly (Manea et al., 2009). The onset of illness within 1 month after birth accounted for 42.2% of cases, and the age of diagnosis was mostly after 1 year of age, indicating that most patients got delayed diagnoses. Severe refractory anemia is a common initial presentation. Some children develop neutropenia and/or thrombocytopenia during the course of the disease. Pancytopenia was reported as an initial symptom in some cases (Falcon and Howard, 2017; Tadiotto

et al., 2018). In this case, the patient's initial presentation was an episode of moderate anemia. After 10 months, the patient required repeated blood transfusions. In the literature review, refractory anemia as the initial symptom accounted for 44.6% of cases. It was closed to 36.4% from patients with neonatal onset (Manea et al., 2009). Refractory anemia can easily be misdiagnosed as Diamond-Blackfan anemia (DBA) or other hematological disorders (Gagne et al., 2014). Gastrointestinal symptoms, including diarrhea, vomiting, and feeding difficulties were among the initial symptoms for 26.9% of cases. Only a small number of patients had gastrointestinal symptoms as the only initial symptoms (Niaudet et al., 1994). Only 6.2% of cases had initial symptoms of pancreatic exocrine insufficiency. There were 2 cases (1.5%) with pancreatic endocrine dysfunction, resulting in hyperglycemia and diabetes mellitus. Metabolic disorders, including hyperlactic academia and metabolic acidosis as initial symptoms, occurred in 19 patients (14.6%). It was 9% from patients with neonatal onset (Manea et al., 2009).

Multiple symptoms were observed as the disease progresses. In this case, several disorders were happened, including pancreatic exocrine function insufficiency, gastrointestinal disorders, metabolic imbalance, vision disorder, and central nervous disorders, while growth and renal function were spared. Based on the literature review, hematological symptoms was present in all patients, presented as anemia with or without neutropenia and/or thrombocytopenia. It was reported that the percentage of anemia, neutropenia and thrombocytopenia was 98%, 67% and 73%, respectively (Pronman et al., 2009). Bone marrow aspiration reveals ring sideroblasts or vacuolization of bone marrow precursor cells. In some patients, early bone marrow biopsy often fails to show these characteristic changes, and multiple biopsies are required (Pearson et al., 1979; Superti-Furga et al., 1993; Mkaouar-Rebai et al., 2013). Besides, the diagnosis may be missed by bone marrow examiners with no relevant experience. For our patient, in two bone marrow aspirations, the presence of active myeloproliferation and visible sideroblasts were typical factors, while the diagnosis was delayed. In most cases, gastrointestinal symptoms, such as diarrhea, elevated liver enzymes, cholestasis, enlarged liver, and liver failure, are responsible for mortality (Rötig et al., 1990; Rötig et al., 1995). Recurrent infection was happened in 42.5% of patients, it was not reported by other publications. Many patients died of multiple organ failure caused by infection (Crippa et al., 2015). Renal disorders (42.5%)was mainly manifested as Fanconi syndrome, characterized by aminoaciduria, proteinuria, diabetes mellitus, and electrolyte disturbance, with increased renal volume on Ultrasonography (McShane et al., 1991; Lichter-Konecki et al., 1993; Santorelli et al., 1996; Crippa et al., 2015). The percentage of renal disorder, pancreatic exocrine insufficiency and cardiac disease were similar to those reported by literature (Pronman et al., 2009). Mitochondrial inheritance is characterized by heteroplasmy and threshold effect, leading to diverse clinical phenotypes. The possibility of PS should be considered in children with anemia associated with other systemic changes.

PS is mainly caused by the heteroplasmic deletion of mitochondrial DNA. In this case, there was a *de novo* heteroplasmic deletion of 3.063 kb (nt 6,224–9,287), including part of MT-CO1, all MT-TS1, MT-TD, MT-CO2, MT-TK, MT-ATP8, MT-ATP6, MT-CO3. The heteroplasmy was 75% in peripheral blood. The common gene mutation is a heteroplasmic deletion of 4.977 kb (nt 8,489–13,447) which is involved in mitochondrial energy metabolism and electron transfer (Rötig et al., 1990; Rötig et al., 1995). This deletion mutation was found in 22.2% of the cases in the literature, while other uncommon deletions accounted for 77.8%. It was suggestive of diversity in gene mutation of PS. The different sizes of the deleted segments and the different effects on mitochondrial respiratory chain function may be one of the reasons for the diverse clinical presentation. The clinical manifestations were also affected by the heteroplasmy of mitochondrial mutations (McShane et al., 1991). Limited autopsy cases have shown heteroplasmy in mitochondrial deletion in other tissues that are different from those in bone marrow or peripheral blood (Superti-Furga et al., 1993; Jacobs et al., 2004). The heteroplasmy of mitochondrial deletions in peripheral blood is not significantly correlated with the age of onset and may be related to the different sizes of mitochondrial deletion fragments and different mitochondrial genes. There was no correlation between genetic heteroplasmy of 4.977 kp deletion in peripheral blood and age, indicating that there might be some other factors involved, such as heteroplasmy of mitochondrial deletion in other tissues and organs. Since the data of these PS cases were collected from the literature, there was no further analysis of the correlation between 4.977 kb gene deletion and severity of anemia. In addition, due to the unbalanced distribution of mitochondrial mutations in cell division, whether the heteroplasmy at a certain time can represent the initial level needs to be further studied. Our results showed that regardless of mitochondrial fragment size, the percentage of mitochondrial heteroplasmy in peripheral blood of the death was significantly higher than that in survivals. Since most children died from septic shock and multiple organ system failures, the heteroplasmy of other tissues may also be a factor affecting mortality. The specific threshold of mitochondrial DNA deletion in PS was still not clear. The results of blood heteroplasmy have shown that the minimum mitochondrial heteroplasmy is 15% (Rötig, A. et al., 1995).

There was a lack of effective treatment with a poor prognosis and high mortality. Children with anemia require repeated blood transfusions. Most patients died due to the metabolic crisis and multi-system failure after infection. The mortality was 52.3% among the reported cases, and the majority of deaths were among infants and young children under 3 years of age. The leading causes of death were septic shock, multiple organ failure, and leukemia. Anemia was corrected in survivors without repeated blood transfusions, and adult cases developed KSS. If the symptoms of bone marrow failure are corrected early, patients can survive until 3 years of age, improving the prognosis. In this case, the patient needed repeated blood transfusions and still developed metabolic acidosis, hyperlactic academia, and elevated liver enzymes despite normal levels of platelets

and neutrophils. The patient died at 31 months of age due to a severe infection.

In conclusion, this case report enriches the mitochondrial gene mutation spectrum and clinical features of PS. The literature review found that in addition to hematological and pancreatic dysfunction, PS also has a high incidence of gastrointestinal and renal tubular diseases. In clinical practice, if refractory anemia is accompanied by other systemic manifestations, the possibility of PS should be highly suspected.

DATA AVAILABILITY STATEMENT

The datasets for this article are not publicly available due to concerns regarding participant/patient anonymity. Requests to access the datasets should be directed to the corresponding author.

ETHICS STATEMENT

The studies involving human participants were reviewed and approved by the Ethics Committee of Tongji Hospital, Tongji Medical College, Huazhong University of Science and Technology. Written informed consent to participate in this study was provided by the participants' legal guardian/next of kin.

AUTHOR CONTRIBUTIONS

YY were responsible for the data acquisition of this study and revised the manuscript critically for important intellectual content. YL, XL, and MW made contributions to drafting and revising this article. All authors commented on drafts of the paper. All authors read and approved the final manuscript.

FUNDING

This study was supported by the national key R&D program of China (2018YFC1002400).

ACKNOWLEDGMENTS

We are grateful to the family members who participated in this study.

SUPPLEMENTARY MATERIAL

The Supplementary Material for this article can be found online at: https://www.frontiersin.org/articles/10.3389/fgene.2022.802402/full#supplementary-material

REFERENCES

Crippa, B. L., Leon, E., Calhoun, A., Lowichik, A., Pasquali, M., and Longo, N. (2015). Biochemical Abnormalities in Pearson Syndrome. *Am. J. Med. Genet.* 167, 621–628. doi:10.1002/ajmg.a.36939

Falcon, C. P., and Howard, T. H. (2017). An Infant with Pearson Syndrome: a Rare Cause of Congenital Sideroblastic Anemia and Bone Marrow Failure. *Blood* 129, 2710. doi:10.1182/blood-2017-02-766881

Gagne, K. E., Ghazvinian, R., Yuan, D., Zon, R. L., Storm, K., Mazur-Popinska, M., et al. (2014). Pearson Marrow Pancreas Syndrome in Patients Suspected to Have Diamond-Blackfan Anemia. *Blood* 124, 437–440. doi:10.1182/blood-2014-01-545830

Giese, A., Kirschner-Schwabe, R., Blumchen, K., Wronski, L., Shalapour, S., Prada, J., et al. (2007). Driever Pablo Hernáiz., Brauer Martin., Schuelke Markus., Henze Günter., Seeger KarlPrenatal Manifestation of Pancytopenia in Pearson Marrow-Pancreas Syndrome Caused by a Mitochondrial DNA Deletion. *Am. J. Med. Genet.* 143A, 285–288. doi:10.1002/ajmg.a.31493

Jacobs, L. J. A. M., Jongbloed, R. J. E., Wijburg, F. A., de Klerk, J. B. C., Geraedts, J. P. M., Nijland, J. G., et al. (2004). Pearson Syndrome and the Role of Deletion Dimers and Duplications in the mtDNA. *J. Inherit. Metab. Dis.* 27, 47–55. doi:10.1023/B:BOLI.0000016601.49372.18

Köklü, S., Akbal, E., Koçak, E., and Alioğlu, B. (2010). Celiac Disease in Siblings with Pearson Syndrome. *Am. J. Med. Sci.* 339, 392–394. doi:10.1097/MAJ.0b013e3181cefba3

Liang, Y., Du, C., Wei, H., Zhang, C., Zhang, M., Hu, M., et al. (2020). Genotypic and Clinical Analysis of 49 Chinese Children with Hepatic Glycogen Storage Diseases. *Mol. Genet. Genomic Med.* 8, e1444. doi:10.1002/mgg3.1444

Lichter-Konecki, U., Trefz, F. K., Rötig, A., Munnich, A., Pfeil, A., and Bremer, H. J. (1993). 3-Methylglutaconic Aciduria in a Patient with Pearson Syndrome. *Eur. J. Pediatr.* 152, 378–379. doi:10.1007/BF01956761

Manea, E. M., Leverger, G., Bellmann, F., Stanescu, P. A., Mircea, A., Lèbre, A.-S., et al. (2009). Pearson Syndrome in the Neonatal Period: Two Case Reports and Review of the Literature. *J. Pediatr. Hematol. Oncol.* 31, 947–951. doi:10.1097/MPH.0b013e3181bbc4ef

McShane, M. A., Hammans, S. R., Sweeney, M., Holt, I. J., Beattie, T. J., Brett, E. M., et al. (1991). Pearson Syndrome and Mitochondrial Encephalomyopathy in a Patient with a Deletion of mtDNA. *Am. J. Hum. Genet.* 48, 39

Mkaouar-Rebai, E., Chamkha, I., Mezghani, N., Ayed, I. B., and Fakhfakh, F. (2013). Screening of Mitochondrial Mutations in Tunisian Patients with Mitochondrial Disorders: an Overview Study. *Mitochondrial DNA* 24, 163–178. doi:10.3109/19401736.2012.748045

Niaudet, P., Heidet, L., Munnich, A., Schmitz, J., Bouissou, F. o., Gubler, M. C., et al. (1994). Deletion of the mitochondrial DNA in a case of de Toni-Deb-Fanconi syndrome and Pearson syndrome. *Pediatr. Nephrol.* 8, 164–168. doi:10.1007/BF00865468

Pearson, H. A., Lobel, J. S., Kocoshis, S. A., Naiman, J. L., Windmiller, J., Lammi, A. T., et al. (1979). A New Syndrome of Refractory Sideroblastic Anemia with Vacuolization of Marrow Precursors and Exocrine Pancreatic Dysfunction. *J. Pediatr.* 95, 976–984. doi:10.1016/s0022-3476(79)80286-3

Pronman, L., Rondinelli, M., Burkardt, D. D. C., Velayuthan, S., Khalili, A. S., and Bedoyan, J. K. (2019). Pearson Syndrome: A Rare Cause of Failure to Thrive in Infants. *Clin. Pediatr. (Phila)* 58, 819–824. doi:10.1177/0009922819834285

Rötig, A., Bourgeron, T., Chretien, D., Rustin, P., and Munnich, A. (1995). Spectrum of Mitochondrial DNA Rearrangements in the Pearson Marrow-Pancreas Syndrome. *Hum. Mol. Genet.* 4, 1327–1330. doi:10.1093/hmg/4.8.1327

Rötig, A., Cormier, V., Blanche, S., Bonnefont, J. P., Ledeist, F., Romero, N., et al. (1990). Pearson's Marrow-Pancreas Syndrome. A Multisystem Mitochondrial Disorder in Infancy. *J. Clin. Invest.* 86, 1601–1608. doi:10.1172/JCI114881

Santorelli, F. M., Barmada, M. A., Pons, R., Zhang, L. L., and DiMauro, S. (1996). Leigh-type Neuropathology in Pearson Syndrome Associated with Impaired ATP Production and a Novel mtDNA Deletion. *Neurology* 47, 1320–1323. doi:10.1212/wnl.47.5.1320

Smith, O. P., Hann, I. M., Woodward, C. E., and Brockington, M. (1995). Pearson's Marrow/pancreas Syndrome: Haematological Features Associated with Deletion and Duplication of Mitochondrial DNA. *Br. J. Haematol.* 90, 469–472. doi:10.1111/j.1365-2141.1995.tb05178.x

Superti-Furga, A., Schoenle, E., Tuchschmid, P., Caduff, R., Sabato, V., DeMattia, D., et al. (1993). Pearson Bone Marrow-Pancreas Syndrome with Insulin-dependent Diabetes, Progressive Renal Tubulopathy, Organic Aciduria and Elevated Fetal Haemoglobin Caused by Deletion and Duplication of Mitochondrial DNA. *Eur. J. Pediatr.* 152, 44–50. doi:10.1007/BF02072515

Tadiotto, E., Maines, E., Degani, D., Balter, R., Bordugo, A., and Cesaro, S. (2018). Bone Marrow Features in Pearson Syndrome with Neonatal Onset: A Case Report and Review of the Literature. *Pediatr. Blood Cancer* 65, e26939. doi:10.1002/pbc.26939

Tumino, M., Meli, C., Farruggia, P., La Spina, M., Faraci, M., Castana, C., et al. (2011). Clinical Manifestations and Management of Four Children with Pearson Syndrome. *Am. J. Med. Genet.* 155, 3063–3066. doi:10.1002/ajmg.a.34288

Williams, T. B., Daniels, M., Puthenveetil, G., Chang, R., Wang, R. Y., and Abdenur, J. E. (2012). Pearson Syndrome: Unique Endocrine Manifestations Including Neonatal Diabetes and Adrenal Insufficiency. *Mol. Genet. Metabolism* 106, 104–107. doi:10.1016/j.ymgme.2012.01.018

Conflict of Interest: The authors declare that the research was conducted in the absence of any commercial or financial relationships that could be construed as a potential conflict of interest.

Publisher's Note: All claims expressed in this article are solely those of the authors and do not necessarily represent those of their affiliated organizations, or those of the publisher, the editors and the reviewers. Any product that may be evaluated in this article, or claim that may be made by its manufacturer, is not guaranteed or endorsed by the publisher.

frontiers | Frontiers in Pediatrics

ORIGINAL RESEARCH
published: 24 May 2022
doi: 10.3389/fped.2022.887214

Pathogenicity and Long-Term Outcomes of Liddle Syndrome Caused by a Nonsense Mutation of *SCNN1G* in a Chinese Family

Di Zhang[1], Yi Qu[1], Xue-Qi Dong[1], Yi-Ting Lu[1], Kun-Qi Yang[1], Xin-Chang Liu[1], Peng Fan[1], Yu-Xiao Hu[2], Chun-Xue Yang[2], Ling-Gen Gao[3], Ya-Xin Liu[2] and Xian-Liang Zhou[1]**

[1] Department of Cardiology, National Center for Cardiovascular Diseases, Chinese Academy of Medical Sciences and Peking Union Medical College, Fuwai Hospital, Beijing, China, [2] Emergency and Critical Care Center, National Center for Cardiovascular Diseases, Chinese Academy of Medical Sciences and Peking Union Medical College, Fuwai Hospital, Beijing, China, [3] Department of Geriatric Cardiology, Chinese People's Liberation Army (PLA) General Hospital, Beijing, China

Objective: Liddle syndrome (LS) is a monogenic hypertension consistent with autosomal dominant inheritance, often with early onset high blood pressure in childhood or adolescence. This study aimed to identify the pathogenicity of a nonsense mutation in *SCNN1G* in a Chinese family with LS and the long-term outcomes of tailored treatment with amiloride.

Methods: To explore the pathogenicity of candidate variant reported in 2015 by our team, we constructed mutant and wild-type models *in vitro* and measured amiloride-sensitive current in *Chinese Hamster Ovary* (*CHO*) cells using patch clamp technique. Participants were followed up for 7 years after tailored treatment with amiloride.

Results: A nonsense variant was detected in six members, two of whom were pediatric patients. This mutation resulted in a termination codon at codon 572, truncating the Pro-Pro-Pro-X-Tyr motif. The mutant epithelial sodium channels displayed higher amiloride-sensitive currents than the wild-type channels ($P < 0.05$). Tailored treatment with amiloride achieved ideal blood pressure control in all patients with normal cardiorenal function, and no adverse events occurred during follow-up.

Conclusion: We found the pathogenicity of a nonsense *SCNN1G* mutation (p.Glu571*) with enhanced amiloride-sensitive currents in a LS family with young patients. Tailored treatment with amiloride may be an effective strategy for the long-term control of blood pressure and protection from target organ damage or cardiovascular events, including children and youth patients with LS.

Keywords: Liddle syndrome, pathogenicity, pediatrics, amiloride-sensitive current, longterm prognosis

OPEN ACCESS

Edited by:
Naglaa M. Kamal,
Cairo University, Egypt

Reviewed by:
Vandana Jain,
All India Institute of Medical Sciences, India
Thomas Kleyman,
University of Pittsburgh, United States

****Correspondence:***
Ya-Xin Liu
yaxinliu1978@hotmail.com
Xian-Liang Zhou
zhouxianliang0326@hotmail.com

Specialty section:
This article was submitted to Genetics of Common and Rare Diseases, a section of the journal Frontiers in Pediatrics

Received: *01 March 2022*
Accepted: *02 May 2022*
Published: *24 May 2022*

Citation:
Zhang D, Qu Y, Dong X-Q, Lu Y-T, Yang K-Q, Liu X-C, Fan P, Hu Y-X, Yang C-X, Gao L-G, Liu Y-X and Zhou X-L (2022) Pathogenicity and Long-Term Outcomes of Liddle Syndrome Caused by a Nonsense Mutation of SCNN1G in a Chinese Family. Front. Pediatr. 10:887214. doi: 10.3389/fped.2022.887214

INTRODUCTION

Liddle syndrome (LS) was first reported at 1963 by Liddle et al. (1). It is a monogenic hypertension caused by mutations in genes encoding epithelial sodium channels (ENaCs) (2). ENaCs are composed of three subunits: α, β, and γ (encoded by *SCNN1A*, *SCNN1B*, and *SCNN1G*, respectively) (3). Proline-rich segments, referred to as Pro-Pro-Pro-X Tyr (PY) motifs, in the

carboxyl terminal regions of β and γ subunits are binding sites for WW domains of neural precursor cell expressed, developmentally Down-regulated 4 (NEDD4), an E3 ubiquitin-protein ligase (4). By binding the ubiquitin-protein ligase domain, PY motifs inactivate ENaCs (5). LS is characterized with increased sodium reabsorption in collecting tubules resulted from ENaCs dysfunction, including inactivation disorders, and abnormal opening frequencies (3, 6–8). The function of ENaCs usually is examined by patch clamp techniques.

The typical manifestations of LS include early-onset hypertension, hypokalemia and suppression of plasma renin activity (PRA), and plasma aldosterone concentration (PAC) (3, 9). Some LS patients lack a typical presentation and are not diagnosed and treated in time, which can lead to major complications such as stroke and early death because of poor control of hypertension (10–13). Genetic sequencing is recommended for LS screening for *SCNN1A*, *SCNN1B,* and *SCNN1G* mutations, especially in families with a history of early-onset hypertension (3). Through family screening, it often screens for children who carried mutations in family (11, 14). Genetic sequencing screened LS patients, but the pathogenicity of most variants has not been verified by functional experiments. For LS patients diagnosed based on sequencing results and silico analysis prediction, the usual follow-up after beginning amiloride treatment is approximately 1 or 2 months and the long-term outcomes of LS patient remains unclear.

In this study, we explored the pathogenicity of a nonsense mutation (c.1171G > T) in exon 13 of *SCNN1G* reported in 2015 year by our team and efficiency of blood pressure control by amiloride. We used patch-clamp to verify functional mechanism of this mutation, and found that amiloride-sensitive currents differed significantly between wild-type and mutant groups. All members harboring the c.1171 G > T mutation in *SCNN1G* with hypertension and/or abnormal biochemical presentations were diagnosed with LS. Over a 7-year follow-up, the results show efficacy with tailored treatment of amiloride in blood pressure control and prevention of target organ damage.

MATERIALS AND METHODS

Clinical Characteristics

Subjects

The index case was an 18-year-old woman (III-2) with early-onset, refractory, and unexplained hypertension and hypokalemia, accompanied by suppressed PRA. The diagnosis of hypertension for children is made when repeat BP values on three different measurements are greater than the 95th percentile for the age, sex, and height of the patient (15). The proband and five members carrying the nonsense mutation were included for the clinical, biochemical analysis in this family. This study was approved by the Ethics Committee of Fuwai Hospital and all participants signed their written informed consent (The informed consent of the deceased patient was obtained from his immediate family) in accordance with the Declaration of Helsinki.

Tailored Treatment and Follow-Up

All biochemical tests, such as of electrolytes, were performed using standard methods. Patients carrying *SCNN1G* mutation were required to follow a salt-restricted diet and received oral amiloride (5.0 mg/day for adults and 2.5 mg/day for children) intervention. Blood pressure and potassium levels were measured during follow-up period. Indicators of assessing cardiorenal function and cardiovascular events were followed up over 7 years. Indicators included creatinine, urea nitrogen, echocardiography, and cardiovascular events. Events contain heart failure, stroke, and all-cause death.

Functional Analysis of the γG571 Stop Mutation in Epithelial Sodium Channels

Site-Directed Mutagenesis and Chinese Hamster Ovary Cell Incubation

The sequence of human *SCNN1A*, *SCNN1B*, and *SCNN1G* was obtained from the University of California Santa Cruz database, and cDNAs encoding human ENaC were synthesized exogenously. The *SCNN1G* gene mutation (c.1171G > T) was induced using a QuikChange Site-Directed Mutagenesis Kit (Statagene). ENaC expression vectors were gifts from Dr. Cecilia Canessa, Yale University. *Chinese Hamster Ovary* (*CHO*) cells were used for expression human ENaC. *CHO* cells were cultured under standard conditions (10% fetal bovine serum in Dulbecco's modified Eagle's medium, 1% penicillin/streptomycin, 37°C, 5% CO_2). Before transfection, cells were seeded on poly-lysine coated slides. pcDNA3.1-ENaCα, ENaCβ, ENaCγ, or ENaCγ-mut together with pEGFP-N1 were transfected into cells in a 1:1:1:1 ratio using Lipofectamine 2000 (Invitrogen, Carlsbad, CA, United States). Green fluorescent protein was used to identify transfected cells. Amiloride (10 μM) was added to culture medium until just prior to the electrophysiological experiments (48 h after transfection).

Electrophysiological Measurements

Whole-cell current recordings were acquired using a MultiClamp 700B amplifier (Molecular Devices, San Jose, CA, United States). Signals were collected by a Micro 1401 MKII (Cambridge Electronic Design, Cambridge, United Kingdom) using Spike 2 acquisition software. The electrophysiological methods were as previously described (16). In brief, the pipette solution (in mM) was 120 CsCl, 5 NaCl, 5 EGTA, 2 $MgCl_2$, 2 Mg-ATP, 0.1 GTP, and 10 HEPES (pH 7.4). The bath solution (in mM) was 150 NaCl, 1 $CaCl_2$, 2 $MgCl_2$, and 10 HEPES (pH 7.4). Whole-cell capacitance was recorded for normalizing ENaC currents. Current through ENaC was elicited by voltage ramping from 20 to -140 mV over a 300 ms period. At the end of each recording, 10 μM amiloride was added to identify amiloride-sensitive currents. ENaC activity was assessed as the amiloride-sensitive current.

Systematic Review of Published Studies Regarding Liddle Syndrome Patients Carrying SCNN1G Mutations

We systematically searched MEDLINE (*via* PubMed), Embase, Cochrane, and Web of Science databases for relevant articles

TABLE 1 | Clinical, biochemical characteristics and results of follow-up of patients in this family.

Cases	Sex	Age (years)	Max BP (mmHg)	Serum K + (mmol/L)	Follow-up at 1 month		Follow-up at 7 years							
					BP (mmHg)	Serum K + (mmol/L)	BP (mmHg)	Serum K + (mmol/L)	Creatinine (μmol/L)	Urea nitrogen (mmol/L)	LVEDD (mm)	IVS thickness	LVEF (%)	Events
I-1	F	78	176/106	2.83	134/78	4.22	NA	NA	NA	NA	NA	NA	NA	No
II-1	F	58	194/116	2.76	126/80	4.59	110–130/82–90	3.62–4.9	89.68	6.20	60	11	55	No
II-2	M	54	210/120	2.00	130/74	4.22	128–136/78–84	4.51–4.66	74.41	5.20	49	12	69	Previous Stroke
II-3	M	32	NA	NA	NA	NA	NA	NA	NA	NA	NA	NA	NA	Death
III-1	F	31	140/110	2.62	138/76	3.92	112–129/80–92	3.80–4.55	56	2.92	40	10	70	No
III-2	F	18	216/118	2.50	126/80	4.24	120–130/85–90	3.45–4.12	62	3.02	45	13	72	No
IV-1	M	7	120/72	3.32	NA	NA	102–120/60-80	3.56–4.0	108	4.85	43	10	60	No

F, female; M, male; BP, blood pressure; the reference of serum K^+: 3.5–5.5 mmol/L; the reference of creatinine: 44–133 μmol/L; the reference of urea nitrogen: 2.86–7.9 mmol/L; LVEDD, left ventricular end-diastolic dimension; IVS, interventricular septum; LVEF, left ventricular ejection fraction; NA, not available.

published in English up to December 31, 2020, with the search terms "Liddle syndrome," "Liddle's syndrome," "pseudoaldosteronism," and *SCNN1G*. Studies that reported patient clinical characteristics, outcomes as well as phenotype and genotype relation of Liddle syndrome patients carrying *SCNN1G* mutations and pathogenicity of variants were included.

Statistical Analysis

Differences in amiloride-sensitive sodium currents between wild-type and mutant ENaCs in *CHO* cells were analyzed using the unpaired *t*-test. *P*-values less than 0.05 were considered statistically significant.

RESULTS

Clinical and Biochemical Characteristics

All members participating in this study presented with varying degree of hypertension. The echocardiographic findings of the proband (III-2) suggest concentric left ventricular hypertrophy, so it is presumed that hypertension occurred earlier than 18 years old. The I-1 and II-2 were paralyzed and bedridden from hypertensive cerebral hemorrhage prior the start of the study and the II-3 was diagnosed with hypertension and died of hypertensive stroke at 32 years of age. The IV-1, a 7 years old boy, was diagnosed with hypertension for BP values (120/72 mmHg) greater than 95th percentile reference (110/71 mmHg). All participants underwent biochemical examinations, and the results are shown in **Table 1**.

Tailored Medicine for Mutation Carriers

The proband and other members diagnosed with LS were recommended to follow a low-salt diet and receive oral amiloride treatment. The blood pressures and serum potassium levels of all family members were in the normal range (**Table 1**) during follow-up period. Creatinine, urea nitrogen and the result of echocardiography were normal, and none of the family members had cardiovascular events during the 7-year period of regular treatment (**Table 1**).

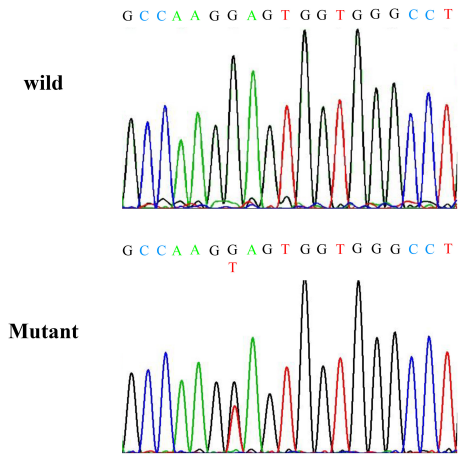

FIGURE 1 | Results of Sanger sequencing. Sanger sequencing indicates a nonsense mutation at codon position 562 of exon 13 of *SCNN1G*.

Electrophysiology

A truncation mutation in exon 13 of *SCNN1G* was identified and reported in this family and this mutation led to a stop codon after glutamic acid (Glu) (p.Glu571*; c.1171G > T; **Figure 1**). We compared amiloride-sensitive sodium currents in p.Glu571* mutant and wild-type *CHO* cells. The amiloride-sensitive currents of the mutant control group were 3.7 times of the wild-type control group (3.7 vs. 1.0, $P < 0.05$; **Figure 2A**). After cells were incubated for 48 h after the addition of amiloride, we detected and compared the current changes in wild-type and mutant ENaCs cells. There was a significant difference between the mutant control and mutant amiloride-added groups (152.4 ± 41.6 pA/pF vs. 84.2 ± 26.3 pA/p, $P = 0.013$), indicating

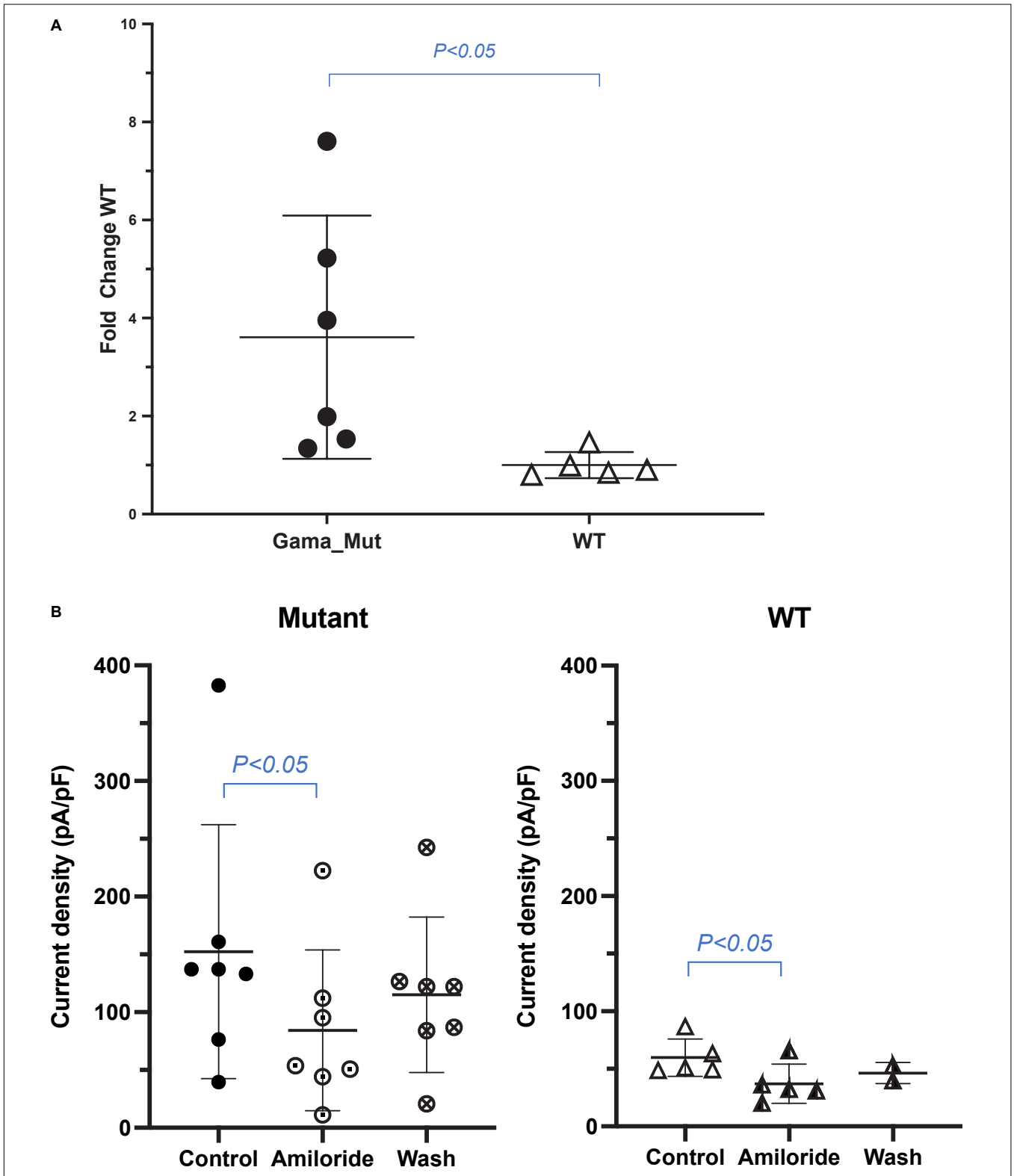

FIGURE 2 | (A) Sodium current between wild and mutant group. Amiloride-sensitive sodium current was increased in CHO expressing mutant ENaC compared with those expressing wild type channels. Values are significantly different between wild type. **(B)** Amiloride inhibition of sodium current in wild and mutant group. Amiloride-sensitive sodium current was decreased in *CHO* of mutant ENaC after adding amiloride compared with controlled group. Values are significantly different between with amiloride and without amiloride ($P < 0.05$).

that the sodium current was inhibited by amiloride, an ENaC inhibitor (**Figure 2B**).

Results of Systematic Review

According to the search strategy, A total of 29 patients from 7 families, and 3 sporadic patients harbored different mutations were included (**Table 2**). Ten *SCNN1G* mutations, including 4 nonsense mutations, 3 missense mutations, and 3 frameshift mutations were found, 3 of them were validated for pathogenicity by patch-clamp monitoring of amiloride-sensitive sodium currents. Except for the patients with missing blood pressure values, all other patients were diagnosed with hypertension. Among included patients, 69% had hypokalemia, 38% had suppressed PAC, and 79% had suppressed PRA. Four patients (14%) had cerebrovascular events.

DISCUSSION

In this study, the pathogenicity of a nonsense mutation (c.1171 G > T) in *SCNN1G* was confirmed by functional experiments. The blood pressure and electrolyte concentrations of LS patients in this family returned to normal after 1 month of amiloride treatment, and no target organ damage and cardiovascular events occurred over a 7-year follow-up.

LS is a rare autosomal dominant disease, the prevalence reported as 0.91 and 1.52%, respectively (2, 17). LS is caused by mutations in *SCNN1A*, *SCNN1B*, and *SCNN1G*, which encode ENaCs in kidney tubules, affecting sodium reabsorption (18). Proline-rich segments in the C terminals of β and γ subunits, which are critical for function, are known as PY motifs (19). The ubiquitin ligase NEDD4 binds to ENaC PY motifs, leading to the ubiquitination and degradation of ENaC (20). Mutations typically prevent the ubiquitination of subunits, thus inhibiting the rate at which they are internalized from the membrane, resulting in increased ENaC enrichment and elevated channel activity (3). However, a minority of mutations increase ENaC activity by changing the open probability in the membrane (20, 21). In 2017, a *SCNN1A* mutation, a gain-of-function mutation in the extracellular domain of the α subunit, was reported, which primarily increased channel open probability rather than channel surface density (8). By altering ENaC activity, sodium reabsorption increases, which leads to volume expansion and hypertension.

There are 29 mutation sites linked to LS, and nearly all mutations delete or alter PY motifs, and include frameshift, nonsense, or missense mutations (12, 20, 22–24). Among the *SCNN1G* genetic spectrum, 10 sites have been detected (3, 13, 22, 23), including four nonsense mutations, three missense mutations, and three frameshift mutations (**Table 2**). The first identified *SCNN1G* mutation was a nonsense mutation (p.Trp573*) reported by Hansson et al.; *Xenopus oocytes* expressing mutant p.Trp573* displayed 7.5-fold increase in amiloride-sensitive sodium current than wild-type (25). In the following years, a nonsense mutation site (p.Trp575*) was detected in a sporadic case with hypertension in Japan (26), and Shi et al. and Zhang et al. reported a p.Gln567* mutation in a Chinese family and sporadic case, respectively (27, 28). However, pathogenic functional experiments were not conducted for the p.Gln567* mutation. Three frame mutations and one missense site have been reported in different families, and their clinical features are summarized in **Table 2**. Most mutation sites impact PY motifs, except for p.Asn530Ser. The p.Asn530Ser mutation is in the extracellular domain and does not influence the PY motif, but it does cause an LS phenotype (21). In patch-clamp experiments, the p.Asn530Ser mutation presented twofold higher amiloride-sensitive currents compared with the wild type, by increasing the open probability of channels (21). The p.Glu571* mutation was first reported by our team in a Chinese family, and this variant has also been identified in another Chinese family (2, 17). In the present functional experiments, cells with the p.Glu571* mutation displayed 3.7-fold amiloride-sensitive currents of wild-type cells.

LS is a kind of channelopathy, and patch-clamp experiments are very important for verifying ion channel diseases. According to previous research, pathogenic mutations in *SCNN1G* mostly affect the PY motif, but pathogenicity has only been functionally verified in three sites. The physiological characteristics of ENaCs expressed in *Xenopus oocytes* are similar to those of ENaCs in human distal renal tubules (29); thus, functional experiments usually use *Xenopus oocytes* for detecting current variations in patch-clamp experiments. In the present study, however, we use *CHO* cells to detect current variations. *CHO* cells are used in patch-clamp electrophysiological experiments because of their low endogenous expression of ion channels (30). Amiloride-sensitive-sodium currents were suppressed after adding amiloride in the present study, indicating drug efficacy from an ion channel aspect. Different variants display different degrees of amiloride-induced sodium current changes, which may be associated with the effects of mutation sites on PY motifs and the cell model. Compared with extracellular domain mutations, PY motif mutations expressed higher amiloride-sensitive currents, indicating that PY motif mutations have a greater impact on ENaC activity.

Phenotypes vary greatly in patients harboring different mutations, as well as for the same mutation in a pedigree (**Table 2**). A systematic review conducted in 2018 reported that 92.4% of patients with LS presented hypertension (3). In the current pedigree, all members carrying the p.Glu571* variant presented hypertension, and some even had hypertensive stroke. Moreover, one of the typical features of LS is early-onset hypertension; most patients develop hypertension before 30 years. The youngest reported patients are a 10-week-old baby, who was a sporadic case, and a 2-year-old child from an LS family (9, 31). According to the largest retrospective analysis of LS patients, the average onset age of hypertension is 15.5 ± 3.3 years (7). In our research, the index case was diagnosed with hypertension at 18 years old with left ventricular concentric hypertrophy. We speculated that the proband probably had hypertension in child, and she had no obvious symptoms and had not been diagnosed in time. Another 7-year-old pediatric patient had hypertension, hypokalemia, and no target organ damage, as well he had no obvious symptoms and his onset age is unclear.

TABLE 2 | Results of systematic review of published studies regarding LS patients carrying SCNN1G mutations.

Mutation sites	Pedigree sporadic cases	Subjects	Sex	Onset of age (years)	Stroke	BP (mmHg)	Hypokalemia	Suppression of PAC	Suppression of PRA	Vitro studies	Amiloride-sensitive current
p.Asn530Ser	Family	Case1	M	25	No	180/120	Yes	Yes	Yes	*Xenopus oocytes*	2.0-fold
		Case2	F	40	No	160/105	Yes	NA	Yes		
p.Gln567*	Family	Case1	M	20	No	180/120	Yes	Yes	Yes	NA	NA
		Case2	M	NA	No	NA	NA	NA	NA		
		Case3	M	NA	No	191/118	NA	NA	NA		
p.Glu571*	Family	Case1	F	18	No	216/118	Yes	No	Yes	*CHO* cells	3.7-fold
		Case2	F	31	Yes	176/106	Yes	No	Yes		
		Case3	M	19	Yes	210/120	Yes	No	Yes		
		Case4	F	18	No	140/110	Yes	No	Yes		
		Case5	M	NA	Yes	NA	NA	NA	NA		
		Case6	M	7	No	120/72	Yes	No	Yes		
p.Trp573*	Family	Case1	F	17	No	180/106	Yes	Yes	Yes	*Xenopus oocytes*	7.5-fold
		Case2	F	22	No	150/100	Yes	No	Yes		
		Case3	M	15	No	147/90	No	No	Yes		
		Case4	M	12	No	187/114	Yes	Yes	Yes		
		Case5	F	26	No	160/110	Yes	No	Yes		
		Case6	F	26	No	170/110	Yes	No	Yes		
p.Trp575*	Sporadic	Case1	F	14	No	156/108	Yes	Yes	Yes	NA	NA
p.Glu583Aspfs*585	Sporadic	Case1	M	13	No	NA	Yes	No	Yes	NA	NA
p.Gly590Alafs	Family	Case1	M	12	No	159/109	Yes	No	Yes	NA	NA
		Case2	F	14	No	160/100	No	Yes	Yes		
p.Arg586Valfs*598	Family	Case1	F	NA	No	120/86	No	No	No	NA	NA
		Case2	M	19	No	180/110	No	Yes	Yes		
		Case3	M	14	No	190/120	No	Yes	Yes		
p.Pro625Leu	Family	Case1	M	14	No	160/100	No	No	No	NA	NA
		Case2	F	28	Yes	180/110	Yes	Yes	Yes		
		Case3	M	30	No	180/120	Yes	Yes	Yes		
		Case4	M	3	No	120/80	Yes	Yes	Yes		
p.Pro625Arg	Sporadic	Case1	M	13	No	>140/90	Yes	NA	NA	NA	NA

*F, female; M, male; BP, blood pressure; CHO, Chinese Hamster Ovary; PRA, plasma renin activity; PAC, plasma aldosterone concentration. *PRA and *PAC were tested after being kept in a standing position for 2 h; NA, not available.*

The remaining family members diagnosed with hypertension are almost less than 30 years old.

In this family, there was heterogeneity not only in the occurrence of high blood pressure, but also in the severity of hypertension and complications. Reported complications of persistent hypertension in LS patients include cerebrovascular accidents, early death, renal insufficiency, nose bleeds, and retinal damage (7, 12, 32). Cerebrovascular accidents before the age of 40 were common in this LS family, especially stroke, which causes a heavy burden to patients and their families. The reason for the high incidence of stroke in this family may include poor management of blood pressure, genotype, and environmental factors.

Hypokalemia is present in 71.8% of cases of LS (3). In the current study, all mutation-carrying participants exhibited hypokalemia. Tamura et al. and Fan Peng et al. reached a similar conclusion: that some LS patients have hypertension but exhibit normokalemia (13, 33). The suppression of PRA and PAC is considered a typical presentation, and can be used to differentiate other possible causes of secondary hypertension (34). In our study, all members presented with suppression of PRA, which is in line with the typical characteristics of LS. However, the PAC levels of all members were within the normal range, and members harboring the same variant in another LS pedigree also presented normal PAC (17). The presentation of PAC shows clear heterogeneity compared with other variant-related phenotypes. The reasons for the heterogeneity of LS may be related to aspects including environmental factors and gene polymorphisms. LS patients with *SCNN1A* mutation may presented with mild phenotype than typical LS, which may attribute to different pathogenetic mechanisms (8). Therefore, for patients with suspected LS phenotype but milder symptoms, the possibility of carrying *SCNN1A* mutation should be considered.

Clinical presentations and laboratory findings in LS are heterogeneous, which can hamper its diagnosis. Family history can provide clues, and combined with early-onset hypertension

and laboratory results, can be used to identify suspected LS patients. Inadequate symptoms and insufficient awareness of children with monogenic hypertension leading to fail to intervene in time, and most of them have developed complications in youth (12). According to the previous study, 90% pediatric patients had LS family history, so genetic screening can provide definitive confirmation of adult, and pediatric LS (22, 35). Additionally, investigation of the pathogenicity of variants based on amiloride-sensitive currents is needed.

There were several limitations in the present study. This site was not a novel mutation—it has been briefly mentioned in a review by our team. Furthermore, we only compared the amiloride-sensitive sodium currents of γGlu571* mutations with wild-type channels, and not with other truncation mutations of the γ subunit, which may explain the heterogeneous results to some extent. The tailored treatment with amiloride efficacy in blood pressure control and avoiding cardiovascular events has only been validated in the long-term follow-up results of this family, which cannot be representative of all LS patients. A cohort study of LS patients is needed to explore the efficacy of amiloride in improving prognosis and blood pressure control.

CONCLUSION

In conclusion, wen identified the pathogenicity of a nonsense mutation by functional analysis. This discovery not only expands the spectrum of *SCNN1G* mutations, but also increases the pathogenicity grades. Tailored treatment with amiloride may be an effective treatment for long-term blood pressure management and preventing cardiovascular events, so timely intervention makes a difference for adult and pediatric patients.

DATA AVAILABILITY STATEMENT

The original contributions presented in the study are included in the article/supplementary material, further inquiries can be directed to the corresponding author/s.

ETHICS STATEMENT

The studies involving human participants were reviewed and approved by the Fuwai Hospital, National Center for Cardiovascular Diseases. Written informed consent to participate in this study was provided by the participants' legal guardian/next of kin.

AUTHOR CONTRIBUTIONS

DZ, Y-XL, and X-LZ designed the study and modified the manuscript. DZ, YQ, X-QD, C-XY, and X-CL collected clinical information and performed data analysis. DZ, Y-TL, K-QY, PF, YX-H, and L-GG performed experiments. DZ wrote the manuscript. All authors reviewed this work.

FUNDING

This work was supported by the National Key Research and Development Program of China (2016YFC1300100), the National Natural Science Foundation of China (81974042), and the Non-profit Central Research Institute Fund of Chinese Academy of Medical Sciences (2019XK320058 and 2019XK320057).

ACKNOWLEDGMENTS

We thank all participants for taking part in this study and agencies that aided the efforts of the authors.

REFERENCES

1. Liddle GW. A familial renal disorder stimulating primary aldosteronism but with negligible aldosterone secretion. *Trans Assoc Am Physicians.* (1963) 76:199–213.
2. Wang LP, Yang KQ, Jiang XJ, Wu HY, Zhang HM, Zou YB, et al. Prevalence of liddle syndrome among young hypertension patients of undetermined cause in a Chinese population. *J Clin Hypertens (Greenwich).* (2015) 17:902–7. doi: 10.1111/jch.12598
3. Tetti M, Monticone S, Burrello J, Matarazzo P, Veglio F, Pasini B, et al. Liddle syndrome: review of the literature and description of a new case. *Int J Mol Sci.* (2018) 19:812. doi: 10.3390/ijms19030812
4. Staub O, Abriel H, Plant P, Ishikawa T, Kanelis V, Saleki R, et al. Regulation of the epithelial Na^+ channel by Nedd4 and ubiquitination. *Kidney Int.* (2000) 57:809–15. doi: 10.1046/j.1523-1755.2000.00919.x
5. Zhou R, Kabra R, Olson DR, Piper RC, Snyder PM. Hrs controls sorting of the epithelial Na^+ channel between endosomal degradation and recycling pathways. *J Biol Chem.* (2010) 285:30523–30. doi: 10.1074/jbc.M110.150755
6. Botero-Velez M, Curtis JJ, Warnock DG. Brief report: Liddle's syndrome revisited–a disorder of sodium reabsorption in the distal tubule. *N Engl J Med.* (1994) 330:178–81. doi: 10.1056/NEJM199401203300305
7. Cui Y, Tong A, Jiang J, Wang F, Li C. Liddle syndrome: clinical and genetic profiles. *J Clin Hypertens (Greenwich).* (2017) 19:524–9. doi: 10.1111/jch.12949
8. Salih M, Gautschi I, van Bemmelen MX, Di Benedetto M, Brooks AS, Lugtenberg D, et al. A missense mutation in the extracellular domain of alphaenac causes Liddle syndrome. *J Am Soc Nephrol.* (2017) 28:3291–9. doi: 10.1681/ASN.2016111163
9. Findling JW, Raff H, Hansson JH, Lifton RP. Liddle's syndrome: prospective genetic screening and suppressed aldosterone secretion in an extended kindred. *J Clin Endocrinol Metab.* (1997) 82:1071–4. doi: 10.1210/jcem.82.4.3862
10. Rayner BL, Owen EP, King JA, Soule SG, Vreede H, Opie LH, et al. A new mutation, R563q, of the beta subunit of the epithelial sodium channel associated with low-renin, low-aldosterone hypertension. *J Hypertens.* (2003) 21:921–6. doi: 10.1097/00004872-200305000-00016
11. Fan P, Lu CX, Zhang D, Yang KQ, Lu PP, Zhang Y, et al. Liddle syndrome misdiagnosed as primary aldosteronism resulting from a novel frameshift mutation of Scnn1b. *Endocr Connect.* (2018) 7:1528–34. doi: 10.1530/EC-18-0484
12. Fan P, Zhang D, Pan XC, Yang KQ, Zhang QY, Lu YT, et al. Premature stroke secondary to severe hypertension results from liddle syndrome caused

by a novel Scnn1b mutation. *Kidney Blood Press Res.* (2020) 45:603–11. doi: 10.1159/000507580
13. Fan P, Zhao YM, Zhang D, Liao Y, Yang KQ, Tian T, et al. A Novel frameshift mutation of Scnn1g causing Liddle syndrome with normokalemia. *Am J Hypertens.* (2019) 32:752–8. doi: 10.1093/ajh/hpz053
14. Fan P, Lu CX, Yang KQ, Lu PP, Hao SF, Luo F, et al. Truncated epithelial sodium channel beta subunit responsible for Liddle syndrome in a Chinese family. *Kidney Blood Press Res.* (2019) 44:942–9. doi: 10.1159/000500919
15. Flynn JT, Kaelber DC, Baker-Smith CM, Blowey D, Carroll AE, Daniels SR, et al. Clinical practice guideline for screening and management of high blood pressure in children and adolescents. *Pediatrics.* (2017) 140:e20171904. doi: 10.1542/peds.2017-1904
16. Ilatovskaya DV, Pavlov TS, Levchenko V, Negulyaev YA, Staruschenko AJTFJ. Cortical actin binding protein cortactin mediates enac activity via Arp2/3 complex. *FASEB J.* (2011) 25:2688–99. doi: 10.1096/fj.10-167262
17. Liu K, Qin F, Sun X, Zhang Y, Wang J, Wu Y, et al. Analysis of the genes involved in mendelian forms of low-renin hypertension in Chinese early-onset hypertensive patients. *J Hypertens.* (2018) 36:502–9. doi: 10.1097/HJH.0000000000001556
18. Rossier BC. Epithelial sodium channel (Enac) and the control of blood pressure. *Curr Opin Pharmacol.* (2014) 15:33–46. doi: 10.1016/j.coph.2013.11.010
19. Schild L, Lu Y, Gautschi I, Schneeberger E, Lifton RP, Rossier BC. Identification of a Py motif in the epithelial na channel subunits as a target sequence for mutations causing channel activation found in Liddle syndrome. *Embo J.* (1996) 15:2381–7. doi: 10.1002/j.1460-2075.1996.tb00594.x
20. Enslow BT, Stockand JD, Berman JM. Liddle's syndrome mechanisms, diagnosis and management. *Integr Blood Press Control.* (2019) 12:13–22. doi: 10.2147/IBPC.S188869
21. Hiltunen TP, Hannila-Handelberg T, Petajaniemi N, Kantola I, Tikkanen I, Virtamo J, et al. Liddle's syndrome associated with a point mutation in the extracellular domain of the epithelial sodium channel gamma subunit. *J Hypertens.* (2002) 20:2383–90. doi: 10.1097/01.hjh.0000042881.24999.fc
22. Fan P, Pan XC, Zhang D, Yang KQ, Zhang Y, Tian T, et al. Pediatric Liddle syndrome caused by a novel Scnn1g variant in a chinese family and characterized by early-onset hypertension. *Am J Hypertens.* (2020) 33:670–5. doi: 10.1093/ajh/hpaa037
23. Lata S, Marasa M, Li Y, Fasel DA, Groopman E, Jobanputra V, et al. Whole-exome sequencing in adults with chronic kidney disease: a pilot study. *Ann Intern Med.* (2018) 168:100–9. doi: 10.7326/M17-1319
24. Brower RK, Ghlichloo IA, Shabgahi V, Elsholz D, Menon RK, Vyas AK. Liddle syndrome due to a novel C.1713 deletion in the epithelial sodium channel beta-subunit in a normotensive adolescent. *AACE Clin Case Rep.* (2021) 7:65–8. doi: 10.1016/j.aace.2020.11.017
25. Hansson JH, Nelson-Williams C, Suzuki H, Schild L, Shimkets R, Lu Y, et al. Hypertension caused by a truncated epithelial sodium channel gamma subunit: genetic heterogeneity of Liddle syndrome. *Nat Genet.* (1995) 11:76–82. doi: 10.1038/ng0995-76
26. Yamashita Y, Koga M, Takeda Y, Enomoto N, Uchida S, Hashimoto K, et al. Two sporadic cases of Liddle's syndrome caused by de novo enac mutations. *Am J Kidney Dis.* (2001) 37:499–504. doi: 10.1053/ajkd.2001.22072
27. Shi JY, Chen X, Ren Y, Long Y, Tian HM. [Liddle's syndrome caused by a novel mutation of the gamma-subunit of epithelial sodium channel gene Scnn1g in Chinese]. *Zhonghua Yi Xue Yi Chuan Xue Za Zhi.* (2010) 27:132–5. doi: 10.3760/cma.j.issn.1003-9406.2010.02.003
28. Zhang P, Kong LQ, Huang DJ. [Liddle syndrome complicating with nonfunctional adrenal cortical adenoma: a case report]. *Zhonghua Xin Xue Guan Bing Za Zhi.* (2017) 45:331–2. doi: 10.3760/cma.j.issn.0253-3758.2017.04.015
29. Canessa CM, Schild L, Buell G, Thorens B, Gautschi I, Horisberger JD, et al. Amiloride-sensitive epithelial Na^+ channel is made of three homologous subunits. *Nature.* (1994) 367:463–7. doi: 10.1038/367463a0
30. Gamper N, Stockand JD, Shapiro MS. The use of Chinese hamster ovary (Cho) cells in the study of ion channels. *J Pharmacol Toxicol Methods.* (2005) 51:177–85. doi: 10.1016/j.vascn.2004.08.008
31. Assadi FK, Kimura RE, Subramanian U, Patel S. Liddle syndrome in a newborn infant. *Pediatr Nephrol.* (2002) 17:609–11. doi: 10.1007/s00467-002-0897-z
32. Gong L, Chen J, Shao L, Song W, Hui R, Wang Y. Phenotype-genotype analysis in two Chinese families with Liddle syndrome. *Mol Biol Rep.* (2014) 41:1569–75. doi: 10.1007/s11033-013-3003-7
33. Tamura H, Schild L, Enomoto N, Matsui N, Marumo F, Rossier BC. Liddle disease caused by a missense mutation of beta subunit of the epithelial sodium channel gene. *J Clin Invest.* (1996) 97:1780–4. doi: 10.1172/JCI118606
34. Mumford E, Unwin RJ, Walsh SB. Liquorice, Liddle, Bartter or Gitelman-how to differentiate? *Nephrol Dial Transplant.* (2019) 34:38–9. doi: 10.1093/ndt/gfy199
35. Büyükkaragöz B, Yilmaz AC, Karcaaltincaba D, Ozdemir O, Ludwig M. Liddle syndrome in a Turkish family with heterogeneous phenotypes. *Pediatr Int.* (2016) 58:801–4. doi: 10.1111/ped.12985

Conflict of Interest: The authors declare that the research was conducted in the absence of any commercial or financial relationships that could be construed as a potential conflict of interest.

Publisher's Note: All claims expressed in this article are solely those of the authors and do not necessarily represent those of their affiliated organizations, or those of the publisher, the editors and the reviewers. Any product that may be evaluated in this article, or claim that may be made by its manufacturer, is not guaranteed or endorsed by the publisher.

frontiers | Frontiers in Pediatrics

CASE REPORT
published: 25 May 2022
doi: 10.3389/fped.2022.855210

Case Report: Dubin-Johnson Syndrome Presenting With Infantile Cholestasis: An Overlooked Diagnosis in an Extended Family

Naglaa M. Kamal[1], Omar Saadah[2], Hamdan Alghamdi[3], Ali Algarni[4], Mortada H. F. El-Shabrawi[1], Laila M. Sherief[5] and Salma A. S. Abosabie[6]*

[1] Department of Pediatrics and Pediatric Hepatology, Faculty of Medicine, Cairo University, Cairo, Egypt, [2] Department of Pediatrics, Faculty of Medicine, King Abdulaziz University, Jeddah, Saudi Arabia, [3] Department of Pediatrics, Alhada Armed Forces Hospital, Taif, Saudi Arabia, [4] Department of Pediatrics, Taif Children Hospital, Taif, Saudi Arabia, [5] Faculty of Medicine, Zagazig University, Zagazig, Egypt, [6] Faculty of Medicine, Julius-Maximilians-Universität Würzburg, Würzburg, Germany

Dubin-Johnson syndrome (DJS) is an often-missed diagnosis of neonatal cholestasis. We report two patients with DJS, who presented with neonatal cholestasis. The first patient underwent extensive investigations for infantile cholestasis with no definitive etiology reached; the diagnosis of DJS was missed until the age of 14 years old. The diagnosis was confirmed genetically with c.2273G > T, p.G758V mutation in exon 18 of the ABCC2 gene. The 2nd patient is a 7-day-old baby, the son of the 1st patient who gave birth to him at the age of 21 years old. He was diagnosed with DJS at the age of 2 weeks based on normal clinical and laboratory workup apart from direct hyperbilirubinemia. He had the same mutation as his mother in homozygous status. The husband was heterozygous for the same mutation. DJS is one of the often-missed differential diagnoses of neonatal cholestasis. It should be suspected in patients of infantile cholestasis, who have an, otherwise, normal physical examination, and laboratory investigations to avoid unnecessary lengthy, invasive, and expensive workups.

Keywords: Dubin-Johnson syndrome, infant, cholestasis, ABCC2 gene, mutation

OPEN ACCESS

Edited by:
Pietro Vajro,
University of Salerno, Italy

Reviewed by:
Patryk Lipiński,
Children's Memorial Health Institute (IPCZD), Poland
Giulia Paolella,
Ca' Granda Foundation Maggiore Policlinico Hospital (IRCCS), Italy

****Correspondence:***
Naglaa M. Kamal
Nagla.Kamal@medicine.cu.edu.eg

Specialty section:
This article was submitted to Genetics of Common and Rare Diseases, a section of the journal Frontiers in Pediatrics

Received: *14 January 2022*
Accepted: *31 March 2022*
Published: *25 May 2022*

Citation:
Kamal NM, Saadah O, Alghamdi H, Algarni A, El-Shabrawi MHF, Sherief LM and Abosabie SAS (2022) Case Report: Dubin-Johnson Syndrome Presenting With Infantile Cholestasis: An Overlooked Diagnosis in an Extended Family. Front. Pediatr. 10:855210. doi: 10.3389/fped.2022.855210

INTRODUCTION

Dubin-Johnson syndrome (DJS) was first reported in 1954 by Dubin and Johnson (1) as a rare autosomal recessive disease with clinical features of chronic-conjugated hyperbilirubinemia due to a defect in the excretion of the anionic conjugate from the hepatocytes into the bile (2). Most patients manifest as intermittent or chronic jaundice aggravated by intercurrent illness (1). Physical examination is frequently unremarkable (1). Liver enzymes are usually within normal limits, while bilirubin levels fluctuate (1).

The syndrome occurs due to expression defects of the MRP2 gene, an ATP-dependent canalicular membrane transporter (3–5). The diagnosis is established by performing the bromsulphalein test, oral cholecystography, HIDA scan, and liver biopsy (6–8). Liver biopsy is the

Abbreviations: DJS, Dubin-Johnson syndrome.

gold standard diagnostic test for this syndrome. It shows the presence of brown pigment granules in the centrilobular hepatocytes (9–11). Molecular genetic testing of the ABCC2 gene is the definitive diagnosis (12). We, herein, report a Saudi female child who presented as having cholestasis at the age of 1 month with a missed diagnosis of DJS until the age of 14 years. Her molecular genetic testing revealed the c.2273G > T, p.G758V mutation in Exon 18 of the ABCC2 gene.

CASE REPORT

A 14-year-old female child was born to consanguineous Saudi first-degree cousins who are descents from a tribe with highly consanguineous marriage. She was referred to a pediatric gastroenterology clinic as a case of persistent conjugated hyperbilirubinemia for investigations.

Tracing her history revealed that jaundice started at the age of 4 days with elevated total bilirubin (350 μmol/L), mainly indirect. Her direct bilirubin was 30 μmol/L with normal alanine and aspartate transaminases (ALT and AST). Phototherapy was started, and the patient was discharged in good condition after 3 days.

She returned to her primary physician at the age of 40 days with unresolved jaundice and mild abdominal distension with no organ enlargement. Her investigations revealed mild direct hyperbilirubinemia. Her total and direct bilirubins were 50 and 35 μmol/L, respectively. Her ALT, AST, gamma-glutamyl transpeptidase (GGT), prothrombin time/concentration, and abdominal ultrasonography were all normal. Extensive workups of cholestasis, including complete blood count, retics, coombs, hemoglobin electrophoresis, urine and blood cultures, TORCH screening, serum bile acids, thyroid profile, tandem metabolic screening, and non-glucose-reducing substances in the urine, were all normal. HIDA scan and MRCP were not available in that hospital and were not done. Liver biopsy was refused by the parents, and she was discharged against medical advice in good general condition without a definitive diagnosis. Her total and direct bilirubin at time of discharge was 48 and 40 μmol/L, respectively.

Since that time and until her presentation to our care at the age of 14 years, the parents used to visit different health care facilities when their child's jaundice deepened with different intercurrent illnesses. Laboratory workups, including liver function tests and hepatitis markers, were done many times with normal results apart from direct hyperbilirubinemia.

On presentation to our hospital, she had tinge jaundice with stable vital signs, normal abdominal examination with no organomegaly, and normal assessment of different body systems. Her laboratory investigation showed high total bilirubin of 32 μmol/L, mainly in the form of direct bilirubin (31 μmol/L), with normal ALT, AST, GGT, complete blood picture, and a renal profile with normal abdominal US. The diagnosis of DJS was suspected, and a 99^{m} Tc-HIDA scan was requested. The HIDA scan serial images revealed rapid clearance of blood pool activity with a good hepatocyte function as evidenced by the adequate ascending limb of the dynamic curve. However, there was a slow excretion of radioactivity into the biliary radicles with retained activity in the liver up to 6 h. The gall bladder was seen at 1 h and the small intestine at 2 h. This good hepatocyte uptake function with impairment of excretory function in absence of obstruction was highly suggesting DJS. Urinary coproporphyrins were not done (the test was not available in our hospital).

Molecular genetic testing for DJS, the ABCC2 gene, was requested to confirm the diagnosis.

MOLECULAR GENETIC ANALYSIS OF THE ABCC2 GENE

PCR amplification and direct sequencing of all coding exons and flanking intronic sequence (ABCC2 gene, GenBank NM_000392.3, NC_000010.10) gene dosage analysis by quantitative real-time PCR (qPCR) with 5 amplifications (in exons 1, 7, 15, 24, and 32) (13).

RESULTS

Unclassified variant c.2273G⟩T, pG785V in Exon 18 of the gene ABCC2 gene in the homozygous state. By qPCR, no deletion or duplication was detected, **Figure 1**.

INTERPRETATION

Molecular analysis confirmed the clinical suspicion of DJS syndrome. The variant c.2273G⟩T, pG785V in Exon 18 of the gene ABCC2 gene was detected in homozygous state.

The patient was diagnosed in 2014, and, at that time, this mutation was a novel mutation, which has not been described yet (HGMD professional 2014.2). "Polyphen2" (14) predicts the consequence of pG785V for the ABCC2 protein as "probably damaging" and "mutation taster" (15) called the variant "disease-causing" At that time, we assumed that the variant represented a pathogenic mutation, but the parents' missed follow-up with their child, and we failed to outreach to them to get consent for publication. Hence, we could not publish our case report at the time of detection of the novel mutation.

In October 2021, the parents presented to us once again with the patient who was a 21-year young adult female. She got married to her cousin, and she experienced an intermittent deepening of her jaundice during pregnancy with no associated pruritus or dark urine. Her liver biochemistry was within normal values apart from direct hyperbilirubinemia.

She gave birth to a 3.5 kg male baby by normal vertex delivery with uneventful antenatal and perinatal histories. Her baby developed jaundice at the age of 1 week with no history of pallor, blood transfusion, or medications intake.

At the age of 4 weeks, she thought about our medical advice for her newly born jaundiced baby. On assessment, his physical examination was normal apart from mild jaundice with no organomegaly. His workup was assuring with normal abdominal ultrasound, ALT, AST, albumin, prothrombin

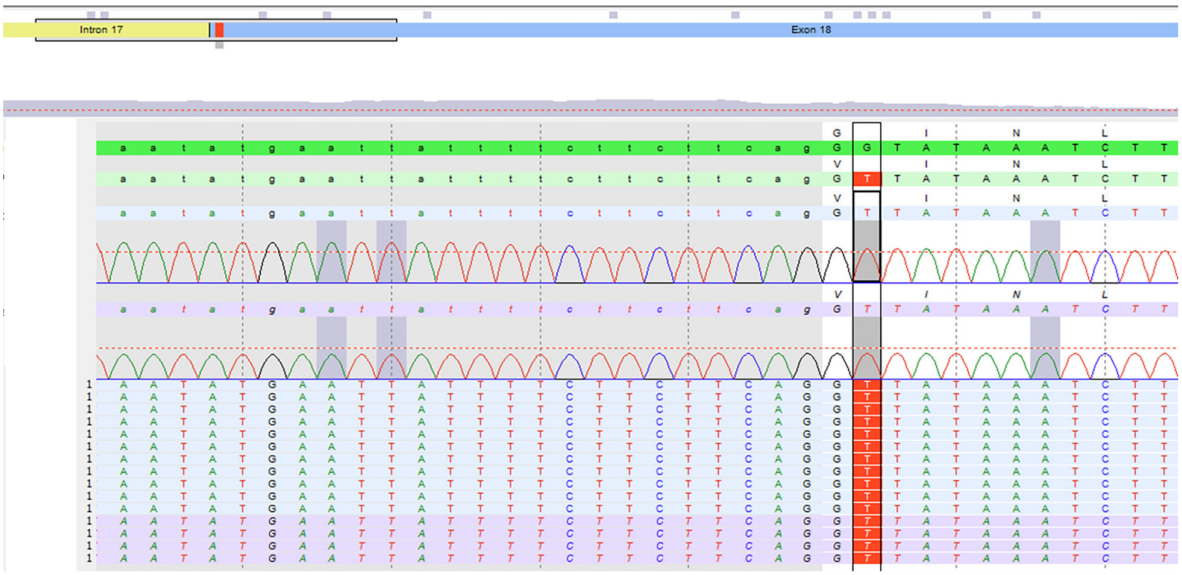

FIGURE 1 | Molecular genetic testing of the patient.

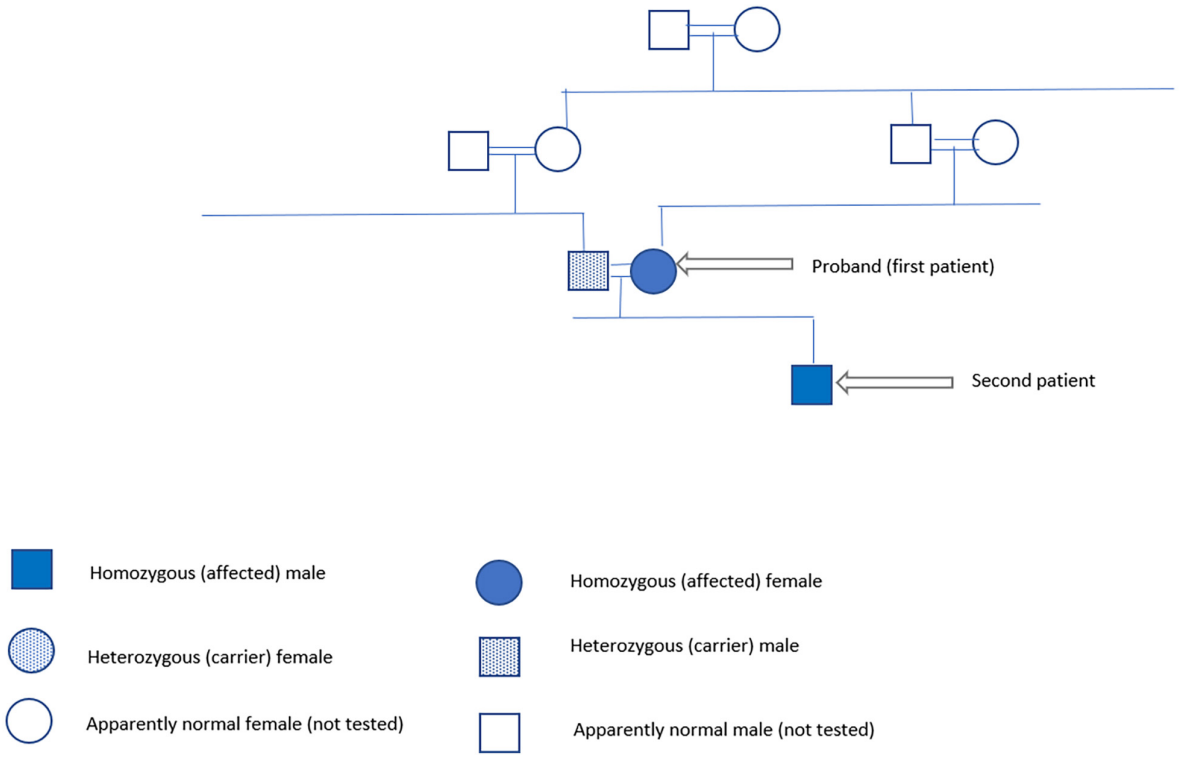

FIGURE 2 | Family pedigree.

time/concentration, and GGT with a high total bilirubin of 78 μmol/L and high direct bilirubin of 43 μmol/L, suggesting the diagnosis of DJS.

Sanger sequencing of the p.G785V variant detected in his mother was performed for him, which came out to be positive. The husband was also tested and was heterozygous for the same mutation.

In January 2022, we got the consent of the patient and her husband for publishing their family case series. The family pedigree is illustrated in **Figure 2**.

DISCUSSION

Dubin-Johnson syndrome is a rare hereditary disease, inherited as autosomal recessive inheritance mainly, but some cases with an autosomal dominant mode of transmission had been reported (10, 11). The first description of the disease was in 1954 (1). It occurs most commonly in Iranian Jews 1:1,300 (16).

Many cases were reported worldwide with the ABCC2 gene mutation (17). Our patient was the first to be detected with c.2273G > T; p.Gly758Val mutation in Exon 18 of the ABCC2 gene, which was in 2014. The patient presented to us 7 years later with her baby having cholestasis, and molecular genetic testing of the same DJS mutation detected in her was tested in her baby and her husband, who were positive to the same mutation in homozygous and heterozygous states, respectively.

Two reports were released from Saudi Arabia, one with a large series of 28 genetically proven cases with DJS (18) and the other one with one non-genetically proven case (19). Twenty-three out of the 28 patients of Al-Hussaini series had the same mutation detected in our family (18).

Patients with DJS have metabolic defect since birth, but it rarely presents in infancy and usually becomes more apparent in the late teens. In our reported two patients and in the series of Al-Hussaini and his colleagues, jaundice started in early infancy.

The first case was missed until the age of 14 years with extensive workup of cholestasis in infancy up to a liver biopsy with more than 20 physicians' visits afterward, but the diagnosis of DJS was overlooked. This unfortunate course reflects a lack of knowledge about DJS, which should have been the first differential diagnosis of direct hyperbilirubinemia in otherwise normal patients with unremarkable clinical and laboratory workups.

A HIDA scan is a good diagnostic modality for DJS (20, 21), and it was suggestive of the diagnosis in our patient, but molecular genetic testing is the definitive diagnosis. The homozygous variant c.2273G⟩T, pG785V in Exon 18 of the gene ABCC2 gene confirmed the diagnosis in our patient.

CONCLUSION

The presence of cholestasis in well-appearing neonates and infants, who have an otherwise normal examination with normal liver biochemical functions and hepatocytes and biliary enzymes, should alert physicians to the possibility of the diagnosis of DJS. A high index of suspicion for DJS in those patients prevents unnecessary lengthy, costly, and invasive workup. Molecular genetic testing of the ABCC2 gene is confirmatory.

DATA AVAILABILITY STATEMENT

The datasets for this article are not publicly available due to concerns regarding participant/patient anonymity. Requests to access the datasets should be directed to the corresponding author.

ETHICS STATEMENT

The studies involving human participants were reviewed and approved by IRB Committee of Alhada Armed Forces Hospital, Taif, Saudi Arabia. Written informed consent was obtained from the individual(s), and minor(s)' legal guardian/next of kin, for the publication of any potentially identifiable images or data included in this article.

AUTHOR CONTRIBUTIONS

NK diagnosed the patient, set the idea of the study, and designed the study. NK, OS, SA, LS, ME, HA, and AA reviewed literature, drafted the manuscript, and critically analyzed the data. SA, NK, HA, and AA collected patient's data. All authors reviewed and approved the manuscript for final publication.

REFERENCES

1. Dubin IN, Johnson FB. Chronic idiopathic jaundice with unidentified pigment in liver cells: new clinicopathologic entity with report of 12 cases. *Medicine.* (1954) 33:155–97. doi: 10.1097/00005792-195409000-00001
2. Kondo T, Kuchiba K, Ohtsuka Y, Yanagisawa W, Shiomura T, Taminato T. Clinical and genetic studies on Dubin-Johnson syndrome in a cluster area in Japan. *JPN J Hum Genet.* (1974) 18:378–92.
3. Cebecauerova D, Jirasek T, Budisova L, Mandys V, Volf U, Novotna Z, et al. Dual hereditary jaundice: simultaneous occurrence of mutations causing Gilbert's and Dubin-Johnson syndrome. *Gastroenterology.* (2005) 129:315–20. doi: 10.1053/j.gastro.2004.10.009
4. Paulusma CC, Kool M, Bosma PJ, Scheffer GL, Borg F, Sheper RJ, et al. A mutation in the human canalicularmultispecific organic anion transporter gene causes the Dubin-Johnson syndrome. *Hepatology.* (1997) 25:1539–42. doi: 10.1002/hep.510250635
5. Stapelbroek JM, Van Erpecum KJ, Klomp LWJ, Houwen RHJ. Liver disease associated with canalicular transport defects: current and future therapies. *J Hepatol.* (2010) 52:258–71. doi: 10.1016/j.jhep.2009.11.012
6. Kondo T, Yagy R, Kuchiba K. Dubin-Johnson syndrome in neonate. *N Engl J Med.* (1975) 292:1028–9. doi: 10.1056/nejm197505082921913
7. Rastogi A, Krishnani N, Pandey R. Dubin-Johnson syndrome, a clinicopathologic study of twenty cases. *Indian J PatholMicrobiol.* (2006) 49:500–4.
8. Dubin IN. Chronic idiopathic jaundice with a review of fifty cases. *Am J Med.* (1958) 24:268–92. doi: 10.1016/0002-9343(58)90315-2
9. Baba N, Ruppert RD. The Dubin-Johnson syndrome: electron microscopic observation of hepatic pigment–a case study. *Am J Clin Pathol.* (1972) 57:306–10. doi: 10.1093/ajcp/57.3.306
10. Sobaniec-Lotwska ME, Lebensztejn DM. Ultrastructure of Kupffer cells and hepatocytes in the Dubin-Johnson syndrome: a case report. *World J Gastroenterol.* (2006) 12:987–9. doi: 10.3748/wjg.v12.i6.987
11. Yasawy MI, Al-Karawi M, Coode P. Dubin-Johnson syndrome (black liver disease): report of two cases. *Ann Saudi Med.* (1988) 8:382–5. doi: 10.5144/0256-4947.1988.382
12. Dubin-Johnson Syndrome [DJS], # 237500. *HYPERBILIRUBINEMIA, DUBIN-JOHNSON TYPE; HBLRDJHYPERBILIRUBINEMIA II.* (2022). Available online at: https://www.omim.org/entry/237500 (accessed January 14, 2022).

13. Borozdin W, Boehm D, Leipoldt M, Wilhelm C, Reardon W, Clayton-Smith J, et al. SALL4 deletions are a common cause of Okihiro and acro-renal-ocular syndromes and confirm haploinsufficiency as the pathogenic mechanism. *Method Anal.* (2004) 41, 1–8. doi: 10.1136/jmg.2004.019901
14. PolyPhen-2. *Prediction of Functional Effects of Human nsSNPs*. (2014). Available online at: http://genetics.bwh.harvard.edu/pph2/ (accessed January 13, 2022).
15. Mutation Taster. *Mutation t@sting*. (2014). Available online at: www.mutationtaster.org (accessed January 13, 2022).
16. Tanner S. *Jaundice in Paediatric Hepatology*. Edinburgh: Churchill Livingstone (1989).
17. Kanda D, Takagi H, Kawahara Y, Yata Y, Takakusagi T, Hatanaka T, et al. Novel large-scale deletion (whole exon 7) in the ABCC2 gene in a patient with the Dubin-Johnson syndrome. *Drug Metab Pharmacokinet.* (2009) 24:464–8. doi: 10.2133/dmpk.24.464
18. Al-Hussaini A, AlSaleem B, AlHomaidani H, Asery A, Alruwaithi M, Alameer M, et al. Clinical, biochemical, and molecular characterization of neonatal-onset Dubin-Johnson syndrome in a large case series from the Arabs. *Front Pediatr.* (2021) 9:741835. doi: 10.3389/fped.2021.741835
19. Nadroo AM, Al-Zaben A, Bilan M, Baez-Giangreco A. Dubin-Johnson syndrome in a Saudi neonate. *Ann Saudi Med.* (1996) 16:695–7. doi: 10.5144/0256-4947.1996.695
20. Bar-Meir S, Baron J, Seligson U, Gottesfeld F, Levy R, Gilat T. 99mTc-HIDA cholescintigraphy in Dubin-Johnson and Rotor syndromes. *Radiology*. (1982) 142:743–6. doi: 10.1148/radiology.142.3.7063695
21. Bujanover Y, Bar-Meir S, Hayman I, Baron J. 99mTc-HIDA cholescintigraphy in children with Dubin-Johnson syndrome. *J Pediatr Gastroenterol Nutr*. (1983) 2:311–2. doi: 10.1097/00005176-198305000-00017

Conflict of Interest: The authors declare that the research was conducted in the absence of any commercial or financial relationships that could be construed as a potential conflict of interest.

Publisher's Note: All claims expressed in this article are solely those of the authors and do not necessarily represent those of their affiliated organizations, or those of the publisher, the editors and the reviewers. Any product that may be evaluated in this article, or claim that may be made by its manufacturer, is not guaranteed or endorsed by the publisher.

frontiers | Frontiers in Genetics

CASE REPORT
published: 05 July 2022
doi: 10.3389/fgene.2022.885589

Case Report: Severe Gonadal Dysgenesis Causing 46,XY Disorder of Sex Development Due to a Novel *NR5A1* Variant

Kheloud M. Alhamoudi[1], *Balgees Alghamdi*[1], *Abeer Aljomaiah*[2], *Meshael Alswailem*[1], *Hindi Al-Hindi*[3] *and Ali S. Alzahrani*[1,2]*

[1]Department of Molecular Oncology, King Faisal Specialist Hospital and Research Centre, Riyadh, Saudi Arabia, [2]Department of Medicine, King Faisal Specialist Hospital and Research Centre, Riyadh, Saudi Arabia, [3]Department of Pathology and Laboratory Medicine, King Faisal Specialist Hospital and Research Centre, Riyadh, Saudi Arabia

Mutations in the nuclear receptor subfamily 5 group A member 1 (*NR5A1*) are the underlying cause of 10–20% of 46,XY disorders of sex development (DSDs). We describe a young girl with 46,XY DSD due to a unique novel mutation of the *NR5A1* gene. An 11-year-old subject, raised as a female, was noticed to have clitromegly. She looked otherwise normal. However, her evaluation revealed a 46,XY karyotype, moderate clitromegly but otherwise normal female external genitalia, undescended atrophied testes, rudimentary uterus, no ovaries, and lack of breast development. Serum testosterone and estradiol were low, and gonadotropins were elevated. Adrenocortical function was normal. DNA was isolated from the peripheral leucocytes and used for whole exome sequencing. The results were confirmed by Sanger sequencing. We identified a novel mutation in *NR5A1* changing the second nucleotide of the translation initiation codon (ATG>ACG) and resulting in a change of the first amino acid, methionine to threonine (p.Met1The). This led to severe gonadal dysgenesis with deficiency of testosterone and anti-Müllerian hormone (AMH) secretion. Lack of the former led to the development of female external genitalia, and lack of the latter allowed the Müllerian duct to develop into the uterus and the upper vagina. The patient has a female gender identity. Bilateral orchidectomy was performed and showed severely atrophic testes. Estrogen/progesterone therapy was initiated with excellent breast development and normal cyclical menses. In summary, we describe a severely affected case of 46,XY DSD due to a novel *NR5A1* mutation involving the initiation codon that fully explains the clinical phenotype in this subject.

Keywords: NR5A1 mutation and gonadal dysgenesis, DSD, disorders of sex development, ambiguous genitalia, gonadal dysgenesis, NR5A1

OPEN ACCESS

Edited by:
Naglaa M. Kamal,
Cairo University, Egypt

Reviewed by:
Mohammed Ali Al Balwi,
King Saud bin Abdulaziz University for Health Sciences, Saudi Arabia
Saba Khaliq,
University of Health Sciences, Pakistan

***Correspondence:**
Ali S. Alzahrani
aliz@kfshrc.edu.sa

Specialty section:
This article was submitted to Genetics of Common and Rare Diseases, a section of the journal Frontiers in Genetics

Received: *28 February 2022*
Accepted: *03 June 2022*
Published: *05 July 2022*

Citation:
Alhamoudi KM, Alghamdi B, Aljomaiah A, Alswailem M, Al-Hindi H and Alzahrani AS (2022) Case Report: Severe Gonadal Dysgenesis Causing 46,XY Disorder of Sex Development Due to a Novel NR5A1 Variant. Front. Genet. 13:885589. doi: 10.3389/fgene.2022.885589

INTRODUCTION

Disorders of sex development (DSDs) are a group of congenital conditions characterized by impaired development of chromosomal, gonadal, and/or phenotypic sex (Ono and Harley, 2013). Depending on the etiology of the disease, DSDs have been classified into several categories including sex chromosome DSDs, 46,XX DSDs, and 46,XY DSDs (Witchel, 2018). The 46,XY DSDs are characterized by ambiguous external genitalia with a 46,XY karyotype (García-Acero et al.,

2020). The 46,XY DSD patients, however, are known to be phenotypically and etiologically heterogeneous and may develop variable genital manifestations.

The ongoing advances in the genomics applications have been instrumental in revealing the etiology of several DSDs (Baxter et al., 2015; Audi et al., 2018; Witchel, 2018). Numerous genes have been associated with 46,XY DSD such as ARX, ATRX, CBX2, DHH, DMRT2, FGFR2, GATA4, MAP3K1, NR0B1, NR5A1, SOX9, SRY, TSPYL1, WNT4, WT1, WWOX, ZFPM2, AKR1C2, AKR1C4, AMH, CYB5A, CYP11A1, CYP17A1, HSD17B3, HSD3B2, LHCGR, POR, SRD5A2, STAR, AMHR2, and androgen receptor (AR) (Audi et al., 2018). In the last few years, Nuclear receptor subfamily 5 group A member 1 (*NR5A*1) mutations have been detected in about 10–20% of 46,XY DSD cases as the major causes of gonadal dysgenesis in males and ovarian insufficiency in genetic females (Ferraz-de-Souza et al., 2011; Voican et al., 2013; Suntharalingham et al., 2015).

*NR5A*1 (OMIM: 184757), also abbreviated as steroidogenic factor 1 (*SF*1) or adrenal 4-binding protein (*Ad4BP*), is a member of the nuclear receptor family (Morohashi and Omura, 1996). The *NR5A*1 gene resides on chromosome 9q33.3 and contains seven exons: one nontranslated exon (exon 1) and six other coding exons (exons 2–7) (Hoivik et al., 2010). Structurally, the NR5A1 protein consists of a DNA-binding domain (DBD), a ligand-binding domain (LBD), two functional activation domains (AF-1 and AF-2), and a hinge region. It has been demonstrated that NR5A1 is highly expressed in Sertoli and Leydig cells of the fetal and adult gonads as well as the adrenal cortex, placenta, ovary, testis, hypothalamus, and anterior pituitary (Luo et al., 1994; Parker et al., 2002; Zhao et al., 2007; Lin and Achermann, 2008; Ferraz-de-Souza et al., 2011).

To date, more than 150 disease-causing mutations in the *NR5A*1 gene associated with 46,XY disorders have been reported in the Human Gene Mutation Database (HGMD) database (Lin et al., 2007; Philibert et al., 2007; Köhler et al., 2008; Soardi et al., 2010; Allali et al., 2011; Tantawy et al., 2014). Here, we report a 46,XY patient with a female external genitalia phenotype, rudimentary uterus, primary amenorrhea, lack of secondary sexual characteristics, and bilateral undescended inguinal testes. We identified a novel heterozygous missense *NR5A1* variant (c.2T>C, p.Met1Thr) that explains her phenotype and adds to the spectrum of *NR5A1* mutations that cause gonadal dysgenesis and DSDs.

PATIENT AND METHODS

Human Subject and Ethical Approval

The proband underwent a comprehensive clinical, biochemical and radiological evaluation by an experienced endocrinologist and genetic evaluation and counseling by a geneticist. Ethical approval of this study was obtained from King Faisal Specialist Hospital and Research Centre Institutional Review Board (RAC number 2130-012). An informed consent was obtained from the patient and her parents.

Genomic DNA Extraction and Screening of Candidate Genes

Genomic DNA was extracted from peripheral leucocytes using a commercial DNA extraction kit (QIAamp Blood Midi Kit, Qiagen, Hilden, Germany) according to the manufacturer's instructions. Initial genetic testing was directed to the 5-alpha reductase (*SRD5A2*) and AR using Sanger sequencing of all exons and exon–intron boundaries according to previously reported methods (Alswailem et al., 2021). This showed no potential variants in any of these two genes.

Whole Exome Sequencing

Whole exome sequencing (WES) was performed on the DNA of the affected proband using the Illumina HiSeq 2500 platform to capture regions of interest from the fragmented DNA library. A minimum coverage of 30× of 95% of the target regions was performed, and the sequence data from the proband was mapped to the human genome build UCSC hg19 reference sequence. The quality and coverage assessment for targeted coding exons of the protein-coding genes were ascertained.

Bioinformatics Filtration Step

Primary filtering was performed using the standard method, including filtering out low-quality reads and potential artifacts. All phenotype-driven genes reported in the Human Phenotype Ontology, the HGMD, the 1000 Genomes database, the NHLBI GO Exome Sequencing Project, the OMIM and PubMed databases were considered. Briefly, copy number variation (CNV) calling was used. Following this, all disease-causing variants reported in the HGMD (Stenson et al., 2014), in ClinVar (Landrum et al., 2016), and in CentoMD in addition to all variants with minor allele frequency below 1% in the genomAD and the Exome Aggregation Consortium (ExAC) database (Lek et al., 2016) were given priority. Variant filtration steps also focused on coding exons and flanking ±20 intronic bases. All pertinent inheritance patterns were considered. The family history and patient clinical information provided were used to evaluate the variants that were eventually identified in genes associated with 46,XY DSD. Variants that were filtered after WES were characterized with respect to their pathogenicity and causality using the published American Collage of Medical Genetics and Genomics guidelines (Richards et al., 2015). All variants related to the phenotype of the patient, except for benign or likely benign variants, were reported. CNVs of unknown significance were not reported.

Mutation Confirmation and Sequencing Analysis

Sanger sequencing was carried out to validate the identified variant. The identified missense mutation in the *NR5A1* gene (NM_004959.5, c.2T > C) was validated using primers: F: 5′-CGA TCTTGCAGCTCTGGC-3′ and R: 5′-TCTCAGACAAACGAA TCCCAA-3′. A standard PCR using the platinum II Hot-Start Green PCR Master Mix was performed following the manufacturer's instruction and an annealing temperature of

55°C. Direct sequencing reaction was performed using BigDye Terminator version 3.1, cycle sequencing reaction kit and an ABI PRISM 3730XL genetic analyzer (Applied Biosystems).

RESULTS

Clinical Description

An 11-year-old person, raised as a girl, born to non-consanguineous parents, presented to our clinic after her mother noticed atypical genital appearance with large clitoris. The patient was born at full term *via* a normal vaginal delivery, with normal pregnancy history. She looked a normal baby girl and was not noticed to have any physical abnormality at birth. During childhood, she was raised as a normal girl with no history of abnormal behavior or significant medical events. She was the first child of five siblings younger than her. None of them was reported to have any genital or somatic abnormality. She had no family history of infertility, amenorrhea, or abnormal development of external genitalia.

At the time of presentation at 11 years of age, physical examination revealed no dysmorphic features. Vital signs were within normal limits with weight of 46 kg on the 50th centile, height of 135 cm on the 45th percentile, and BMI of 25.2. Her blood pressure was normal at 105/65 mm Hg. Genitalia examination revealed mild clitromegaly with one orifice for the urethral meatus and another inferior separate vaginal meatus, partially fused labioscrotal fold, normal hymen, and no masses in labioscrotal folds. There was a firm mass of about 2-cm length in the right inguinal canal. Breast examination showed Tanner stage I. Hair distribution was normal without facial, chest, or abdominal hair but normal early pubic hair (Tanner II). The rest of her physical examination was normal.

Laboratory workup showed creatinine 51 μmol/L (46–96), Na 142 mmol/L (135–145), K 4.2 (3.5–5.0), CO_2 24 mmol/L (22–31), follicle-stimulating hormone (FSH) 63 u/L (1.5–12.4), luteinizing hormone (LH) 31 u/L (1.7–8.6), testosterone 3.55 nmol/L (0.2–2.9), estradiol 36 pmol/L (28–156), progesterone 0.4 nmol/L (follicular phase levels, 0.6–4.7), 17α-hydroxyprogesterone 0.6 nmol/L (normal <3.0), dihydrotestosterone 87 pg/ml (normal <200), DHEAS 2.48 μmol/L (1.8–8.3), morning ACTH 38 ng/L (5–60), morning cortisol 208 nmol/L (166–507), and post-ACTH stimulation 580 nmol/L. The human chorionic gonadotropin stimulation test showed an increase in testosterone level from 3.5 to 7.5 nmol/L. Pelvis ultrasound examination showed vaginal pouch in the pelvis; however, the uterus was not visualized. There was an oval-shaped isoechoic structure noted in the right inguinal region, measuring 1.99 × 1.09 cm and shows inner vascularity. Pelvic magnetic resonance imaging showed hypoplastic small uterus measuring about 2.4 × 0.7 × 0.2 cm in craniocaudal and transverse diameter with small, thin endometrial stripe. The ovaries, seminal vesicles, and prostate could not be visualized. The cytogenetics results revealed that the patient had a 46,XY karyotype. Psychosocial evaluation repeatedly confirmed that she has a female gender identity.

After extensive counseling of the patient and her parents, she underwent laparoscopy, left inguinal exploration, and bilateral orchiectomy (the left testis was found atrophied). The histopathological examination using hematoxylin and eosin staining showed a left undescended testis, atrophied with vasa efferentia, and epididymal tissue, negative for neoplasm at ×20 magnification (**Figure 1A**). The right testis showed total loss of germ cells in the seminiferous tubules, which were lined by mature Sertoli cells and negative for neoplasm or intratubular germ cell neoplasm at ×100 magnification (**Figure 1B**).

At age 15 years, the patient was started on hormonal replacement in the form of Premarin 0.625 mg days 1–25 of each month with medroxyprogesterone 10 mg daily days 16–25 of each month. With that, she started to have regular menstrual cycles and noticed further development of her breasts. Following orchidectomy, she also had regression of the clitromegly and significant breast development (Tanner IV). The patient is currently 21 years old. Her weight is 79 kg, height 162 cm, and BMI 30 kg/m^2. She continues to feel well and is comfortable with her gender identity with excellent educational and social progress.

Identification of Causal Mutation

The WES data analysis and Sanger sequencing (**Figure 2A**) revealed a heterozygous missense variant in the first transcribed exon of the *NR5A1* gene (NM_004959.5, c.2T>C, p.Met1Thr) This novel mutation was located on chr:127,265,673 and resulted in replacement of the first initiation codon ATG (methionine) by ACG (threonine).

In Silico Classification of *NR5A1*-Identified Mutation

The classification analysis, including the pathogenicity analysis for this identified missense variant, was determined based on various *in silico* parameters to be pathogenic including the pathogenic scores obtained using SIFT (damaging); PolyPhen2, which was used to predict possible impacts of amino acid substitutions on protein structure and function (probably damaging); MutationTaster (disease causing); PROVEAN (damaging); and FATHMM (pathogenic). ENCODE annotation on the UCSC genome browser revealed that the variant falls in a functional region of *NR5A1* and thus predicted to be pathogenic (**Figure 2B**). The variant was predicted to fall in several transcriptional factor binding motifs such as EZH2, NR3C1, and SUZ12 (**Figure 2B**). The identified variant was not observed in the heterozygous state in the ExAC, 1000 Genomes, and genomAD and not in the Saudi Genome Project of >5,000 individual full exome sequencing data (https://shgp.kacst.edu.sa/index.en.html).

Phylogenetic Conservation

The variant falls in a functional region of the N-terminal region of *NR5A1* and disrupts the start codon in the first coding exon, exon 2 (**Figure 3A**). Full-length orthologous protein sequences from a range of animal species were retrieved from the UniProt database

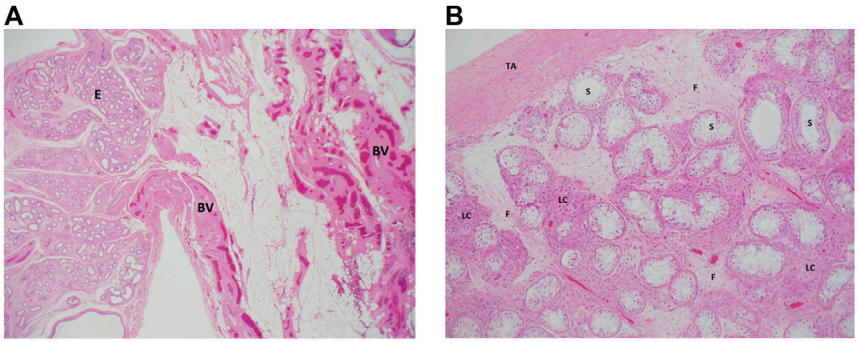

FIGURE 1 | Histologic examination of the proband's testicular biopsies. **(A)** Left testes: a low magnification (×20) from the surgical specimen of the left "testis" where epididymal tissue (E) is seen along with adjacent fatty tissue that is rich in blood vessels (BV). Note the total absence of any testicular tissue. **(B)** Right testis: an intermediate magnification (×100) image from the right testis showing seminiferous tubules (ST) that lack germ cells (lined by Sertoli cells only). The interstitium between the tubules shows clusters of hyperplastic Leydig cells (ILC) and fibrosis (F) secondary to tubular atrophy. TA, tunica albuginea. Both sections were stained using hematoxylin and eosin staining.

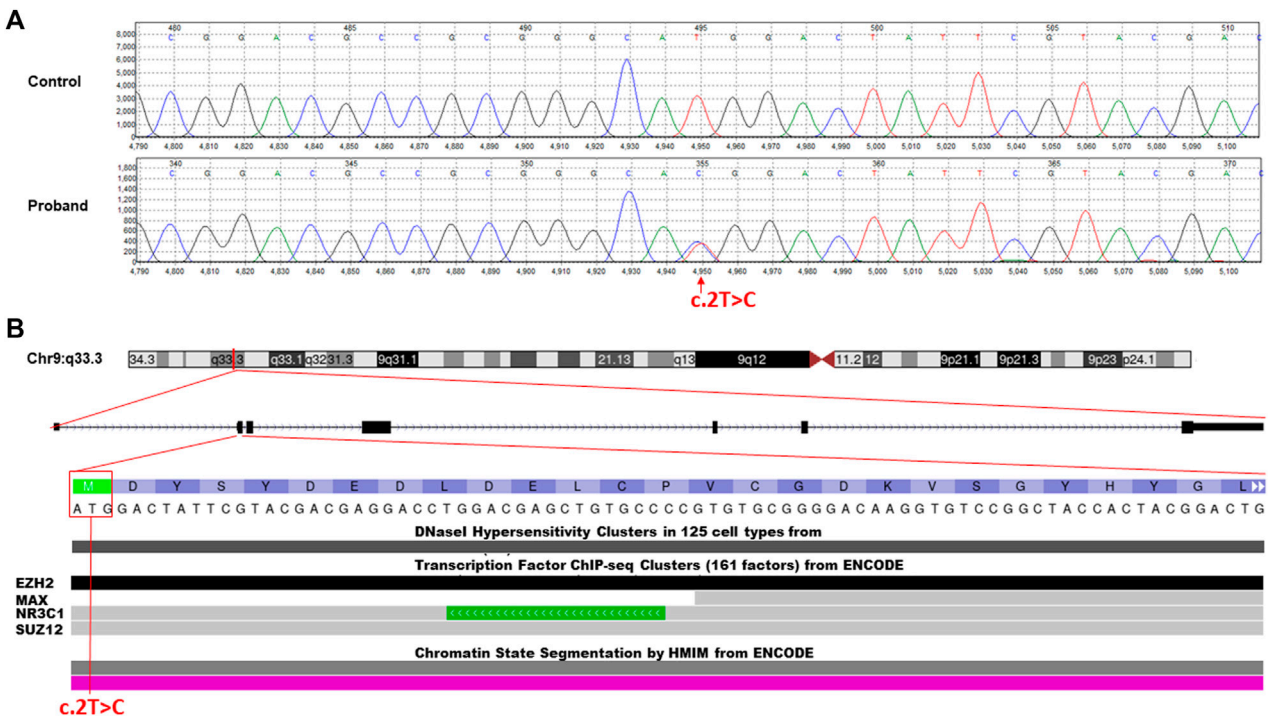

FIGURE 2 | Molecular characterization of the identified c.2T>C missense variant in the *NR5A1* gene. **(A)** Chromatogram of Sanger sequencing segregation analysis of the wild-type control and affected proband. Red arrow represents the identified variant. **(B)** Annotation of the identified missense variant in the *NR5A1* gene (c.2T>C, p.Met1Thr) is located on chromosome 9p33.3. The variant falls in the first transcribed exon (exon 2) of the N-terminal region and interrupts the starting codon (ATG>ACG). The variant located in some of the ENCODE functional data tracks in the USCS genome browser (http://genome.ucsc.edu/). The variant interrupt DNaseI hypersensitivity and some predicted transcription factor binding sites (TFBSs) such as EZH2, NR3C1, and SUZ12.

and aligned using UniProt Align, and final processing was performed in ESPript. Alignment of the sequence of H. Sapiens NR5A1 (UniProt: Q13285) with the Mouse NR5A1 (UniProt: P33242), Pig NR5A1 (UniProt: P79387), Rat NR5A1 (UniProt: P50569), Horse NR5A1 (UniProt: Q9GKL2) and Bovine NR5A1 (UniProt: Q04752) was generated (**Figure 3B**). The p.Met1Thr variant is located in a highly conserved position across mammals and higher eukaryotes, and thus, this strengthens the pathogenicity of the identified variant (**Figure 3B**). The STRING protein interaction shows that there is a strong interaction between NR5A1 and several other DSD proteins such as SOX9 (**Figure 3C**).

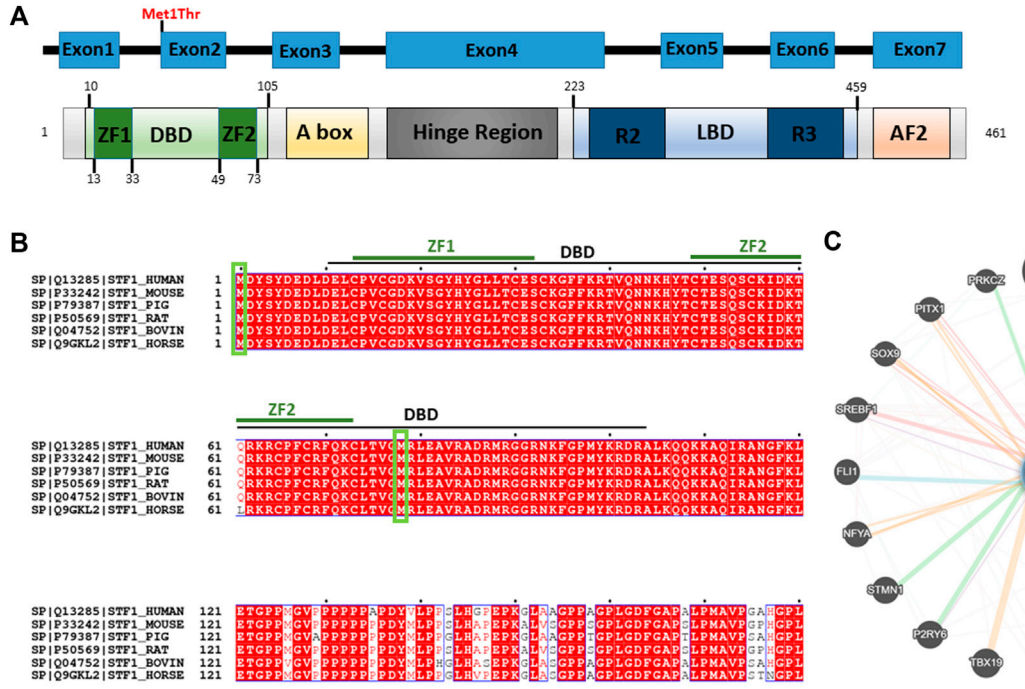

FIGURE 3 | Predicted effect of Met1Thr mutation on NR5A1 function. **(A)** Schematic diagram of the identified variant at amino acid 1 is located on the DBD (green) in the N-terminus of NR5A1. The diagram was generated using PROSITE (https://prosite.expasy.org/cgi-bin/prosite). **(B)** Alignment of the sequences of H. Sapiens NR5A1 (UniProt: Q13285) with the Mouse NR5A1 (UniProt: P33242), Pig NR5A1 (UniProt: P79387), Rat NR5A1 (UniProt: P50569), Bovin NR5A1 (Uniprot: Q04752), and Horse NR5A1 (UniProt: Q9GKL2). The alignment was generated using UniProt Align (http://www.uniprot.org/align/). Start codon (Met) are represented by green rectangles. The alignment file was generated using UniProt Align (http://www.uniprot.org/align/), and final processing was performed in ESPript (http://espript.ibcp.fr). **(C)** Schematic representation of the NR5A1 interactions with other proteins using GeneMANIA (http://genemania.org/): physical interaction with other proteins (pink lines), genetics interaction (green lines), co-localization (blue lines), and predicted interaction (orange lines).

DISCUSSION

In this study, we describe an interesting case of 46,XY DSD. The patient has severe gonadal dysgenesis, and the likely pathogenesis is related to lack of androgens and anti-Müllerian hormone (AMH) from the severely dysgenetic testes during the first few weeks of life. Lack of androgens led to the development of the female external genitalia phenotype and probably was also the reason for the undescended testes. Lack of the AMH resulted in the formation of the uterus and upper third of the vagina. Although NR5A1 is an important factor for normal adrenocortical development, this patient had no evidence of adrenal insufficiency. Previous studies showed that *NR5A1* mutations, especially heterozygous ones, do not usually affect adrenocortical function, while homozygous mutations may be associated with gonadal and adrenocortical insufficiency (Lin et al., 2007; Song et al., 2018).

NR5A1 is expressed in the bipotential gonads during the early gonadal development. It modulates the expression of critical genes for male gonadal development including *SRY* and *SOX9* (De Santa Barbara et al., 1998; Sekido and Lovell-Badge, 2008). It also activates the expression of the AMH that is responsible for regression of the Müllerian duct, the origin of internal female genitalia (Shen et al., 1994; Lasala et al., 2011). Finally, it stimulates testosterone biosynthesis by Leydig cells (Shen et al., 1994; De Santa Barbara et al., 1998). Therefore, impairment of its structure and function by mutations such as the one in our patient is likely to affect all of these regulatory functions and explains the clinical phenotype of our patient and similar cases. The clinical spectrum of patients with *NR5A1* mutations in subjects with a 46,XY karyotype is wide ranging from hypospadias only to a micropenis to a complete female external genitalia like that in our patient. This wide spectrum in the phenotypes of patients with *NR5A1* mutations is probably related to the type of mutations, their locations in the gene, and their effects on its function. In our patient, since the causative mutation involves the initiation codon, it probably has major effects on the gene function resulting in severe phenotype with complete sex reversal.

The novel *NR5A1* variant we detected in this patient is a heterozygous missense c.2T>C, (p.Met1Thr) variant located in the first transcribed exon (exon 2) of the N-terminal region and interrupts the starting codon (ATG>ACG). The disruption of the start codon in Met1Thr mutation affects the initial translation and formation of the DBD (10–105 aa) that contains two zinc finger motifs (ZF1: 13–33 aa; Zf2: 49–73 aa), but not the other domains in NR5A1, and thus may partially affect the overall function. Lourenço et al. (2009) have identified another variant that affects the initiation codon (c.3G>A,

p.M1I) in two girls with 46,XY and 46,XX karyotypes. The first one (46,XY) was a 12-year-old girl who presented in a similar way to our patient with clitromegly, primary amenorrhea, and small breasts and uterus. Her surgically removed testes showed fibrous tissue, disorganized tubules, and Leydig cell hyperplasia. The second one (46,XX) was a 16-year-old girl who presented with secondary amenorrhea, small breasts, and no pubic hair, and her ovarian tissue showed only fibrous tissue with no follicles. Their 46-year-old mother reported normal menses. Genetic testing revealed an *NR5A1* mutation in the third nucleotide of the initiation codon (c.3G>A, p.M1I) in the two affected siblings and their mother but not in another normal sister and the father (Lourenço et al., 2009). The authors explained the absence of phenotypic abnormalities in the mother by the variable penetrance of the mutant allele due to variable translation defect, existence of modifier genes, or environmental defects as was previously seen in monozygotic twins with an *N5RA1* mutation and variable penetrance (Philibert et al., 2007). Similarly, in another report, Philibert et al. (2010) described a pathogenic heterozygous variant in the first nucleotide of the initiation codon (c.1A>G, p.M1V) in a female patient. It was speculated that this variant will abolish the transcriptional initiation and probably affects the protein activity.

Each domain of NR5A1 has been shown to play a critical and distinctive role. The DBD is crucial for transcription factor binding to promoters. The DBD contains a core with two Cys4 zinc finger motifs and a highly conserved Ftz-F1 box motif that is considered as a stabilizing region and involved in SF-1 to DNA interaction (Parker and Schimmer, 1997; Little et al., 2006). Owing to this impaired DBD, the protein–protein interaction and the anchoring will probably be affected, and the stabilizing ability might get disrupted. In addition, the impaired DBD might not have the ability to bind, interact, or trans-activate several proteins and subsequently could affect the overall NR5A1 nuclear receptor function. The STRING protein interaction revealed that NR5A1 physically interacts with SOX9. It has been demonstrated that NR5A1 trans-activates Sox9/SOX9 and nuclear receptor subfamily 0 group B member 1 (Nr0b1/NR0B1) through interacting with sex-determining region Y (SRY) (Sekido and Lovell-Badge, 2008). It has been demonstrated that during testicular development in mice, NR5A1 activates the testis enhancer sequence core element (TESCO) of Sox9/SOX9 (Sekido and Lovell-Badge, 2008). In addition, the impaired NR5A1 might lose the ability to modulate the genes that are involved in steroidogenesis such as steroidogenic acute regulatory protein (StAR) and cytochrome P450 steroid hydroxylase (CYP) enzymes including CYP11A1 and CYP17A1 in Leydig cells, which are required for testosterone biosynthesis (Lin and Achermann, 2008). In addition, NR5A1 was found to play a pivotal role in the transcriptional regulation of the expression of luteinizing hormone receptor (LHCGR) in both theca and granulosa cells (Luo et al., 1994). Furthermore, NR5A1 regulates cholesterol mobilization including AMH, HMGCoA synthase, and 3b-hydroxysteroid dehydrogenase (3bHSD). In contrast, it has been demonstrated that NR5A1 upregulates the insulin-like polypeptide 3 (INSL3) expression, which regulates testicular descent (Schimmer and White, 2010). However, owing to the presence of another start codon at position 78 (**Figure 3B**), the transcription of other NR5A1 domains such as A-box, LBD, AF-1, and AF-2 is probably unaffected. Therefore, this variant might not affect the transcriptional activation or suppression of some parts of the gene. It has been demonstrated that A-box binds to hormone response elements, which respond to steroid receptors and initiate the gene signaling pathway by the steroid hormones (Little et al., 2006). Therefore, this mutation may not cause hormonal alteration. It has been demonstrated that mutations located in the DBD (c.90T>G) and the DBD ZF1 box domain of the DBD (c.58G>C; c.70C>T and c.70delC) lead to affected individuals having partial or complete gonadal dysgenesis (Camats et al., 2012). Similar heterozygous c.18delC, V15M, C16X, C33S, and G35E variants located in the Ftz-ZF domain of the *NR5A*1 gene have also been documented in another study with a similar clinical phenotype (Köhler et al., 2008). Overall, it has been speculated that this variant may be subjected to partial or complete loss of a functional DBD in the NR5A1 protein.

This case adds to the rare and unique mutations of *NR5A1*. Although functional assessment was not performed, the *in silico* prediction was highly suggestive of the pathogenic nature of this variant. Since this variant involves the initiation codon, it is expected to have a detrimental effect on the protein translation. However, the final protein function pathogenicity effect may require further functional verification, which is not carried out in this study.

In conclusion, we have described the clinical and molecular genetics of a case of 46,XY DSD and identified a novel heterozygous missense c.2T>C variant changing the initiation codon of the *N5RA1* gene from methionine to threonine in this patient. This variant is predicted to impair the DBD and subsequently affect the NR5A1 nuclear receptor function.

DATA AVAILABILITY STATEMENT

The datasets for this article are not publicly available due to concerns regarding participant/patient anonymity. Requests to access the datasets should be directed to the corresponding author.

ETHICS STATEMENT

Ethical approval of this study was obtained from the King Faisal Specialist Hospital and Research Centre Institutional Review Board (RAC number 2130-012). Written informed consent to participate in this study was provided by the participant's legal guardian/next of kin. Written informed consent was obtained from the individual(s), or the minor(s)' legal guardian/next of kin, for the publication of any potentially identifiable images or data included in this article.

AUTHOR CONTRIBUTIONS

KA wrote the manuscript; BA performed DNA extraction, PCR, and Sanger sequencing experiments; AbA summarized and reported the clinical diagnosis; MA performed the WES and other laboratory work; HA-H reviewed the pathology and prepared the figures; AlA contributed to the inception of the research idea, designed the experiments, supervised the work, and edited the manuscript.

ACKNOWLEDGMENTS

We wish to thank the patient and her family for their participation.

REFERENCES

Allali, S., Muller, J.-B., Brauner, R., Lourenço, D., Boudjenah, R., Karageorgou, V., et al. (2011). Mutation Analysis of NR5A1 Encoding Steroidogenic Factor 1 in 77 Patients with 46, XY Disorders of Sex Development (DSD) Including Hypospadias. *PLoS One* 6 (10), e24117. doi:10.1371/journal.pone.0024117

Alswailem, M., Alsagheir, A., Abbas, B. B., Alzahrani, O., and Alzahrani, A. S. (2021). Molecular Genetics of Disorders of Sex Development in a Highly Consanguineous Population. *J. Steroid Biochem. Mol. Biol.* 208, 105736. doi:10.1016/j.jsbmb.2020.105736

Audí, L., Ahmed, S. F., Krone, N., Cools, M., McElreavey, K., Holterhus, P. M., et al. (2018). GENETICS IN ENDOCRINOLOGY: Approaches to Molecular Genetic Diagnosis in the Management of Differences/disorders of Sex Development (DSD): Position Paper of EU COST Action BM 1303 'DSDnet'. *Eur. J. Endocrinol.* 179 (4), R197–r206. doi:10.1530/eje-18-0256

Baxter, R. M., Arboleda, V. A., Lee, H., Barseghyan, H., Adam, M. P., Fechner, P. Y., et al. (2015). Exome Sequencing for the Diagnosis of 46,XY Disorders of Sex Development. *J. Clin. Endocrinol. Metab.* 100 (2), E333–E344. doi:10.1210/jc.2014-2605

Camats, N., Pandey, A. V., Fernández-Cancio, M., Andaluz, P., Janner, M., Torán, N., et al. (2012). Ten Novel Mutations in the NR5A1 Gene Cause Disordered Sex Development in 46,XY and Ovarian Insufficiency in 46,XX Individuals. *J. Clin. Endocrinol. Metab.* 97 (7), E1294–E1306. doi:10.1210/jc.2011-3169

De Santa Barbara, P., Bonneaud, N., Boizet, B., Desclozeaux, M., Moniot, B., Sudbeck, P., et al. (1998). Direct Interaction of SRY-Related Protein SOX9 and Steroidogenic Factor 1 Regulates Transcription of the Human Anti-müllerian Hormone Gene. *Mol. Cell Biol.* 18 (11), 6653–6665. doi:10.1128/mcb.18.11.6653

Ferraz-de-Souza, B., Lin, L., and Achermann, J. C. (2011). Steroidogenic Factor-1 (SF-1, NR5A1) and Human Disease. *Mol. Cell. Endocrinol.* 336 (1-2), 198–205. doi:10.1016/j.mce.2010.11.006

García-Acero, M., Moreno-Niño, O., Suárez-Obando, F., Molina, M. n., Manotas, M. a., Prieto, J., et al. (2020). Disorders of Sex Development: Genetic Characterization of a Patient Cohort. *Mol. Med. Rep.* 21 (1), 97–106. doi:10.3892/mmr.2019.10819

Hoivik, E. A., Lewis, A. E., Aumo, L., and Bakke, M. (2010). Molecular Aspects of Steroidogenic Factor 1 (SF-1). *Mol. Cell. Endocrinol.* 315 (1-2), 27–39. doi:10.1016/j.mce.2009.07.003

Köhler, B., Lin, L., Ferraz-de-Souza, B., Wieacker, P., Heidemann, P., Schröder, V., et al. (2008). Five Novel Mutations in Steroidogenic Factor 1 (SF1,NR5A1) in 46,XY Patients with Severe Underandrogenization but without Adrenal Insufficiency. *Hum. Mutat.* 29 (1), 59–64. doi:10.1002/humu.20588

Landrum, M. J., Lee, J. M., Benson, M., Brown, G., Chao, C., Chitipiralla, S., et al. (2016). ClinVar: Public Archive of Interpretations of Clinically Relevant Variants. *Nucleic Acids Res.* 44 (D1), D862–D868. doi:10.1093/nar/gkv1222

Lasala, C., Schteingart, H. F., Arouche, N., Bedecarrás, P., Grinspon, R. P., Picard, J.-Y., et al. (2011). SOX9 and SF1 Are Involved in Cyclic AMP-Mediated Upregulation of Anti-müllerian Gene Expression in the Testicular Prepubertal Sertoli Cell Line SMAT1. *Am. J. Physiology-Endocrinology Metabolism* 301 (3), E539–E547. doi:10.1152/ajpendo.00187.2011

Lek, M., Karczewski, K. J., Minikel, E. V., Samocha, K. E., Banks, E., Fennell, T., et al. (2016). Analysis of Protein-Coding Genetic Variation in 60,706 Humans. *Nature* 536 (7616), 285–291. doi:10.1038/nature19057

Lin, L., and Achermann, J. C. (2008). Steroidogenic Factor-1 (SF-1, Ad4BP, NR5A1) and Disorders of Testis Development. *Sex. Dev.* 2 (4-5), 200–209. doi:10.1159/000152036

Lin, L., Philibert, P., Ferraz-de-Souza, B., Kelberman, D., Homfray, T., Albanese, A., et al. (2007). Heterozygous Missense Mutations in Steroidogenic Factor 1 (SF1/Ad4BP, NR5A1) Are Associated with 46,XY Disorders of Sex Development with Normal Adrenal Function. *J. Clin. Endocrinol. Metab.* 92 (3), 991–999. doi:10.1210/jc.2006-1672

Little, T. H., Zhang, Y., Matulis, C. K., Weck, J., Zhang, Z., Ramachandran, A., et al. (2006). Sequence-specific Deoxyribonucleic Acid (DNA) Recognition by Steroidogenic Factor 1: a Helix at the Carboxy Terminus of the DNA Binding Domain Is Necessary for Complex Stability. *Mol. Endocrinol.* 20 (4), 831–843. doi:10.1210/me.2005-0384

Lourenço, D., Brauner, R., Lin, L., De Perdigo, A., Weryha, G., Muresan, M., et al. (2009). Mutations inNR5A1Associated with Ovarian Insufficiency. *N. Engl. J. Med.* 360 (12), 1200–1210. doi:10.1056/NEJMoa0806228

Luo, X., Ikeda, Y., and Parker, K. L. (1994). A Cell-specific Nuclear Receptor Is Essential for Adrenal and Gonadal Development and Sexual Differentiation. *Cell* 77 (4), 481–490. doi:10.1016/0092-8674(94)90211-9

Morohashi, K. I., and Omura, T. (1996). Ad4BP/SF-1, a Transcription Factor Essential for the Transcription of Steroidogenic Cytochrome P450 Genes and for the Establishment of the Reproductive Function. *FASEB J.* 10 (14), 1569–1577. doi:10.1096/fasebj.10.14.9002548

Ono, M., and Harley, V. R. (2013). Disorders of Sex Development: New Genes, New Concepts. *Nat. Rev. Endocrinol.* 9 (2), 79–91. doi:10.1038/nrendo.2012.235

Parker, K. L., Rice, D. A., Lala, D. S., Ikeda, Y., Luo, X., Wong, M., et al. (2002). Steroidogenic Factor 1: an Essential Mediator of Endocrine Development. *Recent Prog. Hormone Res.* 57, 19–36. doi:10.1210/rp.57.1.19

Parker, K. L., and Schimmer, B. P. (1997). Steroidogenic Factor 1: a Key Determinant of Endocrine Development and Function. *Endocr. Rev.* 18 (3), 361–377. doi:10.1210/edrv.18.3.0301

Philibert, P., Leprieur, E., Zenaty, D., Thibaud, E., Polak, M., Frances, A.-M., et al. (2010). Steroidogenic Factor-1 (SF-1) Gene Mutation as a Frequent Cause of Primary Amenorrhea in 46,XY Female Adolescents with Low Testosterone Concentration. *Reprod. Biol. Endocrinol.* 8, 28. doi:10.1186/1477-7827-8-28

Philibert, P., Zenaty, D., Lin, L., Soskin, S., Audran, F., Leger, J., et al. (2007). Mutational Analysis of Steroidogenic Factor 1 (NR5a1) in 24 Boys with Bilateral Anorchia: a French Collaborative Study. *Hum. Reprod.* 22 (12), 3255–3261. doi:10.1093/humrep/dem278

Richards, S., Aziz, N., Bale, S., Bick, D., Das, S., Gastier-Foster, J., et al. (2015). Standards and Guidelines for the Interpretation of Sequence Variants: a Joint Consensus Recommendation of the American College of Medical Genetics and Genomics and the Association for Molecular Pathology. *Genet. Med.* 17 (5), 405–424. doi:10.1038/gim.2015.30

Schimmer, B. P., and White, P. C. (2010). Minireview: Steroidogenic Factor 1: its Roles in Differentiation, Development, and Disease. *Mol. Endocrinol.* 24 (7), 1322–1337. doi:10.1210/me.2009-0519

Sekido, R., and Lovell-Badge, R. (2008). Sex Determination Involves Synergistic Action of SRY and SF1 on a Specific Sox9 Enhancer. *Nature* 453 (7197), 930–934. doi:10.1038/nature06944

Shen, W.-H., Moore, C. C. D., Ikeda, Y., Parker, K. L., and Ingraham, H. A. (1994). Nuclear Receptor Steroidogenic Factor 1 Regulates the Müllerian Inhibiting Substance Gene: A Link to the Sex Determination Cascade. *Cell* 77 (5), 651–661. doi:10.1016/0092-8674(94)90050-7

Soardi, F. C., Coeli, F. B., Maciel-Guerra, A. T., Guerra-Júnior, G., and Palandi de Mello, M. (2010). Complete XY Gonadal Dysgenesis Due to p.D293N Homozygous Mutation in the NR5A1 Gene: a Case Study. *J. Appl. Genet.* 51 (2), 223–224. doi:10.1007/bf03195733

Song, Y., Fan, L., and Gong, C. (2018). Phenotype and Molecular Characterizations of 30 Children from China with NR5A1 Mutations. *Front. Pharmacol.* 9, 1224. doi:10.3389/fphar.2018.01224

Stenson, P. D., Mort, M., Ball, E. V., Shaw, K., Phillips, A. D., and Cooper, D. N. (2014). The Human Gene Mutation Database: Building a Comprehensive Mutation Repository for Clinical and Molecular Genetics, Diagnostic Testing and Personalized Genomic Medicine. *Hum. Genet.* 133 (1), 1–9. doi:10.1007/s00439-013-1358-4

Suntharalingham, J. P., Buonocore, F., Duncan, A. J., and Achermann, J. C. (2015). DAX-1 (NR0B1) and Steroidogenic Factor-1 (SF-1, NR5A1) in Human Disease. *Best Pract. Res. Clin. Endocrinol. Metabolism* 29 (4), 607–619. doi:10.1016/j.beem.2015.07.004

Tantawy, S., Mazen, I., Soliman, H., Anwar, G., Atef, A., El-Gammal, M., et al. (2014). Analysis of the Gene Coding for Steroidogenic Factor 1 (SF1, NR5A1) in a Cohort of 50 Egyptian Patients with 46,XY Disorders of Sex Development. *Eur. J. Endocrinol.* 170 (5), 759–767. doi:10.1530/eje-13-0965

Voican, A., Bachelot, A., Bouligand, J., Francou, B., Dulon, J., Lombès, M., et al. (2013). NR5A1(SF-1) Mutations Are Not a Major Cause of Primary Ovarian Insufficiency. *J. Clin. Endocrinol. Metab.* 98 (5), E1017–E1021. doi:10.1210/jc.2012-4111

Witchel, S. F. (2018). Disorders of Sex Development. *Best Pract. Res. Clin. Obstetrics Gynaecol.* 48, 90–102. doi:10.1016/j.bpobgyn.2017.11.005

Zhao, H., Li, Z., Cooney, A. J., and Lan, Z. J. (2007). Orphan Nuclear Receptor Function in the Ovary. *Front. Biosci.* 12, 3398–3405. doi:10.2741/2321

Conflict of Interest: The authors declare that the research was conducted in the absence of any commercial or financial relationships that could be construed as a potential conflict of interest.

Publisher's Note: All claims expressed in this article are solely those of the authors and do not necessarily represent those of their affiliated organizations, or those of the publisher, the editors and the reviewers. Any product that may be evaluated in this article, or claim that may be made by its manufacturer, is not guaranteed or endorsed by the publisher.

frontiers | Frontiers in Genetics

ORIGINAL RESEARCH
published: 08 July 2022
doi: 10.3389/fgene.2022.884522

Targeted Next-Generation Sequencing Identified Novel Compound Heterozygous Variants in the *PTPRQ* Gene Causing Autosomal Recessive Hearing Loss in a Chinese Family

Yuan Jin[1†], *Xiao-Zhou Liu*[1†], *Le Xie*[1], *Wen Xie*[1], *Sen Chen*[1] *and Yu Sun*[1,2*]

[1]*Department of Otorhinolaryngology, Union Hospital, Tongji Medical College, Huazhong University of Science and Technology, Wuhan, China,* [2]*Tongji Medical College, Institute of Otorhinolaryngology, Huazhong University of Science and Technology, Wuhan, China*

OPEN ACCESS

Edited by:
Naglaa M. Kamal,
Cairo University, Egypt

Reviewed by:
Renjie Chai,
Southeast University, China
Muhammad Jawad Hassan,
National University of Medical Sciences (NUMS), Pakistan

***Correspondence:**
Yu Sun
sunyu@hust.edu.cn

†These authors have contributed equally to this work

Specialty section:
This article was submitted to Genetics of Common and Rare Diseases, a section of the journal Frontiers in Genetics

Received: *26 February 2022*
Accepted: *26 May 2022*
Published: *08 July 2022*

Citation:
Jin Y, Liu X-Z, Xie L, Xie W, Chen S and Sun Y (2022) Targeted Next-Generation Sequencing Identified Novel Compound Heterozygous Variants in the PTPRQ Gene Causing Autosomal Recessive Hearing Loss in a Chinese Family. Front. Genet. 13:884522. doi: 10.3389/fgene.2022.884522

Hearing loss is among the most common congenital sensory impairments. Genetic causes account for more than 50% of the cases of congenital hearing loss. The *PTPRQ* gene, encoding protein tyrosine phosphatase receptor Q, plays an important role in maintaining the stereocilia structure and function of hair cells. Mutations in the *PTPRQ* gene have been reported to cause hereditary sensorineural hearing loss. By using next-generation sequencing and Sanger sequencing, we identified a novel compound heterozygous mutation (c.997 G > A and c.6603-3 T > G) of the *PTPRQ* gene in a Chinese consanguineous family. This is the first report linking these two mutations to recessive hereditary sensorineural hearing loss. These findings contribute to the understanding of the relationship between genotype and hearing phenotype of *PTPRQ*-related hearing loss, which may be helpful to clinical management and genetic counseling.

Keywords: *PTPRQ* gene, novel compound heterozygous mutation, targeted next-generation sequencing, hearing loss, autosomal recessive inheritance

INTRODUCTION

Hearing loss is the most common sensorineural disorder affecting approximately 6.1% of the world population (Qian et al., 2020; Zhang et al., 2021a; Fu et al., 2021; Lv et al., 2021). It is estimated that more than half of the hearing loss cases are attributable to genetic factors (He et al., 2017; Wang et al., 2022), while the other half of hearing loss cases could be caused by ototoxic drugs, such as aminoglycosides and anti-tumor drugs, aging, excessive noise exposure, and infections (Li et al., 2018a; Li et al., 2018b; Liu et al., 2019a; Cheng et al., 2019; Han et al., 2020; He et al., 2020; Zhong et al., 2020; Zhou et al., 2020; Liu et al., 2021a; Zhang et al., 2021b; Guo et al., 2021; He et al., 2021; Bu et al., 2022; Fu et al., 2022; Jiang et al., 2022). The functions of these hearing loss genes play an essential role in the development and function of hair cells and synaptic transmission of spiral ganglion neurons (Wang et al., 2017; Zhu et al., 2018; Cheng et al., 2021). Thus, hearing loss is often induced by the loss of sensory hair cells and spiral ganglion neurons (Liu et al., 2019b; Guo et al., 2019; He et al., 2019; Qi et al., 2019; Chen et al., 2021; Hu et al., 2021; Wei et al., 2021; Guo et al., 2022; Hu et al., 2022; Jiang et al., 2022) in the inner ear cochlea. Up to 30/8/2021, at least 124 genes have

TABLE 1 | Standard and Colloquial nomenclature for *PTPRQ* mutations and variants.

DNA sequence change*	Amino acid change	Commonly used colloquial nomenclature	Site of mutation	Type of mutation
c.4006C > T	p.Gln1336X	Q1336X	Exon 24	Nonsense
c.6881G > A	p.Trp2294X	W2294X	Exon 45	Nonsense
c.1973T > C	p.Val658Ala	V658A	Exon 14	Missense
c.4472C > T	p.Thr1491Met	T1491M	Exon 26	Missense
c.5592dup	p.(Glu134Glyfs*6)	—	Exon 32	Frame shift
c.6080dup	p.(Asn2027Lys*9)	—	Exon 38	Frame shift
c.6881G > A	p.Trp2294X	T2294X	Exon 45	Nonsense
c.16_17insT	p.Leu8fsX18	128insT	Exon 1	Frame shift
c.2714delA	p.Glu909fsX922	2825delA	Exon 18	Frame shift
c.55-2A > G	—	c.166-2A > G	Intron 1	Splice site
c.2599T > C	p.Ser867Pro	S867P	Exon 17	Missense
c.3125A > G	p.Asp1042Gly	D1042G	Exon 20	Missense
c.5981A > G	p.Glu1994Gly	E1994G	Exon 37	Missense
c.1491T > A	p.Tyr497X (currently Tyr279X)	Y497X	Exon 10	Nonsense
c.1369A > G	p.Arg457Gly (currently Arg239Gly)	R457G	Exon 10	Missense
c.1285C > T	p.Gln429X	Q429X	Exon 9	Nonsense
c.1261C > T	p.Arg421X	R421X	Exon 9	Nonsense
c.166C > G	p.Pro56Ala	P56A	Exon 3	Missense
c.6453 + 3delA	—	c.6564 + 3delA	Intron 41	Splice site
c.4640T > C	p.Met1349Thr	M1349T	Exon 27	Missense
c.1057delC	p.Leu353SfsX8	1168delC	Exon 8	Frame shift

Nucleotide numbering is based on DNA reference sequence NM_001145026.2. The version number of this reference sequence may be frequently updated. The table was made with reference to previous literature (Shuji et al., 2007).

been identified associated with non-syndromic hearing loss genes (https://hereditaryhearingloss.org/).

The *PTPRQ* gene, located in the DFNB84 region of chromosome 12q21.31, is comprised of 58 exons (Schraders et al., 2010). The transcript levels of *PTPRQ* are the highest in fetal kidneys, followed by fetal lungs and fetal cochlea (Schraders et al., 2010). In the cochlea, the PTPRQ protein (Protein Tyrosine Phosphatase Receptor Type Q, which encodes 2,299 amino acids) expresses in the basal region of the stereocilia of hair cells (Ozieblo et al., 2019). Particularly, the PTPRQ protein has a higher expression level in the basal turn of the cochlea corresponding to high-frequency hearing (Goodyear et al., 2003). Studies have shown that PTPRQ is indispensable for the formation of hair bundles. In the early postnatal *Ptprq* −/− mouse model, elongated and fused stereocilia in inner hair cells (IHCs), shortened stereocilia in outer hair cells (OHCs), and loss of hair bundles in both OHCs and IHCs were observed (Goodyear et al., 2003). In the adult *Ptprq* −/− mice, almost all hair cells had degenerated and even the organ of Corti was missing. In addition, PTPRQ protein forms a complex with myosin VI to tether the membrane of the stereocilia to stereocilia, causing reorganization of the actin cytoskeleton, and plays an important role in the mechanical transduction and adaptation of hair cells (Takenawa and Itoh, 2001; Hirono et al., 2004; Sakaguchi et al., 2008). Studies in families with *PTPRQ* mutations show that mutants of the *PTPRQ* gene could cause autosomal recessive or autosomal dominant congenital sensorineural hearing loss, damage all frequency or high frequency, with or without vestibular dysfunction in infancy or early childhood (Li et al., 2018a; Li et al., 2018b; Liu et al., 2019a; Cheng et al., 2019; Zhou et al., 2020; Liu et al., 2021a; Guo et al., 2021; He et al., 2021; Bu et al., 2022; Fu et al., 2022; Jiang et al., 2022). The hearing loss was progressive in some cases. In addition, transcription of *PTPRQ* was highly expressed in adult lung and heart tissues, and there has been no significant evidence showing dysfunction of organs except that of the cochlea (Schraders et al., 2010).

Until now, cases of *PTPRQ*-related hearing loss rarely have been reported (summarized in **Tables 1**, **2**). More cases of gene mutation need to be collected to understand the molecular mechanism. Here, we report a novel heterozygous *PTPRQ* mutation in a Chinese family, which might be helpful to establish a better understanding of the relationship between *PTPRQ* and the phenotype.

MATERIALS AND METHODS

Family Description

The family members are Han Chinese. Proband II-1 is a 29-year-old female. Proband II-2 is a 23-year-old male. Both probands had failed to pass the hearing screening and were diagnosed with sensorineural hearing loss. Neither parent of two probands exhibited similar hearing loss or vestibular dysfunction (**Figure 1**).

Clinical Examination

Both probands underwent audiological examination such as the otoscopic examination, auditory immittance, and auditory steady-state–evoked responses (ASSR). Computed tomography (CT) and magnetic resonance imaging (MRI) of the temporal bone showed no abnormal malformations. Parents reported no

TABLE 2 | *PTPRQ* mutations with hearing phenotypes in families.

Genotype	Protein domain	Inheritance pattern	Frequencies of hearing loss	Vestibular dysfunction	Phenotype	Reference
c.4006C > T/c.4006C > T	FN III	Autosomal recessive	Not mentioned	Yes	Hearing loss	Paridhy et al. (2021)
c.6881G > A/WT	—	Autosomal dominant	Mid to high frequencies	No	Mild to severe hearing loss	Eisenberger et al. (2018)
c.1973T > C/c.4472C > T	FN III	Autosomal recessive	All frequencies	No	Severe to profound hearing loss	Lv et al. (2021)
c.5592dup/c.5592dup	FN III	Autosomal recessive	Not mentioned	No	Profound hearing loss	Ammar-Khodja et al. (2015)
c.6080dup/c.6080dup	FN III	Autosomal recessive	Not mentioned	No	Profound hearing loss	Ammar-Khodja et al. (2015)
c.6881G > A/WT	—	Autosomal dominant	Mid to high frequencies	No	Severe hearing loss	Ozieblo et al. (2019)
c.16_17insT/c.2714delA	—/FN III	Autosomal recessive	All frequencies	No	Severe hearing loss	Sang et al. (2015)
c.55-2A > G/c.55-2A > G	FN III	Autosomal recessive	Mid to high frequencies	No	Severe to profound hearing loss	Mahmood et al. (2021)
c.2599T > C/c.2599T > C	FN III	Autosomal recessive	Not mentioned	Not mentioned	Hearing loss	Talebi et al. (2018)
c.3125A > G/c.5981A > G	FN III/—	Autosomal recessive	All frequencies	No	Moderate to profound hearing loss	Gao et al. (2015)
c.1491T > A/c.1491T > A	—	Autosomal recessive	All frequencies	Yes	Profound hearing loss	Schraders et al. (2010)
c.1369A > G/c.1369A > G	—	Autosomal recessive	All frequencies	Yes	Moderate hearing loss	Schraders et al. (2010)
c.1285C/T/c.1285C/T	FN III	Autosomal recessive	All frequencies	Not mentioned	Moderate to severe hearing loss	Shahin et al. (2010)
c.1261C > T/c.1261C > T	FN III	Autosomal recessive	Mid to high frequencies	Yes	Profound hearing loss	Sakuma et al. (2015)
c.166C > G/c.1261C > T	FN III	Autosomal recessive	All frequencies	No	Profound hearing loss	Sakuma et al. (2015)
c.6453 + 3delA/c.4640T > C	—/FN III	Autosomal recessive	All frequencies	No	Moderate hearing loss	Sakuma et al. (2015)
c.1057delC/c.1057delC	FN III	Autosomal recessive	Not mentioned	Not mentioned	Hearing loss	Yang et al. (2021)

Hearing loss was classified as mild (20–40 dB), moderate (41–60 dB), severe (61–90 dB), or profound (>90 dB); low frequencies mean 125–500 Hz; medium frequencies mean 500–2000 Hz; high frequencies mean 2000–8000 Hz; FN III, fibronectin type III protein domain.

history of miscarriage or stillbirth. The physical examination, otoscopy, and medical history were performed at the outpatient clinic of Wuhan Union Medical College Hospital.

Mutation Detection and Analysis

The method has been described in detail in our previous articles (Chen et al., 2020; Liu et al., 2021b). Briefly, the two probands and their parents each contributed 3–5 ml of venous peripheral blood after the participants had given their informed consent. Genomic DNA was isolated from the blood samples using the QIAamp DNA Blood Midi Kit (Qiagen Inc., Hilden, Germany). Fragmentation of the genomic DNA was performed by using a Covaris LE220 ultrasonicator (Covaris Inc., Woburn, Massachusetts, United States) to generate a paired-end library. The library was enriched after hybridization, elution, and post-capture amplification. The amplified DNA library was sequenced on the BGISEQ-500 platform. Sequencing data were compared with the human genome reference (GRCh37/hg19) to detect target regions, single-nucleotide variants (SNVs), and INDEL calling. Identified SNVs and indels were compared with the information available in multiple databases, such as the National Center for Biotechnology Information GenBank database (https://www.ncbi.nlm.nih.gov/nuccore/), the Database of Single Nucleotide Polymorphisms (dbSNP) (http://www.ncbi.nlm.nih.gov/projects/SNP/), and the 1000 Genomes Database (https://www.internationalgenome.org). According to the sequencing results of two probands, Sanger sequencing was performed to confirm whether their parents had the same mutations. Using online tools such as HSF (http://www.umd.be/HSF3/HSF.shtml), FF (http://www.fruitfly.org/seq_tools/splice.html), SpliceAI (https://spliceailookup.broadinstitute.org/), an assessment was made to determine whether mutations occurring in the introns affected hnRNA splicing.

RESULTS

Clinical Data

Both patients failed the newborn hearing screening and were diagnosed with congenital sensorineural hearing loss. The ASSR of Proband II-1 showed the thresholds of the left ear were 30, 35,

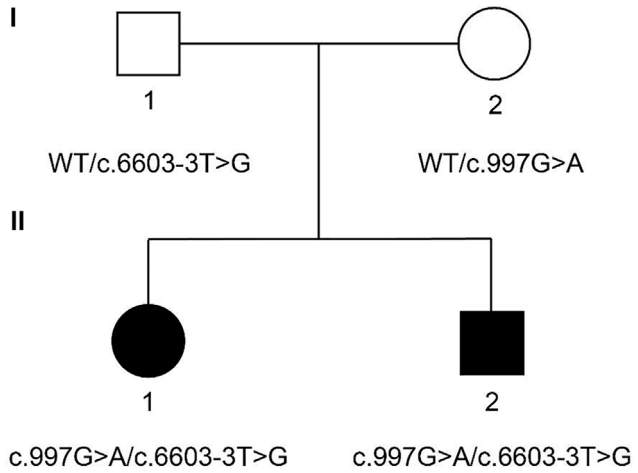

FIGURE 1 | Family pedigree of two probands. Probands II-1 and II-2 carry compound heterozygous mutation c.997 G > A (chr12:80862555) and c.6603-3 T > G (chr12:81066945) of PTPRQ. The mother of the probands carries heterozygous mutation c.997 G > A. The father of the probands carries heterozygous mutation c.6603-3 T > G. Probands are marked in black. WT, wild type.

55, 65, 65, and 70 dBnHL at 0.25, 0.5, 1, 2, 4, and 8 kHz, while the thresholds of the right ear were 30, 45, 70, 65, 70, and 70 dBnHL at 0.25, 0.5, 1, 2, 4, and 8 kHz (**Figures 2A,B**). The ASSR of Proband II-2 showed that the thresholds of the left ear were 55, 70, 65, 70, and 60 dBnHL at 0.25, 0.5, 1, 2, and 4 kHz, while the thresholds of the right ear were 45, 60, 60, 65, and 60 dBnHL at 0.25, 0.5, 1, 2, and 4 kHz (**Figures 2C,D**). The temporal bone CT scan suggested that the shape and size of the bilateral cochleae were not obviously abnormal. Neither proband reported ever suffering from balance manifestation, tinnitus, or vertigo. In addition, the parents of the probands stated that both probands had no symptoms of falling down or frequent standing instability during their childhood. Physical examinations of the two probands revealed no signs of systemic illness. After wearing a hearing aid, the ASSR of Proband II-1 showed the thresholds of the left ear were 30, 35, 40, 40, and 40 dBnHL at 0.25, 0.5, 1, 2, and 4 kHz, while the thresholds of the right ear were 30, 45, 40, 45, and 40 dBnHL at 0.25, 0.5, 1, 2, and 4 kHz (**Figures 2A,B**); the ASSR of Proband II-2 showed the thresholds of the left ear were 40, 35, 35, 30, and 30 dBnHL at 0.25, 0.5, 1, 2, and 4 kHz, while the thresholds of the right ear were 35, 30, 35, 30, and 40 dBnHL at 0.25, 0.5, 1, 2, and 4 kHz (**Figures 2C,D**). Their parents had no history of hearing impairment, nor did their medical history include other organ disorders.

Mutation Identification Data

The genomic DNA sequences of the probands were compared with the human genome reference sequence (GRCh37/hg19). Both probands carried compound heterozygous mutations of *PTPRQ*: c.997 G > A and c.6603-3 T > G. The mutation c.997 G > A occurred in EX7/CDS7 in the *PTPRQ* gene, causing the substitution of no. 997 nucleotide from guanine to adenine (**Figure 3A**). The mutation c.6603-3 T > G is a splice mutation in Intron 42, causing the substitution of no. 6603-3 nucleotide from thymine to guanine (**Figure 3B**). The proband's father and mother were heterozygous carriers of the c.997 G > A and c.6603-3 T > G mutations, respectively (**Figure 1**). The mutation c.6603-3 T > G of *PTPRQ* was inherited from the father and reported a minor allele frequency of 0.000078 in the gnomAD database. The allele frequency of this mutation in the East Asian population is 0.002118. The mutation c.997 G > A of *PTPRQ* was inherited from the mother, and no information on this mutation was found in the gnomAD database.

Functional Analysis of the Mutant Protein

The PTPRQ protein is composed of three types of domains, namely, 18 fibronectin III repeats domain (FN III domain), transmembrane domain, and tyrosine–protein phosphatase domain (PTPase domain). The mutation c.997 G > A causes the original TGG at nucleotide nos. 976–978 to become TAG, which corresponds to the termination codon (**Figure 4A**). The mutation c.997 G > A occurs in the second fibronectin III domain. The mutation c.997 G > A resulted in a truncated protein of only 325 proteins. Thus, the following 1,974 amino acids after this site cannot be synthesized (**Figures 4A,B**). The mutation c.6603-3 T > G causes the original thymine at nucleotide no. 6603-3 in Intron 42 to become guanine, which is near the splice site between Intron 42 and Exon 43 (**Figure 4C**). This mutation type often results in abnormal splicing of hnRNA. The amino acid encoded by Exon 43 is involved in the formation of the PTPase domain. We assessed whether mutation c.6603-3 T > G affects *PTPRQ* hnRNA splicing using the online bioinformatics database. All three database tools, HSF(http://www.umd.be/HSF3/HSF.shtml), FF(http://www.fruitfly.org/seq_tools/splice.html), and SpliceAI (https://spliceailookup.broadinstitute.org/), suggest that mutations c.6603-3 T > G will change the original acceptor site and hnRNA splicing. However, patients did not intend to participate in the minigene splicing assay. Therefore, we did not verify the effect of mutation c.6603-3 T > G in *in vitro* experiments.

DISCUSSION

Both probands failed the newborn hearing screening and were diagnosed with congenital sensorineural hearing loss. The proband's parents were consanguineous. However, they did not provide more detailed information on family members. By using an approach of next-generation sequencing and the Sanger sequencing method, we identified c.997 G > A and c.6603-3 T > G of *PTPRQ* in the family, as the probable cause of sensorineural hearing loss.

Mutation c.997 G > A of *PTPRQ* causes termination of protein synthesis. The mutant protein contains only one complete fibronectin III domain, the other domains are completely deleted (**Figure 4B**). Such proteins basically lose their function. Usually, the 3′ end splicing site of an intron ends with an AG. Mutations occurring in introns and close to this region may result in changes in the transcription sequence, affecting the nucleotide sequence of the final transcript. The

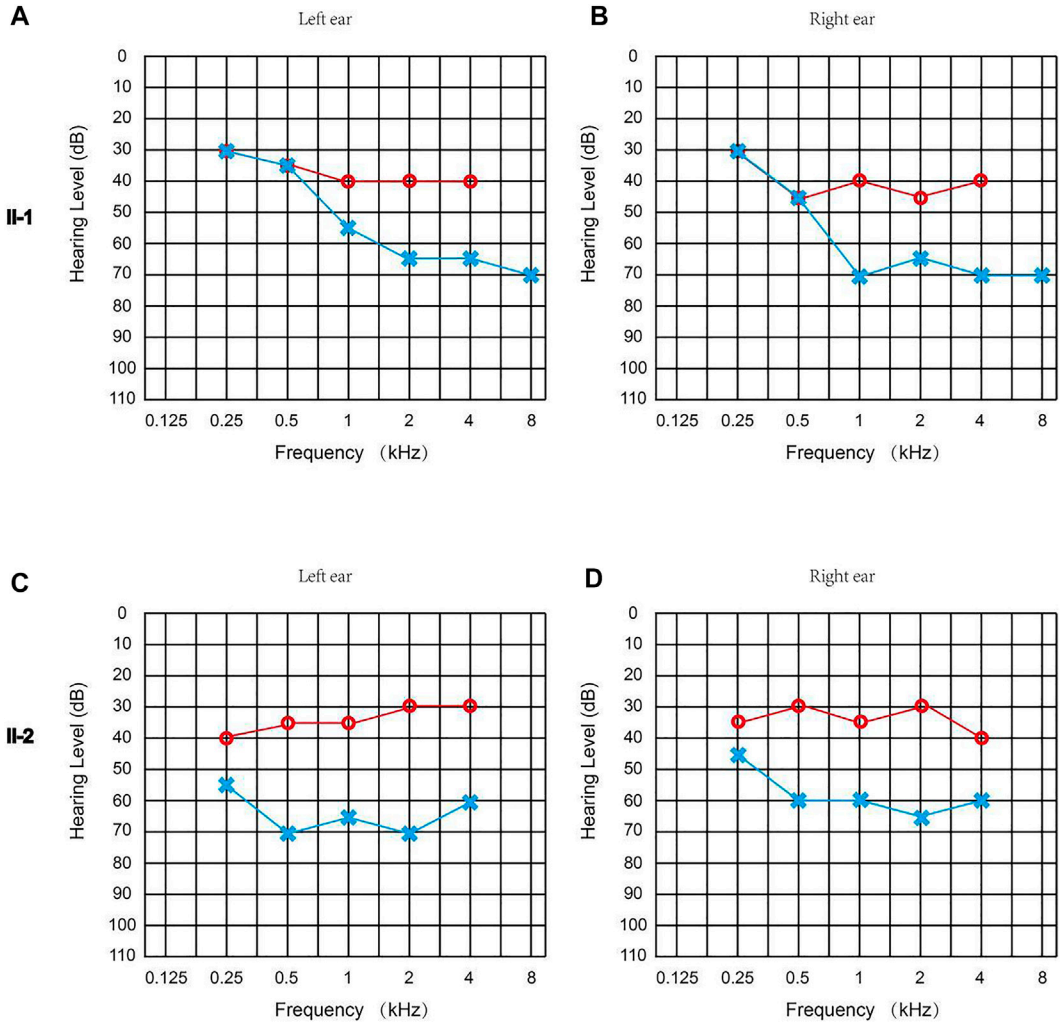

FIGURE 2 | Clinical audiology examination of the probands. **(A)** ASSR of Proband II-1 (left ear): 30, 35, 55, 65, 65, and 70 dBnHL at 0.25, 0.5, 1, 2, 4, and 8 kHz. **(B)** ASSR of Proband II-1 (right ear): 30, 45, 70, 65, 70, and 70 dBnHL at 0.25, 0.5, 1, 2, 4, and 8 kHz. **(C)** ASSR of Proband II-2 (left ear): 55, 70, 65, 70, and 60 dBnHL at 0.25, 0.5, 1, 2, and 4 kHz. **(D)** ASSR of the Proband II-2 (right ear): 45, 60, 60, 65, and 60 dBnHL at 0.25, 0.5, 1, 2, and 4 kHz. The hearing threshold of two probands with a hearing aid is marked in red, and the hearing threshold of two probands without a hearing aid is marked in blue.

mutation c.6603-3 T > G of *PTPRQ* occurs in Intron 42, a region near the boundary of Intron 42 and Exon 43, which may lead to changes in hnRNA splicing. Our assessment of this mutation using database tools revealed that the mutation resulted in the disappearance of the original splice site between Intron 42 and Exon 43, possibly resulting in the skipping of Exon 43 during transcription. More seriously, the mutation c.6603-3 T > G of *PTPRQ* may also lead to all subsequent changes in the amino acid sequence and protein domains. Exon 43 correlates with the synthesis of PTPase domains of PTPRQ proteins. According to the assessment (by HSF, FF, and SpliceAI), mutation c.6603-3 T > G of *PTPRQ* may cause altered hnRNA splicing, which can lead to changes in the composition and function of the PTPase domains. Neither mutant protein in two probands lacks the PTPase domains that are critical for the normal functioning of the PTPRQ protein. The PTPase domains have phosphatidylinositol phosphatase activity, so the PTPRQ protein can regulate the local phosphoinositides' concentration in a specific area. Furthermore, phosphoinositides play a role in cell growth, polarity, and movement by regulating the reorganization of actin filaments (Sakaguchi et al., 2008). In the inner ear, *PTPRQ* maintains the stability of the stereocilia bundle on hair cells (Goodyear et al., 2012). Deletion of the PTPase domain may lead to the degradation of stereocilia bundles. The final mutated protein results in impaired mechanotransduction function of hair cells, resulting in hearing loss.

A total of 21 *PTPRQ* mutations have been reported before this article (**Table 1**). The nucleotide and amino acid changes for these mutations are summarized in **Table 1**. Two mutations mentioned in this article, namely, mutations c.997 G > A of *PTPRQ* and c.6603-3 T > G of *PTPRQ*, have not been reported before. According to reports, some patients with *PTPRQ* mutations suffer from mild- to high-frequency hearing loss, while others suffer hearing loss in all frequencies (Han et al., 2020; He et al.,

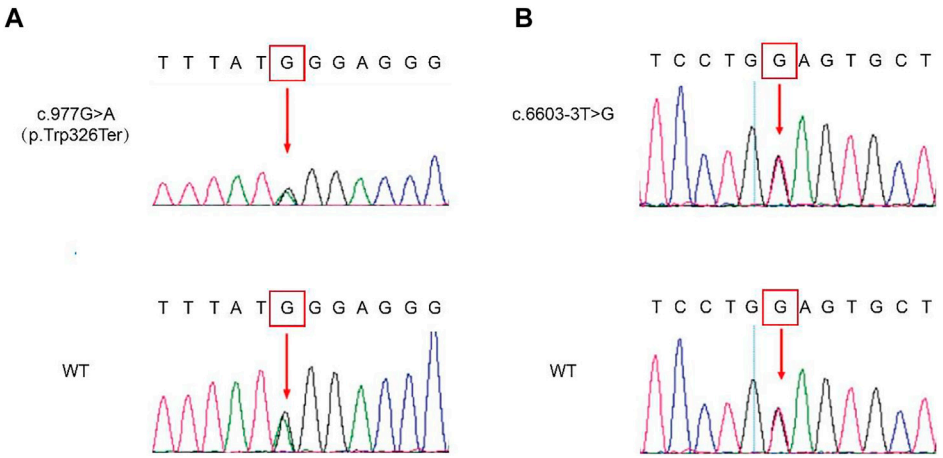

FIGURE 3 | Genetic sequencing results of the probands and their parents. Mutated sequences of the identified c.997 G > A **(A)** and c.6603-3 T > G **(B)** variant. The red arrow indicates the site of the base deletion or substitution.

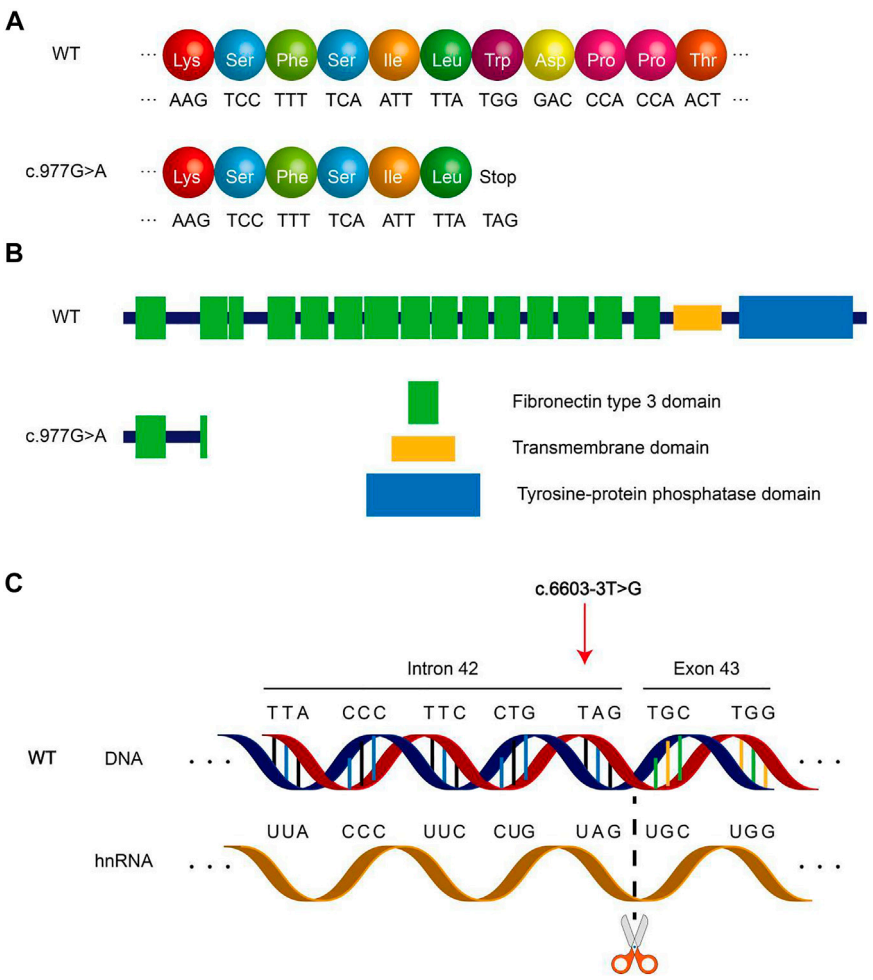

FIGURE 4 | Schematic diagram of *PTPRQ* mutation. **(A)** Amino acid coding diagram of mutation c.997 G > A. **(B)** Schematic diagram of *PTPRQ* peptide chain truncation caused by mutation c.997 G > A. **(C)** Schematic diagram of mutation c.6603-3 T > G altering hnRNA splicing.

2020; Zhang et al., 2021a; Zhang et al., 2021b; Lv et al., 2021). The relationship between the genotype and hearing phenotype in deaf patients carrying PTPRQ mutations is summarized in **Table 2**. In the present study, Proband II-1 suffered from mild- to high-frequency hearing loss, while Proband II-2 with the same mutations suffered hearing loss in all frequencies. Although the hearing loss may progress steadily, the low-frequency hearing threshold of Proband II-2 is much higher than Proband II-1. In addition, some patients with *PTPRQ* mutations have been reported to sustain vestibular dysfunction such as tinnitus or vertigo (Cheng et al., 2019; Zhang et al., 2021b; He et al., 2021; Fu et al., 2022), while others and the probands in this study did not show the same symptoms. We emphasize again that there may be no obvious correlation between genotype and phenotype of *PTPRQ*.

No obvious disease of other organs was found in participants until now. However, this risk remains due to the limited number of reported cases of *PTPRQ* mutations. We recommend cochlear, kidney, lung, and thyroid function tests for patients with *PTPRQ* mutations. In addition, we noticed that the c.6603-3 T > G mutation of *PTPRQ* was only found in the East Asian population in the GnomAD database. In the future, we will continue to pay attention to *PTPRQ*-related reports carried out in the East Asian population.

CONCLUSION

We identified a novel compound heterozygous mutation of *PTPRQ* (c.997 G > A and c.6603-3 T > G) in a Chinese family with non-syndromic sensorineural hearing loss. Our study expanded the spectrum of *PTPRQ* mutations. These findings contribute to the understanding of the relationship between genotype and hearing phenotype of *PTPRQ*-related hearing loss, which may be helpful to clinical management and genetic counseling.

DATA AVAILABILITY STATEMENT

The datasets for this article are not publicly available due to concerns regarding participant/patient anonymity. Requests to access the datasets should be directed to the corresponding author.

ETHICS STATEMENT

The studies involving human participants were reviewed and approved by the responsible committee on human experimentation (Tongji Medical College, Huazhong University of Science and Technology). The patients/participants provided their written informed consent to participate in this study.

AUTHOR CONTRIBUTIONS

YS designed the project and provided clinical examinations for the participants. JY, LX, WX, and SC collected and analyzed the data. JY and X-ZL wrote the article. All authors read and approved the final manuscript.

FUNDING

This work was supported by a grant from the National Nature Science Foundation of China (82071058).

ACKNOWLEDGMENTS

The authors thank the family for their participation in this study.

REFERENCES

Ammar-Khodja, F., Bonnet, C., Dahmani, M., Ouhab, S., Lefèvre, G. M., Ibrahim, H., et al. (2015). Diversity of the Causal Genes in Hearing Impaired Algerian Individuals Identified by Whole Exome Sequencing. *Mol. Genet. Genomic Med.* 3 (3), 189–196. doi:10.1002/mgg3.131

Bu, C., Xu, L., Han, Y., Wang, M., Wang, X., Liu, W., et al. (2022). c-Myb Protects Cochlear Hair Cells from Cisplatin-Induced Damage via the PI3K/Akt Signaling Pathway. *Cell Death Discov.* 8 (1), 78. doi:10.1038/s41420-022-00879-9

Chen, S., Jin, Y., Xie, L., Xie, W., Xu, K., Qiu, Y., et al. (2020). A Novel Spontaneous Mutation of the SOX10 Gene Associated with Waardenburg Syndrome Type II. *Neural Plast.* 2020, 9260807. doi:10.1155/2020/9260807

Chen, Y., Gu, Y., Li, Y., Li, G.-L., Chai, R., Li, W., et al. (2021). Generation of Mature and Functional Hair Cells by Co-expression of Gfi1, Pou4f3, and Atoh1 in the Postnatal Mouse Cochlea. *Cell Rep.* 35 (3), 109016. doi:10.1016/j.celrep.2021.109016

Cheng, C., Wang, Y., Guo, L., Lu, X., Zhu, W., Muhammad, W., et al. (2019). Age-related Transcriptome Changes in Sox2+ Supporting Cells in the Mouse Cochlea. *Stem Cell Res. Ther.* 10 (1), 365. doi:10.1186/s13287-019-1437-0

Cheng, C., Hou, Y., Zhang, Z., Wang, Y., Lu, L., Zhang, L., et al. (2021). Disruption of the Autism-Related Gene Pak1 Causes Stereocilia Disorganization, Hair Cell Loss, and Deafness in Mice. *J. Genet. Genomics* 48 (4), 324–332. doi:10.1016/j.jgg.2021.03.010

Eisenberger, T., Di Donato, N., Decker, C., Delle Vedove, A., Neuhaus, C., Nürnberg, G., et al. (2018). A C-Terminal Nonsense Mutation Links PTPRQ with Autosomal-Dominant Hearing Loss, DFNA73. *Genet. Med.* 20 (6), 614–621. doi:10.1038/gim.2017.155

Fu, X., An, Y., Wang, H., Li, P., Lin, J., Yuan, J., et al. (2021). Deficiency of Klc2 Induces Low-Frequency Sensorineural Hearing Loss in C57BL/6 J Mice and Human. *Mol. Neurobiol.* 58 (9), 4376–4391. doi:10.1007/s12035-021-02422-w

Fu, X., Li, P., Zhang, L., Song, Y., An, Y., Zhang, A., et al. (2022). Activation of Rictor/mTORC2 Signaling Acts as a Pivotal Strategy to Protect against Sensorineural Hearing Loss. *Proc. Natl. Acad. Sci. U. S. A.* 119 (10), e2107357119. doi:10.1073/pnas.2107357119

Gao, X., Su, Y., Chen, Y.-L., Han, M.-Y., Yuan, Y.-Y., Xu, J.-C., et al. (2015). Identification of Two Novel Compound Heterozygous PTPRQ Mutations Associated with Autosomal Recessive Hearing Loss in a Chinese Family. *PLoS One* 10 (4), e0124757. doi:10.1371/journal.pone.0124757

Goodyear, R. J., Legan, P. K., Wright, M. B., Marcotti, W., Oganesian, A., Coats, S. A., et al. (2003). A Receptor-like Inositol Lipid Phosphatase Is Required for the Maturation of Developing Cochlear Hair Bundles. *J. Neurosci.* 23 (27), 9208–9219. doi:10.1523/jneurosci.23-27-09208.2003

Goodyear, R. J., Jones, S. M., Sharifi, L., Forge, A., and Richardson, G. P. (2012). Hair Bundle Defects and Loss of Function in the Vestibular End Organs of Mice

Lacking the Receptor-like Inositol Lipid Phosphatase PTPRQ. *J. Neurosci.* 32 (8), 2762–2772. doi:10.1523/jneurosci.3635-11.2012

Guo, R., Ma, X., Liao, M., Liu, Y., Hu, Y., Qian, X., et al. (2019). Development and Application of Cochlear Implant-Based Electric-Acoustic Stimulation of Spiral Ganglion Neurons. *ACS Biomater. Sci. Eng.* 5 (12), 6735–6741. doi:10.1021/acsbiomaterials.9b01265

Guo, L., Cao, W., Niu, Y., He, S., Chai, R., and Yang, J. (2021). Autophagy Regulates the Survival of Hair Cells and Spiral Ganglion Neurons in Cases of Noise, Ototoxic Drug, and Age-Induced Sensorineural Hearing Loss. *Front. Cell. Neurosci.* 15, 760422. doi:10.3389/fncel.2021.760422

Guo, R., Xiao, M., Zhao, W., Zhou, S., Hu, Y., Liao, M., et al. (2022). 2D Ti3C2TxMXene Couples Electrical Stimulation to Promote Proliferation and Neural Differentiation of Neural Stem Cells. *Acta Biomater.* 139, 105–117. doi:10.1016/j.actbio.2020.12.035

Han, S., Xu, Y., Sun, J., Liu, Y., Zhao, Y., Tao, W., et al. (2020). Isolation and Analysis of Extracellular Vesicles in a Morpho Butterfly Wing-Integrated Microvortex Biochip. *Biosens. Bioelectron.* 154, 112073. doi:10.1016/j.bios.2020.112073

He, Z., Guo, L., Shu, Y., Fang, Q., Zhou, H., Liu, Y., et al. (2017). Autophagy Protects Auditory Hair Cells against Neomycin-Induced Damage. *Autophagy* 13 (11), 1884–1904. doi:10.1080/15548627.2017.1359449

He, Z., Fang, Q., Li, H., Shao, B., Zhang, Y., Zhang, Y., et al. (2019). The Role of FOXG1 in the Postnatal Development and Survival of Mouse Cochlear Hair Cells. *Neuropharmacology* 144, 43–57. doi:10.1016/j.neuropharm.2018.10.021

He, Z.-h., Zou, S.-y., Li, M., Liao, F.-l., Wu, X., Sun, H.-y., et al. (2020). The Nuclear Transcription Factor FoxG1 Affects the Sensitivity of Mimetic Aging Hair Cells to Inflammation by Regulating Autophagy Pathways. *Redox Biol.* 28, 101364. doi:10.1016/j.redox.2019.101364

He, Z.-H., Li, M., Fang, Q.-J., Liao, F.-L., Zou, S.-Y., Wu, X., et al. (2021). FOXG1 Promotes Aging Inner Ear Hair Cell Survival through Activation of the Autophagy Pathway. *Autophagy* 17 (12), 4341–4362. doi:10.1080/15548627.2021.1916194

Hirono, M., Denis, C. S., Richardson, G. P., and Gillespie, P. G. (2004). Hair Cells Require Phosphatidylinositol 4,5-bisphosphate for Mechanical Transduction and Adaptation. *Neuron* 44 (2), 309–320. doi:10.1016/j.neuron.2004.09.020

Hu, Y., Li, D., Wei, H., Zhou, S., Chen, W., Yan, X., et al. (2021). Neurite Extension and Orientation of Spiral Ganglion Neurons Can Be Directed by Superparamagnetic Iron Oxide Nanoparticles in a Magnetic Field. *Ijn* 16, 4515–4526. doi:10.2147/ijn.s313673

Hu, Y., Chen, W., Yin, H., Chen, X., Cai, J., Guo, J., et al. (2022). Super-aligned Carbon Nanotubes and GelMA Hydrogel Composite Scaffolds Promote Spiral Ganglion Neuron Growth and Orientation. *Mater. Today Nano* 18, 100181. doi:10.1016/j.mtnano.2022.100181

Jiang, P., Ma, X., Han, S., Ma, L., Ai, J., Wu, L., et al. (2022). Characterization of the microRNA Transcriptomes and Proteomics of Cochlear Tissue-Derived Small Extracellular Vesicles from Mice of Different Ages after Birth. *Cell. Mol. Life Sci.* 79 (3), 154. doi:10.1007/s00018-022-04164-x

Li, A., You, D., Li, W., Cui, Y., He, Y., Li, W., et al. (2018). Novel Compounds Protect Auditory Hair Cells against Gentamycin-Induced Apoptosis by Maintaining the Expression Level of H3K4me2. *Drug Deliv.* 25 (1), 1033–1043. doi:10.1080/10717544.2018.1461277

Li, H., Song, Y., He, Z., Chen, X., Wu, X., Li, X., et al. (2018). Meclofenamic Acid Reduces Reactive Oxygen Species Accumulation and Apoptosis, Inhibits Excessive Autophagy, and Protects Hair Cell-like HEI-OC1 Cells from Cisplatin-Induced Damage. *Front. Cell. Neurosci.* 12, 139. doi:10.3389/fncel.2018.00139

Liu, W., Xu, X., Fan, Z., Sun, G., Han, Y., Zhang, D., et al. (2019). Wnt Signaling Activates TP53-Induced Glycolysis and Apoptosis Regulator and Protects against Cisplatin-Induced Spiral Ganglion Neuron Damage in the Mouse Cochlea. *Antioxidants Redox Signal.* 30 (11), 1389–1410. doi:10.1089/ars.2017.7288

Liu, Y., Qi, J., Chen, X., Tang, M., Chu, C., Zhu, W., et al. (2019). Critical Role of Spectrin in Hearing Development and Deafness. *Sci. Adv.* 5 (4), eaav7803. doi:10.1126/sciadv.aav7803

Liu, W., Xu, L., Wang, X., Zhang, D., Sun, G., Wang, M., et al. (2021). PRDX1 Activates Autophagy via the PTEN-AKT Signaling Pathway to Protect against Cisplatin-Induced Spiral Ganglion Neuron Damage. *Autophagy* 17 (12), 4159–4181. doi:10.1080/15548627.2021.1905466

Liu, X., Chen, S., Sun, Y., and Kong, W. (2021). [Nonsyndromic Deafness Due to Compound Heterozygous Mutation of the CDH23 Gene]. *Lin. Chung Er Bi Yan Hou Tou Jing Wai Ke Za Zhi* 35 (3), 22933794607–22933795237. Chinese. doi:10.13201/j.issn.2096-7993.2021.03.008

Lv, J., Fu, X., Li, Y., Hong, G., Li, P., Lin, J., et al. (2021). Deletion of Kcnj16 in Mice Does Not Alter Auditory Function. *Front. Cell Dev. Biol.* 9, 630361. doi:10.3389/fcell.2021.630361

Mahmood, U., Shazia, A. B., Muhammad, A., Zubair, M. A., and Saima, R. (2021). Identification of Hearing Loss-Associated Variants of PTPRQ, MYO15A, and SERPINB6 in Pakistani Families. *Biomed. Res. Int.* 2021, 5584788. doi:10.1155/2021/5584788

Ozieblo, D., Anna, S., Marcin, L. L., Birgit, S. B., Grażyna, H., Nataliya, D. D., et al. (2019). First Confirmatory Study on PTPRQ as an Autosomal Dominant Non-syndromic Hearing Loss Gene. *J. Transl. Med.* 17 (1), 351. doi:10.1186/s12967-019-2099-5

Paridhy, V. S., Jayasankaran, C., Justin, M. J., Tom, R., Zippora, B., and Mathuravalli, K. (2021). PTPRQ, and SLC12A2-Associated Genetic and Phenotypic Heterogeneity Among Hearing Impaired Assortative Mating Families in Southern India. *Ann. Hum. Genet.* 86 (1), 1–13. doi:10.1111/ahg.12442

Qi, J., Liu, Y., Chu, C., Chen, X., Zhu, W., Shu, Y., et al. (2019). A Cytoskeleton Structure Revealed by Super-resolution Fluorescence Imaging in Inner Ear Hair Cells. *Cell Discov.* 5, 12. doi:10.1038/s41421-018-0076-4

Qian, F., Wang, X., Yin, Z., Xie, G., Yuan, H., Liu, D., et al. (2020). The Slc4a2b Gene Is Required for Hair Cell Development in Zebrafish. *aging* 12 (19), 18804–18821. doi:10.18632/aging.103840

Sakaguchi, H., Tokita, J., Naoz, M., Bowen-Pope, D., Gov, N. S., and Kachar, B. (2008). Dynamic Compartmentalization of Protein Tyrosine Phosphatase Receptor Q at the Proximal End of Stereocilia: Implication of Myosin VI-based Transport. *Cell Motil. Cytoskelet.* 65 (7), 528–538. doi:10.1002/cm.20275

Sakuma, N., Moteki, H., Azaiez, H., Booth, K. T., Takahashi, M., Arai, Y., et al. (2015). Novel PTPRQ Mutations Identified in Three Congenital Hearing Loss Patients with Various Types of Hearing Loss. *Ann. Otol. Rhinol. Laryngol.* 124 (Suppl. 1), 184S–92S. doi:10.1177/0003489415575041

Sang, Q., Mei, H., Kuermanhan, A., Feng, R., Guo, L., Qu, R., et al. (2015). Identification of a Novel Compound Heterozygous Mutation in PTPRQ in a DFNB84 Family with Prelingual Sensorineural Hearing Impairment. *Mol. Genet. Genomics* 290 (3), 1135–1139. doi:10.1007/s00438-014-0979-1

Schraders, M., Oostrik, J., Huygen, P. L. M., Strom, T. M., van Wijk, E., Kunst, H. P. M., et al. (2010). Mutations in PTPRQ Are a Cause of Autosomal-Recessive Nonsyndromic Hearing Impairment DFNB84 and Associated with Vestibular Dysfunction. *Am. J. Hum. Genet.* 86 (4), 604–610. doi:10.1016/j.ajhg.2010.02.015

Shahin, H., Rahil, M., Rayan, A. A., Avraham, K. B., King, M.-C., Kanaan, M., et al. (2010). Nonsense Mutation of the Stereociliar Membrane Protein Gene PTPRQ in Human Hearing Loss DFNB84. *J. Med. Genet.* 47 (9), 643–645. doi:10.1136/jmg.2009.075697

Shuji, O., Margaret, L. G., Johan, T. D., and Robert, B. W. (2007). Standard Mutation Nomenclature in Molecular Diagnostics: Practical and Educational Challenges. *Association for Molecular Patholpogy Training and Education Committtee* 11 (5), 494. doi:10.2353/jmoldx.2007.060081

Takenawa, T., and Itoh, T. (2001). Phosphoinositides, Key Molecules for Regulation of Actin Cytoskeletal Organization and Membrane Traffic from the Plasma Membrane. *Biochimica Biophysica Acta (BBA) - Mol. Cell Biol. Lipids* 1533 (3), 190–206. doi:10.1016/s1388-1981(01)00165-2

Talebi, F., Ghanbari Mardasi, F., Mohammadi Asl, J., Tizno, S., and Najafvand Zadeh, M. (2018). Identification of Novel PTPRQ and MYO1A Mutations in an Iranian Pedigree with Autosomal Recessive Hearing Loss. *Cell J.* 20 (1), 127–131. doi:10.22074/cellj.2018.4805

Wang, Y., Li, J., Yao, X., Li, W., Du, H., Tang, M., et al. (2017). Loss of CIB2 Causes Profound Hearing Loss and Abolishes Mechanoelectrical Transduction in Mice. *Front. Mol. Neurosci.* 10, 401. doi:10.3389/fnmol.2017.00401

Wang, M., Dong, Y., Gao, S., Zhong, Z., Cheng, C., Qiang, R., et al. (2022). Hippo/YAP Signaling Pathway Protects against Neomycin-Induced Hair Cell Damage in the Mouse Cochlea. *Cell. Mol. Life Sci.* 79 (2), 79. doi:10.1007/s00018-021-04029-9

Wei, H., Chen, Z., Hu, Y., Cao, W., Ma, X., Zhang, C., et al. (2021). Topographically Conductive Butterfly Wing Substrates for Directed Spiral Ganglion Neuron Growth. *Small* 17 (38), e2102062. doi:10.1002/smll.202102062

Yang, G., Yin, Y., Tan, Z., Liu, J., Deng, X., and Yang, Y. (2021). Whole-exome Sequencing Identified a Novel Heterozygous Mutation of SALL1 and a New Homozygous Mutation of PTPRQ in a Chinese Family with Townes-Brocks Syndrome and Hearing Loss. *BMC Med. Genomics* 14 (1), 24. doi:10.1186/s12920-021-00871-9

Zhang, S., Dong, Y., Qiang, R., Zhang, Y., Zhang, X., Chen, Y., et al. (2021). Characterization of Strip1 Expression in Mouse Cochlear Hair Cells. *Front. Genet.* 12, 625867. doi:10.3389/fgene.2021.625867

Zhang, Y., Li, Y., Fu, X., Wang, P., Wang, Q., Meng, W., et al. (2021). The Detrimental and Beneficial Functions of Macrophages after Cochlear Injury. *Front. Cell Dev. Biol.* 9, 631904. doi:10.3389/fcell.2021.631904

Zhong, Z., Fu, X., Li, H., Chen, J., Wang, M., Gao, S., et al. (2020). Citicoline Protects Auditory Hair Cells against Neomycin-Induced Damage. *Front. Cell Dev. Biol.* 8, 712. doi:10.3389/fcell.2020.00712

Zhou, H., Qian, X., Xu, N., Zhang, S., Zhu, G., Zhang, Y., et al. (2020). Disruption of Atg7-dependent Autophagy Causes Electromotility Disturbances, Outer Hair Cell Loss, and Deafness in Mice. *Cell Death Dis.* 11 (10), 913. doi:10.1038/s41419-020-03110-8

Zhu, C., Cheng, C., Wang, Y., Muhammad, W., Liu, S., Zhu, W., et al. (2018). Loss of ARHGEF6 Causes Hair Cell Stereocilia Deficits and Hearing Loss in Mice. *Front. Mol. Neurosci.* 11, 362. doi:10.3389/fnmol.2018.00362

Conflict of Interest: The authors declare that the research was conducted in the absence of any commercial or financial relationships that could be construed as a potential conflict of interest.

The reviewer RC declared a past co-authorship with the authors SC and YS to the handling editor.

frontiers | Frontiers in Genetics

TYPE Case Report
PUBLISHED 07 September 2022
DOI 10.3389/fgene.2022.856636

OPEN ACCESS

EDITED BY
Naglaa M. Kamal,
Cairo University, Egypt

REVIEWED BY
Amjad Khan,
Université de Strasbourg, France
Mark E. Hester,
The Research Institute at Nationwide Children's Hospital, United States

*CORRESPONDENCE
Wenfang Yang,
wenfang.yang@xjtu.edu.cn

†These authors have contributed equally to this work

SPECIALTY SECTION
This article was submitted to Genetics of Common and Rare Diseases, a section of the journal Frontiers in Genetics

RECEIVED 17 January 2022
ACCEPTED 05 August 2022
PUBLISHED 07 September 2022

CITATION
Xie G, Zhang Y, Yang W, Yang L, Wang R, Xu M, Sun L, Zhang B and Cui X (2022), Case report: A novel CASK mutation in a Chinese female child with microcephaly with pontine and cerebellar hypoplasia. *Front. Genet.* 13:856636. doi: 10.3389/fgene.2022.856636

Case report: A novel *CASK* mutation in a Chinese female child with microcephaly with pontine and cerebellar hypoplasia

Guilan Xie[1,2†], Yan Zhang[3†], Wenfang Yang[1*], Liren Yang[1,2], Ruiqi Wang[1,2], Mengmeng Xu[1], Landi Sun[1,2], Boxing Zhang[1,2] and Xiaoyi Cui[1,4]

[1]Department of Obstetrics and Gynecology, Maternal and Child Health Center, The First Affiliated Hospital of Xi'an Jiaotong University, Xi'an, China, [2]School of Public Health, Xi'an Jiaotong University Health Science Center, Xi'an, China, [3]Center for Translational Medicine, The First Affiliated Hospital of Xi'an Jiaotong University, Xi'an, China, [4]Peking University Health Science Center, Beijing, China

Objective: Microcephaly with pontine and cerebellar hypoplasia (MICPCH) is a rare X-linked dominant genetic disease, and most MICPCHs are ascribed to *CASK* mutations, while few are revealed in Chinese patients. This study aims to identify the pathogenic mutation in a Chinese proband with MICPCH.

Methods: A 3-year-old female Chinese proband with MICPCH and her parents were included. Clinical data were collected from the medical records and recalled by the proband's mother. Whole genome sequencing and Sanger sequencing were used to find the pathogenic mutation of MICPCH.

Results: The proband presented with postnatal progressive microcephaly, cerebellar hypoplasia, intellectual disability, motor and language development retardation and limb hypertonia. Genetic analysis indicated that there was a novel compound heterozygote nonsynonymous mutation, c.755T>C(p.Leu252Pro) in exon8 of *CASK* gene in the proband, but not in her parents. This *CASK* mutation has not been reported in other databases.

Conclusion: This study broadens the mutation spectrum of the *CASK* gene and is of great value for precise prenatal diagnosis and genetic counseling.

KEYWORDS

CASK gene, whole exome sequencing, microcephaly, cerebellar hypoplasia, intellectual disability

Introduction

Microcephaly with pontine and cerebellar hypoplasia (MICPCH) is a rare X-linked dominant genetic disease characterized by postnatal progressive microcephaly, intellectual disability, pontine cerebellar hypoplasia, epilepsy, sensorineural deafness, and ophthalmologic abnormalities (Nishio et al., 2021; Shelby et al., 2021). Najm et al. (Najm et al., 2008) first ascribed MICPCH to calcium/calmodulin-dependent serine protein kinase (*CASK*) mutations, for they recovered heterozygous loss-of-function *CASK* mutations in individuals with MICPCH. A total of 153 mutations in the *CASK* gene have been reported in the HGMD Professional 2021.4 database, involving missense, nonsense, splicing, deletions, insertions, indels, duplications and complex rearrangements. The loss-of-function mutations in the *CASK* gene usually lead to phenotypic manifestation in females, while resulting *in utero* lethality in males (Moog et al., 2015; Mukherjee et al., 2020).

The *CASK* gene is located at Xp11.4 and encodes the *CASK* protein composed of 926 amino acids (Hackett et al., 2010). The *CASK* protein belongs to the membrane-associated guanylate kinase family and involves multiple functional domains, including L27 (LIN-2 and LIN-7 interaction), PDZ (PSD95, Discs-large, ZO-1), SH3 (src homology 3), and additional N-terminal calcium/calmodulin-dependent kinase (CaMK) and C-terminal guanylate kinase (GK) domains (Hsueh, 2009). In central nervous system synapse, *CASK* assembles multiprotein complexes and is involved in synaptic interaction, protein trafficking, signaling of ion channels, and regulation of gene expression during neural development (Moog et al., 2011).

Despite the known linkages of *CASK* mutations and MICPCH, few were revealed in Chinese patients. Herein, a novel *CASK* mutation in a female Chinese child with MICPCH was reported, and it had not been reported in other databases. This finding might broaden the spectrum of the *CASK* genotype and help to precisely conduct prenatal diagnosis and genetic counseling.

Methods

Study objects

One female Chinese child with MICPCH and her parents were included in this study. The clinical data of the proband, comprising weight, length, head circumference at birth and different stages, progress of motor and intelligence growth, and brain magnetic resonance imaging (MRI) features, were obtained from the medical records and report from her mother. The growth status of head circumference, weight and length of the proband were compared with the growth reference standard for children in China (Department of Maternal and Child Health, National Health Commission of the People's Republic of China, 2009). The history of diseases and medications during pregnancy, family history of related diseases and feeding status in infancy were recalled by her mother. This study was permitted by the Medical Ethics Committee of the First Affiliated Hospital of Xi'an Jiaotong University (No. XJTU1AF2021LSK-382), and written informed consent was obtained from the parents of the proband.

TABLE 1 Clinical and molecular characteristics of the proband.

Variables	Characteristics
Clinical characteristics	
Age	3 years old
Gender	Female
Gestational age at birth	41 weeks
Birth weight	3.4 kg
Birth length	51 cm
Gravidity	First
Parity	First
Delivery model	Vaginal delivery
Apgar scores	
1 min after birth	9 points
5 min after birth	10 points
History of asphyxia	No
History of hypoxia	No
Family history of genetic diseases	No
Family history of microcephaly	No
Microcephaly	Yes
Pontine and cerebellar hypoplasia	Yes
Intellectual disability	Yes
Developmental delay	Yes
Facial feature	Round face, small chin and large ears
Muscular tone	Normal axial tone and limb hypertonia
Seizures	No
Hearing loss	No
Ophthalmologic abnormalities	No
Molecular characteristics	
Position	exon8
Nucleotide change	c.755T>C
Amino-acid change	p.Leu252Pro

Molecular analysis

After gaining the written informed consent from the parents of the proband, 2 ml venous blood samples of the proband and her parents were collected in anticoagulant tubes containing EDTA. Genomic DNA was extracted by a QIAamp DNA extraction kit (QIAGEN, Hilden, Germany), and 3 μg DNA

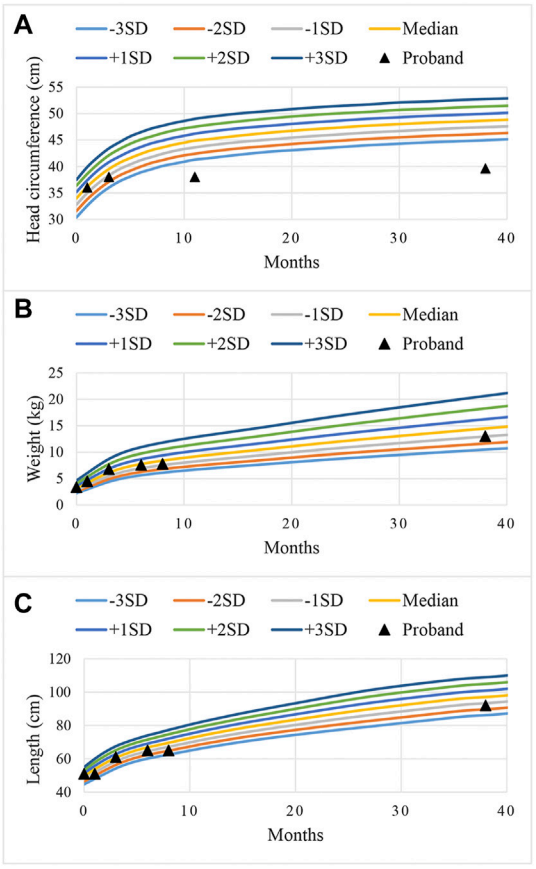

FIGURE 1
Curves of standard deviations (SD) during the growth of head circumference **(A)**, weight **(B)**, and length **(C)** for the proband. The color curves were the referenced growth curves for Chinese girls, and the black triangles were the growth status of the proband at different ages.

was collected as fragments ranging from 150 bp to 200 bp with Covaris S2 (Covaris Company, United States). NEB Next DNA of Illumina (NEB Company, United States) was used to construct the whole genomic DNA library. Liquid phase capture target gene technology was used to capture the human genome gene coding exon regions, and an Illumina Nextseq 6000 (Illumina, San Diego, United States) was used to sequence the genomic DNA of the family with 150 bp pair-end sequencing mode. The low-quality data were removed after the sequencing of the target region, and the sequencing depth, uniformity and probe specificity were analyzed. Single nucleotide polymorphisms (SNPs) and InDels were analyzed with the Verita Trekker® variant site detection system and the Enliven® variant site annotation interpretation system (Berry Genomics, China). The SNPs and InDels were searched in the Berry big data population database, the Exome Aggregation Consortium (ExAC), the 1000 Genome Project, and the Genome Aggregation Database (gnomAD), and the variants with allele frequency lower than 5‰ were filtered. The pathogenicity of the mutation was predicted by SIFT, PolyPhen2, MutationTaster, REVEL, MCAP and LRT. Primers were synthesized and amplified by the PCR method. Sanger sequencing was conducted with an ABI3730xl sequencer (Applied Biosystems, United States), and the results were analyzed and compared with the reference sequence through Mutation Surveyor.

Results

Clinical features

The 3-year-old female Chinese proband was the first gravidity and the first parity of the healthy and non-consanguineous parents. The clinical and molecular characteristics of the proband are outlined in Table 1. She was delivered vaginally, with a gestational age of 41 weeks, birth weight of 3.4 kg and birth length of 51 cm. The Apgar scores were 9 points at 1 min after birth and 10 points at 5 min after birth. There was no history of asphyxia or hypoxia, and the family history of genetic diseases or microcephaly was negative. Her mother did not have gestational hypertension or gestational diabetes mellitus during pregnancy. However, at 6 months of pregnancy, the ultrasound-based gestational age was 3 weeks younger than that of the last menstrual period-based gestational age. Her mother took folate before conception but not during the pregnancy for the emesis gravidarum. Minor facial features were observed, including a round face, small chin and large ears.

The proband was diagnosed with postnatal progressive microcephaly. The growth curves of head circumference, weight and length for the proband are shown in Figure 1. The head circumference was initially within the normal range, but the growth of head circumference nearly came to a standstill at 3 months. Her weight and length were always in the normal range for Chinese girls, although sometimes at the low-normal level. In infancy, she had poor swallowing function, with drooling and feeding difficulties. She also had an intellectual disability and delayed motor development. The results of Gesell Developmental Schedules indicated that her status of adaptive, gross motor, fine motor, language and personal-social behaviors were delayed. When she was at the age of 11 months old, her status matched the age of 20–26 weeks. The brain magnetic resonance imaging (MRI) presented with cerebellar hypoplasia and bilateral enlarged brain ventricles (Figure 2). For the muscle tone, the axial tone was normal but with limb hypertonia. At the age of 3 years, she could only turn over, sit unaided, and crawl with abnormal posture. She could not stand independently. When she stood with support, her knees hyperextended, and her toes touched the ground. In addition, she could not pinch pellets with her thumb and index finger or eat with a spoon. For language development, she could only pronounce “mama” and

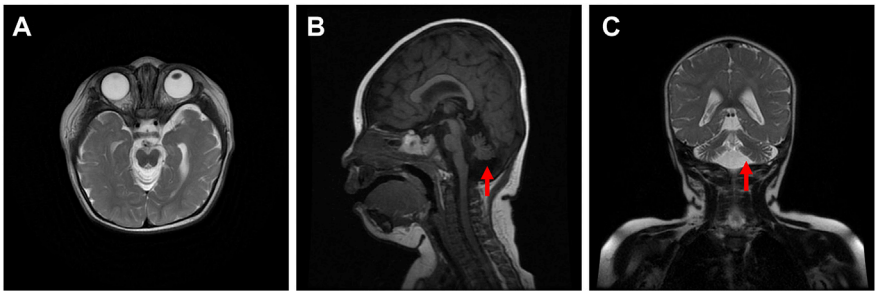

FIGURE 2
Axial **(A)**, sagittal **(B)**, and coronal **(C)** brain magnetic resonance images of the proband.

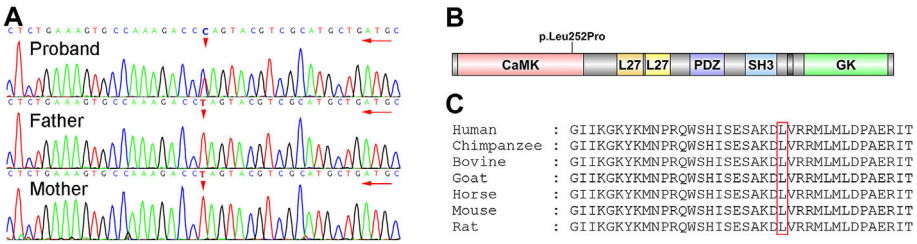

FIGURE 3
Identification of the novel *CASK* mutation. **(A)** results of Sanger sequencing. The proband was heterozygous status with c.755T>C mutation, but her parents were wild-type status. **(B)** functional domains of *CASK*. p.Leu252Pro mutation was in the CaMK domain of *CASK*. **(C)** conservation of the p.Leu252Pro mutation site in different species.

"papa" unconsciously. Her vision and hearing were normal. The proband was given ganglioside and aceglutamide to treat nerve cell damage. Comprehensive rehabilitation training was given to the proband, including repetitive transcranial magnetic stimulation, occupational therapy, and cognitive therapy.

Novel *CASK* mutation

A novel heterozygote nonsynonymous mutation, NM_003688.3:exon8:c.755T>C:p.Leu252Pro in the *CASK* gene (gene position: chrX: 41660515) was identified in the proband (Figure 3), and the amino acid changed from leucine to proline. The influenced codon "L" was conserved. However, the *CASK* mutation was not identified in her parents after Sanger sequencing. According to the American College of Medical Genetics and Genomics (ACMG) guidelines, this *CASK* mutation was categorized as a pathogenic mutation (PS2+PM1+PM2+PP2+PP3) because: 1) this mutation was a novel mutation verified by the venous blood samples of her parents (PS2); 2) this mutation occurred in the CaMK functional domain of *CASK* protein (PM1); 3) this mutation was not found in the Berry big data population database, ExAC, 1000 Genome Project, or gnomAD (PM2); 4) a missense mutation of the *CASK* gene was the common mechanism for the phenotypes of related diseases, and the proportion of benign missense mutation was low (PP2); 5) the results of the in silico prediction algorithms (SIFT, Polyphen2, MutationTaster, REVEL, MCAP and LRT) showed that this *CASK* mutation had damaging or possibly damaging effects on genes or gene products, and the results of SPIDEX showed that the mutation might affect splicing (PP3).

Discussion

The *CASK* protein is highly expressed in the central nervous system and engages in brain development and synaptic function. Intriguingly, the function of the *CASK* gene varies with the periods of brain development (Hsueh, 2006; Rivas et al., 2017). *CASK* mutations lead to interference of the neuronal migration and consequent neurodevelopmental disorder. Accumulated evidence (Hayashi et al., 2017; Nuovo et al., 2021) has demonstrated that most patients with MICPCH arise from *CASK* mutations. Although some reported

maternally inherited *CASK* mutations, the majority were *de novo* (Seto et al., 2017; Pan et al., 2021). Most missense mutations cause alteration of protein structure through a frameshift change of amino acids, while some missense mutations cause misrecognition of specific sites by splicing machinery (Cartegni et al., 2002). The reduced accuracy of splicing yields aberrant transcripts that lead to less-functional protein and ultimate gene inactivation. Piluso et al. (2009) demonstrated that the missense mutation exon2:c.83G>T(p.R28L) in the *CASK* gene did not induce significant alterations in the structure, dynamics, and functions of *CASK*, but they found aberrant exon2-skipped *CASK* mRNA transcripts ascribed to the improper recognition of exonic splicing enhancers. In this study, we found a novel *CASK* mutation in the CaMK domain, and leucine (252nd amino acid) was replaced with proline. Neurexin and other molecules interact with the *CASK* protein through the CaMK domain. A missense mutation (p.Leu209Pro) was reported that could disrupt protein interactions mediated by the CaMK domain but not directly affect the *CASK*-neurexin interaction (LaConte et al., 2019). However, whether the neurexin binding function of *CASK* protein was affected by p.Leu252Pro mutation needs to be further explored.

Several studies have investigated the pattern of X-chromosome inactivation for mutations in the *CASK* gene. Burglen et al. (Burglen et al., 2012) performed an X-inactivation study on nine female patients with *CASK* anomalies and found that all of them had random X-chromosome inactivation. A random skewing X-inactivation pattern was also found in a 12-year-old female with a *CASK* mutation of c.1556T>C: p.Met519Thr (LaConte et al., 2018). However, in a family with a maternally inherited allele carrying a *CASK* mutation, the mother had the skewed X-chromosome inactivation, but the daughter had a paradoxical X-chromosome inactivation (Seto et al., 2017).

The phenotypes of mutations in the *CASK* gene are diverse. *CASK* null alleles lead to severe phenotypes, while missense mutations and slicing mutations in the *CASK* gene lead to mild to moderate phenotypes (Moog et al., 2011). The MRI images of a patient with MICPCH caused by *CASK* mutations often show prominent cerebellar hypoplasia, different degrees of pons hypoplasia, and a normal-sized corpus callosum, which might be important imaging clues for distinguishing the patients with *CASK* mutations from other MICPCH patients (Takanashi et al., 2010). Takanashi et al. (Takanashi et al., 2012) detected a normal to low-normal size corpus callosum in each of 16 patients with intellectual disability and MICPCH with *CASK* mutations. Our proband displayed cerebellar hypoplasia and bilateral enlarged brain ventricles, which was in line with another study (Zhao et al., 2021). Microcephaly, the key feature of MICPCH, could be determined by head circumference smaller than −3SD below the median (DeLuca et al., 2017). Zhao et al. (Zhao et al., 2021) observed four female patients with MICPCH caused by *CASK* mutations whose head circumference ranged from −4.2 SD to −7.7 SD. Hayashi et al. (Hayashi et al., 2012) described that the occipitofrontal circumferences of ten female patients with MICPCH were obviously lower than the normal standard (<−3.2 SD). In our study, the head circumference of the proband was initially within the normal range and nearly stagnant since the age of 3 months. *CASK* regulates mitochondrial respiration and oxidative metabolism, and nutrition and energy deprivation of the rapid growth of brain after birth disproportionately limits the growth of the cerebellum (Srivastava et al., 2016; Zhao et al., 2021). Moreover, the differences in symptoms and manifestations, especially in language and motor function, between patients with microcephaly and healthy children become more and more obvious during the developmental progression (DeLuca et al., 2017). This would explain the phenomenon that MICPCH patients tend to be born with normal head circumference, birth weight and length but experience postnatal progressive microcephaly and growth retardation. Pan et al. (Pan et al., 2021) reported that among six patients with novel *CASK* mutations, four patients had developmental delay or intellectual disability, and three patients had muscular hypertonia, hearing loss and ophthalmologic abnormalities. In ten females with *CASK* mutations, two patients had seizures, and five patients had muscular hypotonia (Hayashi et al., 2012). Due to the variable genotype-phenotype of *CASK*, the diseases arising from *CASK* mutations should be diagnosed with caution.

Conclusion

Collectively, this study reported a novel c.755T>C(p.Leu252Pro) *CASK* mutation in a female Chinese child with MICPCH, which might broaden the spectrum of *CASK* genotype and is of great value for precise prenatal diagnosis and genetic counseling.

Data availability statement

The datasets presented in this study can be found in online repositories. The names of the repository/repositories and accession number(s) can be found below: https://www.ncbi.nlm.nih.gov/, SRR17634755 https://www.ncbi.nlm.nih.gov/, SRR17634754 https://www.ncbi.nlm.nih.gov/, SRR17634753.

Ethics statement

The studies involving human participants were reviewed and approved by the Medical Ethics Committee of the First Affiliated Hospital of Xi'an Jiaotong University (No. XJTU1AF2021LSK-382). Written informed consent to participate in this study was provided by the participant's legal guardian/next of kin.

Author contributions

Conceptualization: GX, YZ, and WY. Data collection: GX, LY, and WY. Data analysis: GX, YZ, LY, RW, MX, LS, BZ, and XC. Writing original draft: GX and YZ. Writing-review and editing: GX, YZ, WY, LY, RW, MX, LS, BZ, and XC. All authors have read and approved the manuscript.

Acknowledgments

We would like to thank the participation of the proband and her parents and the technical support of Berry Genomics.

Conflict of interest

The authors declare that the research was conducted in the absence of any commercial or financial relationships that could be construed as a potential conflict of interest.

Publisher's note

All claims expressed in this article are solely those of the authors and do not necessarily represent those of their affiliated organizations or those of the publisher, the editors and the reviewers. Any product that may be evaluated in this article, or claim that may be made by its manufacturer, is not guaranteed or endorsed by the publisher.

References

Burglen, L., Chantot-Bastaraud, S., Garel, C., Milh, M., Touraine, R., Zanni, G., et al. (2012). Spectrum of pontocerebellar hypoplasia in 13 girls and boys with CASK mutations: Confirmation of a recognizable phenotype and first description of a male mosaic patient. *Orphanet J. Rare Dis.* 7, 18. doi:10.1186/1750-1172-7-18

Cartegni, L., Chew, S. L., and Krainer, A. R. (2002). Listening to silence and understanding nonsense: Exonic mutations that affect splicing. *Nat. Rev. Genet.* 3 (4), 285–298. doi:10.1038/nrg775

DeLuca, S. C., Wallace, D. A., Trucks, M. R., and Mukherjee, K. (2017). A clinical series using intensive neurorehabilitation to promote functional motor and cognitive skills in three girls with CASK mutation. *BMC Res. Notes* 10 (1), 743. doi:10.1186/s13104-017-3065-z

Department of Maternal and Child Health, National Health Commission of the People's Republic of China (2009). Reference standards for growth and development of children under 7 years old in China. Available at: http://www.nhc.gov.cn/fys/s7906/200910/994a7f6e1bd1491a9e8efa8e762a313f.shtml.

Hackett, A., Tarpey, P. S., Licata, A., Cox, J., Whibley, A., Boyle, J., et al. (2010). CASK mutations are frequent in males and cause X-linked nystagmus and variable XLMR phenotypes. *Eur. J. Hum. Genet.* 18 (5), 544–552. doi:10.1038/ejhg.2009.220

Hayashi, S., Okamoto, N., Chinen, Y., Takanashi, J., Makita, Y., Hata, A., et al. (2012). Novel intragenic duplications and mutations of CASK in patients with mental retardation and microcephaly with pontine and cerebellar hypoplasia (MICPCH). *Hum. Genet.* 131 (1), 99–110. doi:10.1007/s00439-011-1047-0

Hayashi, S., Uehara, D. T., Tanimoto, K., Mizuno, S., Chinen, Y., Fukumura, S., et al. (2017). Comprehensive investigation of CASK mutations and other genetic etiologies in 41 patients with intellectual disability and microcephaly with pontine and cerebellar hypoplasia (MICPCH). *PLoS One* 12 (8), e0181791. doi:10.1371/journal.pone.0181791

Hsueh, Y. P. (2009). Calcium/calmodulin-dependent serine protein kinase and mental retardation. *Ann. Neurol.* 66 (4), 438–443. doi:10.1002/ana.21755

Hsueh, Y. P. (2006). The role of the MAGUK protein CASK in neural development and synaptic function. *Curr. Med. Chem.* 13 (16), 1915–1927. doi:10.2174/092986706777585040

LaConte, L. E. W., Chavan, V., DeLuca, S., Rubin, K., Malc, J., Berry, S., et al. (2019). An N-terminal heterozygous missense CASK mutation is associated with microcephaly and bilateral retinal dystrophy plus optic nerve atrophy. *Am. J. Med. Genet. A* 179 (1), 94–103. doi:10.1002/ajmg.a.60687

LaConte, L. E. W., Chavan, V., Elias, A. F., Hudson, C., Schwanke, C., Styren, K., et al. (2018). Two microcephaly-associated novel missense mutations in CASK specifically disrupt the CASK-neurexin interaction. *Hum. Genet.* 137 (3), 231–246. doi:10.1007/s00439-018-1874-3

Moog, U., Bierhals, T., Brand, K., Bautsch, J., Biskup, S., Brune, T., et al. (2015). Phenotypic and molecular insights into CASK-related disorders in males. *Orphanet J. Rare Dis.* 10, 44. doi:10.1186/s13023-015-0256-3

Moog, U., Kutsche, K., Kortüm, F., Chilian, B., Bierhals, T., Apeshiotis, N., et al. (2011). Phenotypic spectrum associated with CASK loss-of-function mutations. *J. Med. Genet.* 48 (11), 741–751. doi:10.1136/jmedgenet-2011-100218

Mukherjee, K., Patel, P. A., Rajan, D. S., LaConte, L. E. W., and Srivastava, S. (2020). Survival of a male patient harboring CASK Arg27Ter mutation to adolescence. *Mol. Genet. Genomic Med.* 8 (10), e1426. doi:10.1002/mgg3.1426

Najm, J., Horn, D., Wimplinger, I., Golden, J. A., Chizhikov, V. V., Sudi, J., et al. (2008). Mutations of CASK cause an X-linked brain malformation phenotype with microcephaly and hypoplasia of the brainstem and cerebellum. *Nat. Genet.* 40 (9), 1065–1067. doi:10.1038/ng.194

Nishio, Y., Kidokoro, H., Takeo, T., Narita, H., Sawamura, F., Narita, K., et al. (2021). The eldest case of MICPCH with CASK mutation exhibiting gross motor regression. *Brain Dev.* 43 (3), 459–463. doi:10.1016/j.braindev.2020.11.007

Nuovo, S., Micalizzi, A., Romaniello, R., Arrigoni, F., Ginevrino, M., Casella, A., et al. (2021). Refining the mutational spectrum and gene-phenotype correlates in pontocerebellar hypoplasia: Results of a multicentric study. *J. Med. Genet.* 59, 399–409. doi:10.1136/jmedgenet-2020-107497

Pan, Y. E., Tibbe, D., Harms, F. L., Reißner, C., Becker, K., Dingmann, B., et al. (2021). Missense mutations in CASK, coding for the calcium-/calmodulin-dependent serine protein kinase, interfere with neurexin binding and neurexin-induced oligomerization. *J. Neurochem.* 157 (4), 1331–1350. doi:10.1111/jnc.15215

Piluso, G., D'Amico, F., Saccone, V., Bismuto, E., Rotundo, I. L., Di Domenico, M., et al. (2009). A missense mutation in CASK causes FG syndrome in an Italian family. *Am. J. Hum. Genet.* 84 (2), 162–177. doi:10.1016/j.ajhg.2008.12.018

Rivas, L., Blanco, Ó., Torreira, C., Repáraz, A., Melcón, C., and Amado, A. (2017). Pontocerebellar hypoplasia secondary to CASK gene deletion: Case report. *Rev. Chil. Pediatr.* 88 (4), 529–533. doi:10.4067/s0370-41062017000400014

Seto, T., Hamazaki, T., Nishigaki, S., Kudo, S., Shintaku, H., Ondo, Y., et al. (2017). A novel CASK mutation identified in siblings exhibiting developmental disorders with/without microcephaly. *Intractable Rare Dis. Res.* 6 (3), 177–182. doi:10.5582/irdr.2017.01031

Shelby, E. S., Lupu, O. T., Axente, M., Leanca, M. C., Badina, M., Padure, L., et al. (2021). New VOUS in CASK gene correlating with the MICPCH phenotype. *Maedica (Bucur)* 16 (1), 135–139. doi:10.26574/maedica.2020.16.1.135

Srivastava, S., McMillan, R., Willis, J., Clark, H., Chavan, V., Liang, C., et al. (2016). X-linked intellectual disability gene CASK regulates postnatal brain growth in a non-cell autonomous manner. *Acta Neuropathol. Commun.* 4, 30. doi:10.1186/s40478-016-0295-6

Takanashi, J., Arai, H., Nabatame, S., Hirai, S., Hayashi, S., Inazawa, J., et al. (2010). Neuroradiologic features of CASK mutations. *AJNR. Am. J. Neuroradiol.* 31 (9), 1619–1622. doi:10.3174/ajnr.A2173

Takanashi, J., Okamoto, N., Yamamoto, Y., Hayashi, S., Arai, H., Takahashi, Y., et al. (2012). Clinical and radiological features of Japanese patients with a severe phenotype due to CASK mutations. *Am. J. Med. Genet. A* 158a (12), 3112–3118. doi:10.1002/ajmg.a.35640

Zhao, J., Hou, M., Wang, H., Liu, Q., Sun, D., and Wei, W. (2021). Microcephaly, disproportionate pontine, and cerebellar hypoplasia syndrome: Two novel mutations in the CASK gene were discovered in Chinese females. *Int. J. Dev. Neurosci.* 81 (3), 277–284. doi:10.1002/jdn.10100

frontiers | Frontiers in Genetics

TYPE Original Research
PUBLISHED 30 September 2022
DOI 10.3389/fgene.2022.801447

OPEN ACCESS

EDITED BY
Naglaa M. Kamal,
Cairo University, Egypt

REVIEWED BY
Urh Groselj,
University of Ljubljana, Slovenia
Kenji Yamada,
Shimane University, Japan
Dehua Zhao,
The Third Affiliated Hospital of Zhengzhou University, China

*CORRESPONDENCE
Chao Zhang,
Suqianzcys@163.com

SPECIALTY SECTION
This article was submitted to Genetics of Common and Rare Diseases, a section of the journal Frontiers in Genetics

RECEIVED 25 October 2021
ACCEPTED 31 August 2022
PUBLISHED 30 September 2022

CITATION
Zhang H, Wang Y, Qiu Y and Zhang C (2022), Expanded newborn screening for inherited metabolic disorders by tandem mass spectrometry in a northern Chinese population. *Front. Genet.* 13:801447. doi: 10.3389/fgene.2022.801447

Expanded newborn screening for inherited metabolic disorders by tandem mass spectrometry in a northern Chinese population

Hong Zhang[1], Yanyun Wang[2], Yali Qiu[1] and Chao Zhang[1]*

[1]Suqian Maternal and Child Health Care Hospital, Suqian, China, [2]Nanjing Maternal and Child Health Care Hospital, Nanjing, China

Tandem mass spectrometry (MS/MS) has been developed as one of the most important diagnostic platforms for the early detection and screening of inherited metabolic disorders (IMDs). To determine the disease spectrum and genetic characteristics of IMDs in Suqian city of Jiangsu province in the northern Chinese population, dried blood spots from 2,04,604 newborns, were assessed for IMDs by MS/MS from January 2016 to November 2020. Suspected positive patients were diagnosed through next-generation sequencing (NGS) and validated by Sanger sequencing. One hundred patients with IMDs were diagnosed, resulting in an overall incidence of 1/2,046, of which 56 (1/3,653), 22 (1/9,300), and 22 (1/9,300) were confirmed amino acids disorders (AAs), organic acids disorders (OAs), fatty acid oxidation disorders (FAODs) positive cases, respectively. The highest incidence of IMDs is phenylalanine hydroxylase deficiency (PAHD) (45 cases), with a total incidence of 1:4,546. Hot spot mutations in phenylalanine hydroxylase (PAH)-related genes are *c.158G > A* (24.44%), *c.728G > A* (16.67%), *c.611A > G* (7.78%), and *c.331C>T* (7.78%). The related hot spot mutation of the *MMACHC* gene is *c.609G > A* (45.45%). Short-chain acyl-CoA dehydrogenase deficiency (SCAD)-related *ACADS* gene hotspot mutations are *c.164C > T* (33.33%) and *c.1031A > G* (33.33%). Our work indicated that the overall incidence of IMDs is high, and the mutations in *PAH*, *ACADS*, and *MMACHC* genes are the leading causes of IMDs in Suqian city.

Abbreviations: IMDs inherited metabolic disorders; NBS newborn screening; MS/MStandem mass spectrometry; NGS next-generation sequencing; AAs amino acids disorders; OAs organic acids disorders; FAODs fatty acid oxidation disorders; MLPA multiplex ligation-dependent probe amplification; PA propionic acidemia; DBS dried blood spots; PPV positive predictive value; PAHD phenylalanine hydroxylase deficiency; BH4D tetrahydrobiopterin deficiency; CD citrin deficiency; HCY homocysteinemia; H-MET hypermethioninemia; OTCD ornithine transcarbamylase deficiency; TYR-II tyrosine aminotransferase type II; CIT-I citrullinemia type I; CUD carnitine uptake defect; SCAD short-chain acyl-CoA dehydrogenase deficiency; VLCADD very long-chain acyl-CoA dehydrogenase deficiency; MCADD medium-chain acyl-CoA dehydrogenase deficiency; CPT-I carnitine palmitoyl transferase-I; CACTD carnitine-acylcarnitine translocase deficiency; 3-MCCD 3-methylcrotonyl; CoA carboxylase deficiency; MAHCC methylmalonic aciduria and homocystinuria cblC type; IBDD isobutyryl-CoA dehydrogenase deficiency; MMA-MUTD methylmalonic aciduria mut type deficiency; GA-II glutaric acidemia type II; GA-I glutaric acidemia type I; 2-MBG 2-methylbutyrylglycinuria; C2 aceylcarnitine; C3 propionylcarnitine; C5 isovalerylcarnitine/2-methylbutyrylcarnitine; C5DC glutarylcarnitine; C5OH 3-hydroxyisovalerylcarnitine/3-hydroxy-2-methylbutyrylcarnitine; C0 free carnitine; C8 octanoylacrnitine; C10 decanoylcarnitine; C12 dodecanoylcarnitine; C14 myristoylcarnitine.

The incidence of AAs in Suqian city is higher than in other Chinese areas. The disease spectrum and genetic backgrounds were elucidated, contributing to the treatment and prenatal genetic counseling of these disorders in this region.

KEYWORDS

newborn screening, inborn errors, tandem mass spectrometry, inherited metabolic disorders, next-generation sequencing

Introduction

Inherited metabolic disorders (IMDs) or inborn errors of metabolism (IEM) are a class of metabolic disorders caused by gene mutations, representing roughly 1,000 different genetic disorders (Ferreira et al., 2019). Even though they are individually rare, their collective prevalence is estimated today at greater than 1: 800 individuals (Wilcox, 2018). The key to clinical management of IMDs is to obtain a definitive genetic diagnosis followed by clinical interventions, such as dietary modification, metabolite administration, or enzyme replacement therapy, to reduce mortality and morbidity and improve quality of life (Tarailo-Graovac et al., 2016). Newborn screening (NBS) is a valuable preventive health measure for early diagnosis, which is diagnostically effective and economically efficient (Zhang et al., 2021).

Tandem mass spectrometry (MS/MS) has been developed as a diagnostic platform for early detection, and screening of genetic disorders and many countries have implemented NBS using MS/MS (Garg and Dasouki, 2006), especially for AAs, OAs, FAODs (Chace et al., 2003; Fabie et al., 2019). The incidence of IMDs detected by MS/MS varies significantly among different countries. The incidence rate of IMDs was 1:8,557 in Japan, 1: 7,030 in Taiwan, and 1:2,200 in Germany (Shibata et al., 2018). Already in 2012, Shi et al. have been reported that the average incidence rate of IMDs was 1/3,795 using the NBS of MS/MS in mainland china (Shi et al., 2012a).

In recent years, more and more regions of China, such as Shanghai, Guangzhou, Zhejiang, and Guangxi, have implemented NBS using MS/MS and reported IMDs incidence in their area (Huang et al., 2012; Guo et al., 2018; Wang et al., 2019; Zhang et al., 2021). Substantial progress in disease prevention, saving lives, and improving patient prognosis has been made in China since screening for IMDs in newborns (Lin et al., 2019; Wang et al., 2019).

In China, children with no clinical symptoms are diagnosed and treated through MS/MS screening technology, reducing the disability rate and mortality. In addition, it has significantly reduced the economic burdens on the family and society (Shi et al., 2012a; Ye et al., 2015; Chen et al., 2018; Wang et al., 2019). With the soaring development of genomics and molecular biology, next-generation sequencing (NGS) has become the gold standard and a common tool used for the diagnostic evaluation of IMDs (Leonard and Morris, 2006; Dai et al., 2019). Focusing on 204,604 newborns, we aimed to determine the disease spectrum and genetic characteristics of IMDs in Suqian city and explore the application value of NBS for IMDs using MS/MS.

Materials and methods

Subjects

2,04,604 infants born in Suqian city were enrolled for expanded NBS by MS/MS from January 2016 to November 2020. The Ethical Committee of Suqian Maternity and Children's Hospital approved this study. Written informed consents were obtained from all the infants' patients.

NBS flow chart

Dried blood spots (DBS) samples were collected following standard procedures to collect DBS in newborns born 48 h-7 days after lactation. DBS samples were delivered by cold-chain transportation to the NBS center of Suqian Maternity and Children's Hospital within 5 days, and then they were analyzed using MS/MS. If the test result is higher or lower than the cut-off value, the initial screening is positive, and the child is recalled for re-examination. Those with abnormal results (suspected positive patients) are recalled for confirmatory tests such as routine biochemical, MS/MS, gas-chromatographic mass spectrometry (GC-MS) and genetic analysis. The description of the process of NBS see Figure 1.

Mass spectrometry analysis

DBS were pre-processed following the instruction of NeoBaseTM non-derivatized MS/MS kit (PerkinElmer, MA, United States), using 1525u high-performance liquid chromatography (HPLC) (Waters Technologies, Milford, MA, United States) and ACQUITY TQD mass spectrometer (Waters, Milford, MA, USA) for quantitative analysis. The analytes included 11 amino acids, 31 acylcarnitine, and 1 Ketone (succinylacetone). The 11 amino acids were alanine (Ala), arginine (Arg), citrulline (Cit), glycine (Gly), leucine/isoleucine (Leu/lle/Pro-OH), methionine (Met), ornithine (Orn), phenylalanine (Phe), proline (Pro), tyrosine (Tyr), and valine (Val); the 31 acylcarnitine were free carnitine (C0), acetylcarnitine (C2), propionylcarnitine (C3),

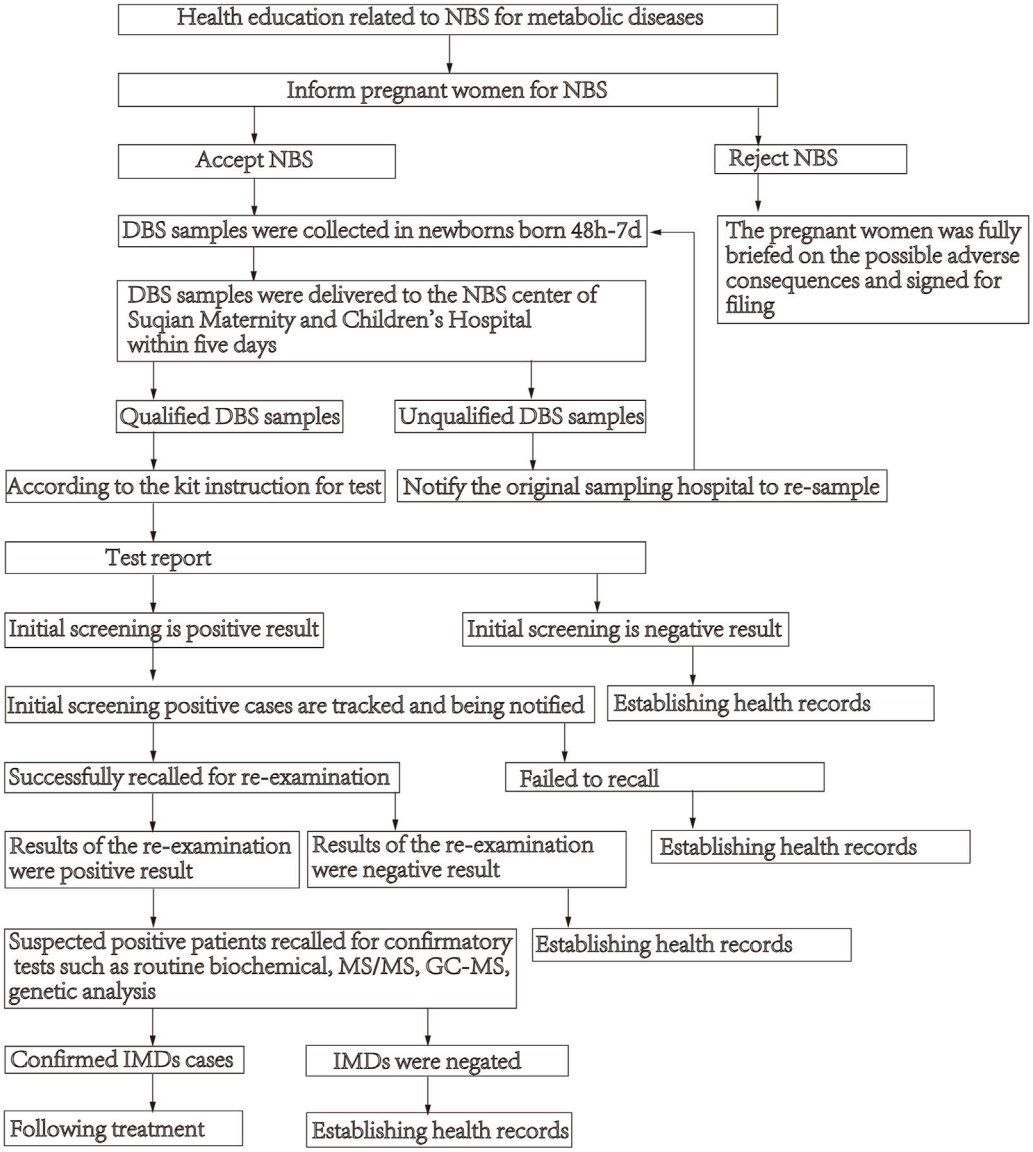

FIGURE 1
Flowchart of newborn screening.

malonylcarnitine/3-hydroxy- butyrylcarnitine (C3DC/C4OH), butyrylcarnitine (C4), methylmalonyl/3-hydroxy-isovalerylcarnitine (C4DC/C5OH), isovalerylcarnitine (C5), tiglylcarnitine (C5:1), glutarylcarnitine/3-Hydroxy-hexanoylcarnitine (C5DC/C6OH), hexanoylcarnitine (C6), adipylcarnitine (C6DC), octanoylcarnitine (C8), octenoylcarnitine (C8:1), decanoylcarnitine (C10), decenoylcarnitine (C10:1), decadienoylcarnitine (C10:2), dodecanoylcarnitine (C12), dodecenoylcarnitine (C12:1), tetradecanoylcarnitine (C14), tetradecenoylcarnitine (C14:1), tetradecadienoylcarnitine (C14:2), 3-Hydroxy-tetradecanoylcarnitine (C14OH), hexadecanoylcarnitine (C16), hexadecenoylcarnitine (C16:1), 3-Hydroxy-hexadecanoylcarnitine (C16OH), 4-Hydroxy-hexadecenoylcarnitine (C16:1OH), octadecanoylcarnitine (C18), octadecenoylcarnitine (C18:1), octadecadienoylcarnitine (C18:2), 3-Hydroxy-Octadecanoylcarnitine (C18OH), 3-Hydroxy-Octadecenoylcarnitine (C18:1OH).

The indoor quality control and the inter-room quality control adopt the quality evaluation standard of NBS by the Clinical Examination Center of the Ministry of Health, and they are all qualified. The cut-off values were initially set by reference to the worldwide collaborative project and other screening centers (Niu et al., 2010; McHugh et al., 2011) and were adjusted over time as the number of samples increased.

Next-generation sequencing analysis

Genetic analysis was performed by Genuine Diagnostics Company (Hangzhou, Zhejiang, China). The detailed process of NGS was as follows. According to the manufacturer's protocol, DBS or peripheral whole blood of suspected positive patients was referred to a laboratory, and genomic DNA was extracted using the QIA amp DNA Blood Midi Kit (Qiagen, Hilden, Germany). Then use Gene Cap gene sequence capture technology to mix standard IMDs pathogenic gene capture probes with the child's whole genome library, and the disease-related gene fragments are hybridized for the examination, and the DNA in the non-target area is eluted. The fragments are washed away, thereby enriching the pathogenic gene fragments. cDNA library was constructed and sequenced using Illumina HiSeq 2000 sequencer (San Diego, CA, United States). After the fragments were filtered and trimmed by the Trim-Galore program, the sequences with reading quality >20 and read length >80 bp are retained. The sequenced reads were aligned to the human reference genome (hg19) using the Burrows-Wheeler Aligner (BWA). Then, the GATH software package was used to collect point mutations, insertion mutations or deletion mutations, etc. Next, all variants identified by NGS were further validated by Sanger sequencing of the parents. In addition, multiple ligation-dependent probe amplification (MLPA) technology is also used to diagnose diseases where NGS has no pathogenic mutations but suspected deletion or duplication mutations, such as non-ketotic hyperglycinemia and propionic acidemia (PA).

Diagnosis and follow-up

Metabolic disease specialists made a definitive diagnosis based on the patients' biochemical performance, genetic mutations, and clinical symptoms. Then, a definitive diagnosis was made by metabolic disease specialists based on the patients' biochemical performance, genetic mutations, and clinical symptoms. Only patients diagnosed by the genetic analysis were included in this study. All infants with negative screening results were included in the children's health care management system for follow-up. All confirmed children were followed up every 3–6 months, and the follow-up data were collected.

Results

Newborn screening

An expanded NBS program screened 2,04,604 newborns. After initial screening, 4,069 (1.99%) newborns, who had positive results, were recalled for a new specimen. 4,021 newborns (98.82%) were successfully recalled and had a repeated test, 100 cases were finally confirmed with IMDs, and the positive predictive value (PPV) was 2.46%. Twenty-two types of IMDs were diagnosed in 100 confirmed cases, and the overall IMDs detection incidence was 1: 2,046; of these, 56 (56.0%) newborns with AAs, 22 (22.0%) with OAs, and 22 (22.0%) with FAODs. AAs, OAs, and FAODs were 1:3,653, 1:9,300, and 1:9,300, respectively. Details are shown in Table 1 and Figure 2A.

Amino acids disorders

Totally eight types of AAs were detected. Phenylalanine hydroxylase deficiency (PAHD) was the most common disorder (45/56, 80.4%), followed by citrin deficiency (CD) (3/56, 5.36%), hypermethioninemia (H-MET, 3/56, 5.36%). There was only one positive case for tetrahydrobiopterin deficiency (BH4D), homocysteinemia (HCY), ornithine transcarbamylase deficiency (OTCD), and tyrosine aminotransferase type II deficiency (TYR II- deficiency). The phenylalanine concentration of 45 PAHD patients exceeded the reference range (reference range: 24–105 μmol/L), and only 3 patients' phenylalanine/tyrosine ratios were within the reference range (reference range: 0.16–1.25 μmol/L). The phenylalanine concentration and phenylalanine/tyrosine ratios of the 3 patients were 120.69, 113.44, 141.12 μmol/L, and 1.168, 1.244, 1.14, respectively. Details are shown in Table 1.

Forty-five patients had *PAH* gene mutations, of whom two patients had concurrent *PTS* gene and *PAH* gene mutations. The most frequent mutation found was *c.158G>A* (22/90, 24.44%), followed by *c.728G>A* (15/90, 16.67%), *c.611A>G* (7/90, 7.78%), *c.331C>T* (7/90, 7.78%). Three patients with CD were female, and mutations were compound heterozygous. The *MAT1A* mutations of two patients with H-MET were heterozygous, and the mutations were *c.777_778insCG* and *c.895C>T*. One patient has a compound heterozygous *c.1003T>C* and *c.188G>T*. Details are shown in Table 1 and Figure 2B. (Supplementary File S1: Supplementary Table S1).

Organic acids disorders

There were eight types of OAs. Of these types, the most common disorder was 3-methylcrotonyl CoA carboxylase deficiency (3-MCCD, 6/22, 27.27%) and methylmalonic aciduria and homocystinuria type C deficiency (MAHCC-deficiency, 6/22, 27.27%), followed by isobutyryl-CoA dehydrogenase deficiency (IBDD, 3/22, 13.63%), methylmalonic aciduria mut type deficiency (MMA-MUTD, 3/22, 13.63%). The remaining four types of OAs were all of one case. Details are shown in Table 1.

TABLE 1 Abnormal MS/MS markers and results statistics of all confirmed infants.

Disorders	Positive cases	Frequency	Abnormal MS/MS marks	Concentration mean (range) (μmol/L)	Reference range (μmol/L)
Amino acids disorders (AAs)	56	1:3653			
Phenylalanine hydroxylase deficiency (PAHD)	45	1:4546	Phe	413.99 (108.57–1631.90)	24–105
			Phe/Tyr	7.52 (1.14–32.95)	0.16–1.25
Tetrahydrobiopterin deficiency (BH4D)	1	1:204604	Phe	267.42	24–105
			Phe/Tyr	3.67	0.16–1.25
Citrin deficiency (CD)	3	1:68201	Cit	116.66 (48.54–218.23)	5.5–30
Homocysteinemia (HCY)	1	1:204604	Met	100.16	6–40
Hypermethioninemia (H-MET)	3	1:68201	Met	205.82 (59.55–296.34)	6–40
			Met/Phe	5.96 (5.12–6.80)	0.12–0.73
Ornithine transcarbamylase deficiency (OTCD)	1	1:204604	Cit	5.45	5.5–30
			Cit/Phe	0.12	0.13–0.89
Tyrosine aminotransferase type II deficiency (TYR II-deficiency)	1	1:204604	Tyr	666.75	35–320
Citrullinemia type I deficiency (CIT I-deficiency)	1	1:204604	Cit	135.68	5.5–30
			Cit/Phe	2.857	0.10–0.75
Organic acids disorders (OAs)	22	1:9300			
Propionic acidemia (PA)	1	1:204604	C3	4.68	0.3–0.45
			C3/C2	0.33	0.01–0.2
3-methylcrotonyl CoA carboxylase deficiency (3-MCCD)	6	1:34100	C4DC/C5OH	3.15 (0.81–8.82)	0.08–0.4
			(C4DC/C5OH)/C0	0.06 (0.04–0.09)	0–0.02
			(C4DC/C5OH)/C8	31.97 (16.50–51.75)	1.2–15
Methylmalonic aciduria and homocystinuria type C deficiency (MAHCC-deficiency)	6	1:34100	C3	6.08 (4.32–8.24)	0.3–0.45
			C3/C0	0.35 (0.15–0.55)	0.02–0.2
			C3/C2	0.82 (0.35–1.95)	0.01–0.2
Isobutyryl-CoA dehydrogenase deficiency (IBDD)	3	1:68201	C4	1.29 (0.73–1.98)	0.08–0.45
			C4/C2	0.13 (0.07–0.17)	0–0.03
			C4/C3	1.00 (0.86–1.09)	0.04–0.39
Methylmalonic aciduria mut type deficiency (MMA-MUTD)	3	1:68201	C3	11.27 (8.28–16.58)	0.3–0.45
			C3/C2	0.54 (0.42–0.67)	0.01–0.2
Glutaric acidemia type II deficiency (GA II-deficiency)	1	1:204604	C4	0.64	0.08–0.45
			C6	0.27	0.01–0.09
			C8	0.46	0.01–0.13
			C10	0.37	0.02–0.21
			C5DC/C6OH	0.49	0.04–0.2
Glutaric acidemia type I deficiency (GA I-deficiency)	1	1:204604	C0	5.52	9.5–65
			C5DC/C6OH	2.01	0.04–0.2
			(C5DC/C6OH)/(C3DC/C4OH)	33.5	0.35–2.33
			(C5DC/C6OH)/(C4DC/C5OH)	9.14	0–1.14
2-methylbutyrylglycinuria deficiency (2-MBG-deficiency)	1	1:204604	C5	0.66	0.03–0.35
			C5/C2	0.02	0–0.04
			C5/C3	0.52	0.02–0.42
Fatty acid oxidation disorders (FAODs)	22	1:9300			
Carnitine uptake defect (CUD)	6	1:34100	C0	5.45 (3.66–6.95)	9–50
Short-chain acyl-CoA dehydrogenase deficiency (SCAD)	11	1:18600	C4	0.99 (0.62–1.46)	0.08–0.45
			C4/C2	0.07 (0.03–0.10)	0–0.03

(Continued on following page)

TABLE 1 (*Continued*) Abnormal MS/MS markers and results statistics of all confirmed infants.

Disorders	Positive cases	Frequency	Abnormal MS/MS marks	Concentration mean (range) (μmol/L)	Reference range (μmol/L)
			C4/C3	0.72 (0.33–1.14)	0.04–0.39
Very long-chain acyl-CoA dehydrogenase deficiency (VLCADD)	1	1:204604	C14:1	3.06	0.02–0.26
Medium-chain acyl-CoA dehydrogenase deficiency (MCADD)	2	1:102302	C6	0.29 (0.28–0.31)	0.01–0.09
			C8	0.80 (0.61–1.00)	0.01–0.15
			C10	0.26 (0.2–0.31)	0.02–0.2
			C8/C2	0.09	0–0.01
Carnitine palmitoyl transferase I deficiency (CPT I-deficiency)	1	1:204604	C0	70.83	9–50
Carnitine-acylcarnitine translocase deficiency (CACTD)	1	1:204604	C0/(C16/C18)	43.19	2.4–35
			C6	0.63	0.01–0.09

Note: Phe, phenylalanine; Tyr, tyrosine; Cit, citrulline; Met, methionine; C2, aceylcarnitine; C3, propionylcarnitine; C5DC, glutarylcarnitine; C5OH, 3-hydroxyisovalerylcarnitine/3-hydroxy-2-methylbutyrylcarnitine; C0, free carnitine; C8, octanoylacrnitine; C10, decanoylcarnitine; C12, dodecanoylcarnitine; C14, myristoylcarnitine; The results did not exceed the reference ranges including amino acids were alanine (Ala), arginine (Arg), glycine (Gly), leucine/isoleucine (Leu/lle/Pro-OH), ornithine (Orn), proline (Pro), valine (Val), tiglylcarnitine (C5:1), adipylcarnitine (C6DC), octenoylcarnitine (C8:1), decenoylcarnitine (C10:1), decadienoylcarnitine (C10:2), dodecanoylcarnitine (C12), dodecenoylcarnitine (C12:1), tetradecanoylcarnitine (C14), tetradecadienoylcarnitine (C14:2), 3-Hydroxy-tetradecanoylcarnitine (C14OH), hexadecanoylcarnitine (C16), hexadecenoylcarnitine (C16:1), 3-Hydroxy-hexadecanoylcarnitine (C16OH), 4-Hydroxy-hexadecenoylcarnitine (C16:1OH), octadecanoylcarnitine (C18), octadecenoylcarnitine (C18:1), octadecadienoylcarnitine (C18:2), 3-Hydroxy-Octadecanoylcarnitine (C18OH), 3-Hydroxy-Octadecenoylcarnitine (C18:1OH).

Six patients with 3-MCCD found a total of 13 site mutations in 5 mutated genes, of whom three patients were compound heterozygous, and one was heterozygous in the *MCCC2* gene, two patients were heterozygous in the *MCCC1* gene. Six patients with MAHCC deficiency had *MAHCC* gene mutations, and the most common mutation was *c.609G>A* (5/11, 45.45%). In patients with MMA-MUTD, the predominant mutation in *MUT* gene was *c.323G>A* and *c.729_730insTT*, with each frequency of 33.33%. Three patients with IBDD have compound heterozygous mutations in the *ACAD8* gene and one with mutations in the *PAH* gene. The remaining patients were either compound heterozygous mutation, and no high frequent mutation was found. Details are shown in Table 1 and Figure 2C. (Supplementary file S2: Supplementary Table S2).

Fatty acid oxidation disorders

Six types of FAODs were detected among the 22 cases. SCAD was the most common disease in this group, which accounted for 50.00%, followed by CUD (6/22, 27.27%), and medium-chain acyl-CoA dehydrogenase deficiency (MCADD, 2/22, 9.09%). The very long-chain acyl- CoA dehydrogenase deficiency (VLCADD), carnitine palmitoyl transferase I deficiency (CPT I-deficiency), and carnitine-acylcarnitine translocase deficiency (CACTD) were comparatively rare. In the initial screening, one case was recalled due to CIT (CIT = 73.55; C0 = 70.83, C0/(C16 + C18) = 43.19). However, Next-generation sequencing detected *PAH* gene *c.473G>A* locus heterozygous mutation, *CPT1A* gene *c.1910C>T* and *c.1065G>A* locus heterozygous mutation, and finally diagnosed as CPT-I deficiency. Details are shown in Table 1.

One case was recalled due to an abnormal concentration of C5 in the initial screening. However, Next-generation sequencing detected *ACADM* gene *c.1085G>A* locus heterozygous mutation, *ACADSB* gene *c.655G>A* and *c.848A>G* locus heterozygous mutation, and finally diagnosed as SCAD. There were six types of FAODs and 27 mutation sites in 25 genes. The most mutation gene was *ACADS* (10/25, 40.00%), and the most common mutation was *c.1031A>G* (6/18, 33.33%) and *c.164C>T* (6/18, 33.33%). Other mutation sites were comparatively rare. Details are shown in Table 1 and Figure 2D. (Supplementary File S3: Supplementary Table S3).

Follow-up in the confirmed cases

The average initial screening time was 14.39 ± 6.59 days, and the second screening was 66.8 ± 148.11 days. Two patients died, one due to recurrent fever, poor response, hypoketotic hypoglycemia, and liver injury (period 21 months), while another was unknown (period 6 months). One patient with MMA-MUTD had normal intelligence but presented with hypotonia and developmental delays. Exception for three patients (one each in MAHCC-deficiency, MMA-MUTD, and PA) whose parents refused to follow up, the remaining 94 children received regular follow-up, and all are generally developing at present. The longest follow-up period is

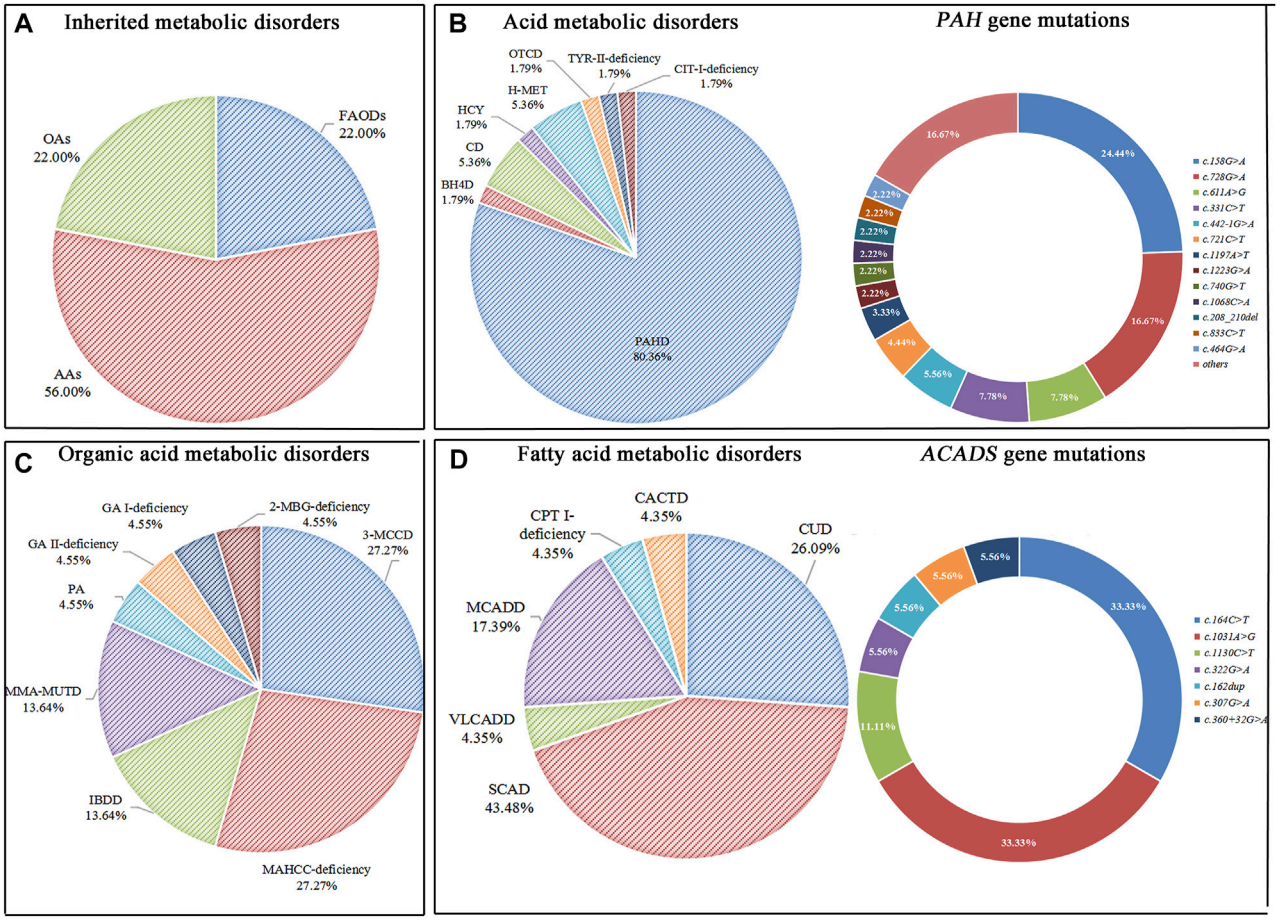

FIGURE 2
Disease spectrum, distribution, and gene mutations of inherited metabolic disorders. **(A)** The percentage of three categories of inherited metabolic disorders. **(B)** The percentage of different types of amino acid metabolic disorders and alleles of *PAH* gene mutations. **(C)** The percentage of different types of organic acid metabolic disorders. **(D)** The percentage of different types of fatty acid metabolic disorders and alleles of *ACADS* gene mutations.

approximately 6 years (Supplementary File S4: Supplementary Table S4)

Discussion

The overall incidence of IMDs detected by MS/MS in northern Chinese, Suqian city is 1: 2,046. Several articles reported the overall incidence of IMDs in other regions of Chinese, for example, northwestern Chinese 1:1,898 (Zhang et al., 2021), eastern China 1:1,178 (Guo et al., 2018), southern Chinese 1:2,804 (18). The overall incidence of IMDs in other countries appeared to be lower than that of Chinese, for example, 1:8,557 in Japan (Shibata et al., 2018), 1:7,030 in Taiwan (Shibata et al., 2018), 1:13,205 in South Korea (Shibata et al., 2018), 1:2,200 in Germany (Shibata et al., 2018), 1:4,942 in the Faroe Islands and Greenland (Lund et al., 2012), 1: 6,000 in European (Smon et al., 2018). The possible cause of the difference is the influence of the government policies on NBS. Nearly all babies in China are tested at birth for rare, serious, and treatable disorders through mandatory province NBS. Another possible reason is that it did not use any second-tier testing regarding MS/MS screening in China (Zhang et al., 2021). The results of this study showed that the AAs were the most common style of IMDs, accounting for 56.00% of patients (1:3,653), followed by OAs (22.00%; 1:9,300) and FAODs (22.00%; 1:9,300). For other Chinese areas, the incidence of AAs, OAs and FAODs was 1:4,176, 1:5,220, 1:12,179 in northwestern Chinese (Zhang et al., 2021), 1:5,084, 1:13,389, 1:9,129 in Suzhou (Wang et al., 2019), 1:8680, 1:9347 and 1:7440 respectively in southern Chinese (Lin et al., 2019). This means that the

incidence of AAs in Suqian city is higher than in other Chinese areas.

PAHD, SCAD, CUD, 3-MCCD, and MAHCC-deficiency are the most common IMDs, and hotspot mutations in pathogenic genes are consistent with Suzhou and the Southern region in China (Lin et al., 2019; Wang et al., 2019). 4,021 suspected positive patients were using MS/MS diagnosis, NGS confirmed 100 cases and the PPV was 2.49%. It shows that MS/MS has a certain degree of false-positive rate when used in screening IMDs. On the one hand, false positives are related to the limitations of MS/MS. For example, the test results are easily affected by factors such as gestational age, newborn weight, and nutritional status. On the other hand, it is related to metabolism, such as abnormal liver and kidney function, drug treatment, diet, and non-metabolic diseases that cause secondary or transient metabolic disorders. Xia et al. (2021) found that vitamin B12 deficiency and acidosis in pregnant women can cause an increase in plasma C3 in their newborns. Arnold et al. (Arnold et al., 2008) reported that the mild secondary increase in 3-hydroxyisovalerylcarnitine (C5OH) in healthy newborns was due to the mother's 3-methylcrotonyl-coenzyme glycinuria. In 2012, Shi et al. (Shi et al., 2012a) reported on NBS for IMDs in mainland China for the previous 30 years. There were only 371,942 neonates screened in Mainland China by MS/MS from 2008 to 2012. However, there are 204,604 infants born in Suqian city enrolled for expanded NBS using MS/MS from January 2016 to November 2020. These substantial changes may be attributed to the efforts of the Chinese government policy and financial support.

In this study, 56 patients with AAs were confirmed, accounting for 56.0% of patients with IMDs, and the incidence rate was 1:3,467. The incidence of PAHD is the highest among all IMDs, reaching 1: 4,546. It is higher than the incidence of PAHD in the Chinese population reported in the literature (total incidence: 1/11,614) (Shi et al., 2012b). According to the concentration of blood phenylalanine, the Chinese Preventive Medicine Association classified PAH deficiency into three types, including mild hyperphenylalaninemia (MHP) (120–360 μmol/L), mild phenylketonuria (mPKU) (360–1,200 μmol/L), classic phenylketonuria (cPKU) (≥1,200 μmol/L) (Association et al., 2019). MHP accounted for 57.78% (26/45) in the present study, and cPKU accounted for 4.44% (2/45) in patients with PAH deficiency. Previous studies show that MHP and mPKU have a higher incidence in the Chinese population than cPKU, which is more prevalent in Eastern Europe (Chen et al., 2018). In the present study, MHP and mPKU accounted for 95.56% of patients with PAHD, consistent with the reports in the literature. This study found 89 different *PAH* gene mutations, of which two cases had mutations in the *PAH* gene and *PTS* gene. The most common mutations were *c.158G>A* (23.5%) and *c.728G>A* (16.8%). It is a hotspot mutation in the Chinese population, and it has also been confirmed that PAHD has a variety of variants and genotypes in different people, and the phenotype is complex (Lin et al., 2019).

In summary, we propose the following conclusions. The advantage of MS/MS is its shorter detection time, super sensitivity, and specificity, making it a powerful tool for screening for IMDs in newborns. The disease occurs of IMDs the Suqian region has the following characteristics. IMDs are not rare in the Suqian region, particularly for AAs. In this region, recurrent mutations of relatively common diseases like PAHD, SCAD, CUD, 3-MCCD, and MAHCC-deficiency were also elucidated. The NBS strategy of combining MS/MS with NGS can improve the early diagnosis of IMDs and facilitate necessary interventions.

There are some limitations of this study. Concerning M/SMS screening efficiency, like most newborn screening centers in China, we did not use any second-tier testing, so we had a high positive rate of initial screening. Moreover, a bias in sample acquisition may exist due to the samples only from hospitals qualified for NBS in Suqian. Therefore, our results may not accurately reflect the urban and rural distribution of IMDs in the Suqian area. Besides, this study could not provide detailed information on the routine biochemistry of patients and their mothers (Bower et al., 2019; Hazan et al., 2020; Raskind and El-Chaar, 2000; Scriver et al., 2001; Tebani et al., 2016; The People's Government of Jiangsu Province, 2019).

Data Availability Statement

The data presented in the study are deposited in the MetaboLights database repository, accession number MTBLS5673.

Ethics Statement

The studies involving human participants were reviewed and approved by the Ethnic Committee of Suqian Maternal and Child Health Care Hospital (Serial number: SMCHCH [2019] ky- 009). All patient-related data were collected retrospectively and anonymously. Written informed consent was obtained from the individual(s), and minor(s)' legal guardian/next of kin, for the publication of any potentially identifiable images or data included in this article.

Author contributions

HZ, YW, and CZ carried out the assays and participated in designing the study. HZ, YW, YQ, and CZ carried out clinical consultations. HZ, YW, YQ, and CZ conceived the study,

participated in its design and coordination, and wrote the manuscript. All authors read and approved the final manuscript.

Funding

This study was supported by grants from the Maternal and Child Health Program of Jiangsu Province (grant no. F202161) and Science and Technology Plan of Suqian City (grant no. Z2021070).

Acknowledgments

The authors most honestly appreciate the patients for their participation in this study and all colleagues in the department of family planning of the Suqian Maternal and Child Health Care Hospital and Nanjing Maternal and Child Health Care Hospital for their assistance in the present study.

Conflict of interest

The authors declare that the research was conducted in the absence of any commercial or financial relationships that could be construed as a potential conflict of interest.

Publisher's note

Supplementary material

The Supplementary Material for this article can be found online at: https://www.frontiersin.org/articles/10.3389/fgene.2022.801447/full#supplementary-material

References

Arnold, G. L., Koeberl, D. D., Matern, D., Barshop, B., Braverman, N., Burton, B., et al. (2008). A Delphi-based consensus clinical practice protocol for the diagnosis and management of 3-methylcrotonyl CoA carboxylase deficiency. *Mol. Genet. Metab.* 93 (4), 363–370. doi:10.1016/j.ymgme.2007.11.002

Association, C. P. M., Association, C. M., and Association, C. M. D. (2019). Consensus statement on dietary treatment and nutritional management for phenylalanine hydroxylase deficiency. *Chin. J. Pediatr.* 57 (6), 405–409. doi:10.3760/cma.j.issn.0578-1310.2019.06.002

Bower, A., Imbard, A., Benoist, J.-F., Pichard, S., Rigal, O., Baud, O., et al. (2019). Diagnostic contribution of metabolic workup for neonatal inherited metabolic disorders in the absence of expanded newborn screening. *Sci. Rep.* 9 (1), 14098. doi:10.1038/s41598-019-50518-0

Chace, D. H., Kalas, T. A., and Naylor, E. W. (2003). Use of tandem mass spectrometry for multianalyte screening of dried blood specimens from newborns. *Clin. Chem.* 49 (11), 1797–1817. doi:10.1373/clinchem.2003.022178

Chen, T., Xu, W., Wu, D., Han, J., Zhu, L., Tong, F., et al. (2018). Mutational and phenotypic spectrum of phenylalanine hydroxylase deficiency in Zhejiang Province, China. *Sci. Rep.* 8 (1), 17137. doi:10.1038/s41598-018-35373-9

Dai, P., Huang, L.-H., Wang, G.-J., Gao, X., Qu, C.-Y., Chen, X.-W., et al. (2019). Concurrent hearing and genetic screening of 180, 469 neonates with follow-up in beijing, China. *Am. J. Hum. Genet.* 105 (4), 803–812. doi:10.1016/j.ajhg.2019.09.003

Fabie, N. A. V., Pappas, K. B., and Feldman, G. L. (2019). The current state of newborn screening in the United States. *Pediatr. Clin. North Am.* 66 (2), 369–386. doi:10.1016/j.pcl.2018.12.007

Ferreira, C. R., van Karnebeek, C. D. M., Vockley, J., and Blau, N. (2019). A proposed nosology of inborn errors of metabolism. *Genet. Med.* 21 (1), 102–106. doi:10.1038/s41436-018-0022-8

Garg, U., and Dasouki, M. (2006). Expanded newborn screening of inherited metabolic disorders by tandem mass spectrometry: Clinical and laboratory aspects. *Clin. Biochem.* 39 (4), 315–332. doi:10.1016/j.clinbiochem.2005.12.009

Guo, K., Zhou, X., Chen, X., Wu, Y., Liu, C., and Kong, Q. (2018). Expanded newborn screening for inborn errors of metabolism and genetic characteristics in a Chinese population. *Front. Genet.* 9, 122. doi:10.3389/fgene.2018.00122

Hazan, G., Hershkovitz, E., and Staretz-Chacham, O. (2020). Incidence of inherited metabolic disorders in southern Israel: A comparison between consanguinity and non-consanguinity communities. *Orphanet J. Rare Dis.* 15 (1), 331. doi:10.1186/s13023-020-01578-3

Huang, X., Yang, L., Tong, F., Yang, R., and Zhao, Z. (2012). Screening for inborn errors of metabolism in high-risk children: A 3-year pilot study in Zhejiang province, China. *BMC Pediatr.* 12 (1), 18. doi:10.1186/1471-2431-12-18

Leonard, J. V., and Morris, A. A. (2006). Diagnosis and early management of inborn errors of metabolism presenting around the time of birth. *Acta Paediatr.* 95 (1), 6–14. doi:10.1080/08035250500349413

Lin, Y., Zheng, Q., Zheng, T., Zheng, Z., Lin, W., and Fu, Q. (2019). Expanded newborn screening for inherited metabolic disorders and genetic characteristics in a southern Chinese population. *Clin. Chim. Acta.* 494, 106–111. doi:10.1016/j.cca.2019.03.1622

Lund, A. M., Hougaard, D. M., Simonsen, H., Andresen, B. S., Christensen, M., Dunø, M., et al. (2012). Biochemical screening of 504, 049 newborns in Denmark, the Faroe Islands and Greenland — experience and development of a routine program for expanded newborn screening. *Mol. Genet. Metab.* 107 (3), 281–293. doi:10.1016/j.ymgme.2012.06.006

McHugh, D., Cameron, C. A., Abdenur, J. E., Abdulrahman, M., Adair, O., Al Nuaimi, S. A., et al. (2011). Clinical validation of cutoff target ranges in newborn screening of metabolic disorders by tandem mass spectrometry: A worldwide collaborative project. *Genet. Med.* 13 (3), 230–254. doi:10.1097/GIM.0b013e31820d5e67

Niu, D. M., Chien, Y. H., Chiang, C. C., Ho, H. C., Hwu, W. L., Kao, S. M., et al. (2010). Nationwide survey of extended newborn screening by tandem mass spectrometry in Taiwan. *J. Inherit. Metab. Dis.* 33 (2), S295–S305. doi:10.1007/s10545-010-9129-z

Raskind, J. Y., and El-Chaar, G. M. (2000). The role of carnitine supplementation during valproic acid therapy. *Ann. Pharmacother.* 34 (5), 630–638. doi:10.1345/aph.19242

Scriver, C., Beaudet, A. L., and Sly, W. S. (2001). *The metabolic and molecular bases of inherited disease*. New York: McGraw-Hill.

Shi, X.-T., Cai, J., Wang, Y.-Y., Tu, W.-J., Wang, W.-P., Gong, L.-M., et al. (2012). "Newborn screening for inborn errors of metabolism in mainland China: 30 Years of experience," in *JIMD reports - case and research reports, 2012/3* (Berlin, Heidelberg: Springer Berlin Heidelberg). doi:10.1007/8904_2011_119

Shi, X. T., Cai, J., Wang, Y. Y., Tu, W. J., Wang, W. P., Gong, L. M., et al. (2012). Newborn screening for inborn errors of metabolism in mainland China: 30 years of experience. *JIMD Rep.* 6, 79–83. doi:10.1007/8904_2011_119

Shibata, N., Hasegawa, Y., Yamada, K., Kobayashi, H., Purevsuren, J., Yang, Y., et al. (2018). Diversity in the incidence and spectrum of organic acidemias, fatty acid oxidation disorders, and amino acid disorders in Asian countries: Selective

screening vs. expanded newborn screening. *Mol. Genet. Metab. Rep.* 16, 5–10. doi:10.1016/j.ymgmr.2018.05.003

Smon, A., Repic Lampret, B., Groselj, U., Zerjav Tansek, M., Kovac, J., Perko, D., et al. (2018). Next generation sequencing as a follow-up test in an expanded newborn screening programme. *Clin. Biochem.* 52, 48–55. doi:10.1016/j.clinbiochem.2017.10.016

Tarailo-Graovac, M., Shyr, C., Ross, C. J., Horvath, G. A., Salvarinova, R., Ye, X. C., et al. (2016). Exome sequencing and the management of neurometabolic disorders. *N. Engl. J. Med.* 374 (23), 2246–2255. doi:10.1056/NEJMoa1515792

Tebani, A., Abily-Donval, L., Afonso, C., Marret, S., and Bekri, S. (2016). Clinical metabolomics: The new metabolic window for inborn errors of metabolism investigations in the post-genomic era. *Int. J. Mol. Sci.* 17 (7), 1167. doi:10.3390/ijms17071167

The People's Government of Jiangsu Province (2019). The guildlines for the prevention and control of Birth Defects in Jiangsu Province. Available at: http://www.jiangsu.gov.cn/art/2021/1/6/art_46143_9626220.html (Accessed December 31, 2020)

Wang, T., Ma, J., Zhang, Q., Gao, A., Wang, Q., Li, H., et al. (2019). Expanded newborn screening for inborn errors of metabolism by tandem mass spectrometry in Suzhou, China: Disease spectrum, prevalence, genetic characteristics in a Chinese population. *Front. Genet.* 10, 1052. doi:10.3389/fgene.2019.01052

Wilcox, G. (2018). Impact of pregnancy on inborn errors of metabolism. *Rev. Endocr. Metab. Disord.* 19 (1), 13–33. doi:10.1007/s11154-018-9455-2

Xia, Q., Chen, Z., He, Y., Jin, Y., Li, M., and Song, J. (2021). A case of infant secondary methylmalonic aciduria caused by maternal vegetarianism. *China Clinical Case Results Database* 03 (01), E159–E159. doi:10.3760/cma.j.cmcr.2021.e00159

Ye, J., Qiu, W. J., Han, L. S., Zhang, H. W., and Gu, X. F. (2015). Phenylalanine hydroxylase deficiency and citrin deficiency in a Chinese infant. *Chin. Med. J.* 128 (21), 2979–2980. doi:10.4103/0366-6999.168084

Zhang, R., Qiang, R., Song, C., Ma, X., Zhang, Y., Li, F., et al. (2021). Spectrum analysis of inborn errors of metabolism for expanded newborn screening in a northwestern Chinese population. *Sci. Rep.* 11 (1), 2699. doi:10.1038/s41598-021-81897-y

Frontiers in Genetics

Highlights genetic and genomic inquiry relating to all domains of life

The most cited genetics and heredity journal, which advances our understanding of genes from humans to plants and other model organisms. It highlights developments in the function and variability of the genome, and the use of genomic tools.

Discover the latest Research Topics

See more →

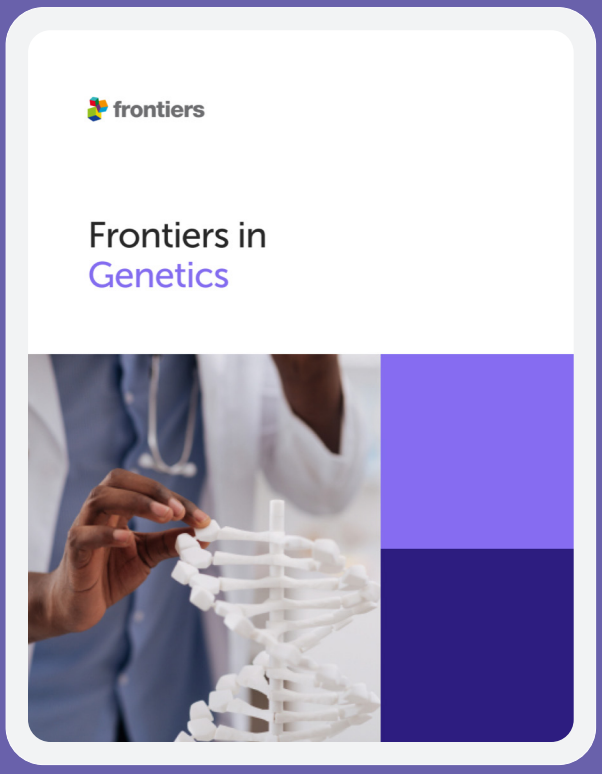

Frontiers

Avenue du Tribunal-Fédéral 34
1005 Lausanne, Switzerland
frontiersin.org

Contact us

+41 (0)21 510 17 00
frontiersin.org/about/contact